CHALMERS
UNIVERSITY OF TECHNOLOGY

Implementation of Stainless Steel Reinforcement in Concrete Bridges

Redesign of Reinforcement using Stainless Steel to Increase Durability and Profitability in Bridge Design.

Master's Thesis in the Master's Programme Structural Engineering and Building Technology

SOFIA ELWIN DAHLSTRÖM
JONAS PERSSON

Architecture and Civil Engineering
Division of Structural Engineering
Concrete Structures
CHALMERS UNIVERSITY OF TECHNOLOGY
Gothenburg, Sweden 2018
Master's Thesis ACEX30-18-37

MASTER'S THESIS ACEX30-18-37

Implementation of Stainless Steel Reinforcement in Concrete Bridges

Redesign of Reinforcement using Stainless Steel to Increase Durability and Profitability in Bridge Design.

Master's Thesis in the Master's Programme Structural Engineering and Building Technology

SOFIA ELWIN DAHLSTRÖM
JONAS PERSSON

Architecture and Civil Engineering

Division of Structural Engineering

Concrete Structures

CHALMERS UNIVERSITY OF TECHNOLOGY

Gothenburg, Sweden 2018

Implementation of Stainless Steel Reinforcement in Concrete Bridges
Redesign of Reinforcement using Stainless Steel to Increase Durability and Profitability in Bridge Design.
SOFIA ELWIN DAHLSTRÖM
JONAS PERSSON

Master's Thesis ACEX30-18-37
ISSN 1652-8557
Architecture and Civil Engineering
Division of Structural Engineering
Concrete Structures
Chalmers University of Technology
SE-412 96 Gothenburg
Sweden
Telephone: +46 (0)31-772 1000

Cover:
The Haynes Inlet bridge in Oregon, U.S. The bridge carries U.S Route 101 over the Haynes Inlet and is constructed with stainless steel reinforcement (Michael Goff, 2008).

Chalmers Reproservice
Gothenburg, Sweden 2018

Implementation of Stainless Steel Reinforcement in Concrete Bridges
Redesign of Reinforcement using Stainless Steel to Increase Durability and Profitability in Bridge Design.
Master's Thesis in the Master's Programme Structural Engineering and Building Technology
SOFIA ELWIN DAHLSTRÖM
JONAS PERSSON
Architecture and Civil Engineering
Division of Structural Engineering
Concrete Structures
Chalmers University of Technology

ABSTRACT

Since reinforced concrete is one of the most common building materials used today, the deterioration mechanisms of the materials and more specifically the corrosion of the steel reinforcement is an extensive problem. The repair of concrete cracks and spalling, which is a direct consequence of corrosion, leads to high repair costs and consequently a request for more durable structures. To increase durability, crack widths are limited, which can result in large amounts of non structural reinforcement.

In order to decrease the consumption of material and create more durable structures, stainless steel reinforcement can be implemented in highly exposed areas of the structures. However, the price of stainless steel is higher than that of ordinary reinforcing steel. Consequently, the purpose of this study is to investigate the applicability and profitability of stainless steel rebars in structural design. This aim is achieved by investigating the stainless steel alternatives available today, with regard to strength and corrosion resistance. Secondly, a retaining wall and a slab-frame bridge, are redesigned using stainless steel reinforcement and a life cycle cost analysis is performed to determine its profitability.

The results of the redesigns showed that a considerable reduction of reinforcement amount was possible when designing with stainless steel reinforcement. For the retaining wall, a decrease of 42 % could be achieved. The reinforcement amount for the slab-frame bridge could be reduced by 16 %. The result of the LCC showed that, when considering only the agency costs, a profit of about 20 % can be expected when using stainless steel reinforcement in the slab-frame bridge, and up to 30 % for the retaining wall. Furthermore, the literature study indicates that stainless steel reinforcement can be used in combination with carbon steel reinforcement without risk of galvanic corrosion, granted that the carbon steel reinforcement is deeply embedded in concrete. Hence, it can be stated that stainless steel reinforcement can be implemented in the outermost layers of the studied reinforced concrete structures in order to increase durability and reduce the total costs.

Keywords: Reinforced concrete, Stainless steel reinforcement, Corrosion resistance of stainless steel, LCC analysis, Bridge construction Slab-frame bridge, Retaining wall, Sustainable construction

Tillämpning av rostfri armering i betongbroar
Omdimensionering av armering med rostfritt stål för att öka hållbarheten och minska kostnaderna inom brokonstruktion.
Examensarbete i Structural Engineering and Building Technology
SOFIA ELWIN DAHLSTRÖM
JONAS PERSSON
Arkitektur och samhällsbyggnadsteknik
Avdelningen för Konstruktionsteknik
Betongbyggnad
Chalmers Tekniska Högskola

SAMMANFATTNING

Då armerad betong är ett av de vanligast förekommande byggnadsmaterialen är nedbrytningen av betongkonstruktioner på grund av korrosion idag ett utbrett problem. Korrosion i armeringsstålet leder till sprickor och splittring av betongen, vilket resulterar i höga reparationskostnader och således ökar behovet av mer hållbara konstruktioner. För att öka hållbarheten i armerade betongkonstruktioner används höga krav på maximal sprickbredd, vilket kan resultera i stora armeringsmängder.

För att minska behovet av armering och för att öka hållbarheten kan istället rostfri armering användas i de mest utsatta delarna av konstruktionen. Det kan dock leda till högre investeringkostnader då rostfri armering är betydligt dyrare än vanlig armeringsstål. Därmed var syftet med den här studien att undersöka lönsamheten och tillämpligheten med rostfri armering i betongbroar. Det utfördes genom att undersöka korrosionsbeständigheten och hållfastheten av rostfria armeringsstål som finns tillgängliga idag. Vidare utfördes detta genom att dimensionera om armeringen i en stödmur och en plattrambro och därefter utföra livscykelkostnadsanalyser för att undersöka lönsamheten.

Resultaten indikerar att en betydlig reduktion av armeringsmängd är möjlig genom användandet av rostfri armering. För stödmuren uppnåddes en minskning av armerings,mängden på 42 % och för plattrambron en minskning av 16 %. Resultaten av LCC analyserna visar att när hänsyn bara tas till kostnader för ägaren kan en vinst på 20 % förväntas för plattrambron, respektive 30 % för stödmuren. Vidare konstateras det att rostfri armering kan användas i kombination med vanlig armeringsstål utan risk för galvanisk korrosion, förutsatt att det vanliga armeringsstålet är djupt inbäddat i betongens passiva miljö. Sammanfattningsvis kan det konstateras att rostfri armering kan tillämpas i det yttersta lagret av de studerade betongkonstruktionerna för att öka hållbarheten, men också minska de totala kostnaderna.

Nyckelord: Armerad betong, Rostfri armering, Korrosionsbeständighet i rostfritt stål, Livscykelkostnads-analys, Brokonstruktion, Plattrambro, Stödmur

Contents

PREFACE

This master's thesis was carried out at the Division of Structural Engineering at Chalmers University of Technology and in cooperation with WSP group during the period of January to June 2018. We would like to take the opportunity in this preface to acknowledge the people who have been supportive and contributed to this thesis and therefore made it possible.

First of all, we would like to express our gratitude to our examiner Ignasi Fernandez and our supervisor Mohsen Heshmati at Chalmers University of Technology and WSP group. During the creation of this thesis, your knowledge, feedback and tireless commitment has been invaluable for the final result.

We would also like to express our gratitude towards the bridge department at WSP in Gothenburg for their cooperation, aid and assistance. This gratitude especially concerns our supervisor Mohsen Heshmati, Daniel Josefsson, who has provided insightful information for the calculations and Peter Dalerstedt, who has provided a workplace for us during the creation of this thesis.

Lastly, we would also like to thank our opponents, Jack Jönsson and Anton Stenseke, for the appreciated feedback they have given us during this study.

Gothenburg, May 2018

Sofia Elwin Dahlström and Jonas Persson

NOMENCLATURE

Abbreviations

ADT	Average daily traffic
BaTMan	Bridge and tunnel management
EC	Eurocode
FLS	Fatigue limit state
LCC	Life cycle cost
RL	Reinforcement Layout
SEK	Swedish crowns
SLS	Serviceability limit state
TDC	Traffic delay cost
ULS	Ultimate limit state
USD	US Dollars
VOC	Vehicle operation cost

Roman upper case letters

A_s	Area of reinforcing steel
C_t	Sum of costs at time t
C_{RL}	Cost of reinforcement layout
E	Modulus of elasticity
E_c	Compressive modulus of elasticity of concrete
E_{cm}	Compressive modulus of elasticity of concrete; mean value
E_s	Modulus of elasticity of reinforcing steel;
E_{sm}	Modulus of elasticity of reinforcing steel; mean value
E_0	Modulus of elasticity of stainless steel reinforcing steel;
F_t	Tensile Force
F_{tot}	Tensile Force capacity in section
N	Number of cycles
P	Profit
T	Studied time period
V_d	Shear force
V_{tot}	Shear force capacity in section

Roman lower case letters

b_c	Width of concrete cross-section

d	Distance to center of bottom reinforcement layer; measured from top edge
d'	Distance to center of top reinforcement layer; measured from top edge
f_c	Compressive cylinder strength of concrete
f_{cd}	Compressive cylinder strength of concrete; designing value
$f_{cd.fat}$	Compressive cylinder strength of concrete; designing fatigue value
f_{ctm}	Tensile strength of concrete; mean value
$f_{0.2}$	0.2% proof stress of reinforcing steel
f_{yd}	Yield strength of reinforcing steel; design value
f_{yk}	Yield strength of reinforcing steel; characteristic value
h_c	Height of concrete cross section
n	Strain hardening rate of stainless steel
r	Interest rate
r_i	Inflation rate
r_L	Discount rate
$s_{r.max}$	Maximum crack distance
t	Age of concrete at first load cycle
w_k	Crack width; characteristic value
$w_{k.allowed}$	Allowed crack width
x_{top}	Distance to neutral axis from top edge

Greek letters

α	Stress block factor for average stress
α_0	Ratio between elastic and plastic deformation for stainless steel
β	Stress block factor for resultant location
β_{cc}	Coefficient for age of concrete at first loading
$\Delta\sigma_{Rsk}$	Allowed steel stress range
$\Delta\sigma_{ss}$	Steel stress range
$\gamma_{s.fat}$	Fatigue safety factor for steel
ε_{cm}	Concrete strain; mean value
ε_{sm}	Steel strain; mean value
$\varepsilon_{0,2}$	Stainless steel strain at 0,2 % plastic elongation
$\sigma_{c.max}$	Maximum concrete stress under fatigue loading
$\sigma_{c.min}$	Minimum concrete stress under fatigue loading
σ_{sm}	Stress in reinforcing steel; mean value
σ_0	Stress in stainless steel at 0,2 % elongation

1 Introduction

The deterioration of infrastructure is a major concern in society today since the maintenance and repair costs are increasing, leading to a request for more durable infrastructure. In this study, the problems concerning carbon steel reinforcement will be introduced, and the possibility of replacing it with stainless steel reinforcement as a possible solution to increase the lifespan of the structures. This is explored by redesigning existing structures and performing a life cycle cost analysis on each structure. This chapter presents the background, problem description, aim and objectives, method, limitations and structure of the thesis.

1.1 Background

Reinforced concrete is one of the most common building materials used in construction today. There are many benefits, such as formability, low price and efficiency in construction. However, there are some disadvantages with the carbon steel reinforcement used. The corrosion of reinforcement is a major concern since it causes deterioration of the structure and induces high maintenance and repair costs. During recent years, the progress in developing more durable and high strength concrete has been significant, but corrosion of steel reinforced concrete structures is still a major issue today. Corrosion takes place in the reinforcement due to ingress of aggressive agents through the concrete surface. When corrosion initiates cracks can appear, which in turn can lead to concrete spalling. Concrete spalling leads to higher exposure of the reinforcement bars and thus increasing the corrosion rate.

To delay the corrosion process and to increase the durability of the structure, design codes limit the maximum allowable crack width under serviceability limit state in order to reduce the ingress of aggressive agents in the concrete. This requirement can lead to very high reinforcement ratios and consequently, only a small capacity of the reinforced concrete section utilized.

Carbon steel can be replaced by using non-corrosive reinforcement as stainless steel, fibre reinforced polymers or galvanized steel among others. By using alternative reinforcement types, crack width limitations can be relaxed, or even ignored, and a higher utilization ratio can thus be obtained, possibly resulting in lower material usage and maintenance costs. Stainless steel is an alternative reinforcement alternative which has been available on the market for some time, but the applications in Sweden are limited, due to lack of knowledge and prior experience in the area.

1.2 Problem Description

Deterioration of concrete structures due to corrosion of reinforcement induces high social costs, especially when concerning concrete bridges exposed to corrosive environments. Alternative reinforcement methods have been suggested to limit these expenses, but there is not sufficient information available to properly evaluate if they are financially profitable and structurally safe. This leads to the following questions:

1. Is it financially profitable to use stainless steel reinforcement in concrete structures, even though the initial costs will be greater?
2. Could the relaxation of crack width limitations lead to reduction of the amount of reinforcement used in design?
3. Is it safe to assume that the crack width limitations can be relaxed, or even ignored when stainless steel reinforcement is used?
4. Can stainless and carbon steel reinforcement be used in the same structural components without risking galvanic corrosion?

1.3 Aim and Objectives

The aim of the study is to create more durable infrastructure by increasing the knowledge of stainless steel in the construction industry, with focus on reinforced concrete bridges. The study aims further at evaluating the profitability of using stainless steel reinforcement and to present design situations where it is advisable to use alternative reinforcement materials. In order to reach the aim of this study, the following objectives are specified:

- Evaluate different grades of stainless steel available on the market.
- Evaluate the corrosion resistance of different grades of stainless steel.
- Investigate the cost of repairs on existing reinforced concrete bridges in Sweden.
- Present concrete structures around the world where stainless steel has been used.
- Define design situations where the use of stainless steel is advantageous.
- Redesign structural bridge elements using stainless steel reinforcement while using different crack width allowances.
- Perform a life-cycle analysis to evaluate the possible profit of replacing some of the carbon steel rebars with stainless steel in reinforced concrete bridges in Sweden.

1.4 Method

Initially, a literature study was carried out to obtain a thorough understanding of the studied field. During this phase, problems concerning carbon steel reinforcement were identified possible solutions to this problem, such as alternative reinforcement material was researched. This was achieved by reviewing current literature regarding stainless steel reinforced concrete structures and presenting the mechanical properties of stainless steel to give a good knowledge base to design a stainless steel reinforced concrete structure.

Secondly, existing concrete bridges with carbon steel reinforcement are researched by reviewing data collected in the Swedish Bridge and Tunnel Management System in order to get a scope of the problem regarding repair costs. Furthermore, concrete bridges using stainless steel reinforcement around the world are researched. The information gathered concerning the repaired bridge components and the application of stainless steel reinforcement form a base for the choice of bridge elements to be redesigned. The structural elements will then be redesigned using relaxed or ignored crack width limitations. After this, the required amount of reinforcement and utilization ratio was evaluated.

Lastly, a life cycle cost analysis was performed in order to study the impact of stainless steel reinforcement on the cost of the bridge over its service life. This study formed the basis to evaluate if stainless steel reinforcement is economically profitable to use in reinforced concrete structures in aggressive environments today. The methodology of the study can be seen in Figure 1.1

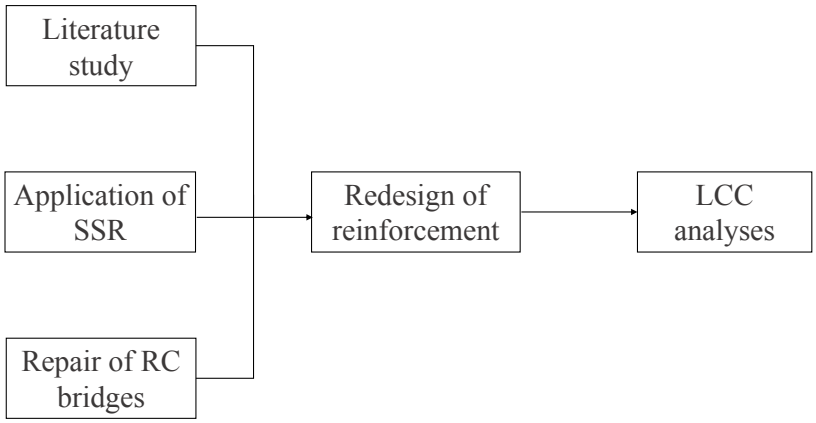

Figure 1.1 Method of the study.

1.5 Limitations

As mentioned in Section 1.1, there are several alternatives to carbon steel reinforcement. In this study, however, the focus lies on the use of stainless steel and the different grades available. Other reinforcement possibilities will be presented briefly to give the reader a general idea, but a more detailed description will not be carried out. Furthermore, the study will not consider concrete quality, which also influences the total cost and durability of an infrastructure project. The study focuses on a small retaining wall and slab-frame bridge. Consequently, it can not be ensured that the results of the study are applicable on larger bridge structures.

1.6 Structure of Thesis

Chapter One: Introduction. This chapter presents the background and the problem of the study as well as the aim, objectives, method and limitations.

Chapter Two: Literature Study. The materials of interest are presented by describing characteristics of the materials such as mechanical properties, durability and chemical composition.

Chapter Three: Repair of Reinforced Concrete Bridges. Six existing reinforced concrete bridges are presented with year of construction, year of reparation and cost of reparation in order to get an idea of the actual repair costs for concrete bridges.

Chapter Four: Application of Stainless Steel Rebars in Bridges. The application and design of stainless steel reinforcement is presented. This includes both the existing design codes and guidance available as well as a short presentation of the current usage in bridges today.

Chapter Five: Case Studies. This chapter presents two case studies where structures originally designed with carbon steel reinforcement are redesigned using stainless steel reinforcement. The cases include a retaining wall and a slab-frame bridge. A short introduction to the cases is presented, followed by the calculation procedure concerning the reinforcement arrangement.

Chapter Six: Life Cycle Cost Analysis. A life cycle cost analysis is conducted for the two different cases. This chapter provides a short introduction to a life cycle cost analysis and states the necessary data and assumptions required in order to perform the analysis.

Chapter Seven: Results. In this chapter, the results of the redesign of reinforcement arrangement and the results of the life cycle cost analysis are presented.

Chapter Eight: Discussion. The results, possible weaknesses and sources of error in the study are discussed and evaluated in this chapter. Furthermore, possible opportunities regarding the use of stainless steel reinforcement that were not utilized in the study are presented.

Chapter Nine: Conclusion. In this chapter, conclusions of the study are drawn based on the questions formulated in the introduction and the weaknesses of the study mentioned in the discussion. Additionally, suggestions for further studies are presented.

2 Literature Study

In the following chapter, a literature study concerning concrete, reinforced concrete, carbon steel reinforcement and stainless steel reinforcement is presented. Furthermore, the durability problems concerning reinforced concrete, and the use of stainless steel reinforcement in concrete as a solution to these problems, are presented.

2.1 Concrete

Concrete is a workable and adaptable, composite material which is one of the most used construction materials in the world today. It has been used as a construction material even before the introduction of reinforcement. In order to use unreinforced concrete, the structure has to be designed to work in pure compression, resulting in heavy, large structures. The introduction of steel in the concrete section makes it possible to design more slender structures that can work in both tension and compression. However, the use of reinforcement has resulted in problems concerning durability, which will be further described in Section 2.3.3.

The earliest applications of concrete took advantage of the fact that concrete has a very high compressive strength, compared to the tensile strength. This was achieved by designing structures that work in pure compression. An early example of the usage of unreinforced concrete in a rather complex structure is the Pantheon in Rome, see Figure 2.1, which was built almost 18 centuries ago (Moore, 1995). The dome is designed to be loaded in compression since it is an unreinforced concrete structure and therefore vulnerable to tensile stresses. Tensile stresses have, however, caused cracking in the dome and in the walls but since there is no presence of reinforcement, the durability problems associated with corrosion of reinforcement has been avoided.

Thus, the Pantheon could be seen as a clear example of how concrete can be very durable when used without corrosive elements. The material has an advantageous use in structures exposed to harsh climate because of its resistance against moisture and wear (Burström, 2007). Another advantage is that concrete could be delivered to a workplace as a formable material, which gives many opportunities for construction companies to have a great impact on the end product.

2.1.1 Material Composition

Concrete is a composite material that consists of both fine and coarse aggregates that are bonded with cement paste. The aggregates define a large part of the concrete mix and contains sand, natural gravel and crushed stone. The cement reacts with the water in a chemical process called cement hydration

Figure 2.1 The dome of the Pantheon in Rome, unreinforced concrete structure constructed 126 AD (Dahlström, 2015).

and together with the aggregates form the concrete material. Additionally, chemical admixtures can be added to the concrete mix to speed up the hydration process, slow down the hydration process, reduce damage during freeze-thaw cycles or increase the workability of fresh concrete. Corrosion inhibitors could also be used in the concrete mixture to increase the chloride threshold value and therefore decrease the corrosion rate of the reinforcing steel.

The most common type of concrete is lime-based containing Portland cement. In Sweden, Portland cement accounts for 75 % of the cement used in the construction industry (Burström, 2007). The cement consists of calcium silicates , aluminates and ferrites and is created when heating limestone, which is a source of calcium, with clay or shale, which is a source of silicon, aluminium and iron. The cement is created when grinding the product with a source of sulfate, i.e gypsum.

In the hydration of Portland cement, calcium hydroxide ($Ca(OH)_2$) forms, which causes the material to be highly alkaline (Burström, 2007). The alkaline environment passivates the reinforcement, giving an initial protection against corrosion, which will be further explained in Section 2.4.1. The calcium hydroxide then reacts with carbon dioxide (CO_2) in the air to form calcium carbonate ($CaCO_3$) in a process called carbonation, which will be further explained in Section 2.4.2.

The alkalinity of concrete is highly dependent on the proportions of the binder and thus the amount of Portland cement, which causes the formation of $Ca(OH)_2$. Basically, the reduction of cement will lower the amount of $Ca(OH)_2$ and cause the initial pH to be lower, resulting in the passivization of the concrete to be reduced.

On the basis of this, cement can be replaced by other cementitious materials and this brings the interest of a group of materials called pozzolans. In the presence of water, these materials react with $Ca(OH)_2$ to form compounds that have similar properties to cement. Fly ash is an example, which is a coal combustion residue product. Fly ash mainly consists of aluminosilicate and the content of aluminosilicate highly affects the fly ash reactivity. The most usual pozzolan used in Sweden is silica fume, which is a fine powder of amorphous silica created as a residue by the manufacturing of alloys to steel (Burström, 2007). Silica fume is a highly reactive pozzolan which improves the concrete cohesion and stability. However, with the addition of silica fume comes an increased need for water, which requires the addition of superplasticizers to be able to benefit from the pozzolan. Ground-granulated blastfurnace slag is another example of a pozzolanic material, which is created when the residual slag from iron production is quenched, dried and ground into a fine powder. Other pozzolans are metakaolin, which is obtained from a clay mineral, and Rice husk ash, which is obtained by burning rice hulls.

These cement replacement materials can overall be said to change the concrete properties. As discussed above, with the use of pozzolanic materials, the pH is changed to a lower grade, reducing the corrosion resistance of the reinforcement. Apart from this, other changes are the improved workability of the fresh concrete due to an increased paste volume, while the cement content remains intact. The cement replacement materials also give an higher early strength by accelerating the strength development of the concrete and because of the fine nature of the pozzolanic materials, the voids in the concrete are more effectively filled, thus limiting the transportation of chlorides and the carbonation process, resulting in increased corrosion resistance.

During the last decades, there has been a considerable development in concrete and thus, new types of concrete has been introduced. High-performance concrete is a relatively new term that considers concrete that is enhanced in comparison to normal concrete. Examples of such properties are; increased workability, strength development, permeability or toughness of the high-performance concrete should be better than normal.

2.1.2 Material Properties

In this study, material properties of concrete are required both to understand the material behaviour and in the analysis conducted. Since concrete has a wide variety of properties, Table 2.1 lists properties of concrete class C35/45 to give approximate values.

Table 2.1 Properties and cost of concrete C35/45 (Burström, 2007) (Jönköpings Betong, 2007).

Parameter	Value
Compressive strength	35 MPa
Tensile strength	3.2 MPa
Modulus of elasticity	34 GPa
Density	2400 kg/m^3
Ultimate compressive strain	0.35%
Thermal expansion coefficient	$12 \cdot 10^{-6}/°C$
Price	1005 SEK/ m^3

2.2 Reinforced Concrete

Reinforcement can be used in concrete structures in order to increase ductility and tensile strength. The reinforcement usually consists of carbon steel reinforcing bars in the size of 6 to 32 mm in diameter and can be used in numerous different applications in order to avoid either cracking or structural failure (Al-Emrani, 2011). Reinforcement is used to provide tensile capacity, due to the low tensile capacity of concrete. Since concrete in itself has high compressive capacity, reinforcement makes it possible to use the material in both tension and compression (Burström, 2007). Although carbon steel reinforcement is the most commonly used, there are several other materials the concrete can be reinforced with. However, in this section, the focus will lie on carbon steel reinforcement as it is the most common reinforcement material. In Section 2.4.7, other reinforcement alternatives will also be presented.

2.3 Carbon Steel Reinforcement

Carbon steel reinforcement is an alloy of iron and carbon, with small concentrations of other metals. The reason why steel is used as a reinforcement material in concrete is its extraordinary properties when considering strength, modulus of elasticity and cost. Another advantage of steel is the formability of the material which makes it possible to create ribbed bars, making the bond between the reinforcing steel and the concrete excellent. However, when using steel in concrete, the main problem is the fact that steel corrodes under standard environmental conditions, which is explained in Section 2.3.3.

2.3.1 Mechanical Properties of Carbon Steel

In this project, material properties of carbon steel reinforcement are of interest for comparison purposes. In Table 2.2, typical mechanical properties of carbon steel reinforcement is presented, which corresponds to reinforcement steel B500B (Al-Emrani, 2011).

Table 2.2 Mechanical properties of carbon steel reinforcement.

Parameter	Value
Yield strength	500 MPa
Modulus of elasticity	200 GPa
Density	7800 kg/m^3
Thermal expansion coefficient	$12 \cdot 10^{-6}/°C$

As can be seen when comparing Table 2.1 with Table 2.2, concrete and carbon steel have similar thermal expansion coefficients. This means that a structural member of reinforced concrete experiences minimal stresses due to temperature changes, which is beneficial in many applications.

2.3.2 Cost, Availability and Sustainability

Steel is a material which is available all over the world. However, steel varies much in quality depending on the composition of the metals used and on the manufacturing method. In September 2017, the price of carbon steel bars was 579 US dollars per metric ton (MEPS, 2018a)

In order to obtain the metals required to create steel, mining is necessary and thus there is an environmental factor that has to be taken into account when using steel. This is however not only related to carbon steel, as is described in this chapter, but is also relevant when considering usage of stainless steel or any other type of steel. Even though mining leads to large disturbance, especially for local environments, the recyclability of steel is also a factor that needs to be considered.

2.3.3 Durability Problems with Carbon Steel Reinforcement

Currently, deterioration of concrete structures due to corrosion of reinforcement is an issue worldwide. Especially exposed areas are roads, marine constructions, bridges and parking decks, which are exposed to harsh climate and de-icing salts. An example of a possible result of the damaging effects can be seen in Figure 2.2.

The consequence of deterioration of infrastructures is that extensive repair-work is needed, causing huge delays and enormous costs for both users and stakeholders. For example, it is estimated that Western Europe spends 5 billion Euros every year to repair corroded concrete infrastructure (Markeset *et al.*, 2006). On basis of this, methods to prevent or reduce corrosion are of high interest. In Section 2.4.7, solutions in order to limit, or prevent, corrosion will be presented and explained. In the following section, the driving mechanisms behind corrosion will be explained as well as the results, and thus the problems that corrosion leads to.

Figure 2.2 Corrosion of reinforcement in concrete, causing rust, cracking and spalling (Concrete Protection, 2017).

2.4 Corrosion of Steel Reinforcement

This section will describe the corrosion process of steel reinforcement embedded in concrete. First, carbon steel reinforcement will be discussed, followed by a comparison to stainless steel reinforcement. Lastly, other corrosion resistant reinforcement alternatives will be briefly mentioned.

2.4.1 Passivation of Steel

Initially, steel reinforcement embedded in concrete is protected from corrosion. This is due to a protective ion-oxide film that is created in the highly alkaline conditions prevailing in the concrete, causing passivation of the steel and thus protecting it from corrosion. This passive condition is obtained if the pH of the concrete is over 12.5.

2.4.2 Chloride Ingress and Carbonation

The protecting film can deteriorate by two different mechanisms. Firstly by chlorides penetrating the concrete and reaching the reinforcement and secondly by carbonation of the concrete, causing the pH of the concrete, and consequently the alkalinity in the pore solution, to diminish.

The first mechanism, chloride ingress, is caused by aggressive chloride ions mainly from sea water and de-icing salts penetrating the concrete. The three different mechanisms that causes the chloride to infiltrate the concrete is capillary suction, diffusion and migration, which makes the corrosion process highly affected by the permeability of the concrete (Silva, 2013). When the chloride reaches the steel surface, chloride ions weakens the iron-oxide layer acting as a passivizing film and chemically reacts with iron cations available on the steel surface to form iron-chloride (Chong *et al.*, 2001). This iron-chloride reacts with hydroxyl ions in the concrete to form ferrous hydroxide, which in turn releases the chloride ions and thus reacts with the iron cations available. This chemical process leads to the dissolution of the passive iron-oxide layer and will in turn cause corrosion to initiate.

The second mechanism, carbonation, is caused by carbon dioxide penetrating the concrete cover. The carbonation process consists of two main reactions. At first, carbon dioxide reaches the pore solution of the concrete causing the carbon dioxide to dissolve, which in turn creates carbonic acid (Bohlin and Snibb, 2016). Secondly, the carbonic acid reacts with calcium hydroxide from the hydration process, described in Section 2.1.1. However, this reaction consumes hydroxide ions and thus reduces the pH of the concrete, causing the alkalinity in the pore solution to be reduced and in turn causing the protecting film to dissolve and therefore exposing the steel to corrosion.

2.4.3 Exposure Classes for Reinforced Concrete

To avoid extensive damage of the structure by corrosion, current standards today defines exposure classes for different components of the structure. The exposure class is defined by the environment that the component is exposed to. For a description of the environments and respective exposure classes, the reader is referred to the standard SS-EN 1992-1-1 Table 4.1. Depending on the exposure class, measures described in SS-EN 1992-1-1 Table 4.3-4.5 need to be taken. These measures include ensuring that the concrete class is appropriate, as well as sufficient thickness of the concrete cover for each structural element is provided.

2.4.4 Corrosion Modes

As described in Section 2.4.2, depassivation of steel embedded in concrete results in initiation of corrosion. This electrochemical reaction consists of cathodic and anodic half-cell reactions (Ziehl and El-Batanouny, 2016). There are several factors that influence the corrosion resistance of a metal, such as alloying elements, amount of impurities, cracks, crevices or lattice imperfections (Silva, 2013). The following section will describe a few of the possible corrosion mechanisms in metal. The described corrosion mechanisms are some of the most common, and they are of interest with regard to stainless steel. The corrosion mechanisms that are discussed in this thesis are the following:

- General / Uniform corrosion
- Pitting corrosion
- Crevice corrosion
- Intergranular corrosion
- Stress corrosion cracking
- Bimetallic/Galvanic corrosion

General / uniform corrosion of metals generally impacts a large part of an exposed surface. This uniform attack is due to local corrosion cell action which means that multiple anodes and cathodes occur on the surface, causing a thin layer of corrosion. Uniform corrosion can result in a significant but predictable loss of section. Laboratory tests are usually sufficient to predict the behaviour, making it a relatively easy corrosion mode to manage (Dillon, 1982).

Regarding stainless steel, general corrosion is usually not an issue since the metal is alloyed with corrosion-resistant elements, see Section 2.5.2. If stainless steel is exposed to a more aggressive environment than it was designed for, general corrosion can still appear. This would be caused by the fact that the content of certain alloys is too low to create a passivating layer, described in Section 2.5, which normally protects the stainless steel from corrosion.

Pitting corrosion is often induced by high relative humidity of the surrounding. It results in a very localized form of corrosion that produces distinct holes in the surface of the material. The produced holes, or pits, are generally quite small in diameter and can be isolated from each other or close together resulting in a rough surface. Pitting corrosion is hard to detect and can occur in all engineering metals and alloys. The potential damage it can cause can be underestimated due to the fact that pitting is sometimes hard to detect in laboratory tests. This is, in turn, caused by the fact that the initiation of the process is difficult to predict as it depends on stochastic variables.

For stainless steel, pitting corrosion can start from a change of environment, late in the service life. If the surface of the steel contains a drop of moisture containing chlorides, the passivity of the steel could be locally diminished, allowing the corrosion process to start. In fact, stainless steel is one of the most sensitive to pitting corrosion, and a high-alloyed steel containing Nickel and Chromium is generally needed to resist this type of corrosion (Dillon, 1982). The pitting corrosion resistance of stainless steel is described further in Section 2.5.6.

Crevice corrosion is similar to pitting corrosion, but it always starts in a crevice, which is a narrow gap or space of some kind. In the gap, crevice corrosion occurs between two metals or between a metal and

a non-metal material. The attack is a result of a concentration cell formed between the electrolyte within the gap, and the electrolyte outside the gap. The electrolyte inside the gap contains lower amounts of oxygen than that of the outside, causing the material within the crevice to act as an anode, while the material on the outside acts a cathode (Dillon, 1982).

In stainless steel, crevice corrosion initiates in the gap where the oxygen content is low, causing the protective oxide film to be unable to reform. The local conditions within the crevice become acid and the corrosion rate accelerates (Callow and Papadakis, 2011).

Intergranular corrosion occurs when grain boundaries or regions are dissolved as a result of potential differences between the grain boundary region and some kind of deposit, intermetallic phase or impurity. The deposits that form on the grain boundaries are often a result of exposure to high temperatures, followed by a cooling period. The deposits can contain a high amount of the alloying elements, causing depletion of the alloying elements in the surrounding matrix (Dillon, 1982).

Stress corrosion cracking is a type of cracking that is caused by the combined effects of a specific corrosive environment together with a tensile stress on the surface. The following three requirements are needed for stress corrosion cracking to be initiated; the metallurgic structure must be susceptible to stress corrosion cracking, the environment must be crack-promoting and the tensile stresses must be larger than a threshold value. Stress corrosion cracking can result in an unforeseen failure under service conditions. It is therefore of great importance to check the susceptibility of the steel, in which the alloy composition is decisive (Dillon, 1982).

Bimetallic/Galvanic corrosion occurs when the metal is coupled to another metal or alloy in the same electrolyte. The following three requirements are needed for the corrosion process to initiate: a common electrolyte, different surface potentials of the materials and a common electrical path. The less noble of the two metals will then be consumed and the more noble stays intact (Dillon, 1982).

Carbon steel is less noble than stainless steel which means that connecting them without an isolating layer would not be advisable as the presence of the stainless steel should increase the corrosion rate of the carbon steel. However, corrosion tests of these materials in concrete have shown a very small rate of galvanic corrosion (Cochrane, 2003), and isolation of the metals is therefore not needed. This is because the metals are both in the passive state while embedded in concrete, a dry, chloride-free environment (Jing and Fang, 2017). For further information on the passivation of metals in concrete, see Section 2.4.1. If chlorides were to penetrate the concrete to the depth of the carbon steel reinforcement, see Section 2.4.2, there is a risk of corrosion of the carbon steel. However, experiments show that no galvanic corrosion occur for the stainless steel grades EN 1.4301, 1.4401, 1.4162 and 1.4462 after two years in carbonated concrete (Sederholm and Almqvist, 2008).

2.4.5 Temperature Dependence of Corrosion

The corrosion process of steel is highly dependent on temperature, which means that an increased temperature usually results in an increased corrosion rate. Initiation of pitting and crevice corrosion of stainless steel are often dependent on temperature, giving a critical corrosion temperature under which corrosion will not initiate (Dillon, 1982).

2.4.6 Damage Due to corrosion

Corrosion of steel rebars results in a loss of steel section which leads to lower load bearing capacity of the structure. However, there is another issue of concern that is usually greater, which is that the corrosion products occupy a larger space than the original steel. This expansion takes place inside the concrete and causes internal stress in the concrete. If these stresses are greater than the tensile stress capacity of the concrete, it can lead to the formation of large cracks and spalling of the concrete surface. This, in turn, leaves the reinforcement fully exposed to an even more aggressive environment which leads to accelerated corrosion (Ziehl and El-Batanouny, 2016). Cracking and spalling of the concrete cover of a bridge deck can be seen in Figure 2.2.

2.4.7 Solutions to Prevent Damage Due to Corrosion

Corrosion of rebars in reinforced concrete is an issue with several possible solutions. They can, however, be divided into three strategies that include:

- Deferring the initiation of corrosion. By delaying the carbonation or chloride ingress in the concrete, the steel can remain in its passive state longer, resulting in a longer service life (Chong *et al.*, 2001). The initiation of corrosion can be deferred either by increasing the density of the concrete or the thickness of the concrete cover, delaying the carbonation or chloride ingress and thus causing the reinforcement to remain passive longer. The process of carbonation and chloride ingress is described in Section 2.4.2.
- Slowing down the rate of corrosion. The use of corrosion resistant steels result in a corrosion rate which is negligible (Chong *et al.*, 2001). By replacing carbon steel with corrosion resistant reinforcing materials, the service life of the structure can be extended without changing the dimensions or properties of the concrete. Examples of such materials are:
  - Galvanized steel
  - Epoxy coated steel
  - Carbon steel with a stainless steel coating
  - Stainless steel

These are metals that are resistant against corrosion. They will corrode eventually but the process is slowed down resulting in a longer service life.

- Use of non-corrosive reinforcing materials, such as fibre reinforced polymers. This means that the desired properties are added to the matrix of the polymer in order to provide high tensile capacities. The polymer can be reinforced with glass-, aramid-, basalt- or carbon fibres among others. The fibres bring different properties to the material, as well as different price, and therefore it is important to differentiate between them.

Mentioned above are several reinforcing options. It is outside the scope of this project to evaluate all of them, but the reader should be aware that multiple options exist. As mentioned in Section 1.5, only stainless steel reinforcement is within the scope of this study.

2.5 Stainless Steel

Stainless steel is a material that has been used successfully in construction for a long time. As mentioned in Section 2.3.3, the main problem in concrete structures is corrosion which causes extensive damage. Unlike carbon steel reinforcement, stainless steel is less sensitive to corrosion and is therefore far superior when considering durability. Stainless steel is a steel alloy containing a minimum chromium content of 10.5 %. It is the presence of chromium which provides the steel with a protective chromium oxide film which increases the corrosion resistance (Markeset *et al.*, 2006). This film covers the surface and is self-healing under right circumstances. If there is not a sufficient amount of oxygen, or if the content of ions, such as chlorides, is too high, the layer will not be able to reform (Callow and Papadakis, 2011).

As an example, a 2100 meter long concrete pier at the port of Progreso in Mexico was constructed using stainless steel reinforcement in 1941. No major maintenance or repair works has been needed, and there has been no corrosion of the reinforcement, despite the harsh marine climate and the low-quality concrete used. As a contrast, a shorter pier was built just 200 meters away in 1972 with carbon steel reinforcement (Markeset *et al.*, 2006). This newer pier is already out of use due to extensive corrosion. Part of the standing Progreso pier and the remains of the newer pier can be seen in Figure 2.3.

Since stainless steel is an alloy, there are many possible configurations. However, they can be sorted into four main groups by their crystalline structure. These structures will be presented in the following section, together with some of their characteristic properties.

Figure 2.3 The remains of the 1972 carbon steel reinforced pier next to Progreso pier constructed with stainless steel in 1941 (Nickel Institute, 2018).

2.5.1 Microstructures

Mechanical properties of stainless steel are characterized by its microstructure. The microstructure has significant impact on the material performance and it is therefore of interest to describe. The estimated stress-strain relationships can be seen in Figure 2.4 for three main microstructures, martensite, austenite, ferrite and duplex, which is a combination of two other.

Martensite is very stiff and strong due to a high content of Carbon. Furthermore, Nitrogen can be added which further enhances the strength (Outokumpu, 2013). This results in a material that is brittle and its resistance against fatigue is poor. Therefore, martensite is not suitable when designing reinforced concrete structures.

Austenite is the most widely used stainless steel. The austentic structure means that it is a surface-based configuration (Nirosta, 2014). The alloy contains Nickel or Nitrogen to ensure the desired properties. The austentic microstructure provides ductile behaviour, non-magnetic properties, good weldability and high corrosion resistance. However, the strength and stiffness is in the lower than for the other microstructures (Markeset *et al.*, 2006).

Ferrite is the third microstructure, which usually has the lowest ultimate strength. The ferretic microstructure is a body-based cubic configuration of iron. To achieve this structure, ferritic stainless steels are alloyed with chromium but usually contain little or no nickel (Nirosta, 2014). This results in a stainless steel with relatively low corrosion resistance (Markeset *et al.*, 2006), but gives a fairly stable price. The strength of ferritic steel is higher than that of austentic, but not as high as that of martensite or duplex steel range.

Duplex (austentic-ferrite) stainless steel has a lattice microstructure which contains ferrite and austentic microstructures in almost equal fractions. This combination of the ferritic and austentic properties provides both high strength and high ductility. The duplex microstucture became commercially available in the 1930s (Liljas and Nilsson, 1999). Duplex steels are rated very high in corrosion resistance and can

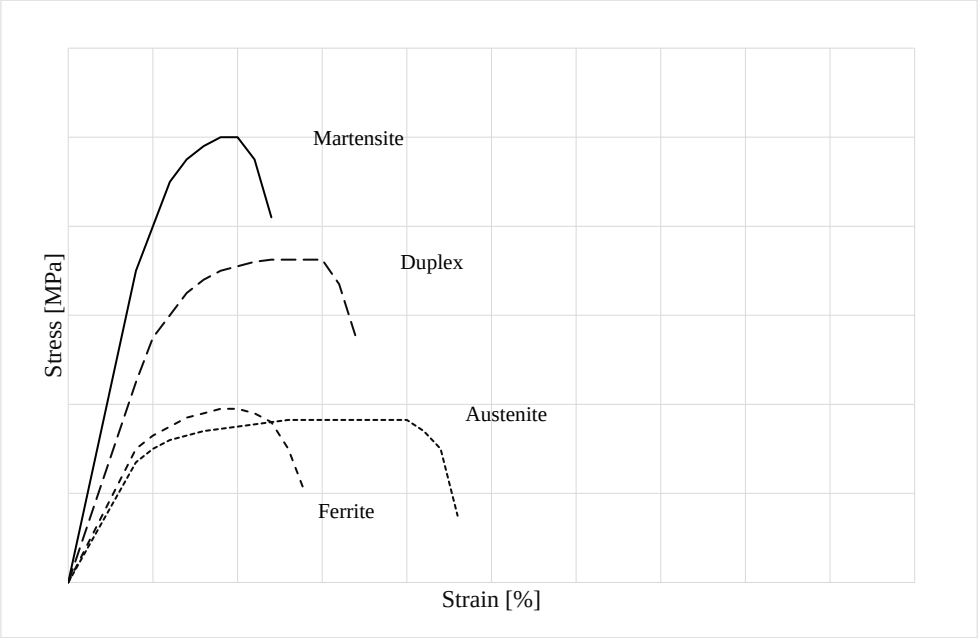

Figure 2.4 Sketch of stress strain relationships for martenstic, austentic, ferrite and duplex steel.

be used in chloride based aggressive environments and in high temperatures. The price of duplex steel varies with the price of its alloying elements.

In order to make duplex steel less sensitive to price changes, a material called lean duplex has been developed. It usually has a very low nickel content making it cheaper to produce than regular duplex steel while still maintaining the high corrosion resistance of the austentic-ferrite crystalline structure. The corrosion resistance of the duplex steel can be measured by the PREN-number, for a definition of PREN, see Section 2.5.6. Table 2.3 shows the classification of duplex steel grades according to PREN-number

Table 2.3 PREN classification of duplex stainless steels.

Classification	**Name**	**PREN-number**
Low-alloyed	Lean duplex	< 32
Intermediate	Duplex	32 - 39
High-alloyed	Super duplex	> 39

2.5.2 Alloying Elements

Stainless steel is an alloy of elements which influence the price as well as the mechanical and chemical properties of the steel. The properties of the steel is a consequence of the alloying elements in combination with heat treatment during production and the impurities contained in the material. The alloying elements can be classified by the microstructure they promote, ferrite or austenite. This section aims to describe the alloying elements that are common in the production of stainless steel. The properties of a certain steel grade can then be predicted by Nickel- or Chromium equivalents (Outokumpu, 2013), given by Equation 2.1 and 2.2

$$NickelEquivalent = \%Ni + 0,5 \cdot \%Mn + 30 \cdot (\%C + \%N) \tag{2.1}$$

$$ChromiumEquivalent = \%Cr + \%Mo + 1,5 \cdot \%Si + 0,5 \cdot \%Nb \tag{2.2}$$

The Equations describe the Nickel- and Chromium Equivalent and these numbers can be used to describe a duplex steel since Nickel contributes to an austentic structure while Chromium promotes a ferritic structure. The austenite and the ferrite structures are described in Section 2.5.1. There are many possible alloys that can be used in stainless steel. The most important ones that are commonly used in the production of stainless steel today are shorty described below.

Chromium (Cr) is, as previously mentioned, what provides the steel with a passive layer protecting it against corrosion. This protective film is invisible and very thin. It reduces the corrosion rate to a negligible amount. This is therefore the most important alloy, and the minimum content, which allows the film to form is about 10,5 %. An increased chromium content gives a higher corrosion resistance, higher resistance to oxidation at high temperatures and benefits a ferritic microstructure (Davis, 2001).

Nickel (Ni), as opposed to Chromium, contributes to an austentic microstructure, increases ductility and toughness while reducing the corrosion rate. Nickel is a very advantageous alloy, except for the fact that the price is generally quite high it is sensitive to price fluctuations. To exemplify, a shortage of nickel during the 20th century caused civil wars in Africa and Asia (Liljas and Nilsson, 1999).

Nitrogen (N) is always present in stainless steel. Earlier it was considered as an impurity and its impact was therefore not studied further. The investigation of the effect of nitrogen on the structure was investigated in the early 1930s when early pioneers saw a possibility for Nitrogen to replace Nickel. It has been shown that Nitrogen increases the strength, promotes an austentic structure while also increasing the corrosion resistance. A high Nitrogen content can give a 50-100% increase of strength, when compared to a normal austentic stainless steel, this while still maintaining the high ductility which characterizes the austentic steels (Liljas and Nilsson, 1999).

Molybdenum (Mo) enhances the resistance against localized and uniform corrosion. It also promotes a ferritic microstructure and increases the mechanical strength. Molybdenum ferritic stainless steels show a good corrosion resistance and surface appearance after long term exposure to marine climates. However, austentic steels alloyed with Molybdenum have some of the lowest corrosion resistance compared with the austentic steels not containing Molybdenum. Similar to Nickel, Molybdenum is an element that is quite costly and a high Molybdenum content will result in an expensive steel (Liljas and Nilsson, 1999).

Carbon (C) strongly promotes an austentic structure. It contributes to high mechanical strength, but also reduces the resistance to intergranular corrosion, which was an issue for early stainless steels. In stainless steel today, the carbon content is kept low to avoid this type of corrosion (Outokumpu, 2013).

Manganese (Mn) has a varying impact on the microstructure, depending on the temperature. Low temperatures promote an austentic structure and high temperatures a ferrite structure (Outokumpu, 2013).

Silicon (Si) is a ferrite stabilizer which is often added to stainless steels in order to enhance the resistance against oxidation (Cunat, 2004). It also improves the mechanical strength (Outokumpu, 2013).

Titanium (Ti) is the most commonly used stabilizing element for stainless steel. It also increases the resistance to pitting corrosion (Cunat, 2004). Titanium is added to austentic steels with high carbon content in order to increase the resistance to intergranular corrosion and increase the mechanical properties at high temperatures. In ferretic steels, it is added to boost the corrosion resistance, toughness and formability (Outokumpu, 2013).

Tungsten (W) is an impurity in most stainless steel, but it can also be added to improve pitting corrosion resistance (Outokumpu, 2013).

Niobium (Nb) reduces the risk of intergranular corrosion in case of high temperatures (Cunat, 2004). It also increases the mechanical strength at high temperatures and it is a ferrite former (Outokumpu, 2013).

2.5.3 Mechanical Strength

The mechanical strength of stainless steel depends on the microstructure and alloying elements, as described in previous sections. Most of the stainless steels used in construction exhibits a similar or even higher mechanical strength than carbon steel.

As opposed to carbon steel, stainless steel usually does not show a pronounced yield point, the stress strain curve shows a distinctly non-linear behaviour, as opposed to that of carbon steel, which can be simplified to a bi-linear relationship. This means that it is hard to define a yield stress for stainless steel. Instead, another method has been developed to determine the mechanical strength of a specific steel grade. This is called the proof strength, and it usually refers to the 0.2 proof strength, which measures the stress at 0.2 % plastic elongation. The proof strength can be defined for any elongation, but 0.2 % is the most common one.

To design a structure using stainless steel reinforcement, it is necessary to approximate the stress strain relationship. A possible method to use is to define the Ramberg-Osgood curve using four parameters: E_0, σ_0, α and n (Pajari, 2011). The expression can be seen in Equation 2.3. The Ramberg-Osgood curve can be seen in comparison with the bi-linear curve, used for design with carbon steel, in Figure 2.5. Design using stainless steel also requires a partial factor for the material. If the design is according to Eurocode 2, the standard procedure can be applied, using the recommended national value for steel, e.g. $\gamma_{steel} = 1,15$ (Pajari, 2011).

$$\varepsilon = \frac{\sigma}{E_0} + \alpha \frac{\sigma_0}{E_0} (\frac{\sigma}{\sigma_0})^n \tag{2.3}$$

where ε is the strain, E_0 refers to the modulus of elasticity at the proof stress, σ_0 refers to the proof stress, α defines the ratio between plastic and elastic deformation, while n determines the strain hardening rate.

2.5.4 Fatigue Strength

The fatigue strength of stainless steel is similar to that of carbon steel. When the steel is used as reinforcement, the critical issue for fatigue is normally the corrosion. Since the corrosion resistance of stainless steel is much greater than that of carbon steel, it would mean that the fatigue strength of stainless steel reinforcement is also increased when two steels of similar mechanical strengths are compared. This is because the fatigue limit is related to the tensile strength of the steel (Markeset *et al.*, 2006).

2.5.5 Thermal Properties

Traditional carbon steel shows a loss of strength at high temperatures (over 500 °C) and are therefore vulnerable to fire exposure. Stainless steel, especially austentic, show greater resistance to higher temperatures and are therefore often used in situations where high temperatures are expected. Carbon steel also shows a loss of ductility when exposed to low temperatures, and most carbon steels have a very brittle behaviour below -20 °C. Contrarily, austentic steels maintain their ductility even in very low temperatures.

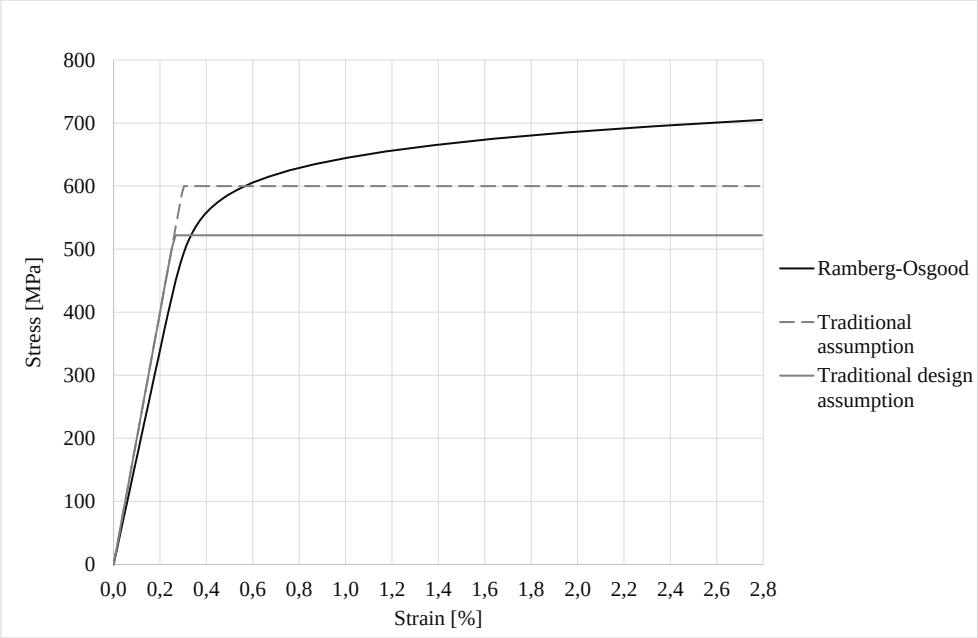

Figure 2.5 Bi-linear curve approach of carbon steel as used in Eurocode 2 in comparison with measured curve for stainless steel.

Although stainless steel shows excellent thermal properties when compared to carbon steel, problems can arise when it is used as reinforcement in concrete. As mentioned in Section 2.3.1, carbon steel and concrete have a very similar coefficient of thermal expansion which is not always the case for stainless steel. The austentic range has a thermal expansion coefficients can be seen in Table 2.4. The difference is not so great as to become a serious problem when designing with stainless steel reinforcement, but it should be noted that internal stresses may arise (Markeset *et al.*, 2006).

Table 2.4 Thermal expansion coefficients for reinforcing steels.

Reinforcement type	**Coefficient of thermal expansion**
Austentic	$16 \cdot 10^{-6}/°C$
Duplex	$13 \cdot 10^{-6}/°C$
Carbon	$12 \cdot 10^{-6}/°C$

2.5.6 Corrosion Resistance of Stainless Steel

As mentioned in Section 2.3.3, corrosion of steel rebars is a major cause for deterioration of reinforced concrete structures. Stainless steel reinforcement can be used to avoid this to some extent. However, no stainless steel is truly stainless but the corrosion rate is slowed down to a great extent. The corrosion rate of stainless steel depends on the alloying elements described in Section 2.5.2. Since the alloying elements also have a great impact on the price of the steel, it is important to choose a steel grade with a corrosion resistance that is appropriate to use in the designated environment. Stainless steel is not sensitive to all kinds of corrosion described in Section 2.4.4. Corrosion in stainless steel is generally caused by pitting or crevice corrosion. Therefore, the PREN-number method to determine the corrosion resistance of stainless steel has been developed. PREN stands for *Pitting Resistance Equivalent Number* and describes the resistance against pitting corrosion. A higher number indicates a better resistance against corrosion. The number is calculated using one of the equations below, depending on the microstructure of the steel (Markeset *et al.*, 2006). If the microstructure is austentic, Equation 2.4 should be used. Equation 2.5 should be used for duplex steels and Equation 2.6 if the duplex steel is alloyed with Tungsten.

$$PREN_{austentic} = \%Cr + 3,3 \cdot \%Mo + 30 \cdot \%N \tag{2.4}$$

$$PREN_{duplex} = \%Cr + 3,3 \cdot \%Mo + 16 \cdot \%N \tag{2.5}$$

$$PREN_{duplex_{W+N}} = \%Cr + 3,3 \cdot (\%Mo + 0,5 \cdot \%W) + 16 \cdot \%N \tag{2.6}$$

where % Cr is the Chromium content in percent, % Mo is the Molybdenum content in percent, % N is the Nitrogen content in percent and % W is the Tungsten content in percent.

2.5.7 Cost, Availability and Sustainability

The price of stainless steel is approximately 6 times higher than that of carbon steel. The difference in price is due to the fact that some of the alloying elements commonly used in stainless steel, see Section 2.5.2, are scarce or difficult to extract, making them more expensive. The price of the stainless steel rebars that will be presented in this study is approximately 3400-4500 USD/ton, which can be seen in Table 4.4.

Regarding the availability of stainless steel, it is generally good. However, if comparing with carbon steel reinforcement it is inferior. This is especially the case for certain stainless steel grades that are not common and long supply times could therefore be expected.

Considering the sustainability of stainless steel, it is also highly dependent on the alloying elements. The alloy which makes the steel stainless, Chromium, is the 13th most common element in the earths crust with a concentration of 400 ppm. At the present rate of consumption, Chromium reserves are predicted to last several centuries. Concerning the more expensive alloying elements, Nickel and Molybdenum, they are the 24th and 38th most abundant elements, making them significantly more scarce with a concentration of only 80 and 15 ppm in the earth crust (Cunat, 2004).

Stainless steel has a slightly larger environmental impact than carbon steel reinforcement when initial construction is concerned. However, this is compensated by a longer service life, requiring less maintenance and repair. At end of life, stainless steel rebars can be recycled at a recovery rate of 90 % (Mistry *et al.*, 2016).

2.5.8 Steel Grades

The chemical composition of a stainless steel is classified according to microstructure and alloying elements. Methods for classification vary in different parts of the world, but in 1995, a European standard was released. This section will describe how the EN- classification is made. This system uses both a material number and a material name to identify the chemical composition (Markeset *et al.*, 2006).

To explain this system, the following example is used:

- **Material number: 1.4462**
  - Where 1 denotes a steel material
  - 44 denotes a group of stainless steels
  - 62 is the identification number of a specific material
- **Material name: X2CrNiMoN22-5-3**
  - X means that it is a high alloy steel.
  - 2 represents the 100 times the carbon content in percent, meaning that the carbon content is 0,02% in this case.
  - CrNiMo are the main alloying elements and the numbers that follow is their nominal content in percent.

2.6 Stainless Steel Reinforcement

Stainless steel combines exceptional durability with high strength, aesthetics and ductility, making it suitable for many applications in construction and especially in reinforced concrete structures. As stated in the beginning of Section 2.5, the use of stainless steel as reinforcement is not a new occurrence as the first usage dates back to the late 30's (BSSA, 2003). Although, during recent years the usage and research has significantly increased. As there are a great number of variations of stainless steel, this Section will describe those that are suitable to use as reinforcement in concrete and how stainless steel reinforcement is used in construction today.

Even though stainless steel exhibits excellent properties with regard to strength, durability and ductility, the main disadvantage is the high cost. As mentioned in Section 2.5.2, stainless steels with high contents of Nickel and Molybdenum are very costly and thus, the price is highly dependent of the alloying elements. However, there are some different ways to deal with this high material cost. One solution would be to only use stainless steel reinforcement in the areas of the construction which are more exposed to harsh environments and thus limiting the material usage. Another solution would be to use less expensive alloys, making it more economically affordable. In the latter case, stainless steels with low Nickel content would be suitable. Consequently, lean duplex is presented as a suitable alternative with very low Nickel content while maintaining very high corrosion resistance.

2.6.1 Corrosion Behaviour in Concrete

Research show that the corrosion resistance of stainless steel reinforcement in concrete differs somewhat from that used in other applications. This means that the PREN-number described in Section 2.5.6 does not transfer directly to reinforcement bars. This is due to the fact that the formulae were developed for high-alloyed stainless steels in neutral or acidic environments, and not for the high pH environment present in concrete (Van Niejenhuis *et al.*, 2016).

Additional PREN-formulae have been developed in order to give a more realistic corrosion resistance of the low-alloyed range, where also the Manganese content has been added. This formulae gives a more realistic value. However, it is not adjusted to reflect the high-pH environment in the surrounding concrete (Van Niejenhuis *et al.*, 2016). The modified equations can be seen in Equations 2.7 and 2.8.

$$PREN_{austentic} = \%Cr + 3,3 \cdot \%Mo + 16 \cdot \%N - \%Mn \tag{2.7}$$

$$PREN_{duplex} = \%Cr + 3,3 \cdot \%Mo + 30 \cdot \%N - \%Mn \tag{2.8}$$

where % Cr is the Chromium content in percent, % Mo is the Molybdenum content in percent, % N is the Nitrogen content in percent and % Mn is the Manganese content in percent.

In recent years, research has been undertaken in order to evaluate the behaviour of stainless steel reinforcement in cracked concrete. Research show that no stainless steel is truly stainless, and will be sensitive to corrosion in harsh environments. On the other hand, it is very difficult to estimate the environment in cracked concrete structures exposed to chloride solutions.

This section aims to describe possible risks of using stainless steel reinforcement in cracked concrete structures. Corrosion of stainless steel reinforcement embedded in cracked concrete varies under several different parameters, such as:

- Alloying elements of the steel
- Ribbed area of the rebar
- Surface treatment of the rebar
- Concrete cover thickness
- Concrete crack width
- Chemical composition of concrete
- Chloride content of solution
- Method of exposure to chloride containing solution.
- Surrounding temperature
- Direction of crack in relation to rebar

In order to better understand the influencing factors and to make an informed decision when choosing steel quality, two research papers will be summarized, explaining the results of the tests shortly. First, a recent research project, published in 2016 will be presented. The second example is an article published in 2011.

Submersion in a de-icing solution containing 21% Cl

A research project was undertaken in Canada, where different commercially available stainless- and carbon steel reinforcing bars were embedded in concrete samples, to simulate bridge decks. The different concrete samples were then cracked longitudinally and transversely to give a realistic exposure environment of the reinforcing bars. The samples where then exposed to a de-icing solution used in Ontario, Canada, containing 21% Cl. The samples were immersed in the salt solution for more than 2 years in a temperature of 20-25 °C. By the end of the test, all of the samples showed signs of corrosion. However, the corrosion of the stainless steel was significantly smaller than that of the carbon steel. (Van Niejenhuis *et al.*, 2016) The results of the tests can be seen in Table 2.5.

Table 2.5 Corrosion of stainless steel reinforcement, test 1, conducted with a 21 % Cl solution, using no additional surface treatment of the rebars. $w_{k.max.m}$ is the maximum average crack width of the concrete samples.

UNS	EN	Microstructure	PREN	Ranking		$w_{k.max.m}$ [mm]	
				trans.	long.	trans.	long.
S32205	1.4462	Duplex	33.5	1st	1st	0.43	0.23
S32304	1.4362	Duplex	23.6	2nd	3rd	0.45	0.40
S32101	1.4162	Lean duplex	20.6	3rd	2nd	0.40	0.33
S30403	1.4306	Austentic	20.9	4th	4th	0.53	0.30
S31653	1.4406	Austentic	27.7	6th	6th	0.40	0.53

Ponding with a de-icing solution containing Cl

The rebars used in this corrosion test were pickled, which is a surface treatment performed to remove impurities and thus increasing the corrosion resistance. The bars were first commercially pickled and then again in the laboratory to ensure that impurities were removed. Two test procedures were carried out, one where chlorides were added to the concrete mix and another where the reinforced concrete was ponded with a chloride solution. The concrete cover was 10 mm, and no cracks were induced in the concrete samples. Corrosion was measured at different chloride contents, up to 8%. The concrete was left to dry in 20°C and 90 % RH. Some of the results of the ponding test can be seen in Table 2.6.

The study also showed that the PREN is not a good indicator when stainless steel reinforcement is chosen. The duplex stainless steels 1.4362 and 1.4162 both have a higher PREN-value than the austenitic steels 1.4311 and 1.4406, but the duplex steels showed a lower corrosion resistance than the austenitic (Bertolini and Gastaldi, 2011),

Table 2.6 Corrosion of stainless steel reinforcement, test 2, using pickling of rebars, both commercially and in the laborory, as surface treatment

EN grade	Microstructure	PREN	Corrosion	Ranking
1.4406	Austentic	28	None at 8% Cl	1st
1.4362	Duplex	26	Initiated at 5% Cl	2nd
1.4311	Austentic	21	Initiated at 5% Cl	3rd
1.4162	Lean duplex	26	Initiated at 3% Cl	4th

2.6.2 Bond-Slip Behaviour

Stainless steel rebars can be manufactured with the ribs as ordinary carbon steel reinforcement. Although the rib area is the most influential parameter when evaluating bond-slip behaviour, tests show that

stainless steel rebars have a slightly lower bond stiffness than the carbon steel rebars. This can be due to the presence of the oxide layer, which can interfere with the mechanical interlock of the steel and concrete (Moen and Sharp, 2016). However, this is not an issue in design, meaning that the same anchorage length can be assumed (Markeset *et al.*, 2006).

2.6.3 Using Stainless Steel Rebars in Construction

When using stainless steel rebars in construction, some care has to be taken in order to protect the steel from corrosion. First, all tools used to cut and shape the rebars must also be of stainless steel. This is due to the fact that the carbon steel can contaminate the stainless steel, causing the corrosion resistance to be diminished.

Secondly, even though most types of welding can be carried out when using stainless steel, care has to be taken to clean the surface of the weld. The welding of the steel causes chromium to oxidize and the passivation layer to thicken. This can lead to chromium depletion of the steel layer underneath. As long as the chromium depleted layer, which can be seen as a dark tint surrounding the weld, is removed, the passivizing layer can be reformed. Another issue concerning welding is the risk of spatter and other irregularities. The irregularities can cause pitting corrosion and initiate fatigue cracks, and therefore they have to be removed.

3 Repair of Reinforced Concrete Bridges

This chapter aims to investigate the repairs which are carried out on reinforced concrete structures of similar size to those used as case studies in the following chapters. A total of six bridges are presented, for which the repair costs are obtained from the Swedish bridge and tunnel management system; BaTMan. BaTMan is a data-base where information concerning the bridges and tunnels in Sweden is collected, such as bridge type, material, year of construction, inspections, damages and repairs. The cost of repairs forms a comparison to the repair cost estimated in the LCC analysis of case study 2, see Section 7.4. The components which were damaged to to corrosion of reinforcement will be redesigned using stainless steel in the same case study, see Section 5.2.

This chapter presents data obtained from BaTMan, where repair and/or maintenance work have been required. The costs that are mentioned are the total costs of the latest repair-package which has been awarded to a contractor, and thus not the total repair costs over the service life of the structure, due to the fact that the total maintenance costs were not available in BaTMan.

3.1 Slab-Frame Bridge over Glasholmaån

Constructed in year 1954, this slab-frame bridge is a part of road 570, with a speed limit of 90 km/h and an average daily traffic (ADT) of 1000 vehicles/day, located in the municipality of Torsås in Kalmar. The bridge, which has a span of 4,4 meters and a width of 7,5 meters, crosses a small river, Glasholmaån. The construction number is 8-381-1 in the Swedish BaTMan system and can be seen in Figure 3.1.

Figure 3.1 Bridge over Glasholmaån in Torsås (Trafikverket, 2018).

In 2003, repairs amounting to 948 000 SEK were carried out on the bridge by the contractor Vägverket Produktion, 49 years after the bridge was constructed. The package included replacement of the edge beams, removal of the steel profiles on the edge beams and replacement of the railings and surfacing.

The damages that were repaired included;

- Leaching of concrete in edge beams
- Corrosion of steel in edge beams

3.2 Slab Bridge over Industrial Track in Oskarshamn

The bridge, see Figure 3.2, is located in Vånevik in the municipality of Oskarshamn in Kalmar. This simply supported slab bridge was constructed in 1934 using carbon steel reinforced concrete. It provides a crossing for road 650 over an industrial railway track and has a width of 7 meters and a length of 6 meters. The road has a speed limit of 70 km/h and an ADT of 1100 vehicles/day. The bridge can be seen in Figure 3.2 and has construction number 8-121-1 in BaTMan. A repair-package was carried out in

Figure 3.2 Bridge over railway track in Oskarshamn (Trafikverket, 2018).

2009 by the contractor TGM, 73 years after the bridge was built. The cost of the repairs amounted to 107 000 SEK. The package included repair of concrete using sprayed concrete on the front and wing walls due to damages;

- Corrosion of reinforcement in front walls
- Corrosion of reinforcement in wing walls

Earlier repairs were carried out in 1995, 61 years after the inauguration of the bridge. These repairs included repair of bridge deck using spray concrete, replacement and impregnation of edge beams, as well as replacement of railings and surfacing. Unfortunately, the costs of these repairs are unknown.

3.3 Slab Bridge over the River Närvaån in Mönsterås

This slab-bridge was constructed in 1924 and forms a crossing for road 602 over the stream Närvaån in the municipality of Mönsterås in Kalmar. The speed limit on the road is 70 km/h and the ADT is approximately 500 vehicles/day. The bridge is 6,2 meters long, 7 meters wide and is constructed in carbon steel reinforced concrete. The bridge has construction number 8-129-1 in the Swedish BaTMan system and can be seen in Figure 3.3.

Figure 3.3 Bridge over Närvaån in Mönsterås (Trafikverket, 2018).

A major repair-package was carried out in 1996 by the contractor SIAB, 72 years after the bridge was constructed. The cost of the repairs amounted to 1 385 000 SEK. The package included replacement of the superstructure of the bridge due to damages. These damages included;

- Corrosion of reinforcement in beams
- Leaching of concrete in bridge deck
- Corrosion of reinforcement in bridge deck
- Corrosion of reinforcement in edge beams
- Corrosion of steel on edge beams
- Damages to surfacing
- Corrosion of steel in parapets/railings

3.4 Slab-Frame Bridge over Strait in Västervik

This slab-frame bridge was constructed in 1950 using carbon steel reinforced concrete. The bridge provides a crossing for road 799 over a strait in the municipality of Västervik in Kalmar. The width of the bridge is 6 meters and the length is 5,4 meters. It has construction number 8-247-1 in the Swedish BaTMan system and can be seen in Figure 3.4. The ADT on the bridge is around 300 vehicles/day and the speed limit is 70 km/h.

Figure 3.4 Bridge over strait in Västervik (Trafikverket, 2018).

The latest repairs on the bridge were carried out in 2015 by the contractor TGM, 65 years after the bridge was constructed. The cost of the repairs amounted to 1 160 000 SEK. The package included replacement and impregnation of the edge beams, replacement of railings as well as repair of the front and wing walls. The damages that were repaired included;

- Leaching of concrete in wing- and front walls
- Corrosion of reinforcement in edge beams

3.5 Slab-Frame Bridge over the River Lillån

The bridge over Lillån, which can be seen in Figure 3.5 is located in the municipality of Karlskrona in Blekinge and forms a crossing for road 726 over the small river Lillån. The ADT is 1200 vehicles/day, with a speed limit of 70 km/h. The bridge is 4,5 meters long and 4,9 meters wide and was constructed in 1935 using carbon steel reinforced concrete. In BaTMan, it has construction number 10-10-1.

Figure 3.5 Bridge over Lillån in Karlskrona (Trafikverket, 2018).

The edge beams and surfacing of the bridge was replaced in 2005, 70 years after the year of construction. The repairs were carried out by the contractor Vägverket Produktion. The total cost of the repair amounted to 680 000 SEK. The damages that were repaired included;

- Leaching of concrete in edge beams

3.6 Slab Bridge over Pedestrian Walkway in Oskarshamn

This bridge, which can be seen in Figure 3.6 is 3,15 meters long and 17,9 meters long. The bridge forms a safe crossing for the road 37, which has an ADT of around 10 000 vehicles/day and a speed limit of 70 km/h, over a pedestrian walkway. It was constructed in 1965, has construction number 8-761-1 in BaTMan and it is located in the municipality of Oskarshamn in Kalmar, Sweden.

In 2012, 47 years after the bridge was constructed, substantial repairs amounting to 990 000 SEK were made on the bridge by the contractor Svevia. These repairs included protecting the front wall and bridge deck from carbonation, repair of concrete in the front- and wing walls, as well as in the bridge deck. The repairs also included replacing the surfacing and railings on the bridge. These repairs were required due to the following damages;

- Concrete spalling in the front walls
- Concrete spalling in the bridge deck
- Concrete spalling in the wing walls

Figure 3.6 Bridge over walk- and bike path in Oskarshamn (Trafikverket, 2018).

- Concrete spalling in parapets/railings
- Leaching of concrete in wing walls
- Leaching of concrete in bridge deck
- Corrosion of steel in railings

3.7 Summary of Bridge Repairs

This section summarizes the findings in BaTMan presented in the previous sections. However, it can be hard to draw any conclusions given the number and size of the studied bridges. Table 3.1 provides a short summary of the studied repairs. It should be noted that the extent of the repair can vary between the studied cases, and that there may have been previous repairs which are not included in the table below.

Table 3.1 The bridge area is given as an indicator of the size of the bridge. The repaired components are abbreviated as follows; EB- edge beams, R - railings, S - surfacing, D - bridge deck, FW - front walls WW - wing walls.

Bridge	**Construction nr.**	**Bridge area** [m^2]	**Year of repair**	**Repaired components**	**Cost** [kSEK]
Glasholmaån	8-381-1	33	49	EB, R, S	948
Railway track	8-121-1	42	73	FW, WW	107
Närvaån	8-129-1	43	72	EB, R, D, S	1 385
Västervik	8-247-1	32	65	EB, R, FW, WW	1 160
Lillån	10-10-1	22	70	EB, S	680
Walkway	8-761-1	56	47	EB, R, S, FW, WW, D	990

4 Implementation of Stainless Steel Rebars in Bridges

In this study, the focus lies on how stainless steel rebars can be arranged in a bridge design to improve its durability in several ways. Therefore, it is of interest to present existing guidelines and design codes for stainless steel rebars. What is also of interest is to present and evaluate on-going projects, as well as already built structures and thus increase the knowledge of how to successfully implement stainless steel in bridge design. In order to get a better idea of the problem, this chapter presents the implementation of stainless steel in either concrete bridge structures, or concrete structures that are representative within the scope of this study, from different places of the world.

4.1 Guidance on the Use of Stainless Steel Reinforcement

Stainless steel reinforcement is a relatively new material when considering widespread use in concrete structures and thus, guidance on the use of stainless steel rebars is limited. The structures can be designed in accordance with Eurocode 2, but there are some disadvantages to this method which are described in the following section. Regarding design codes specifically oriented towards stainless steel reinforcement, the authoritative guidance is almost unexisting. However, some guidance can be found. In this section, different design methods will be presented.

4.1.1 Design According to Eurocode 2

Generally, design using stainless steel rebars in concrete structures has been carried out with the use of design rules developed for reinforced concrete structures with carbon steel reinforcement according to Eurocode 2. Therefore, this method uses the bi-linear stress-strain relationship for carbon steel instead of the non-linear stress-strain relationship for stainless steel. This may result in some uncertainties, which could lead to both uneconomical and unsafe designs (Pajari, 2011).

In fact, when replacing the non-linear stress-strain relationship of a stainless steel with a bi-linear one, as described in Eurocode 2, the potential of the material can be lost when high stresses are developed. Controversially, at low stress levels, the bi-linear method can result in an unsafe design as a consequence of an overly conservative safety factor on the first part of the stress-strain curve. However, in light or medium reinforced beams or slabs, the strength of the stainless steel could be exploited by using sucha simplification. This is especially the case in bridges where deflection control is designing, resulting in deeper concrete sections than what would be required to resist the bending moment (Pajari, 2011).

What is deemed obvious is that new design rules are needed for stainless steel in order to fully exploit the benefits of the material. By replacing the bi-linear stress-strain relationship used today by a non-linear one, stainless steel would be more effective in almost all practical applications and especially, the amount of stainless steel rebars could be lowered by offering similar mechanical resistance (Pajari, 2011).

4.1.2 Design Manual, The Highway Agency, UK

In the UK, the first official guidance for using of stainless steel rebars in concrete structures was released in 2002. This design manual was specifically oriented towards highway structures and specially to parts of structures exposed to corrosive environments. This could, however, easily be extended to other types of structures exposed to corrosive environments.

Locations to Implement Stainless Steel Reinforcement
Guidance is given to which locations in the structure that are appropriate to replace with stainless steel reinforcement. This could, for example, be bridge decks carrying heavy traffic, exposed piers and columns and deck slabs where access is limited (The Highways Agency, 2002). It is also recommended to have stainless steel reinforcement in areas exposed to seawater and especially in the splash zones. This is also the case for structural elements exposed to de-icing salts, as for example edge beams. However, the use of stainless steel should be limited to parts where repair would cause excessive traffic disturbance.

Relaxations of Durability Requirements
Design with stainless steel reinforcement allows some relaxation in durability requirements, compared to carbon steel, which can be seen in Table 4.1. This is regardless of the exposure condition and the concrete quality used.

Table 4.1 Relaxations of durability requirements with stainless steel.

Design condition	Relaxation [mm]
Cover thickness	30
Maximum allowable crack width	0.3

Choice of Stainless Steel Rebar Type
Depending on the different exposure conditions that can occur in a highway structure, this guide describes where to use which kind of stainless steel depending on the type of structural element. This can be seen in Table 4.2

Table 4.2 Type of stainless steel grade depending on exposure condition.

Exposure Condition	EN grade
Embedded in concrete with normal exposure, substructures, edge beams, diaphragm walls and joints	1.4301
Where additional relaxation is needed, when waterproofing cant be guaranteed	1.4436
Direct exposure to chlorides, components that extrude from the concrete	1.4436, 1.4429
Need for higher strength and durability, specific structural requirements	1.4462, 1.4429

Strength
This guide is based on the use of stainless steel with strength grade 500, which material properties is equivalent of grade 460S structural steel (The Highways Agency, 2002). However, there is guidance as well on the usage of strength grade 650 and 200.

If cathodic protection or electrochemical chloride extraction is used, the strength grade of 650 could suffer from hydrogen embrittlement, causing the steel to get a more brittle behaviour. This is why strength grade 500 is preferred (The Highways Agency, 2002).

Fatigue Behaviour
In this design manual, it is assumed that the fatigue performance of stainless steel is equivalent to that of ordinary carbon steel and that the requirements for fatigue testing is also the same (The Highways Agency, 2002). This means that stainless steel, when regarding fatigue performance, should be designed in the same way.

Fixing, Anchorage and Welding
When regarding fixing and anchorage of stainless steel reinforcement, it is assumed that the same applies as for carbon steel reinforcement. However, welding of stainless steel reinforcement is not recommended. This is because of the effect it has on the psychical characteristics (The Highways Agency, 2002).

4.1.3 Guidance, Nordic Innovation Centre

The main reason behind the limited use of stainless steel reinforcement is high investment costs and lack of design codes. In order to encourage the use of stainless steel, Nordic Innovation Centre was formed in 2004. This led to the start of a project called *"Corrosion resistant steel reinforcement in concrete structures (NonCor)"*. Participants of the project are, among others, Norwegian Public Roads Administration, Veidekke, COWI, Danish Road Directorate, Strängbetong and the Swedish Road Administration

(Markeset *et al.*, 2006). The driving force in this project was the Norwegian Building Research Institute. The guide was released in 2006.

The idea behind the guide was to increase durability in concrete structures by eliminating corrosion by focusing on the problem itself, which is the reinforcement. The idea behind the guide was also to promote use of stainless steel by reducing the gap between theoretical knowledge and application.

4.2 Examples of Stainless Steel Rebars in Bridges

One example of a successful stainless steel reinforced concrete structure is, as mentioned in Section 2.5, the Progreso pier in Mexico. However, since then there has been a number of other different successful projects using stainless steel reinforcement, which will be described in this section.

4.2.1 Junction Värtan, Stockholm

In Stockholm, the Värtan junction, see Figure 4.1, was built in 2015 as part of the Norra Länken project, which is Sweden's largest road construction project to date. The idea behind the project of junction Värtan was that it should be largely maintenance free for a very long time. Since roads in northern climates are exposed to very corrosive environments, stainless steel was used. In this case, an austenitic stainless steel of grade EN 1.4404 (ASTM 316) was first chosen (Outukumpu, 2017). However, following the advice of the finnish stainless steel manufacturer Outukumpu, a low-alloyed, lean duplex, stainless steel was chosen instead, LDX 2101, which is equivalent to EN 1.4162. The main reason behind this was the financial aspect, as a stainless steel with a low nickel content is much more cost efficient and suffer less from fluctuations in nickel price. In this project, 12 mm in diameter, ribbed rebars of type LDX 2101 from Outukumpu were used and the approximate amount of stainless steel was 300 tons (Outukumpu, 2017).

Figure 4.1 The Värtan junction in Stockholm, using lean duplex EN 1.4162 (Trafikverket, 2014).

4.2.2 Broadmeadow Bridge, Dublin

Broadmeadow bridge, see Figure 4.2, is located in North Fingal in Ireland and carries the M1 Motorway over the Broadmeadow Eastuary and was completed in June 2003. In order to prolong the service life of the bridge, the pier stems were designed using 316L stainless steel rebars, which is an austentic stainless steel equal to EN 1.4435. The reason behind this was that the piers were exposed to chloride and sulphate conditions and thus requiring attention to fulfill long term durability. In addition to this, the mudflats where the piers were located in made future inspections difficult and therefore assurance was needed to avoid corrosion of the steel. However, stainless steel, at the time, cost six times as much as normal carbon steel (Caffrey, 2003). Apart from the cost, another disadvantage was the long supply time required to have stainless steel delivered on site and it could take up to 12 weeks to have large diameter bars delivered, causing problems for the contractor. The amount of stainless steel reinforcement used in this bridge was approximated to 105 tons. In comparison, the amount of normal carbon steel reinforcement used was 1450 tons (Caffrey, 2003).

Figure 4.2 Broadmeadow bridge in Ireland, with pier steams and columns reinforced with stainless steel rebars (CBDG, n.d).

4.2.3 Hong Kong–Zhuhai–Macau Bridge

The Hong Kong-Zhuhai-Macau bridge is an ongoing project that started in 2009 which will link Hong Kong with Macau and the city of Zhuhai in China with a 29.6km long bridge over the Pearl River. The estimated cost of the project is 10.6 billion US dollars and the service life of the bridge is 120 years. Because of the intended service life and the difficulty to repair the bridge, duplex stainless steel grade EN 1.4362 was chosen. 1.4362 is a lean duplex stainless steel and it was deemed appropriate both because of durability reasons, but also because of its cost efficiency (Jing and Fang, 2017). The total amount of

stainless steel rebars in this project is estimated up to 15000 tons and is mostly made up of 10 to 32 mm, in diameter, ribbed rebars.

In this bridge, stainless steel rebars are mostly used in splash zones, which are the most susceptible to chloride ingress. This includes pile caps and lower parts of the concrete towers, concrete box girder and pier body of the bridges. However, due to economic reasons, stainless steel rebars are only used for reinforcement and stirrups in the outermost layer of the structures more exposed to chlorides. This means that there is a combination of stainless steel reinforcement and carbon steel reinforcement, but as mentioned in Section 2.4.4, there is no need for additional protecting measures due to galvanic corrosion.

Figure 4.3 The Hong Kong-Zhuhai-Macau Bridge which connects Hong Kong with Zhuhai and Macau and is constructed with stainless steel reinforcement (© Arup, 2018).

4.2.4 Hastings Bridge, USA

In Minnesota, the new Hastings Bridge, see Figure 4.4, was built in 2013 to replace the old truss bridge which was determined as functionally obsolete. Due to heavy traffic on the bridge, with about 34000 vehicles per day, the bridge represents a crucial connection. Consequently, any disturbance of the traffic would be very costly which promoted the choice of stainless steel as the most suitable reinforcement alternative. The cost of the bridge was estimated to be about 120 million US dollars and the type of stainless steel used in this project was Arminox UNS S32304, in order to ensure long term durability of the bridge. The manufacturer claimed a corrosion resistance of at least 150 years (American Arminox, 2010). Arminox UNS S32304 is made in the United States but also manufactured under EN standards. It is a lean duplex stainless steel and equals to EN 1.4362. Approximately 300 tons of stainless steel was used in the concrete deck slab, end diaphragms, sidewalk, concrete end posts and railings.

Figure 4.4 The new Hastings bridge in Minnesota, using stainless steel rebars in critical areas (MnDOT, 2018).

4.2.5 Haynes Inlet Bridge

In Oregon, U.S, a stainless steel reinforced concrete bridge was inaugurated in 2004, which carries the U.S route 101 over the Haynes Inlet, see Figure 4.5. The bridge is intended to have a life span of 120 years, almost 2.5 times the life span of the bridge that it replaced (Emerald Insight, 2002). The cost of the bridge was estimated to 12.5 million US dollars. However, using stainless steel rebars is estimated to save 25 million US dollars, by not having to replace or repair the bridge in 50 years.

The Haynes Inlet Bridge used nearly 400 tons of stainless steel rebars, which at the time was more than any other bridge in North America. Because of the harsh environment the bridge was exposed to, considering both chloride ingress and seismic activity, the quality of the stainless steel was crucial. Therefore, a duplex Alloy 2205 stainless steel was used. At this time, the most common stainless steel used for bridges was 316 LN, equivalent to EN 1.4429. However, due to higher demands regarding strength and durability, the Alloy 2205 was chosen instead, which equals EN 1.4462 and is a duplex steel with a mix of austentic and ferritic microstructures.

The bridge was designed with stainless steel rebars in the most exposed areas and normal carbon steel rebars in substructure elements not directly exposed to corrosion. In comparison, 614 tons of carbon steel was used for the bridge. The most exposed parts of the bridge, regarding corrosion, were the bridge deck and T-beams because of bending forces and dynamic loads from heavy trucks, which could cause cracking and chloride intrusion. Therefore, the deck and T-beams of the bridge are reinforced with Alloy 2205 (Emerald Insight, 2002). In this bridge, carbon and stainless steel reinforcement were often used independently in the structural elements. However, at some places both stainless steel and carbon steel reinforcement are used. Here, the stainless steel rebar was covered with a polyethylene sleeve to prevent

galvanic corrosion from occurring (Emerald Insight, 2002). Apart from stainless steel rebars, microsilica concrete is used to increase resistance against corrosive attacks, because of its lower permeability.

Figure 4.5 The Haynes Inlet Slough bridge in Oregon, with Alloy 2205 stainless steel bars in critical areas (Michael Goff, 2008).

4.2.6 Summary

The stainless steel reinforced concrete structures described in the previous sections have many things in common. Although, it is important to state that the structures are supposed to have a service life of over 100 years and they are all built in the last 15 years, making it very hard to assess how successfully stainless steel has been implemented in these cases. However, it is still of interest to see which kind of stainless steel rebars are being used and at which locations they are being implemented.

Type of Stainless Steel Rebars Used

What all of the different bridges, except for Broadmeadow bridge, have in common is the use of a duplex stainless steel. However, Broadmeadow bridge is the first completed of the examples, which could be an explanation as to why an austentic steel was used. Otherwise, a duplex stainless steel with a low nickel content is the common factor, also known as lean duplex. Even though most of the bridges uses lean duplex stainless steel, there is a remarkable difference in nickel content in the different types used, see Table 4.3. In Junction Värtan, EN 1.4162 is used, which has a much lower nickel content than EN 1.4362 used in both Hastings bridge and Hong Kong-Zhuhai-Macau bridge. In turn, EN 1.4362 has a lower nickel content than EN 1.4462 used in Haynes Inlet bridge.

As can be seen in Table 4.3 when comparing year of construction with Nickel and Molybdenum content, the general trend is that the content of Nickel and Molybdenum is decreasing. In Section 2.5.2, it is mentioned that Nickel and Molybdenum are the main reasons behind the high cost of stainless steel and therefore it is clear that the general development is towards a more cost efficient stainless steel.

Table 4.3 Summary of type of stainless steel used in the different projects, with Nickel and Molybdenum content (Euro Inox, 2007).

Bridge	**Year**	**EN**	**Type**	**Ni** [%]	**Mo** [%]
Broadmeadow	2003	1.4435	Austentic	12.5-15.0	2.5-3.0
Haynes Inlet	2004	1.4462	Duplex	4.5-6.0	2.5-3.5
Hastings	2013	1.4362	Duplex	3.5-5.5	0.1-0.6
Junction Värtan	2015	1.4162	Duplex	1.35-1.7	0.1-0.8
Hong Kong-Zhuhai-Macau	On-going	1.4362	Duplex	3.5-5.5	0.1-0.6

Implementation of Stainless Steel Rebars

In the aforementioned applications, stainless steel rebars are used only in parts of the structure by replacing carbon steel reinforcement only in the most critical areas of the bridge.

First of all, it is important to state that the bridges are of different character, both considering structural system and location, which means that the critical areas of the bridges differs between each other. In the case of Broadmeadow bridge, the most critical area is the pier stems and columns, see Figure 4.2. These are critical areas because they are located in splash zones and therefore exposed to higher chloride intrusion. Similarly, in the Hong Kong-Zhuhai-Macau bridge, the pier shaft, tower foundation and bridge bearing platform are considered to be the most critical due to the harsh sea they are exposed to. In Hastings bridge, however, the most critical parts are deemed to be the concrete deck slab, end diaphragms, the sidewalk and the concrete end posts. In Haynes Inlet bridge, the bridge deck and T-beams are seen as most critical.

What can be concluded from this is that the use of stainless steel rebars is restricted to areas either exposed to splash zones or cracking. This could mean areas exposed to splash zones from the marine environment, as the lower part of columns and foundations or splash zones from de-icing salts, as the bridge deck, sidewalks and end diaphragms. It is also worth noting that some critical areas where stainless steel rebars are used are the areas where cracking occurs, causing accelerated chloride intrusion and these areas could be the bridge deck and T-beams. To summarize, in order to properly implement stainless steel rebars in a bridge, it is crucial to first understand which areas of the bridge are the most affected due to corrosion.

What is also worth mentioning in the implementation of stainless steel rebars is that the Haynes Inlet bridge uses polyethylene sleeves to protect the metals from galvanic corrosion where there is a mix of stainless and carbon steel reinforcement. As mentioned in Section 2.4.4, this could be unnecessary simply because of the small rate of galvanic corrosion that takes place when the metals are embedded in concrete.

Table 4.4 Material properties (Outukumpu, 2018) and cost (MEPS, 2018b).

Parameter	**EN 1.4162**	**EN 1.4662**	**EN 1.4362**	**EN 1.4462**	**EN 1.4406**
Type	Lean duplex	Lean duplex	Duplex	Duplex	Austentic
Corrosion resistance	Good	Good	Very good	Very good	Superior
Density [kg/m^3]	7800	7700	7800	7800	8000
Thermal exp. [$\cdot 10^{-6}/°C$]	13.0	13.0	13.0	13.0	16.0
Modulus of elasticity [GPa]	200	205	200	200	200
Elongation [%]	> 30	> 25	> 20	> 20	> 70
Proof strength [MPa]	610	640	620	690	300
Ultimate strength [MPa]	810	850	790	880	625
Cost [USD/ton]	3411	4210	4028	4536	3629

4.3 Stainless Steel Rebars Most Suitable for Bridge Design

In this section, a summary of the most suitabl stainless steel grades for application in concrete bridges is presented. Hence, the choice of stainless steel rebars presented is based on the literature study, design manuals and examples of actual constructions.

The corrosion resistance of stainless steel rebars is very hard to predict, as mentioned in Section 2.5.6. However, it is safe to say that duplex steel grades have the best corrosion resistance of the stainless steels tested, superior to that of the lean duplex and austentic grades, as can be seen in Section 2.6.1. What is also safe to say is that high-alloyed duplex steel has significantly better corrosion resistance than low-alloyed. This is why austentic, duplex and lean duplex types of steel are presented and compared in the following section.

As can be seen in Table 4.4, the austentic steel is inferior in strength to that of the duplex types. Even though the austentic steel has superior corrosion resistance, it is not deemed appropriate in this kind of structural design, as it would require large amounts of reinforcement. The most appropriate alternative for bridge design, if looking only at performance, is the duplex stainless steel. This is due to both mechanical strength and corrosion resistance. Although, the lean duplex steels are less expensive, the lower corrosion resistance is a disadvantage.

However, what is of great interest in this study is the relation between strength and cost, as can be seen in Table 4.5. Based on this, the most appropriate stainless steel rebars to implement in the case study is the lean duplex EN 1.4162 and the duplex EN 1.4462. The lean duplex grade EN 1.4162 has, as can be seen in Table 4.5, superior mechanical properties when considering cost. Although, it is also of interest to consider corrosion resistance and therefore the duplex grade EN 1.4462 is also suitable for bridge

design. This is according to what is mentioned in Section 2.6.1.

Table 4.5 Comparison of strength and cost as of September 2017 (MEPS, 2018b).

Parameter	**B500B**	**EN 1.4162**	**EN 1.4662**	**EN 1.4362**	**EN 1.4462**	**EN 1.4406**
Proof Strength [MPa]	500	610	640	620	690	300
Cost [USD/ton]	579	3411	4210	4028	4536	3629
Strength/Cost [-]	0,863	0,179	0,152	0,154	0,152	0,083
Price Index [%]	100	589	727	696	783	627

5 Case Studies

This chapter presents two case studies, which are carried out to determine the impact of replacing carbon steel with a stainless one, and keeping the same structural performance. Firstly, the reasons behind choosing the particular case to study are discussed, followed by a short introduction to the case. Then the applicable design codes and assumptions applying to the case are presented, together with the design process of the structural elements. Finally, the results of the re-design are presented, focusing on amount of reinforcement and concrete, which will serve as input data for the life cycle cost analysis, presented in Chapter 6.

5.1 Retaining Wall

A retaining wall was chosen as a first case in this study since it is a common bridge application irrespective of the bridge type. It is often implemented in the vicinity of heavily trafficked roads, and exposed to de-icing salts. The repair of retaining wall structures can cause significant traffic disturbance, causing delays for the users resulting in high costs for the society as well as costs for the owner.

The retaining wall to be redesigned using stainless steel reinforcement in this study is a part of a bridge structure in Örebro, Sweden. The bridge, which can be seen in Figure 5.1, forms a crossing of the road 675 over the railway line segment 524 Hallsberg-Örebro, and it was constructed in 2018 with a service life of 100 years. The geometry and layout of the reinforcement can be seen in Figure 5.2 and 5.3. The design of the retaining wall was carried out in accordance with the following standards;

- TK BRO 11 TRV publ nr 2011:085
- TR BRO 11 TRV publ nr 2011:086
- TRVFS 2011:12
- TK GEO 13 (BVS 1585.001, VV 2009:46)
- Eurocode 1: Actions on structures, SS-EN 1991-2
- Eurocode 2: Design of concrete structures , SS-EN 1992-1-1:2005
- Eurocode 7: Geotechnical design, SS-EN 1997-1:2005

Figure 5.1 Picture of the slab-frame bridge, of which the retaining wall is a component, during construction (Trafikverket, 2018).

5.1.1 Calculation Procedure using Stainless Steel Reinforcement

At first, input data for the materials were defined and characteristics of the design were specified. Regarding the reinforcement, stainless steel with different proof stress, ranging from 450 MPa to 850 MPa, were used in order to conduct a parametric study. To describe the non-linearity of the stainless steel reinforcement and the elongation of the steel at proof stress, Ramberg-Osgood parameters were specified, which are described in Section 2.5.3. To complete the study, design using characteristics of the original reinforcement B500B was also carried out for comparison purposes. The concrete class used was C35/45 in the whole structure.

Secondly, the prerequisites of the original design process were listed. The safety class of the structure was 2 and service life was 100 years, which resulted in the following requirements regarding the crack width limitation and concrete cover thickness

- The maximum allowed crack width under serviceability limit state (SLS) was 0,4 mm (Trafikverket, 2011), both for the base plate and the front wall exposed to the soil. The side facing open air has a stricter maximum allowed crack width of 0,2 mm.
- The thickness of the concrete cover was set to 40 mm (Trafikverket, 2011), where the maximum aggregate size was the designing factor.

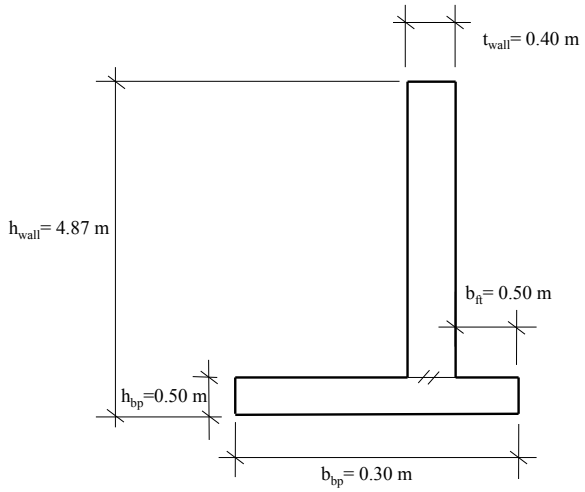

Figure 5.2 The geometry of the retaining wall.

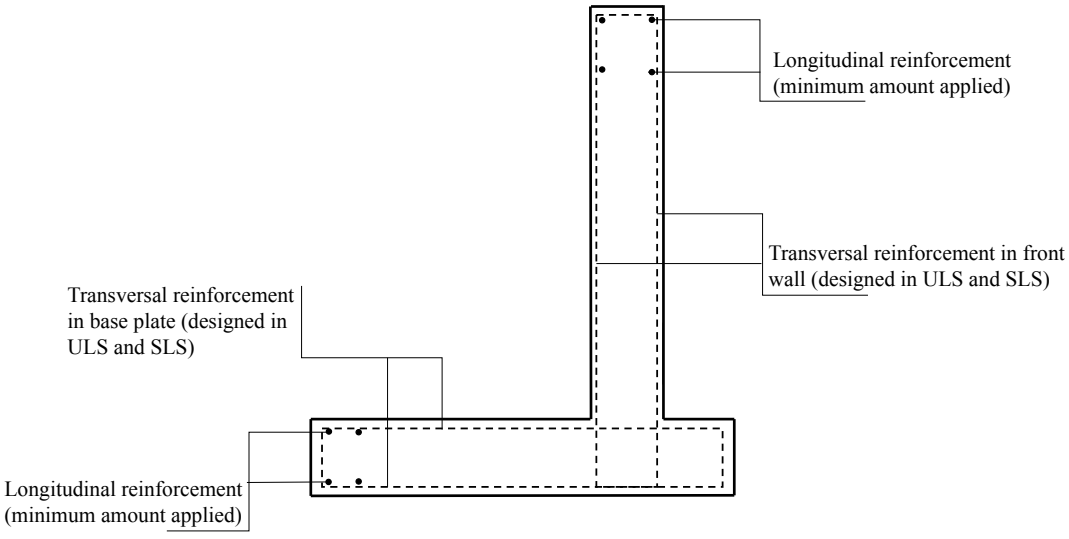

Figure 5.3 Schematic overview of the reinforcement layout of the retaining wall.

The requirement regarding the crack width limitation was applied in the redesign process at first. However, due to the improved corrosion resistance of stainless steel, the maximum allowable crack width can be increased (Markeset *et al.*, 2006). This resulted in a redesign of the reinforcement, using a maximum allowable crack width of 0,6 and 0,8 mm, respectively. The thickness of the concrete cover could not be reduced, even though stainless steel can allow a thinner concrete cover, see Section 2.4. This was due to the fact that maximum aggregate size in the concrete mix was the designing parameter and it is not within the scope of this study to change the mix of the concrete.

The geometry of the wall was defined in accordance to Figure 5.2, and the length of the wall was set to six meters. However, when designing the reinforcement, only a strip of one meter of the wall is considered. The permanent and variable loads acting on the one meter strip are;

- Permanent loads
  - Self-weight of structure
  - Self-weight of soil
  - Soil pressure
- Variable loads
  - Vertical traffic load
  - Horizontal traffic load
  - Wind load

The loads, which can be seen in Figure 5.4, were defined according to EC 1. Based on these loads, the designing moments and sectional forces were calculated. The loads were combined in accordance with TRVFS 2011.12, where geotechnical loads and loads from the structure are treated separately. The load combinations resulted in 12 cases and the designing load combinations were used to make the necessary checks.

Firstly, the geotechnical aspects of the structure were controlled. The calculation procedure regarding these checks are included in Appendix A, but will not be commented further in this thesis as it is not of interest when regarding the redesign of reinforcement. These checks include;

- Overturn
- Gliding
- Soil pressure in ULS and SLS
- Cast joint

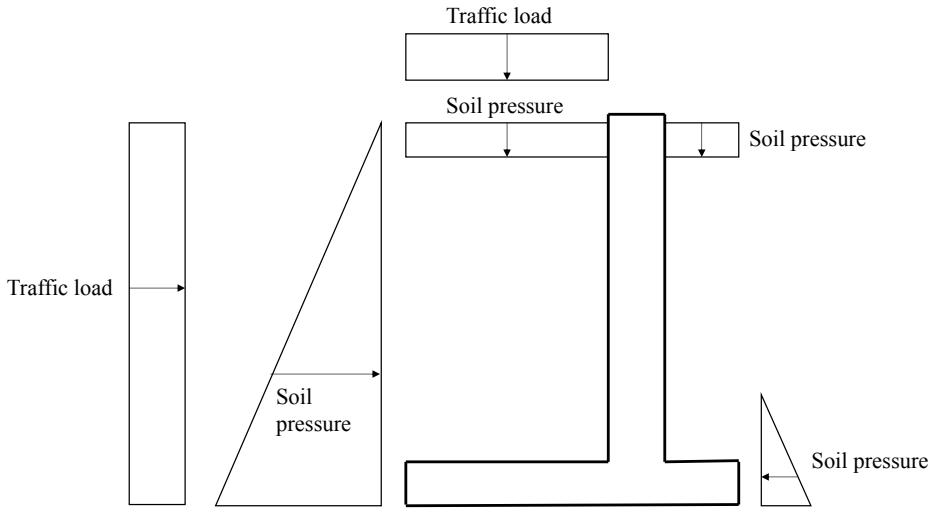

Figure 5.4 Schematic sketch over the loads acting on the retaining wall.

Subsequently, the reinforcement amount and arrangement were controlled. These were done separately for the base slab, described in Section 5.1.2 and front wall, in Section 5.1.3. Regarding the stress-strain relationship for stainless steel reinforcement, it was defined differently compared to carbon steel reinforcement. As mentioned in Section 2.5.3, the stress-strain behaviour can instead be described by Ramberg-Osgood equation. The stress strain relationship for stainless steel is given by Equation 5.1.

$$\varepsilon = \frac{\sigma}{E_0} + \alpha \frac{\sigma_0}{E_0} \left(\frac{\sigma}{\sigma_0}\right)^n \tag{5.1}$$

where ε is the strain [%], σ is the actual stress, E_0 and σ_0 is the modulus of elasticity and stress at 0,2 % plastic strain, α is the ratio between plastic and elastic deformation and n is the strain hardening parameter.

Table 5.1 Parameters used in the calculation of the stress strain relationship of the stainless steel reinforcement.

Parameter	**Value**
E_0	170 GPa
α	0,6
n	15
σ_0	450-800 MPa

In the ultimate limit state (ULS), the traditional bi-linear stress strain relationship is applied since the design is conservative when dealing with high stresses and strains. However, to ensure yielding of reinforcement in ULS, the strain of the reinforcement is controlled by the non-linear behaviour described by the Ramberg-Osgood equation.

In SLS, the stresses are smaller, which means that there is a risk of the design being on the unsafe side, which can be seen schematically in Figure 2.5 and is explained in Section 2.5.3. Therefore, the non-linearity of the steel is taken into account. However, since the Ramberg-Osgood modulus of elasticity, E_0, was used instead of the higher initial modulus E_s the non-linearity did not have a significant impact on the design, which can be seen in Appendix A.

To differentiate between the reinforcement amount required for ULS and SLS, the retaining wall was first designed in ULS, disregarding any crack width limitations. As previously mentioned, in the design, strength grades for the reinforcement ranged from 450 to 850 MPa. If the SLS was not verified, more reinforcement was added to fulfill the crack width limitations measured from 0,4 to 0,8 mm, as previously mentioned. The required amounts for SLS and ULS were then compared to see how much additional reinforcement was required to fulfill the crack width limitations for each of the strength grades. Finally, surface reinforcement or minimum reinforcement was arranged in the bottom of the base slab in transverse and longitudinal directions. Minimum reinforcement was also applied at the top of the base slab in the longitudinal direction and in the air-facing side of the front wall in both directions, as well as the longitudinal direction of the soil-facing side, see Figure 5.3. The required amount of reinforcement was given by Equations 5.2 to 5.7. Equation 5.3, 5.4, 5.5, 5.7 can be found in TDOK 2016:0204 (D.1.1.1) and Equation 5.6 can be found in SS-EN 1992-1-1:2005 (7.3.2).

$$A_{s.min} = max(A_{s.min.1}, A_{s.min.2}, A_{s.min.3}, A_{s.min.4}, A_{s.min.5}) \tag{5.2}$$

$$A_{s.min.1} = \frac{4 \cdot f_{ctm}}{3 \cdot b_c} \frac{mm^2}{m} \tag{5.3}$$

$$A_{s.min.2} = 400 \cdot \frac{mm^2}{m} \tag{5.4}$$

$$A_{s.min.3} = 0,08\% \cdot h_c \frac{mm^2}{m} \tag{5.5}$$

$$A_{s.min.4} = max(0,26 \cdot \frac{f_{ctm}}{f_{yk}} \cdot d, 0,0013 \cdot d) \frac{mm^2}{m} \tag{5.6}$$

$$A_{s.min.5} = \frac{\pi}{400} \cdot \frac{16^2}{4} \frac{mm^2}{m} \tag{5.7}$$

where f_{ctm} is the average tensile strength of the concrete, h_c and b_c is the height and width of the concrete section, d is the distance from the reinforcement to the edge in compression and f_{yk} characteristic yield strength of the steel, defined as the 0,2 % proof strength.

5.1.2 Design of Base Slab

The base slab is in exposure class XC2/XF3, on both the upper and lower face of the slab. The exposure class gives a value for the maximum allowable crack width (0,4 mm), as well as the cover thickness of the concrete. When the reinforcement of the base slab of the retaining wall was redesigned, the objective was to achieve a high utilization ratio in ULS. The most critical sections were identified, and the reinforcement was designed accordingly. The designing factor was the moment capacity with regard to the upper reinforcement, where utilization rates of at least 95 % was aimed for. In addition to the moment capacity, several other checks regarding the base plate were made in SLS and ULS as listed below;

Moment capacity in ULS according to Equation 5.8

$$A_{s.ULS} = \frac{\alpha_c \cdot f_{cd} \cdot x_{top}}{f_{yd}} < A_{s.top} \tag{5.8}$$

where α_c is a coefficient describing the compressive block of concrete, which is set to 0,81 according to SS-EN 1992-1-1 3.1.7 (3), f_{cd} is the designing concrete stress, x_{top} is the distance from the neutral layer to the compressed edge and f_{yd} is the designing steel stress.

Yielding of top reinforcement in ULS using one linear and one non-linear term and checking that the strain is larger than the 0,2 % proof strain according to Equation 5.9

$$\varepsilon_{sm} = \frac{\sigma_{s.m}}{E_0} + \alpha \frac{\sigma_0}{E_0} (\frac{\sigma_{s.m}}{\sigma_0})^n > \varepsilon_{s0,2\%} \tag{5.9}$$

where ε_{sm} is the average steel strain, $\sigma_{s.m}$ is the average steel stress and $\varepsilon_{s0,2\%}$ is the strain at 0,2 % elongation.

Ductility of top reinforcement in ULS according to Equation 5.10

$$x_{top} < 0,45 \cdot d \tag{5.10}$$

where x_{top} is the distance from the neutral layer to the compressed edge and d is the distance between the reinforcement and the compressed edge of the cross section.

Crack width on top of the plate in SLS according to Equation 5.11, where the average steel strain is calculated by using the non-linear stress strain distribution given by Equation 5.1.

$$w_k = s_{r.max} \cdot max(\varepsilon_{sm} - \varepsilon_{cm}, \varepsilon_{sm} \cdot 0,6) < w_{k.allowed} \tag{5.11}$$

where w_k is the characteristic crack width, $s_{r.max}$ is the maximum crack distance, ε_{sm} is the average steel strain, ε_{cm} is the average concrete strain and $w_{k.allowed}$ is the maximum allowable crack width, which was varied from 0,4 mm to 0,8 mm.

Assumed Young's-modulus in SLS, where the assumed modulus of elasticity E_0 is checked by ensuring that the strain is in the linear region, which is given by Equation 5.12.

$$\varepsilon_{sm} < \varepsilon_{s0,2\%} \tag{5.12}$$

where ε_{sm} is the average steel strain and $\varepsilon_{s0,2\%}$ is the strain at 0,2 % elongation.

Minimum reinforcement is applied as bottom reinforcement and checked to have sufficient capacity for **shear force**, **shear slip failure**, **stress limit in strut** and **angle of strut** in ULS.

5.1.3 Design of Front Wall

The design of the front wall was in many cases similar to that of the base slab. The side of the wall facing the air is in class XD1/XF4, and the side facing the soil is in class XC2/XF3. The exposure conditions resulted in the same concrete cover thickness, as well as the same designing crack width limitations. The crack width limitation concerning the side of the wall exposed to air is 0,2 mm. This side of the wall is considered to be in compression, thus no load-induced cracks are expected. By extension, this face of the wall does not need to be checked for load-induced cracks.

The same design procedure as for the base plate was implemented; first, the reinforcement was designed to fulfill the requirements in ULS and then in SLS. Difference in the required amounts was documented and form the basis of the results. The calculations and checks required for the design of the front wall are similar to those regarding the base slab. Instead of controlling only the most critical sections, the calculations were performed for several points along the vertical axes of the wall. The capacity of the wall is then checked along the its height with regard to the obtained values. The checks required for the front wall contain;

Tensile force capacity in ULS according to Equation 5.13

$$F_t(x) < F_{tot}(x) \qquad F_t(x) = \alpha_c \cdot x_{ULS}(x) \cdot f_{cd} \qquad F_{tot}(x) = A_s(x) \cdot f_{yd} \tag{5.13}$$

where α_c is is a coefficient describing the compressive block of concrete, x_{ULS} is the distance from the neutral layer to the compressed edge, f_{cd} is the designing concrete compressive strength, $A_s(x)$ is the

reinforcement area of the section, which varies along the height of the wall and f_{yd} is the designing yield strength of the steel. $F_t(x)$ is the tensile force over the height of the wall and $F_{tot}(x)$ is the tensile force capacity in the given section.

Shear force capacity in ULS according to Equation 5.14

$$V_d(x) < V_{tot}(x) \tag{5.14}$$

where $V_t(x)$ is the shear force over along the length axis of the wall and $V_{tot}(x)$ is the shear force capacity of the concrete with regard to reinforcement content in the given section.

Crack width on soil-facing side of the wall in SLS according to Equation 5.15

$$w_k(x) = s_{r.max} \cdot (\varepsilon_{sm}(x) - \varepsilon_{cm}(x)) < w_{k.allowed} \tag{5.15}$$

Where w_k is the characteristic crack width, $s_{r.max}$ is the maximum crack distance, ε_{sm} is the average steel strain, ε_{cm} is the average concrete strain and $w_{k.allowed}$ is the maximum allowable crack width, which was varied from 0,4 mm to 0,8 mm.

Assumed Young's modulus in SLS, where the assumed modulus of elasticity E_0 is checked by ensuring that the strain is in the linear region,which is given by Equation 5.16.

$$\varepsilon_{sm} < \varepsilon_{s0,2\%} \tag{5.16}$$

Where ε_{sm} is the average steel strain and $\varepsilon_{s0,2\%}$ is the strain at 0,2 % elongation.

5.1.4 Calculation Procedure using Carbon Steel Reinforcement

The retaining wall was originally designed using carbon steel reinforcement, which is the as-built design. The reinforcement amount used in the original design is included in the analysis to give reasonable values to compare with the stainless steel design. The design of the carbon steel reinforcement was carried out using a similar design procedure as described in Section 5.1.1. However, the carbon steel reinforcement was designed assuming a traditional bi-linear stress strain relationship. The material parameters for reinforcement steel B500B were used and the crack width limitation of 0,4 mm according to Eurocode 2 and TRVFS:2011 was implemented.

5.1.5 Reinforcement Layouts to Implement in LCC

Moving forward in this study, it is necessary to limit the number of studied reinforcement solutions on which to perform a LCC. The following seven reinforcement layouts are included in the study;

- **Reinforcement Layout 1** - As built design with carbon steel reinforcement B500B, design process focusing on buildability and thus requiring significantly higher amounts of reinforcement. Design in accordance with current standards.

- **Reinforcement Layout 2** - Design using carbon steel reinforcement, optimized with regard to lowest possible amount of reinforcement. However, still within the limits of the current standards regarding carbon steel reinforced concrete structures.
- **Reinforcement Layout 3** - Design using stainless steel grade EN 1.4162, using material properties given in EN 1993-1-4:2006/A1:2015, and applying the current standard maximum crack width limitation.
- **Reinforcement Layout 4** - Design using stainless steel grade EN 1.4162, using material properties obtained through tests (Pajari, 2011). The current standard maximum crack width limitation is applied.
- **Reinforcement Layout 5** - Design using stainless steel grade EN 1.4162, using material properties obtained through tests (Pajari, 2011), and increasing the maximum crack width limitation to 0,6 mm.
- **Reinforcement Layout 6** - Design using stainless steel grade EN 1.4462, using material properties given by the manufacturer (Outukumpu, 2018), and increasing the maximum crack width limitation to 0,6 mm.
- **Reinforcement Layout 7** - Design using a stainless steel with a proof strength of 800 MPa (which is not currently available) and a crack width limitation of 0,8 mm.

These above listed layouts were chosen to be studied further in the LCC because they are all interesting options to compare in the LCC. Reinforcement layout 1 (RL 1) is included to provide a realistic comparison of the LCC. RL 2 is included as a comparison of the amount of carbon steel required when designing in a similar way as when the stainless steel reinforcement is designed.

Concerning the choice of the stainless steel grades to be implemented, the previous use of lean duplex steel grade EN 1.4162 and duplex grade EN 1.4462 in existing concrete bridges can be seen in Section 4.2. The aforementioned stainless steel grades have been tested against corrosion and have been found to have good to superior corrosion resistance, which is described in Section 2.6.1.

Regarding RL 3, where steel material properties according to Eurocode 3 are used, the same tensile strength should be used for both EN 1.4162 and EN 1.4462 ($f_{yk} = 450$ MPa), which would result in the same amount of reinforcement. On the basis of this, lean duplex steel grade EN 1.4162 is used in this comparison due to its lower price.

Stainless steel grade EN 1.4162 is also used in RL 4, which is similar to RL 3. However, this design uses a higher tensile strength than is advised in Eurocode. This tensile strength has been determined in tests, and is therefore considered to be reasonable to assume as a material parameter (Pajari, 2011).

Respecting the crack width limitation, enough experimental data has not yet been collected to determine the exact maximum allowable crack width, which could be applied without danger of extensive corrosion. However, it has been argued that it can be increased by up to 100 % (Markeset *et al.*, 2006). Due to the uncertainties regarding this assumption, as well as the results of the redesign, an increase in maximum allowable crack width by 50 %, to 0,6 mm, has been deemed reasonable. This limitation was implemented in RL 5 and 6. As can be seen in Figure 7.1, the additional gain of allowing even larger crack widths is very small.

RL 6 is the only one where duplex steel EN 1.4462 is implemented. This is due to the fact that duplex steel grade EN 1.4462 is significantly more expensive than lean duplex grade EN 1.4162, which can be seen in Table 4.5. Thus, this stainless steel grade is only implemented where higher maximum crack widths are allowed.

RL 7 uses a stainless steel with a tensile strength of 800 MPa, which is not available on the market. This is included in the analysis to see if there are possible gains when higher strength reinforcement steel is developed. The crack width limitation is set to 0,8 mm in order to take full advantage of the high strength of the steel. A summary of the reinforcement layouts, amounts and general conditions can be seen in Table 5.2

Table 5.2 Summary of general conditions for the seven considered reinforcement layouts. Reinforcement amounts in ton, where amount in ULS and SLS refers to the reinforcement required in the designing sections. The minimum reinforcement amount refers to all of the surface reinforcement, as well as the main reinforcement where only minimum reinforcement was required to fulfill the requirements

Parameter	**RL 1**	**RL 2**	**RL 3**	**RL 4**	**RL 5**	**RL 6**	**RL 7**
Reinforcement type	B500B	B500B	EN 1.4162	EN 1.4162	EN 1.4162	EN 1.4462	-
f_{yk} < [MPa]	500	500	450	600	600	690	800
w_k < [mm]	0,4	0,4	0,4	0,4	0,6	0,6	0,8
ULS [ton]	0,6226	0,4586	0,5043	0,3919	0,3919	0,3325	0,3077
SLS [ton]	-	-	-	0,0686	-	0,025	-
Minimum [ton]	0,8898	0,7756	0,8556	0,6417	0,6417	0,6016	0,6016
Total [ton]	1,5124	1,2342	1,3599	1,1022	1,0336	0,9591	0,9093

5.2 Slab-Frame Bridge

The second structure to be redesigned using stainless steel reinforcement is a slab-frame bridge constructed in 2015. The bridge has construction number 100-147-1 and can be seen in Figure 5.5. The reason behind this choice of structure is both its commonness and exposure to de-icing salts. The bridge will be redesigned by changing the outermost layer of reinforcement in the bridge deck, edge beams, front wall and wing wall to stainless steel, but keeping the foundation slab as it is designed.

Figure 5.5 Picture of the slab-frame bridge during construction (Trafikverket, 2018).

The bridge is located in Robertsfors and provides a crossing over the stream Långtjärnsbäcken. The width of the bridge is 7,0 meters and the length is 5,88 meters. The geometry of the bridge can be seen from the side in Figure 5.6 and from above in Figure 5.7. See Appendix B for detailed drawings.

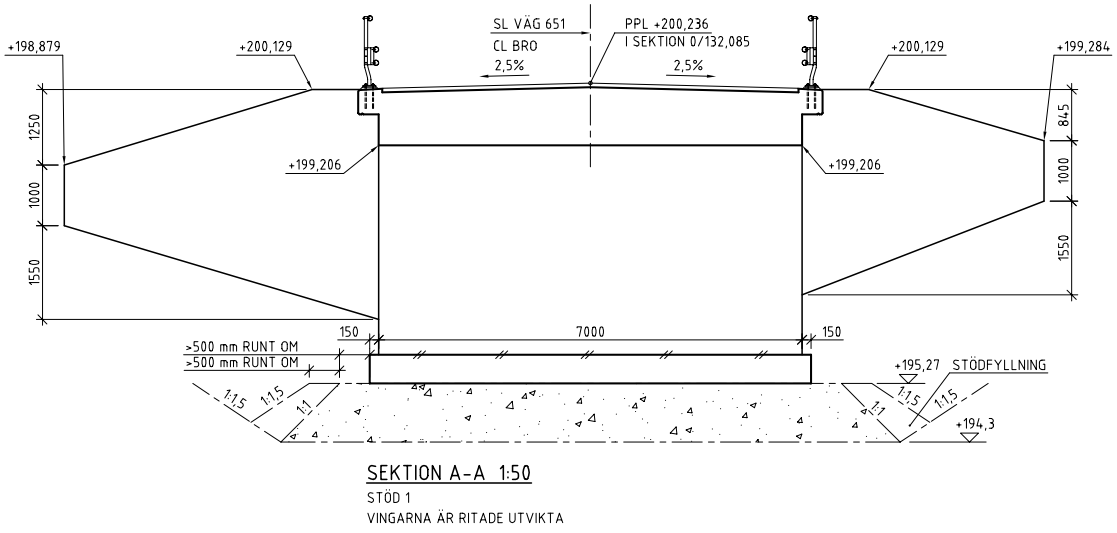

Figure 5.6 The geometry of the slab-frame bridge, seen from the side.

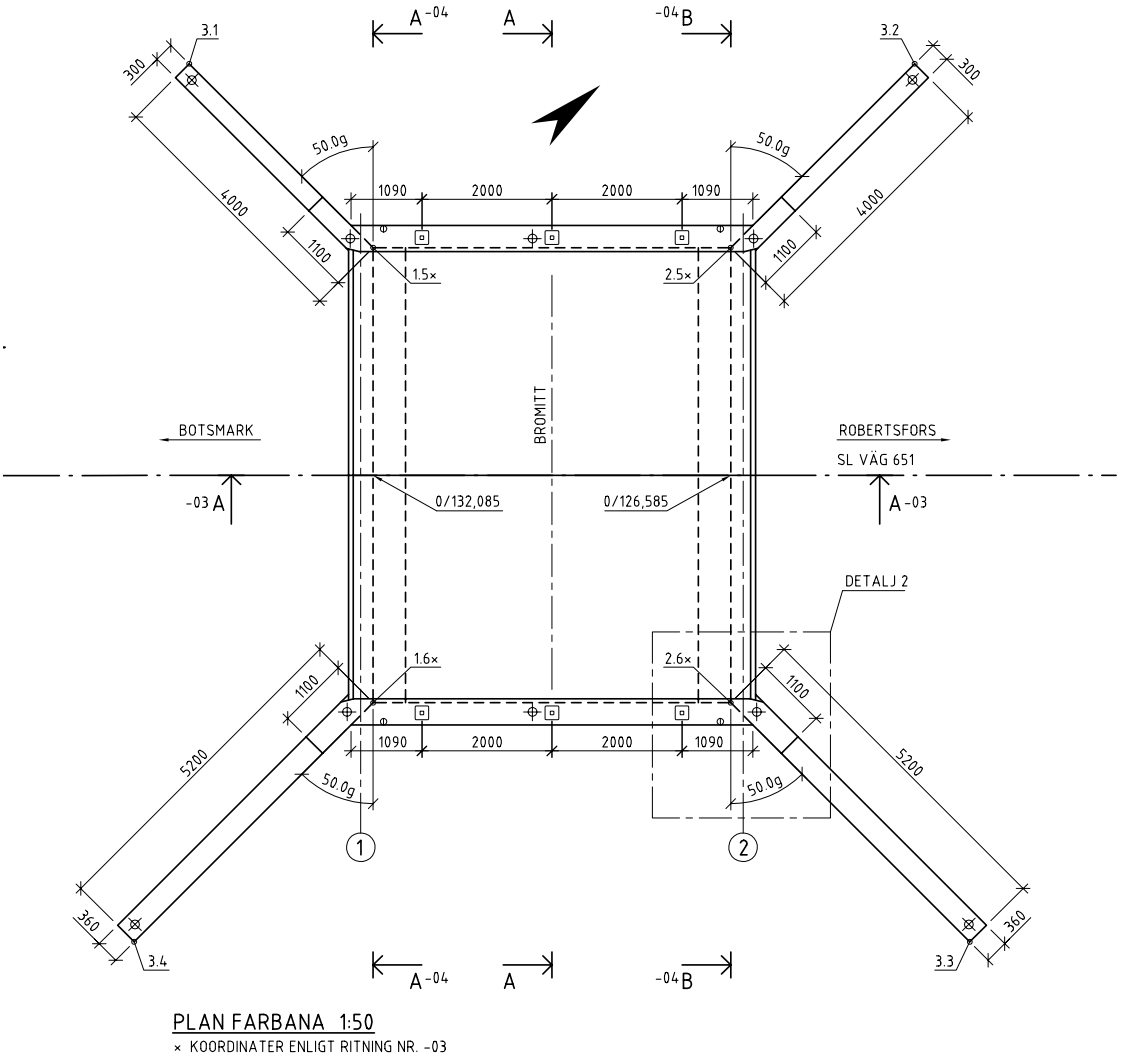

Figure 5.7 The geometry of the slab-frame bridge, seen from above.

The slab-frame bridge was designed using 5 different reinforcement types;

- **RL 1** - Original carbon steel reinforcement B500B. This was used in order to verify the hand calculations and to provide a comparison for the LCC analysis.
- **RL 2** - Lean duplex stainless steel grade EN 1.4162 using parameters and crack width limitations according to Eurocode.
- **RL 3** - Lean duplex stainless steel grade EN 1.4162 using parameters according to tests and allowing the crack width to exceed the limitations by a 100 % (Pajari, 2011).

- **RL 4** - Duplex stainless steel grade EN 1.4462 using parameters according to tests and allowing the crack width to exceed the limitations by a 100 % (Outukumpu, 2018).
- **RL 5** - Fictional stainless steel with $f_{yk} = 800$ MPa, and allowing the crack width to exceed the limitations by a 100 %

5.2.1 Calculation Procedure

The redesign process was carried out using results from a previous analysis of the wall using the program ConcreteDesigner Bridge, where loads, geometry and material is given as input, resulting in sectional forces and reinforcement amounts which are given as output. This program uses carbon steel reinforcement B500B, and it is not possible to give a non-linear material as input. Therefore, the designing sectional forces were identified using the results provided by the program. The sectional forces were then and used in hand calculations where the non-linear relationship could be applied. The reinforcement ratios and lengths were not changed in relation to the original design, so as to be able to assume the same moment distribution as obtained by the program.

The designing sections were analyzed in ULS, SLS and fatigue limit state (FLS). In ULS, the sections were checked to have sufficient moment capacity. In SLS, the crack width was calculated and in FLS, the stress range was calculated. Regarding shear force capacity, it was assumed that the same amount of reinforcement as the original carbon steel design was sufficient, and thus, no checks were needed.

First, the designing sectional forces in span and support, as well as in which section they occur, were obtained from the previous analysis. In order to verify the model, carbon steel reinforcement B500B was first implemented to compare with the results from ConcreteDesigner Bridge. The moment capacity in ULS, the obtained stress ranges in FLS and the crack width in SLS were verified to be in the same range as those obtained by the program. Secondly, the reinforcement was redesigned using stainless steel (RL 2-5) to achieve a high utilization ratio of moment capacity in ULS. Furthermore, the reinforcement amount was also checked to be larger than the minimum amount of reinforcement according to Equation 5.2. Then, RL 2 was also checked to fulfill the crack width limitation in SLS, while the crack width was allowed to be larger for RL 3, 4 and 5. Finally, the stress ranges in FLS were checked for the slab and the walls.

The **moment capacity** was calculated according to Equation 5.17, and checked using the designing moment in ULS.

$$M_{Rd} = \alpha \cdot f_{cd} \cdot b \cdot x \cdot (d_{ss} - \beta \cdot x) + A'_{ss} \cdot \sigma_0 \cdot (d_{ss} - d'_{ss}) - A_{cs} \cdot f_{yd} \cdot (d_{ss} - d_{cs}) + N_{Ed.ULS} \cdot (d_{ss} - \frac{h}{2}) > M_{Ed.ULS} \tag{5.17}$$

where α and β are coefficients describing the pressure block of concrete, f_{cd} is the designing concrete stress, x is the distance from the neutral layer to the compressed edge, d_{ss} is the distance to the bottom layer of stainless steel reinforcement, A'_{ss} is the area of stainless steel reinforcement in the top d'_{ss} is the distance to the top layer of stainless steel reinforcement, A_{cs} is the area of carbon steel reinforcement in the bottom layer, d_{cs} is the distance to the bottom layer of carbon steel reinforcement, and f_{yd} is the designing steel stress.

Subsequently the **crack width** in SLS was calculated and checked according to Equation 5.18. When designing with stainless steel, the crack width was allowed to exceed the limitation for RL 3, 4 and 5, but not for RL 1 and 2, where design is in accordance with Eurocode.

$$w_k = s_{r.max}(max(\varepsilon_{cm} - \varepsilon_{sm}; 0,6 \cdot \frac{\sigma_{ss}}{E_0})) < w_{k.allowed} \tag{5.18}$$

where w_k is the characteristic crack width, $s_{r.max}$ is the maximum crack distance, ε_{sm} is the average steel strain, ε_{cm} is the average concrete strain, σ_{ss} is the stress in the stainless steel at the outer layer, E_0 is the Young modulus of the steel and $w_{k.allowed}$ is the maximum allowable crack width.

The fatigue life of the structure was set to $5 \cdot 10^5$ cycles, and the **allowable steel stress range** was calculated according to Equation 5.19 and

$$\Delta\sigma_{Rsk} = \sqrt[k_1]{165,5^5 \cdot \frac{10^5}{N}} \tag{5.19}$$

where $\Delta\sigma_{Rsk}$ is the allowed stress range, k_1 and 165,5 are values associated with the Wöhler-curve of reinforcing steel and N is the number of cycles.

The **allowed stress range in the concrete** was calculated according to Equation 5.20

$$f_{cd.fat} = k_1 \cdot \beta_{cc} \cdot f_{cd} \cdot (1 - \frac{f_{ck}}{250}) \tag{5.20}$$

where $f_{cd.fat}$ is the designing concrete strength for fatigue , k_1 is a parameter set to 0,85 according to SS-EN 1992-1-1 (6.8), β_{cc} is a parameter according to Equation 5.21 and f_{cd} and f_{ck} are the designing and characteristic concrete strengths.

$$\beta_{cc} = exp(s \cdot (1 - \sqrt{\frac{t}{28}})) \tag{5.21}$$

where β_{cc} is a coefficient which takes the age of the concrete at first loading into account, s is set to 0,25 according to SS-EN 1992-1-1 (3.2) and t is assumed to be 28 days.

The **steel and concrete stresses in FLS** were calculated according to Betonghandboken 4.3:34 and checked according to Equation 5.22 and 5.23

$$\Delta\sigma_{Rsk} > \gamma_{s.fat} \cdot \Delta\sigma_{ss} \tag{5.22}$$

where $\Delta\sigma_{Rsk}$ is the allowed stress range, $\gamma_{s.fat}$ is the fatigue safety factor according to SS-EN 1992-1-1 and $\Delta\sigma_{ss}$ is the difference in minimum and maximum steel stress in the tensile reinforcement under fatigue loading.

$$\frac{\sigma_{c.max}}{f_{cd.fat}} < 0,5 + 0,45 \cdot \frac{\sigma_{c.min}}{f_{cd.fat}} < 0,9 \tag{5.23}$$

where $f_{cd.fat}$ is the designing concrete strength for fatigue, $\sigma_{c.max}$ and $\sigma_{c.min}$ are the maximum and minimum concrete stresses.

5.2.2 Design of Bridge Deck

The bridge deck was redesigned with regard to bending, fatigue and crack width and is analyzed longitudinally and transversely in ConcreteDesigner Bridge using 25 sections in each direction to carry out the analysis. The redesign can be seen in further detail in Appendix D. The bridge deck is fixed at the ends in the longitudinal direction, which results in tension at the top of the deck at the supports, resulting in negative moments being designing. In the span section, there will be tension in the bottom, resulting in a positive moment. The designing moments and the reinforcement configuration can be seen in Appendix C. In the longitudinal direction, the following reinforcement configuration was applied;

- Span section:
  - Tensile reinforcement: Outer layer of stainless steel reinforcement, and inner layer of carbon steel reinforcement.
  - Compressive reinforcement: One layer of stainless steel reinforcement.
- Support section:
  - Tensile reinforcement: Outer layer of stainless steel reinforcement, and inner layer of carbon steel reinforcement.
  - Compressive reinforcement: Outer layer of stainless steel reinforcement and an inner layer of carbon steel reinforcement.

In the transverse direction of the deck negative moments appear at the support sections for some load cases, although they are significantly smaller than in the longitudinal direction, which can be seen in Appendix C. The designing moment in the span is positive and larger than the support moment. Concerning the reinforcement configuration in the transverse direction of the deck, the same amount

of reinforcement is applied in the span and in the support. This configuration consists of one layer of stainless steel reinforcement in the top, and one layer in the bottom of the deck.

5.2.3 Design of Front Wall

The front wall was also redesigned with regard to bending, fatigue and crack width. The wall was analyzed longitudinally and transversely in ConcreteDesigner Bridge using 25 sections in the longitudinal direction and 16 elements in the vertical direction, the resulting moments can be seen in Appendix C.

In the vertical direction, the wall is fixed at the base and in the top, resulting in high support moments at the top of the wall, where it is connected to the slab. These moments varies according to the load case and can be both negative and positive. In order to simplify the analysis, the reinforcement was assumed to be applied symmetrically, resulting in the same reinforcement configuration in the top and bottom of the section, even though it could be optimized further. In the middle of the wall (span), the moments in ULS are smaller and only one layer of reinforcement is applied in the top and in the bottom of the section. Finally, at the base of the wall, the reinforcement was designed to withstand the support moment which appears there. To summarize, the following configuration was implemented;

- Top (support) section:
  - Top reinforcement: Outer layer of stainless steel reinforcement, and inner layer of carbon steel reinforcement.
  - Bottom reinforcement: Outer layer of stainless steel reinforcement, and inner layer of carbon steel reinforcement.
- Middle (span) section:
  - Top reinforcement: One layer of stainless steel reinforcement.
  - Bottom reinforcement: One layer of stainless steel reinforcement.
- Bottom (support) section:
  - Top reinforcement: One layer of stainless steel reinforcement.
  - Bottom reinforcement: One layer of stainless steel reinforcement.

The transverse direction of the wall can be seen as partially fixed at the ends (the wing walls), which results in a symmetric moment distribution with a span moment in the middle and support moments at the ends. Regarding the reinforcement configuration, the span section requires one layer of stainless steel in the top and in the bottom. In the support sections, an additional layer of carbon steel reinforcement is added in the top as a second layer to the stainless steel reinforcement.

5.2.4 Design of Wing-Walls

The wing walls were redesigned with regard to bending and crack width limitations. There is one short wing wall and one long wing wall on each side of the bridge, which can be seen in Figure 5.7. The long wing wall was analyzed longitudinally and transversely in ConcreteDesigner Bridge using 18 sections in both directions. The short wing wall was analyzed using 14 elements in each direction. The resulting moment distributions can be seen in Appendix C.

In the vertical direction, both the short and the long wing walls are fixed at the base and free at the top, resulting in zero moments at the top of the wall and higher support moments at the base of the wall, where it is connected to the slab. To simplify the analysis, only the designing sections at the base of the walls are analyzed. The moments in the base sections varies according to the load case and can be both negative and positive. As for the case of the front wall, the reinforcement was assumed to be applied symmetrically, resulting in the same reinforcement configuration in the top and bottom of the section, even though it could be optimized further. The following configuration was implemented;

- Middle (span) section:
  - Top reinforcement: One layer of stainless steel reinforcement.
  - Bottom reinforcement: One layer of stainless steel reinforcement.
- Bottom (support) section:
  - Top reinforcement: One layer of stainless steel reinforcement and an inner layer of carbon steel reinforcement.
  - Bottom reinforcement: One layer of stainless steel reinforcement and an inner layer of carbon steel reinforcement.

The horizontal direction of the wall can be seen as partially fixed at the ends (where it is connected to the front wall). This results in larger moments at the connection and therefore, only this section is analyzed. Regarding the reinforcement configuration, the span section requires one layer of stainless steel in the top and in the bottom. In the support sections, an additional layer of carbon steel reinforcement is added in the top as a second layer inside of the stainless steel reinforcement.

5.2.5 Design of Base Slab

No repairs were needed for the base slab in the LCC analysis of the retaining wall, as can be seen in Section 6.2. Therefore, it is assumed that the base slab can be designed using carbon steel reinforcement, without inducing high repair costs later in the life cycle of the structure. The amount of carbon steel reinforcement in the base slab was consequently calculated and applied for all of the layouts.

6 Life Cycle Cost Analysis

This chapter describes the life cycle cost or "cradle to grave" cost for the case studies presented in Chapter 5. The analysis is conducted to give an optimized design, considering both the investment cost and the cost of maintenance and repair. Firstly, an introduction to the LCC (Life Cycle Cost Analysis) will be made, followed by costs used in the analyses. Finally, individual data required for the studied cases is presented.

6.1 Introduction to LCC

In this thesis, a LCC method developed at the Royal Institute of Technology in Stockholm will be used to perform the analysis. The method is described by Sundquist and Karoumi, 2008. The following section provides a short introduction to this method, however, the reader is referred to Sundquist and Karoumi for a more detailed account. An Excel-program is also provided by Sundquist and Karoumi, which is used to make the calculation of the LCC more effective.

6.1.1 Costs

Usually, LCCs divide the cost of a project in three parts to obtain a better overview; agency cost, user cost and costs for the society. This division is natural, since different organizations within the society will be responsible for each cost. The costs are then usually summed up by using the net present value method, described in Section 6.1.2. These costs can then be compared for the different cases in order to make an informed decision, regarding the total life cycle cost of the structure.

The agency costs are some of the easiest to define, such as; planning and design, construction, maintenance, repair and disposal. The maintenance costs can in turn be subdivided into; operational, inspection, repair and upgrading costs. Among the agency costs, the cost of planning and design, together with construction are the easiest to predict. The cost of maintenance and repair is harder to estimate since they occur in a more distant future. In Sweden, there is a tool for the management of maintenance called BaTMan where data concerning maintenance has been collected, which makes it a reliable source for estimating the maintenance costs in this study. Regarding the cost of disposal, it can be approximated to 10 % of the investment cost.

The user costs affect the users, such as drivers of vehicles, commuters or pedestrians in terms of delays or rerouting due to maintenance or repair works. The user delay costs can be approximated by using the average daily traffic, allowed speed and length of construction works needed for repair. The

user costs also specify an hourly rate for drivers and commercial traffic, as well as the time required for the completion of the construction works.

Costs for the society affect the society as a whole, such as environmental impact, use of limited natural resources and costs of medical aid in case of a traffic accident. To account for the use of non-renewable materials, costs for reproducing or recycling the materials at the end of life of the construction can be added. To estimate the costs of deaths and health care in case of a traffic accident related to roadwork, additional information about accident rate per vehicle kilometers and accident rate during roadwork is required.

6.1.2 Net Present Value Method

In order to get a good approximation of the profitability of the cases, the net present value method is used. This method takes the time value of money into account. The net present value is the difference between the present value of cash inflow and outflow, where a positive net present value equals a profitable project or investment.

In a LCC analysis, the net present value is used to get an estimation of its actual value after a certain time period or in this case, the service life of the bridge. This value is however highly dependent on the interest rate used, see Equation 6.1.

$$LCC_{cost} = \sum_{t=0}^{T} \frac{C_t}{(1+r)^t} \tag{6.1}$$

where C_t is the sum of costs at time t, r is the interest rate and T is the studied time period

In turn, the interest rate is based on the discount rate and the inflation rate, as can be seen in Equation 6.2. In Sweden, as of February 2018, the inflation rate in society was 1.7 % (SCB, 2018). This is however not representative for the construction sector, which is of interest in this study. In the construction sector, the inflation rate is 1-1.5 % higher (Sundquist and Karoumi, 2008) than the inflation rate for society in general. For the discount rate, the recommended value in Sweden is 3.5-4.0 % (Trafikverket, 2014).

$$r = \frac{r_L - r_i}{1 + r_i} \tag{6.2}$$

where r_L is the discount rate (%) and r_i is the inflation rate (%)

The interest rate is then applied to calculate the value of future costs today, to make an analysis of the most profitable option possible. There are also some guidelines regarding the interest rate when

studying bridges in particular and for the case of bridges, an interest rate of 2 % is recommended (Safi, 2013).

6.1.3 Sensitivity Analysis

There are several factors that have a large influence on the result of a LCC analysis and therefore it is of interest to identify these factors. These could for example be the interest rate, average daily traffic or speed limit. Small variations in these factors can significantly change the outcome of the LCC analysis. Thus, in order to get accurate results, a sensitivity analysis is needed where the values of the factors are varied.

6.2 Life Cycle Costs for Case Studies

The retaining wall and the slab-frame bridge were constructed quite recently, 2018 and 2015 respectively. Therefore, there is no data registered in BaTMan concerning the maintenance and repair of these structures. However, using the LCC method designed by Sundquist and Karoumi, the maintenance and repair costs can be estimated using historical data concerning bridges in different parts of Sweden.

6.2.1 Investment Cost

The investment costs include materials, transportation, design and planning, as well as construction. The construction phase takes formwork and rebar installation, casting of concrete and formwork removal into account. The investment costs are approximated in the Excel-based program provided by Sundquist and Karoumi by entering the required amount and price of the required materials.

In the excel-based program, default values are given for the material costs as of year 2010. In the LCC analysis, these values has to be adapted to 2018. This is done by taking the inflation rate of 3,2 % for the construction industry into account, as mentioned in Section 6.1.2. However, the default value given for reinforcement is for ordinary carbon steel and therefore it is necessary to calculate the material cost for stainless steel reinforcement. This is done by subtracting the raw material cost for carbon steel reinforcement and adding the cost for the specific stainless steel product, which can be seen in Table 4.5. Concerning the reinforcement type "800 MPa", there is no specific cost given for the material as it currently does not exist on the market. In order to make the calculations, a price of 5800 US dollars is assumed by linearly interpolating duplex grade EN 1.4362 and EN 1.4462 and thus obtaining a reasonable price for a 800 MPa strength duplex steel. The costs related to the investment are listed in Table 6.1. It can be seen that the investment costs is not only related to the price of the raw material but includes transportation and labor. For the carbon steel reinforcement, the raw material cost consists of a much smaller part of the total investment than compared to the stainless steel reinforcements.

Table 6.1 Material costs used in the LCC analyses. Investment costs for the materials (including labor, transportation, material cost), raw material cost per unit and the raw material cost as a fraction of the total material cost.

Material	Unit	Price/unit [SEK]	Raw material cost/unit [SEK]	Raw material cost/unit [%]
Formwork	m^3	1 673	-	-
Concrete	m^3	5 146	1 000	19,4
Reinforcement B500B	ton	51 463	4 765	9,3
Reinforcement EN 1.4162	ton	74 771	28 072	37,5
Reinforcement EN 1.4462	ton	84 029	37 331	44,4
Reinforcement f_{yk}=800 MPa	ton	94 432	47 734	50,5

6.2.2 Operation and Inspection Cost

The cost of operation and inspection is considered to be equal for all the proposed traffic conditions and reinforcement layouts, since stainless steel reinforcement is a relatively new material. Therefore, inspections will have to be made to ensure that the material is behaving as expected. The costs of operation and inspection are approximated by using the aforementioned LCC analysis program, where values regarding the cost and time intervals needed for inspections are given, which are listed in Table 6.2. In the excel-based program provided by Sundquist and Karoumi, the cost for yearly surveillance is assumed to be 0,3 % of the investment cost, resulting in different costs for the seven reinforcement layouts. In this case, this is not a reasonable assumption, as the surveillance will be independent of the reinforcement layout. The cost of yearly surveillance is therefore set to 0,3 % of the investment cost of the original reinforcement layout.

Table 6.2 Inspection and repair costs, duration and time intervals, as well as the road length which will be affected by the inspection or repair (Sifra, n.d.).

Action	Unit	Price/unit [SEK]	Interval [year]	Duration [days]	Affected road length [m]
Superficial inspection	-	3 240	3	0,1	200
Main inspection	-	18 900	6	0,5	200
Cleaning	m^2	2	1	0,2	200

6.2.3 Repair Cost

The cost of repairing the structure is of great importance when considering the LCC, and it is one of the issues with reinforced concrete structures, which is discussed in Chapter 2. When performing the LCC

analysis using only carbon steel reinforcement, default values of the time intervals required for repair given in the LCC analysis program will be used. This assumption is viable considering the fact that RL 1 and RL 2 of the retaining wall, and RL 1 of the slab-frame bridge use carbon steel reinforcement, which is the reinforcement type traditionally used in reinforced concrete structures in Sweden. The costs of inspection and repair can be seen in Table 6.2

Table 6.3 Costs relating to the repair of the structures (Trafikverket, 2017). The repair cost is stated per unit, along with the interval at which it is assumed that repair occurs, the duration of repair and the length of road that is assumed to be affected by the repair work.

Action	**Unit**	**Price/unit [SEK]**	**Interval [year]**	**Duration [days]**	**Affected road length [m]**
Retaining wall	m^2	7 300	50	30	300
Front wall	m^2	7 300	25	30	300
Wing wall	m^2	7 300	25	30	300
Bridge deck	m^2	4 400	25	30	300
Edge beam	m	9 000	25	22	300
Insulation	m^2	1 800	25	30	300
Surfacing	m^2	1 000	25	30	300
Parapets	m	4 500	25	15	300

6.2.4 User Costs

The user costs are generated by the traffic disturbance that is caused by the inspection and repair of the structure. The user costs are calculated separately for the operation and inspection and the repair costs. The user costs concerning the operation and inspection will be similar for all the considered cases. However, user costs related to repair will be non-existing for the stainless steel options, as it is assumed that no repair will be required for these structures.

The reduced speed due to repair works is set to 30 or 50 km/h, depending on the original speed. The reduced speed limit has been based on assumptions regarding the maximum speed limit when roadwork is undertaken. In order to have a reduced speed of 70 km/h, extensive protective measures are required, such as a crash barrier (Trafikverket, 2014). Since it is assumed that the duration of the work is short, it is assumed that a reduction in speed to 50 km/h is reasonable. This speed limit requires a safety zone of 2,5 meter between the traffic and the workplace (Trafikverket, 2014). It has been assumed that larger roads are wider, and that there is therefore more space to create a safe workplace, thus allowing higher maximum speed passing the construction site. Regarding the third case, where 50 km/h is the original speed limit, it is therefore assumed that the speed needs to be reduced to 30 km/h, and thus not requiring the 2,5 meter safety zone (Trafikverket, 2014). However, this is not valid for all cases, and information

about the current road width should be used to make an approximation of how the traffic flow would be affected by repair works.

Table 6.4 summarizes the assumptions that were made when calculating the user costs of the LCC. Parameters that are subjected to the sensitivity analysis described in the next section are given in the intervals in which they vary.

Table 6.4 User costs when inspecting or repairing the retaining wall (Sifra, n.d.).

Parameter	**Unit**	**Value**
Percentage of heavy traffic	%	7
Affected roadway length (maintenance)	m	200
Affected roadway length (repair)	m	300
Speed reduction TC 1	km/h	50 to 30
Speed reduction TC 2	km/h	80 to 50
Speed reduction TC 3	km/h	110 to 50
Average daily traffic (ADT)	vehicles/day	5 000 - 20 000
Operation cost for passenger vehicle	SEK/h	145
Operation cost for heavy traffic	SEK/h	540
Interest rate	%	0,0 - 6,0

6.2.5 Sensitivity Analysis

In order to analyze the influence of important parameters, a sensitivity analysis was conducted for three different cases where the maximum speed limit is set to 50, 80 or 110 km/h. In each of the three cases, the ADT is set to 5 000, 10 000 and 20 000 vehicles per day. For each of the nine cases, the interest rate was varied between 0 to 6,0 %. The sensitivity analysis was made as a comparison of the original carbon steel layout and one using the stainless steel grade EN 1.4162.

6.3 Retaining Wall

The retaining wall which has been redesigned using stainless steel reinforcement is presented in Section 5.1. The structure is located in Örebro, Sweden and was built in 2018. As of today, there has been no maintenance or repair works reported in BaTman, the Swedish bridge and tunnel management system. The general conditions of the bridge and bridge site need to be specified in the LCC analysis, which requires some assumptions. Regarding the rate of deterioration due to exposure to hard environments, the climate zone was specified to middle Sweden, and the road salting was assumed to be normal. The calculus period was set to the service life, 100 years.

Concerning traffic on the bridge, no data is available for the specific road, 675, in Örebro. On the other hand, it is of interest to see the influence of traffic on the final result. Consequently, the average daily traffic (ADT) will vary from that of a small, non-urban road to that of a larger road in an urban area, making it possible to identify the conditions where it is most advantageous to apply stainless steel reinforcement. In the same way, it can be argued that the speed limit should also be allowed to vary. Another important parameter, which has a large impact on the final results, is the interest rate, which is independent of the conditions of the specific structure, but is nonetheless important to study. The upper and lower limits for these parameters are presented in Section 6.2.5. Other influencing parameters are the vehicle operation cost (VOC), traffic delay costs (TDC) and percentage of heavy traffic on the road. These parameters are given in Section 6.2.4.

In reinforcement layouts 3, 4, 5, 6 and 7, stainless steel reinforcement is used. The stainless steel has much higher corrosion resistance than ordinary carbon steel, leading to the assumption that the structure will be much more durable. This assumption can be made on the basis of studying existing stainless steel reinforced concrete structures, in particular the Progreso pier, described in Section 2.5. The structure has been exposed to harsh sea-climate for more than 80 years, without needing any significant repair works (Mistry *et al.*, 2016). On the basis of this, the interval between repair works for the stainless steel reinforced cases (RL 3, 4, 5, 6 and 7) is assumed to be longer than the service life of the structure, which is 100 years. The costs and other related parameters required to calculate the costs of operation, inspection and repair are given in Table 6.2. The cost of repair is given from the Swedish Road Administration (Trafikverket, 2017).

6.4 Slab-Frame Bridge

The slab-frame bridge which is redesigned using stainless steel is presented in Section 5.2. In similarity to the retaining wall, there has been no reported maintenance or repair works conducted for the slab-frame bridge, making it necessary to estimate costs using historical data concerning bridges in Sweden. The general conditions of the bridge and bridge site need to be specified in the LCC analysis. The climate zone was specified to lower part of northern Sweden, and the road salting was assumed to be normal, which concerns the rate of deterioration due to exposure to hard environments. The calculus period was set to the service life which is 50 years.

Regarding important parameters, as the speed limit or number of vehicles passing the bridge every day, the LCC for the slab-frame bridge was conducted in a similar way as for the retaining wall, using a sensitivity analysis to identify the least and most beneficial cases. The upper and lower values of these parameters can be seen in Section 6.2.5.

The investment cost for the slab-frame bridge is estimated using the costs in Table 6.1. For the slab-frame bridge, there is an increased number of elements to consider, as the wing walls, bridge deck and foundation slab.

The service life of the bridge is 50 years and based on data collected from existing slab-frame bridges, the assumption was made to repair the bridge one time during its service life. This is however only for RL 1, since the stainless steel designs are considered to last the whole service life. Although, repairs such as insulation, surfacing and parapet replacement, which can be seen in Table 6.3 is conducted for all designs. The costs for the bridge repair is retrieved from the Swedish Road Administration (Trafikverket, 2017).

For the slab-frame bridge, the important parameters are similar to that of the retaining wall, see Section 6.2.5 and thus, the sensitivity analysis has been conducted with the same method. The sensitivity analysis for the slab-frame bridge was made for RL 1, which is the original carbon steel design and RL 3, which is the design with EN 1.4162.

7 Results

The following chapter presents the results obtained from the redesign of reinforcement and the life cycle cost analysis conducted for the two case studies presented previously. The resulting reinforcement amounts are based on the calculations presented in Chapter 5. The following results of the LCC are based on the assumptions and calculations presented in Chapter 6. First, the results for seven reinforcement layouts used in the LCC of the retaining wall are presented, along with different environmental and economical conditions that have an impact on the results. Secondly, the results of the slab-frame bridge are presented in a similar manner but for the reinforcement layouts are limited to five cases.

7.1 Reinforcement Amounts for Retaining Wall

An overview of the results of the reinforcement redesign is given in Figure 7.1. The largest reduction in material usage can be achieved by applying a crack width limitation of 0,8 mm and using a steel with f_{yk} = 800 MPa. However, it can also be seen that the additional savings are small when using a steel of f_{yk} >700 MPa.

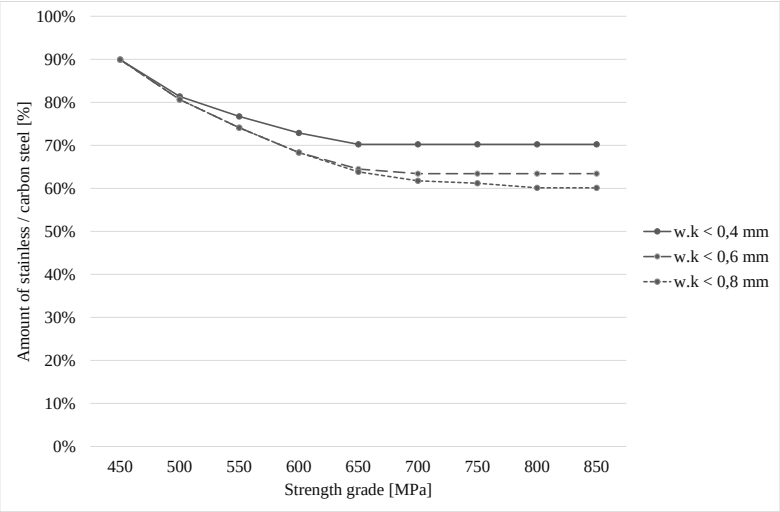

Figure 7.1 Possible reduction in material usage when using stainless steel compared to the original reinforcement arrangement using B500B and a crack width limitation of 0,4 mm. The results are presented using stainless steel strengths ranging from 450 to 850 MPa and crack width limitations ranging from 0,4 to 0,8 mm.

Regarding the difference between the reinforcement required in ULS and SLS for the crack width limitation of 0,4 mm, the amounts are presented in Figure 7.2. The reinforcement amount required for the minimum reinforcement is also given separately and is applied as surface reinforcement, as well as in the bottom of the base plate and on the outer side of the front wall. The required amount of surface reinforcement varies with the yield stress of the reinforcement. In Figure 7.3 and 7.4, it can be seen that the amount required to fulfill the demand in SLS decreases as a result of the increasing crack width limitation. Regarding the amount required in ULS, it decreases with increasing tensile strength.

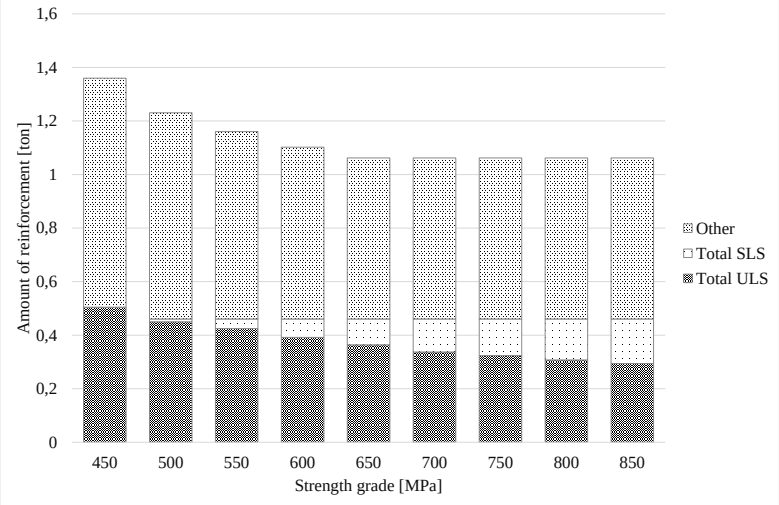

Figure 7.2 Total amounts of reinforcement required in SLS and ULS when a crack width limitation of 0,4 mm is applied. The amount required in SLS is the additional amount needed, as well as the amount in ULS, to fulfill the crack width limitation. The reinforcement categorized under "other" is the minimum amount of reinforcement which is applied where neither SLS nor ULS is designing.

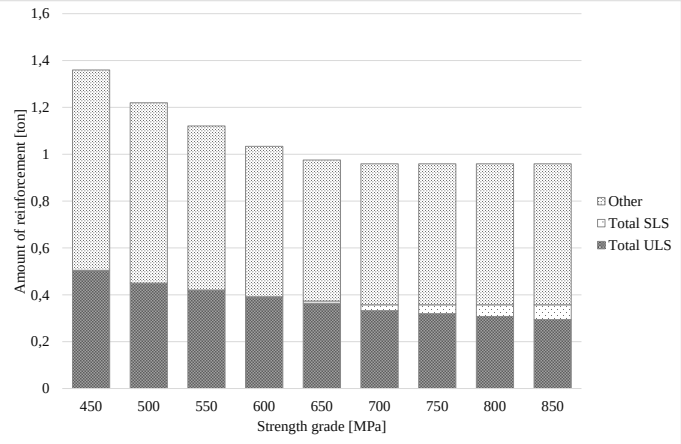

Figure 7.3 Total amounts of reinforcement required in SLS and ULS when a crack width limitation of 0,6 mm is applied. The amount required in SLS is the additional amount needed, as well as the amount in ULS, to fulfill the crack width limitation. The reinforcement categorized under "other" is the minimum amount of reinforcement which is applied where neither SLS nor ULS is designing.

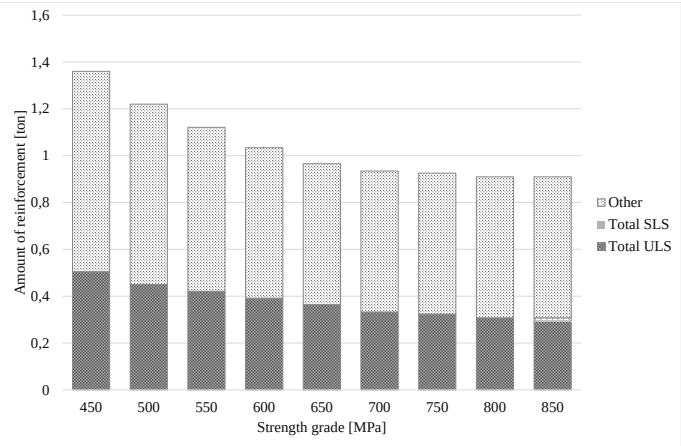

Figure 7.4 Total amounts of reinforcement required in SLS and ULS when a crack width limitation of 0,8 mm is applied. The amount required in SLS is the additional amount needed, as well as the amount in ULS, to fulfill the crack width limitation. The reinforcement categorized under "other" is the minimum amount of reinforcement which is applied where neither SLS nor ULS is designing.

7.1.1 Redesign of the Reinforcement in the Base Plate

In the design of the top reinforcement of the base plate, the designing factor in ULS was determined to be the moment capacity. In SLS, the crack width limitation was the designing parameter and additional reinforcement had to be added when using a steel strength higher than 450 MPa and designing according to the current crack width limitation of 0,4 mm, which can be seen in Figure 7.5. In order to completely eliminate the situations when SLS is designing, a crack width limitation of 0,8 mm can be implemented for all of the used steel strengths. At high steel strengths ($\sigma_0 > 700$ MPa), minimum reinforcement could be used to fulfill the requirements in the checks, meaning that there is no additional reduction of reinforcement amount when using a steel strength higher than 700 MPa and a crack width limitation of 0,8 mm.

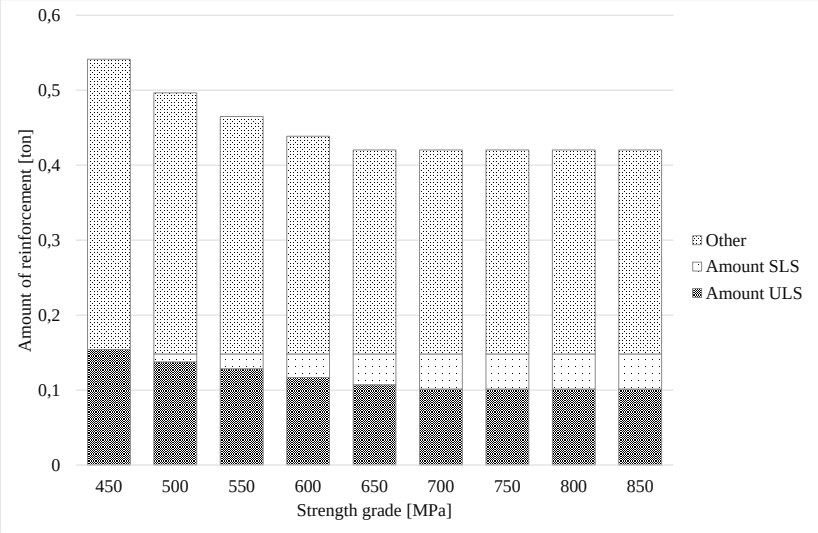

Figure 7.5 Amount of reinforcement in the base plate of the retaining wall required for steel strengths varying from 450 MPa to 850 MPa when the crack width limitation was set to 0,4 mm.

7.1.2 Redesign of the Reinforcement in the Front Wall

Regarding the front wall, the designing factor in ULS was the tensile force capacity and in SLS the crack width limitations, as could be expected. When higher strength steels were used, ULS always required higher amounts of reinforcement than minimum. The crack width limitation of 0,6 mm results in additional reinforcement required for strength grades higher than 650 MPa. Using a crack width limitation of 0,8 mm and a steel strength of 800 MPa or lower, no additional reinforcement was required to fulfill the demands in SLS. When designing according to the current standards, using a crack width

limitation of 0,4 mm, the required amounts of reinforcement can be seen in Figure 7.6.

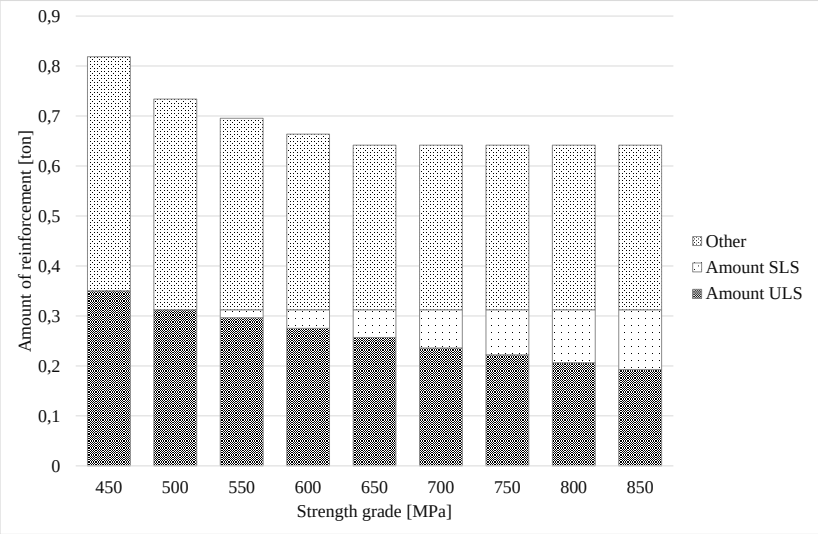

Figure 7.6 Amount of reinforcement required for steel strengths varying from 450 MPa to 850 MPa in the front wall when the crack width limitation was set to 0,4 mm.

When comparing the results of the optimization to the original layout of the reinforcement, it can be seen that the objective when designing the original carbon steel reinforcement was to provide a structure which is easy to build. Considering the fact that stainless steel is about six times more expensive than ordinary carbon steel, another optimization process was required when redesigning the stainless steel reinforcement. Instead, the focus was having a high utilization ratio and a small amount of reinforcement, resulting in significantly smaller amount of reinforcement being required.

7.2 Results of LCC Analysis for the Retaining Wall

The result of the LCC analysis conducted for the seven different reinforcement layouts will be summarized in this section. First, the investment costs for the layouts will be presented, followed by the total costs depending on the conditions of the LCC. An interest rate of 2 % is assumed when presenting the general results of the LCC, which is recommended for bridge construction (Safi, 2013). Furthermore, the results for an urban area (ADT of 20 000 vehicles per day and speed limit of 50 km/h) are compared to that of a non-urban area (ADT of 5 000 vehicles per day and speed limit of 80 km/h). These two environments are set in order to compare the results of how successfully stainless steel reinforcement can be implemented in different areas.

7.2.1 Agency Costs

When considering only the agency cost of the seven different alternatives, it remains constant and unaffected by the conditions of the LCC, such as ADT, interest rate and so on. The investment costs are presented in Table 7.1. It can be seen that the stainless steel alternatives are more expensive than the original design, except for RL 5, which is marginally cheaper than the original design.

Table 7.1 Investment costs as a part of the total agency costs for the seven reinforcement layouts. The possible total profit for the agency is stayed, as well as the increase or decrease of investment cost compared to the original reinforcement layout.

	RL 1	**RL 2**	**RL 3**	**RL 4**	**RL 5**	**RL 6**	**RL 7**
Agency costs [SEK]	667 224	651 475	534 958	513 762	508 121	511 762	517 563
Profit agency cost [%]	0	2	25	30	31	30	29
Investment cost [SEK]	296 895	282 578	320 743	301 474	296 345	299 655	304 929
Investment cost [%]	0	-5	+8	+2	-0,2	+1	+3

7.2.2 Total Costs

The total cost during the life cycle of the structure depend on the conditions of the site where the structure is located, as well as the economical climate. The following two sections presents how the results are affected by the area of application. The first area is an urban area, followed by a non urban area.

7.2.2.1 Urban Area

When assuming an interest rate of 2 %, together with a speed limit of 50 km/h and an ADT of 20 000 vehicles/day, which could be assumed for an urban area, the results show that the most cost efficient design is reinforcement layout 5, see Figure 7.7. This layout is the stainless steel design with the lowest investment cost. This design contains stainless steel grade EN 1.4162 with a crack width limitation of 0,6 mm, as is mentioned in Section 5.1.5. The possible financial gains over the total life cycle of the structure can be seen in Table 7.2. When using RL 5, the total cost over the service life can be reduced by 50 % in comparison to the original reinforcement layout.

Table 7.2 Possible win or loss when implementing the seven reinforcement layouts in an urban area, assuming an interest rate of 2 %. The possible profit when implementing RL 2-6 are compared to the cost of RL 1.

Cost	**RL 1**	**RL 2**	**RL 3**	**RL 4**	**RL 5**	**RL 6**	**RL 7**
Net present value [SEK]	944 506	928 757	658 294	637 098	631 457	635 098	640 899
Profit [%]	0	2	43	48	50	49	47

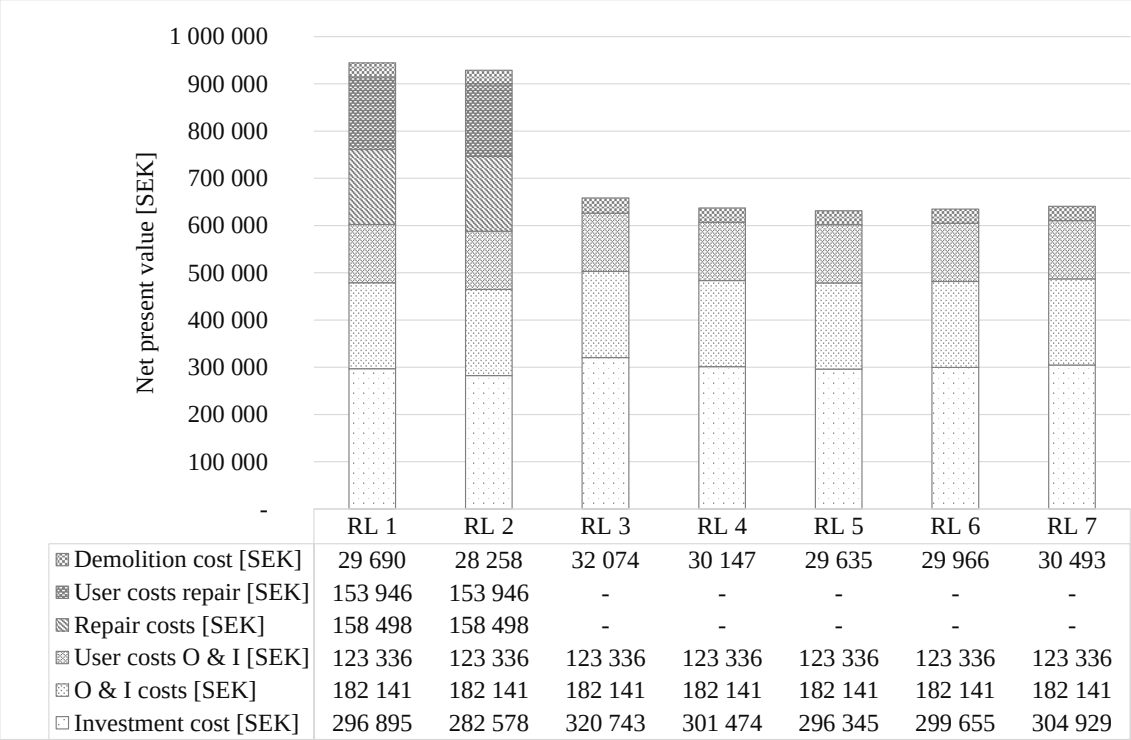

	RL 1	RL 2	RL 3	RL 4	RL 5	RL 6	RL 7
Demolition cost [SEK]	29 690	28 258	32 074	30 147	29 635	29 966	30 493
User costs repair [SEK]	153 946	153 946	-	-	-	-	-
Repair costs [SEK]	158 498	158 498	-	-	-	-	-
User costs O & I [SEK]	123 336	123 336	123 336	123 336	123 336	123 336	123 336
O & I costs [SEK]	182 141	182 141	182 141	182 141	182 141	182 141	182 141
Investment cost [SEK]	296 895	282 578	320 743	301 474	296 345	299 655	304 929

Figure 7.7 Results of LCC for the seven reinforcement layouts when assuming an interest rate of 2 %, ADT of 20 000 vehicles/day and speed limit set to 50 km/h.

Concerning the cost of demolition, it is estimated to 10 % of the investment cost, as mentioned in Section 6.1.1. This assumption results in higher demolition costs when using the stainless steel, due to the higher investment costs. The costs associated with repair can be divided into user costs and the cost of the actual repair, which is an agency cost. In Figure 7.7, it can be seen that the present value of the repair cost arises to over 100 000 SEK. These costs affect only RL 1 and 2, resulting in lower costs for all of the stainless steel alternatives (RL 3-7) when considering only the agency costs, see Table 7.3.

Table 7.3 Possible win or loss for the users when implementing the seven reinforcement layouts, assuming an interest rate of 2 %. The user costs are also given in percentage of the total costs.

Cost	**RL 1**	**RL 2**	**RL 3**	**RL 4**	**RL 5**	**RL 6**	**RL 7**
User costs [SEK]	277 282	277 282	123 336	123 336	123 336	123 336	123 336
User costs/total cost [%]	29,4	29,8	18,7	19,4	19,5	19,4	19,2

To summarize the results of the LCC when comparing different reinforcement solutions in an urban area with a high traffic flow, it can be seen that all of the stainless steel solutions offer lower costs when considering the whole life span of the structure. It can also be seen that the user costs amount to 30 % of the total costs for RL 1, which is the original carbon steel reinforcement design. When implementing the most cost-beneficial reinforcement design, RL 5, the user costs amount to 20 % of the net present value of the total life cycle costs.

When considering the costs over the life cycle of the structure, it can be seen that all of the stainless steel options become more profitable than the carbon steel reinforced layout after 50 years, which is the anticipated time for the first repair of the front wall. Up to that point, the costs occurring after the inauguration are equal for all of the studied reinforcement layouts since equal costs for operation and maintenance are assumed. However, when concerning RL 5, the break-even point is obtained earlier, since the investment cost is slightly lower than that of RL 1, which can be seen in Table 7.1. This difference is very small, but highlights the fact that even the investment cost could be reduced when designing with stainless steel reinforcement.

7.2.2.2 Non-Urban Area

When implementing stainless steel reinforcement in an area with less traffic (5 000 vehicles/day) and a higher initial speed limit (80 km/h), the total life cycle costs of the structure are reduced for all of the studied reinforcement layouts, which can be seen in Figure 7.8. The reduction of costs is due to lower user costs associated with the lower volume of traffic, than compared to an urban area. However, in Table 7.4, it can be seen that stainless steel is still economically beneficial when considering the total life cycle costs of the structure, saving 34 % if reinforcement layout 5 is chosen. If RL 3 is chosen, which is in accordance with current standards, 28 % of the total life cycle costs can be saved.

Table 7.4 Possible win or loss when implementing the seven reinforcement layouts in a non-urban area, assuming an interest rate of 2 %. The possible profit when implementing RL 2-6 are compared to the cost of RL 1.

Cost	**RL 1**	**RL 2**	**RL 3**	**RL 4**	**RL 5**	**RL 6**	**RL 7**
Net present value [SEK]	706 217	690 468	552 302	531 106	525 465	529 106	534 907
Profit [%]	0	2	28	33	34	33	32

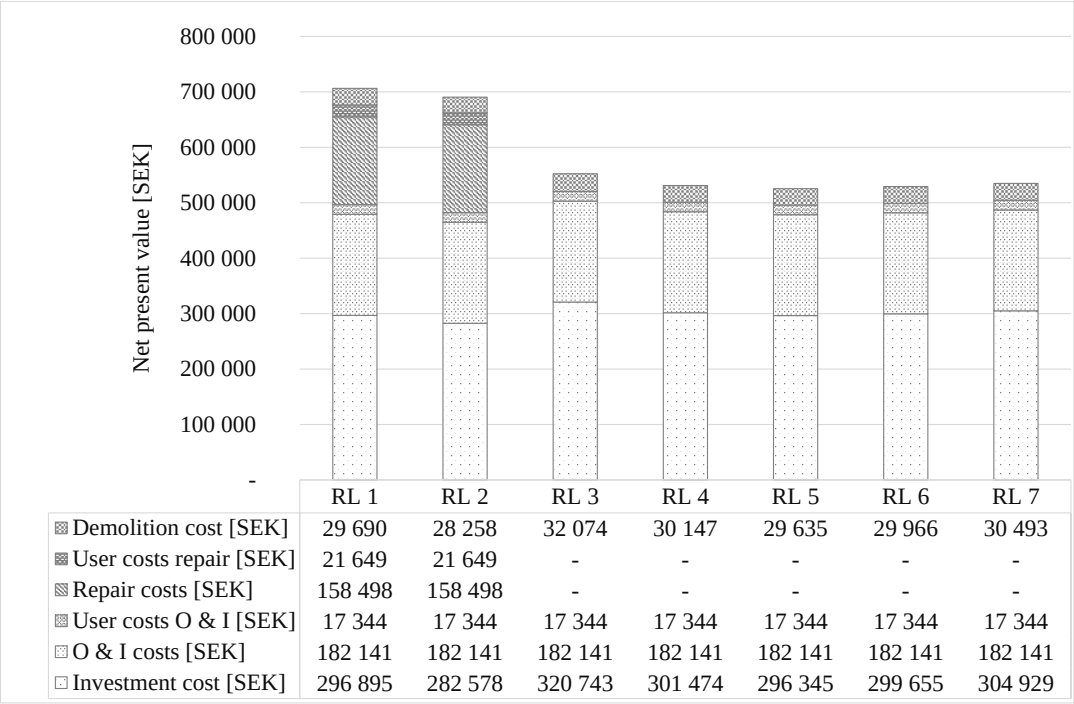

	RL 1	RL 2	RL 3	RL 4	RL 5	RL 6	RL 7
Demolition cost [SEK]	29 690	28 258	32 074	30 147	29 635	29 966	30 493
User costs repair [SEK]	21 649	21 649	-	-	-	-	-
Repair costs [SEK]	158 498	158 498	-	-	-	-	-
User costs O & I [SEK]	17 344	17 344	17 344	17 344	17 344	17 344	17 344
O & I costs [SEK]	182 141	182 141	182 141	182 141	182 141	182 141	182 141
Investment cost [SEK]	296 895	282 578	320 743	301 474	296 345	299 655	304 929

Figure 7.8 Result of LCC using an interest rate of 2 % and assuming conditions of a non-urban area; an ADT of 5 000 vehicles per day and a speed limit 80 km/h.

Table 7.5 Possible win or loss for the users when implementing the seven reinforcement layouts, assuming an interest rate of 2 %. The user costs of each RL are compared to the total life cycle cost of the same RL.

Cost	**RL 1**	**RL 2**	**RL 3**	**RL 4**	**RL 5**	**RL 6**	**RL 7**
User cost [SEK]	38 993	38 993	17 344	17 344	17 344	17 344	17 344
User cost/total cost [%]	5,5	5,6	3,1	3,2	3,3	3,3	3,2

When considering only the agency cost of the structure in a non-urban environment, they remain the same as for the case of an urban environment, which can be seen when comparing Table 7.5 and 7.3. This is due to the fact that only the user costs are affected by the ADT and the speed limit. However, it can be seen that the user costs are reduced when compared to that of an urban environment, and amount to 6 % of the net present value for RL 1. When considering RL 5, the user costs make up about 3 % of the net present value. The higher user costs of RL 1 is due to the repair needed for the structures containing carbon steel reinforcement.

In order to see how the total life cycle cost is influenced by the investment cost and how the possible fluctuation of stainless steel prices influence the analysis, it is of interest to see how much the price of stainless steel could increase. The total life cycle costs for RL 5, using the values assumed in this section were compared to that of RL 1. This comparison showed that in order for RL 5 to become less profitable than RL 1, the lean duplex EN 1.4162 would have to cost ca. 180 000 SEK/ton, which is approximately 6.5 times its current price (28 000 SEK/ton).

7.2.3 Sensitivity Analysis of Results

The results presented above only show two cases, and there are an infinite number of conditions that will affect the results of the LCC. In order to study the effect of the different parameters, a sensitivity analysis is performed. The upper and lower limits of the parameters (ADT, speed limit and interest rate) are presented in Section 6.2.5. This section will show how the aforementioned parameters affect the economical profit of the LCC.

The sensitivity analysis is performed for two of the reinforcement layouts; RL 1, which is the original design using carbon steel reinforcement and RL 5, which is the most cost-efficient design using stainless steel. The sensitivity analysis compares the net present value of the total costs of RL 1 to that of RL 5, and the potential gain of using RL 5 is given as a profit [%], which can be seen in Equation 7.1.

$$P = \frac{C_{RL1}}{C_{RL5}} - 1 \tag{7.1}$$

where P is the profit [%], C_{RL1} and C_{RL5} are the net present values [SEK] using RL 1 and RL 5.

The results of the sensitivity analysis using speed limit 50 km/h can be seen in Figure 7.9, along with the results when the speed limit is set 80 km/h, in Figure 7.10, and 110 km/h in Figure 7.11. The results show that a lower interest rate results in stainless steel reinforcement being more profitable than carbon steel reinforcement. A real interest rate of 0 %, in combination with an ADT of 20 000 vehicles per day results in the cost of RL 5 being 81 % lower than that of RL 1. These conditons give the most favourable results for RL 5. In contrast, a high real interest rate in combination with a low ADT results in the profit of using RL 5 only amounts to 8 %.

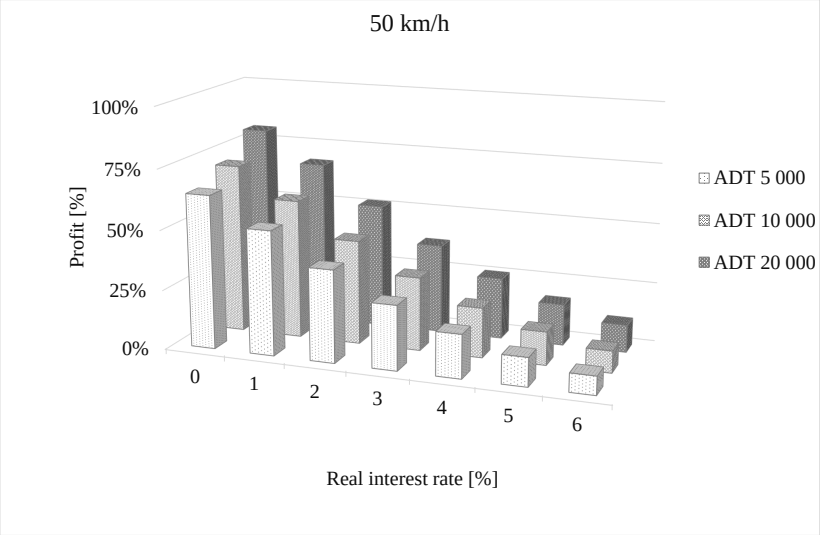

Figure 7.9 The result of a sensitivity analysis showing how the possible profit is affected by the interest rate and the ADT, when the speed limit is set to 50 km/h and the reduced speed limit to 30 km/h.

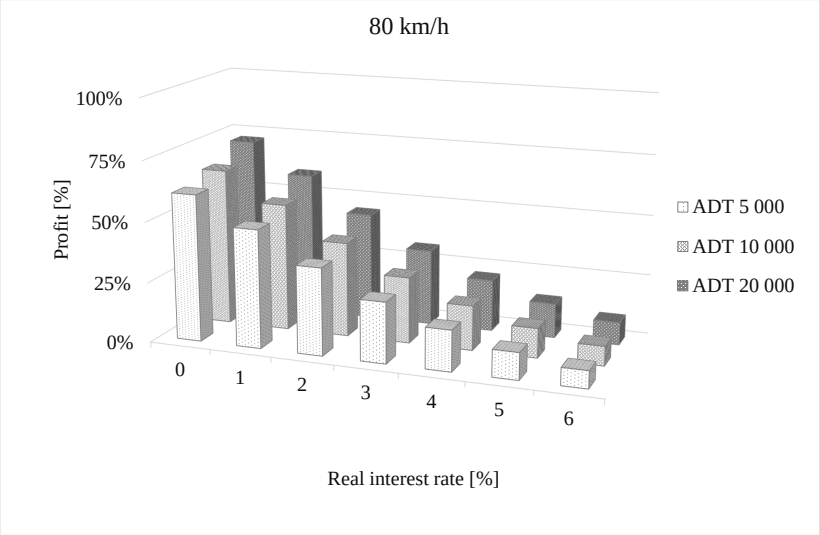

Figure 7.10 The result of a sensitivity analysis showing how the possible profit is affected by the interest rate and the ADT, when the speed limit is set to 80 km/h and the reduced speed limit to 50 km/h.

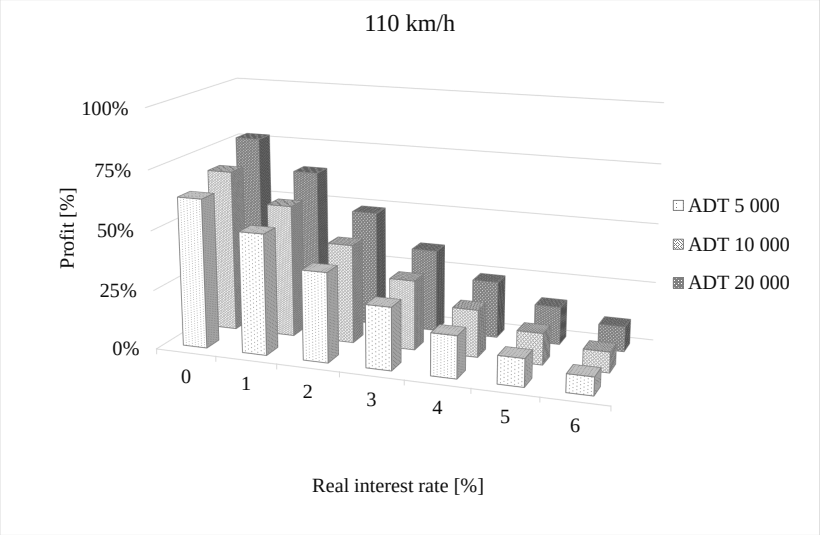

Figure 7.11 The result of a sensitivity analysis showing how the possible profit is affected by the interest rate and the ADT, when the speed limit is set to 110 km/h and the reduced speed limit to 50 km/h.

Similar results can be seen when a speed limit of 80 km/h and reduced speed limit of 50 km/h is applied. Although, it can be seen that the profit is less for the case of 80 km/h than for the case of 50 km/h, which can be explained by the difference in reduced speed limit. The profit of using RL 5 compared to RL 1 varies from 7 % to 72 % when the speed limit is set to 80 km/h. A profit of only 7 % when using the stainless steel reinforcement compared to the original reinforcement layout is the least profitable scenario and this is obtained when the ADT is 5 000 vehicles per day, the interest rate is 6 % and the speed limit is 80 km/h.

The results of the analysis using a speed limit of 110 km/h and reduced speed limit of 50 km/h can also be seen in Figure 7.11. The profit is higher than for the case of 80 km/h but still less than for the case of 50 km/h and varies between 8 % and 77 %. The lowest value in the interval is achieved when the ADT is 5000 vehicles per day and the interest rate is 6 %, and the highest profit is when the ADT is 20 000 vehicles per day and the interest rate is zero.

7.2.4 "Best and Worst Case Scenarios" when Implementing Stainless Steel Reinforcement

The sensitivity analysis showed that the difference in profit margin between the stainless and carbon steel designs increases with the average daily traffic. This results in stainless steel becoming more cost efficient and therefore more favorable with the increasing traffic flow, resulting in cases where stainless steel is profitable to use and where it is not profitable to use. In order to fully investigate the profitability of stainless steel reinforcement, additional LCCs were performed for the seven reinforcement layouts described in Section 5.1.5. The additional LCCs were performed assuming best and worst scenarios.

In Figure 7.12 the result of an analysis conducted assuming the conditions where stainless steel reinforcement is the least favourable - the worst case scenario. This scenario results in very low user, repair and inspection costs since a high interest rate is assumed in combination with a low ADT. It can be seen that the investment costs accounts for about 75 % for all of the seven reinforcement layouts. It can also be noted that the use of RL 3, which is design in accordance with current standards, results in total costs higher than the original reinforcement design, RL 1. The other stainless steel reinforcement layouts all give profitable results, even when assuming the "worst case" scenario.

When assuming conditions which are the most profitable for stainless steel reinforcement, the resulting total costs are much higher, as can be seen in Figure 7.13. This is due to a combination of the fact that the interest rate on costs occurring in the future is very low and that the user costs are high (high ADT, low speed limit). The low interest rate results in high repair, maintenance and user costs, amounting up to 900 % of the investment costs. This "best case" scenario results in the costs of the carbon steel reinforcement layouts being about 1,8 times more expensive than the layouts using stainless steel reinforcement.

7.2.5 Summary of LCC Results for Retaining Wall

In Table 7.6, the results of the urban and non-urban area conditions presented in Section 7.2.2.1 and 7.2.2.2 are compared with the "best and worst case" scenarios. It can be seen that the "best case" scenario results in costs for the stainless steel reinforcement layouts (RL 3-7) amounting to about 55 % of the original carbon steel reinforcement design (RL 1). When assuming the "worst case" the cost of RL 3-7 vary from 94 % to 100 % of RL 1.

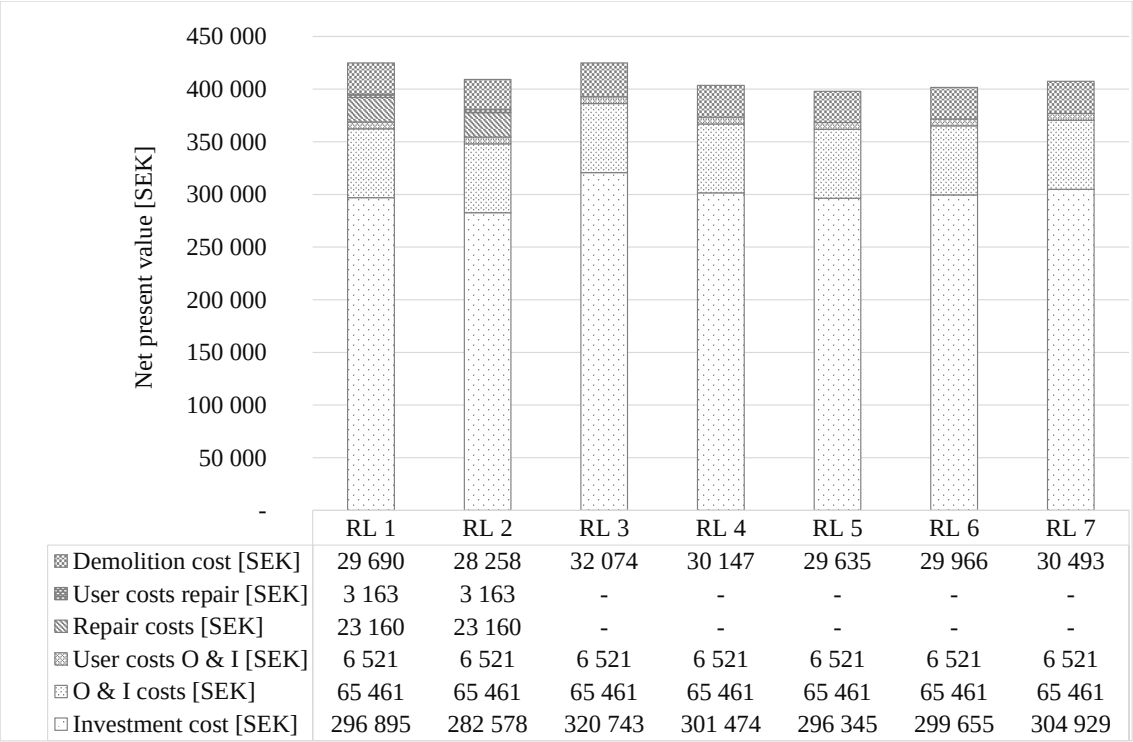

	RL 1	RL 2	RL 3	RL 4	RL 5	RL 6	RL 7
Demolition cost [SEK]	29 690	28 258	32 074	30 147	29 635	29 966	30 493
User costs repair [SEK]	3 163	3 163	-	-	-	-	-
Repair costs [SEK]	23 160	23 160	-	-	-	-	-
User costs O & I [SEK]	6 521	6 521	6 521	6 521	6 521	6 521	6 521
O & I costs [SEK]	65 461	65 461	65 461	65 461	65 461	65 461	65 461
Investment cost [SEK]	296 895	282 578	320 743	301 474	296 345	299 655	304 929

Figure 7.12 The total life cycle costs for the seven reinforcement layouts when assuming conditions that are least favourable to stainless steel reinforcement.

Table 7.6 Profit that can be made for the different reinforcement layouts and cases, in comparison to the original design.

Case	**RL 2**	**RL 3**	**RL 4**	**RL 5**	**RL 6**	**RL 7**
Worst case [%]	4	0	5	7	6	4
Non-urban area [%]	2	28	33	34	33	32
Urban area [%]	2	43	48	50	49	47
Best case [%]	1	76	80	81	80	79

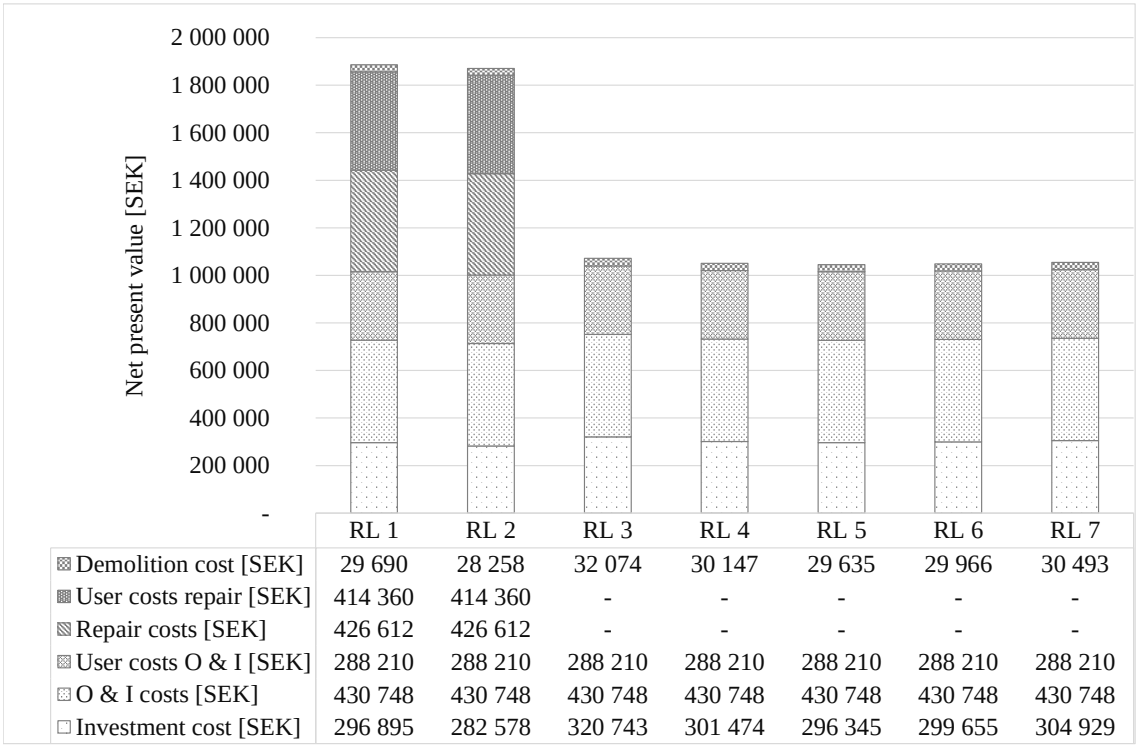

	RL 1	RL 2	RL 3	RL 4	RL 5	RL 6	RL 7
Demolition cost [SEK]	29 690	28 258	32 074	30 147	29 635	29 966	30 493
User costs repair [SEK]	414 360	414 360	-	-	-	-	-
Repair costs [SEK]	426 612	426 612	-	-	-	-	-
User costs O & I [SEK]	288 210	288 210	288 210	288 210	288 210	288 210	288 210
O & I costs [SEK]	430 748	430 748	430 748	430 748	430 748	430 748	430 748
Investment cost [SEK]	296 895	282 578	320 743	301 474	296 345	299 655	304 929

Figure 7.13 The total life cycle costs for the seven reinforcement layouts when assuming conditions that are most favourable to stainless steel reinforcement.

7.3 Reinforcement Amounts for Slab-Frame Bridge

The results of the re-design process, such as the resulting stainless and carbon steel amounts and the utilization ratios in ULS and SLS will be presented in this section. The required reinforcement amounts were calculated separately for each element of the bridge and then added to the total amount. The total amount of reinforcement can be seen in Table 7.7 and more graphically in Figure 7.14.

Table 7.7 Total amount of reinforcement in the Slab-Frame Bridge.

Reinforcement type	RL	Total amount [ton]	Carbon steel [ton]	Stainless steel [ton]	Reduction [%]
B500B	1	6,44	6,44	0	0 %
EN 1.4162 EC	2	6,81	2,25	4,56	-5 %
EN 1.4162	3	5,87	2,04	3,83	10 %
EN 1.4462	4	5,53	2,01	3,52	16 %
800 MPa	5	5,13	1,79	3,34	26 %

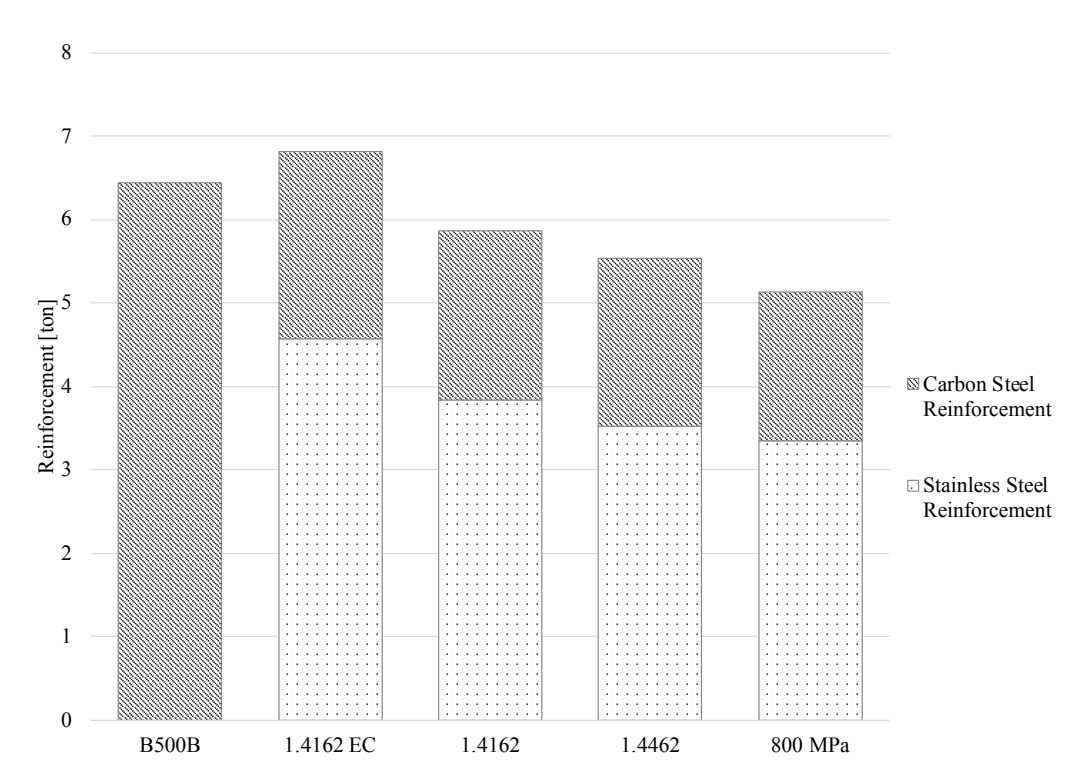

Figure 7.14 Total amount of reinforcement in the slab-frame bridge for the five reinforcement types.

7.3.1 Redesign of Reinforcement in the Bridge Deck

The required amount of reinforcement in the bridge deck can be seen in Figure 7.15. When considering RL 2 compared to RL 1, it can be seen that there is an increase of 2% in the required amount of reinforcement. Regarding the other stainless steel reinforcement layouts, the amount of reinforcement can be reduced by 13 % for RL 3, 20 % for RL 4 and 30 % for RL 5.

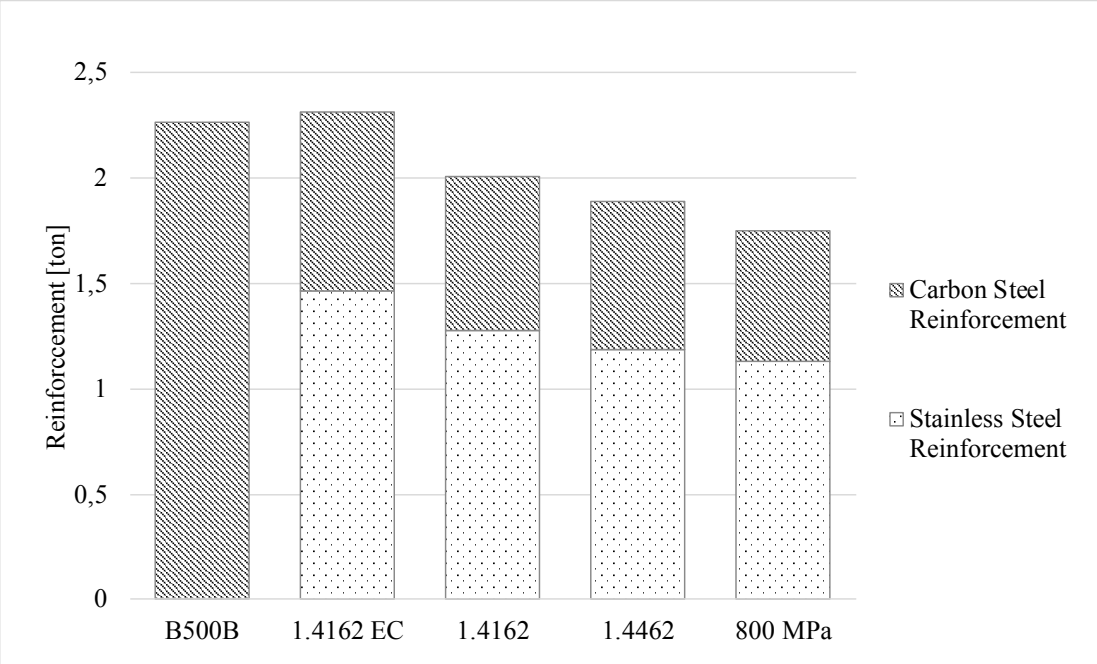

Figure 7.15 Amount of reinforcement in the bridge deck for the five reinforcement types.

Regarding the designing state of the bridge deck, there was no differentiation between the amount required in ULS and SLS, as was done for the retaining wall. Instead, the utilization ratios were noted to provide an idea of whether ULS or SLS is designing and it can be seen that ULS was designing in RL 1, 2 and 3. SLS was only designing when steel strengths higher than 690 MPa were used. These ratios can be seen in Table 7.8. The utilization ratios in FLS were not included in the table since they were never a designing factor.

Table 7.8 Utilization ratios when re-designing the bridge deck.

	Span				Support			
	Longitudinal		Transversal		Longitudinal		Transversal	
Reinforcement type	**ULS**	**SLS**	**ULS**	**SLS**	**ULS**	**SLS**	**ULS**	**SLS**
B500B (RL 1)	94 %	21 %	90%	43%	92 %	61 %	79 %	24 %
EN 1.4162 EC (RL 2)	100 %	27 %	98%	41%	97 %	85 %	98 %	29 %
EN 1.4162 (RL 3)	100 %	33 %	98%	69%	98 %	98 %	98 %	37 %
EN 1.4462 (RL 4)	100 %	36 %	98%	88%	98 %	108 %	98 %	51 %
800 MPa (RL 5)	100 %	40 %	97%	81%	98 %	120 %	100 %	65 %

7.3.2 Redesign of Reinforcement in the Front Wall

The required amount of reinforcement in the front wall can be seen in Figure 7.16. When comparing RL 2,3,4 and 5 to RL 1, it can be seen that RL 2 results in an increase of reinforcement by 9 % and a reduction by 9 %, 19 % and 27 % for RL 3, 4 and 5 respectively.

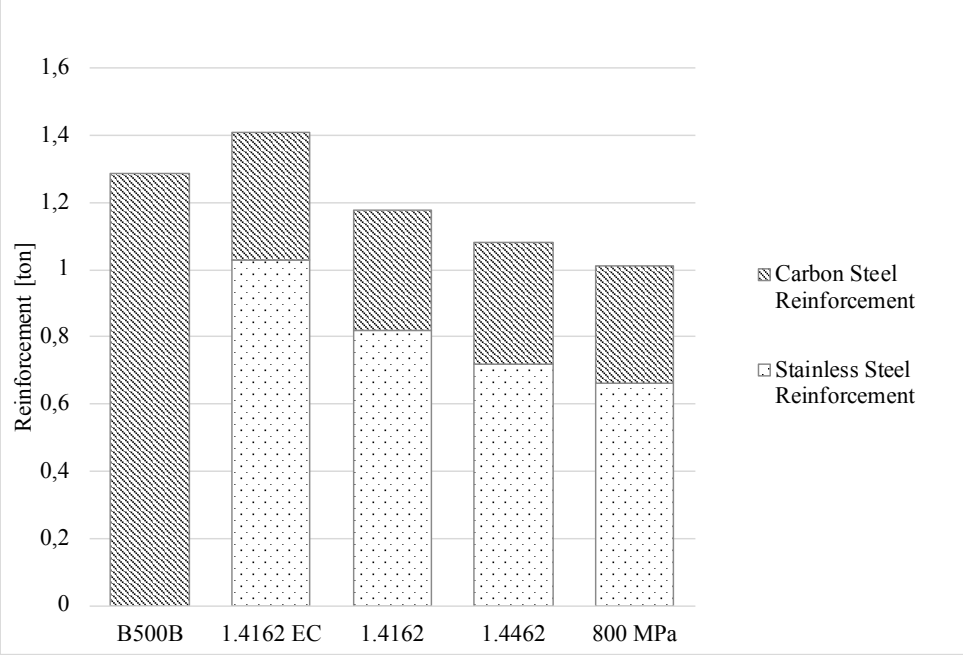

Figure 7.16 Total amount of reinforcement in the front wall of the slab-frame bridge for the five considered reinforcement types.

Concerning whether ULS, SLS or FLS is designing in the front wall, it can be seen that ULS was designing when the crack width limitation is implemented, (RL 1 and 2). If the same limitation was implemented for RL 3, 4 and 5, SLS would have been designing. However, since these designs use

stainless steel in the outer layers, it is assumed that the utilization ratio for thecrack width limitation can be increased to 200 %, resulting in ULS being designing for these cases as well. The utilization ratios can be seen in Table 7.9.

Table 7.9 Utilization ratios when re-designing the front wall.

	Longitudinal				**Vertical**			
	Span		**Support**		**Top**		**Bottom**	
Reinforcement type	**ULS**	**SLS**	**ULS**	**SLS**	**ULS**	**SLS**	**ULS**	**SLS**
B500B	93 %	50 %	111 %	100 %	100 %	27 %	97 %	71 %
EN 1.4162 EC	96 %	44 %	90 %	98 %	100 %	25 %	99 %	61 %
EN 1.4162	97 %	74 %	98 %	127 %	100 %	27 %	99 %	101 %
EN 1.4462	99 %	97 %	100 %	154 %	99 %	31 %	100 %	127 %
800 MPa	100 %	94 %	98 %	158 %	99 %	37 %	98 %	166 %

7.3.3 Redesign of Reinforcement in the Wing Walls

The total required amount of reinforcement in all the four wings can be seen in Figure 7.17. The possible reduction in reinforcement amounts for the short and the long wing wall are very similar. RL 2 results in an increase of material usage of 5 % for both the walls. A reduction of material usage of 10 % (RL 3), 12 % (RL 4) and 24 % (RL 5) is possible for the long wing wall and 5% (RL 3), 9 % (RL 4) and 23 % (RL 5) for the short wing wall.

Concerning whether ULS or SLS were designing in the wing walls, it can be seen that ULS was designing for RL 1 and 2 in the transversal direction. However, in the longitudinal direction SLS is designing for RL 2, and high utilization ratios are reached for both the short and the long wing wall. These ratios can be seen in Table 7.10 and 7.11.

Table 7.10 Utilization ratios when re-designing the short wing wall.

	Longitudinal		**Vertical**	
Reinforcement type	**ULS**	**SLS**	**ULS**	**SLS**
B500B	81,4 %	66,0%	109,0%	27,0%
EN 1.4162 EC	98,4 %	100,0%	97,7%	30,0%
EN 1.4162	98,2 %	153,0%	95,3%	34,0%
EN 1.4462	99,6 %	152,0%	70,5%	32,0%
800 MPa	97,2 %	160,0%	87,4%	42,0%

Table 7.11 Utilization ratios when re-designing the long wing wall.

	Longitudinal		Transversal	
Reinforcement type	**ULS**	**SLS**	**ULS**	**SLS**
B500B	105,2 %	93,0 %	93,0 %	45,0 %
EN 1.4162 EC	90,0 %	98,0 %	98,2 %	44,0 %
EN 1.4162	94,8 %	161,0 %	84,2 %	50,0 %
EN 1.4462	95,0 %	145,0 %	69,3 %	50,0 %
800 MPa	96,1 %	177,0 %	85,0 %	71,0 %

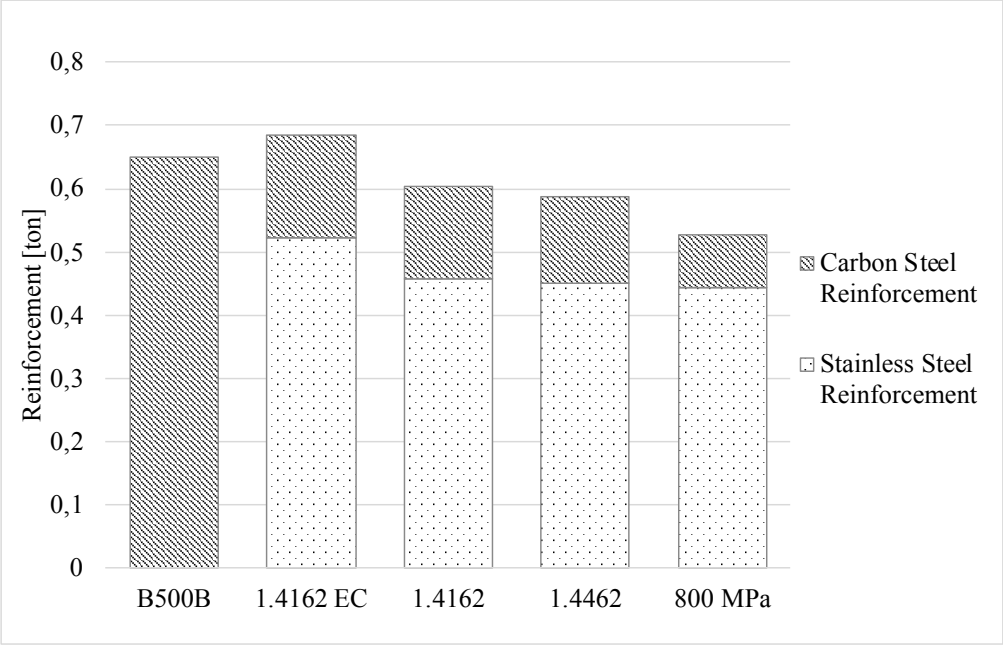

Figure 7.17 Total amount of reinforcement in the wing walls of the slab-frame bridge for the five considered reinforcement types.

7.4 Results of LCC Analysis for Slab-Frame Bridge

In this section, the results of the LCC analysis of the slab-frame bridge will be presented. These results consist of five different design layouts in several different conditions, as mentioned in Section 5.2. These results are then evaluated based on a sensitivity analysis, where the speed limit, ADT and interest rate is varied to both find sensible parameters and the scenarios where stainless steel is the most and least favourable. Finally, the results of these "best and worst case" scenarios are presented.

7.4.1 Agency Costs

When considering only the agency cost of the five different alternatives, the cost remains constant and unaffected by the conditions of the LCC, such as ADT. The agency and investment costs are presented in Table 7.12. It can be seen that the stainless steel alternatives are less expensive than the original design, but requires a higher investment cost.

Table 7.12 Agency and investment costs for the five reinforcement layouts.

	B500B	**1.4162 EC**	**1.4162**	**1.4462**	**800 MPa**
Agency costs [SEK]	2 237 064	1 810 845	1 738 761	1 747 785	1 756 897
Profit agency cost [%]	0	19,1	22,3	21,9	21,5
Investment cost [SEK]	1 185 444	1 410 463	1 344 932	1 353 135	1 361 419
Difference investment cost [%]	0	+19	+13	+14	+15

7.4.2 Total Costs

The total cost during the life cycle of the structure depend on the conditions of the site where the structure is located, as well as the economical climate. The following two sections presents how the results are affected by the area of application. Firstly, the result of a bridge located in an urban area will be presented. This will be followed by the results of a bridge located in a non-urban area in order to get an estimation of where stainless steel is the most suitable to implement.

7.4.2.1 Urban Area

The results of the LCC analysis when implementing the reinforcement layouts in an urban area, using an interest rate of 2 % with a speed limit of 50 km/h and an ADT of 20 000 vehicles/day can be seen in Table 7.13. The result also shows that when designing with reinforcement layout 3 instead of the original design, a total saving of 55 % can be achieved.

Table 7.13 Possible win or loss when implementing the five reinforcement layouts in an urban area, assuming an interest rate of 2 %. The possible profit when implementing RL 2-5 are compared to the cost of RL 1.

Cost	RL 1	RL 2	RL 3	RL 4	RL 5
Net present value [SEK]	4 213 652	2 791 328	2 719 244	2 728 268	2 737 380
Profit total cost [%]	0	51	55	54	54

In Figure 7.18, it can be seen that the investment cost of the stainless steel alternatives (RL 2-5) is between 159 000-250 000 SEK higher than for the original design. However, the repair costs and the user costs induced by repair are 1 669 000 SEK more expensive for the carbon steel design than for the stainless steel design. Thus, considering the whole service life of the bridge, all stainless steel designs are more cost-efficient with a margin that can be seen in Table 7.13.

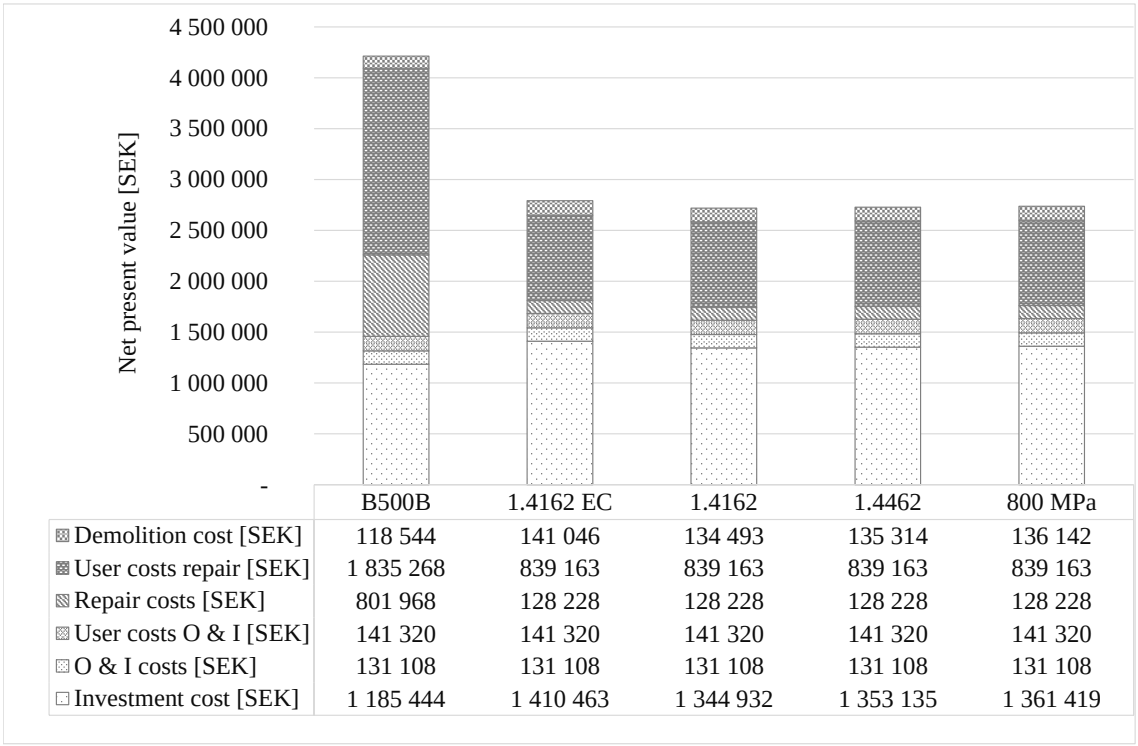

	B500B	1.4162 EC	1.4162	1.4462	800 MPa
Demolition cost [SEK]	118 544	141 046	134 493	135 314	136 142
User costs repair [SEK]	1 835 268	839 163	839 163	839 163	839 163
Repair costs [SEK]	801 968	128 228	128 228	128 228	128 228
User costs O & I [SEK]	141 320	141 320	141 320	141 320	141 320
O & I costs [SEK]	131 108	131 108	131 108	131 108	131 108
Investment cost [SEK]	1 185 444	1 410 463	1 344 932	1 353 135	1 361 419

Figure 7.18 The total life cycle costs for the five reinforcement layouts when assuming conditions that corresponds to an urban area and assuming an interest rate of 2 %.

7.4.2.2 Non-urban Area

The results of this LCC analysis are based on the conditions of a non-urban area, with a speed limit of 80 km/h, a reduced speed limit of 50 km/h and an ADT of 5 000 vehicles/day. The LCC analysis was made using the five reinforcement layouts described in Section 5.2

In Figure 7.19, it can be seen that the investment costs for the alternatives are equivalent to the urban area. However, the user costs induced by repair are heavily reduced. For this case, the repair and user costs induced by repair are 813 000 SEK more expensive for the carbon steel alternative than for the stainless steel alternatives, making the stainless steel designs more profitable over the service life.

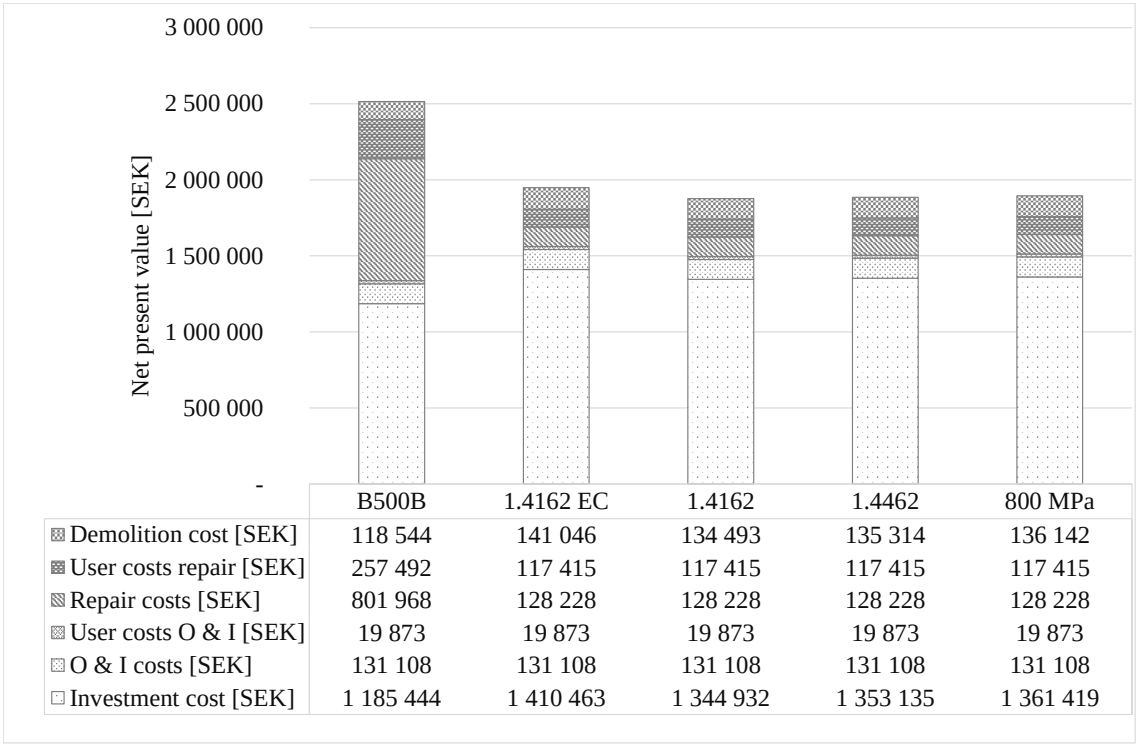

	B500B	1.4162 EC	1.4162	1.4462	800 MPa
Demolition cost [SEK]	118 544	141 046	134 493	135 314	136 142
User costs repair [SEK]	257 492	117 415	117 415	117 415	117 415
Repair costs [SEK]	801 968	128 228	128 228	128 228	128 228
User costs O & I [SEK]	19 873	19 873	19 873	19 873	19 873
O & I costs [SEK]	131 108	131 108	131 108	131 108	131 108
Investment cost [SEK]	1 185 444	1 410 463	1 344 932	1 353 135	1 361 419

Figure 7.19 The total life cycle costs for the five reinforcement layouts when assuming conditions that are least favourable to stainless steel reinforcement.

In Table 7.14, the profit of the different alternatives can be seen. The design with EN 1.4162 according to Eurocode (RL 2) is the least cost efficient alternative, but still has a profit of 29 % in comparison to the original design.

Table 7.14 Possible win or loss when implementing the five reinforcement layouts in a non-urban area, assuming an interest rate of 2 %. The possible profit when implementing RL 2-5 are compared to the cost of RL 1.

Cost	**RL 1**	**RL 2**	**RL 3**	**RL 4**	**RL 5**
Net present value [SEK]	2 514 429	1 948 133	1 876 049	1 885 076	1 894 185
Profit [%]	0	29	34	33	33

7.4.3 Sensitivity Analysis of Results

The sensitivity analysis compares the net present value of the two design alternatives when the speed limit, ADT and interest rate is varied. The upper and lower bound for these parameters can be seen in Section 7.2.3. The analysis is performed for two of the reinforcement layouts; RL 1, which is the original design using carbon steel reinforcement and RL 3, which is the most cost-efficient design using stainless steel.

The results of the sensitivity analysis using speed limit 50 km/h can be seen in Figure 7.20, The results when the speed limit is set to 80 km/h can be seen in Figure 7.21 and 110 km/h in 7.22 respectively. The results show that a lower interest rate and a higher ADT results in stainless steel reinforcement being more profitable than carbon steel reinforcement. The results of the sensitivity analysis are described below;

- When combining a speed limit of 50 km/h, a real interest rate of 0 %, an ADT of 20 000 vehicles per day and a reduced speed limit of 30 km/h, a saving of 70 % can be made when using RL 3, which is equivalent of the most favourable case. In contrast, when using a real interest rate of 6 % and an ADT of 5 000 vehicles per day, the profit of using RL 3 is only up to 12 %.
- When increasing the speed limit to 80 km/h and the reduced speed limit to 50 km/h, a real interest rate of 0 % and ADT of 20 000 vehicles per day results in a saving of 64 %. A real interest rate of 6 % and ADT of 5 000 vehicles per day results in a saving of 10 %, which corresponds to the least favourable case.
- When further increasing the speed limit to 110 km/h, but keeping the reduced speed limit to 50 km/h, the saving makes up to 68 % when using a real interest rate of 0 % and an ADT of 20 000 vehicles per day. For the case of 0 % interest rate and ADT of 5 000 vehicles per day, the possible saving is 11 %.

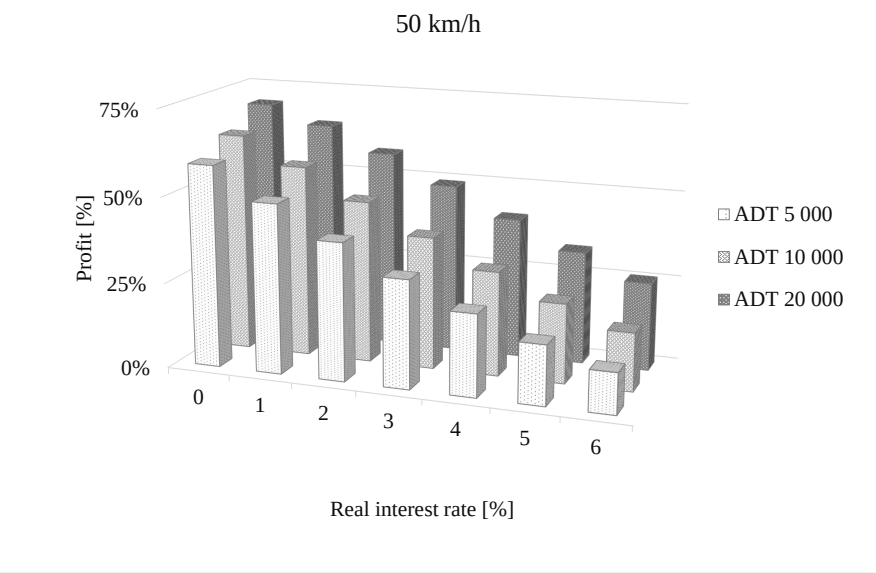

Figure 7.20 The result of a sensitivity analysis showing how the possible profit is affected by the interest rate and the ADT, when the speed limit is set to 50 km/h and the reduced speed limit to 30 km/h.

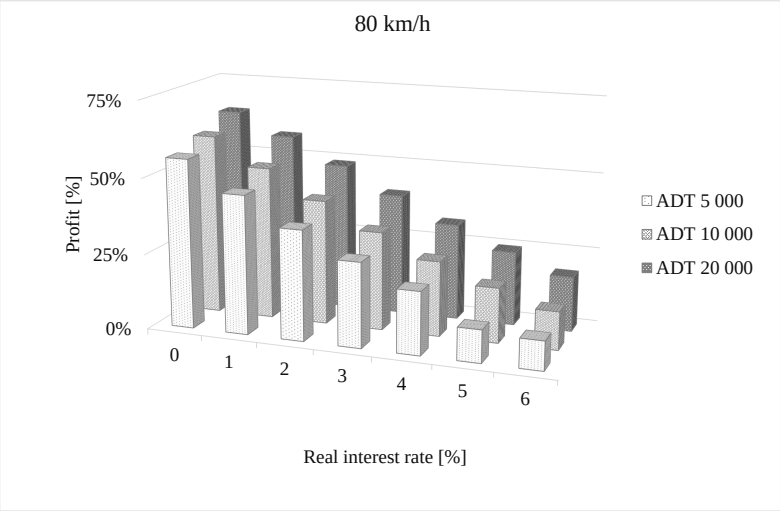

Figure 7.21 The result of a sensitivity analysis showing how the possible profit is affected by the interest rate and the ADT, when the speed limit is set to 80 km/h and the reduced speed limit to 50 km/h.

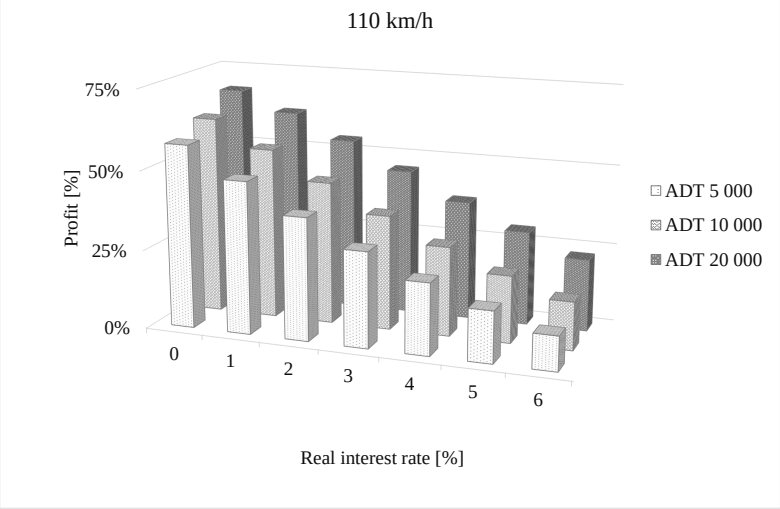

Figure 7.22 The result of a sensitivity analysis showing how the possible profit is affected by the interest rate and the ADT, when the speed limit is set to 110 km/h and the reduced speed limit to 50 km/h.

7.4.4 "Best and Worst Case Scenarios" when Implementing Stainless Steel Reinforcement

The results of the sensitivity analysis showed how the profit of the stainless steel alternative increases with the increasing traffic and decreasing interest rate. In order to fully investigate the profitability of stainless steel in different conditions, additional LCCs were performed for the five different reinforcement layouts, assuming a best and a worst case scenario.

Figure 7.23 presents the result of an analysis conducted assuming the conditions where stainless steel reinforcement is the most favourable, which is an interest rate of 0 %, an ADT of 20 000 vehicles per day, speed limit of 50 km/h and reduced speed limit of 30 km/h. Even for the stainless steel design with EN 1.4162 according to standards today (RL 2), the possible gain is 2 784 000 SEK, in comparison to the original design with carbon steel. When using the most cost efficient stainless steel design (RL 3), the possible gain is estimated to 2 856 000 SEK.

On the contrary, Figure 7.24 presents the result of an analysis conducted assuming the least favourable conditions for stainless steel reinforcement. The conditions are an interest rate of 6 %, an ADT of 5 000 vehicles per day, speed limit of 80 km/h and reduced speed limit of 50 km/h. These conditions still results in the design with EN 1.4162 according to standards today (RL 2) being 55 000 SEK less expensive. When using the most cost efficient stainless steel design (RL 3), the possible gain makes up to 127 000 SEK, even when assuming the worst case scenario.

7.4.5 Summary of LCC Results for Slab-frame Bridge

In order to summarize the results of the LCC conducted for the slab-frame bridge, the profit is presented for the different cases and reinforcement layouts in Table 7.15. Here, the results of the urban and non-urban area are presented with the results of the "best" and "worst" case scenarios.

Table 7.15 Profit that can be made for the different reinforcement layouts and cases, in comparison to the original design.

Case	RL 2	RL 3	RL 4	RL 5
Worst case [%]	3	8	7	7
Non-urban area [%]	29	34	33	33
Urban area [%]	51	55	54	54
Best case [%]	68	71	70	70

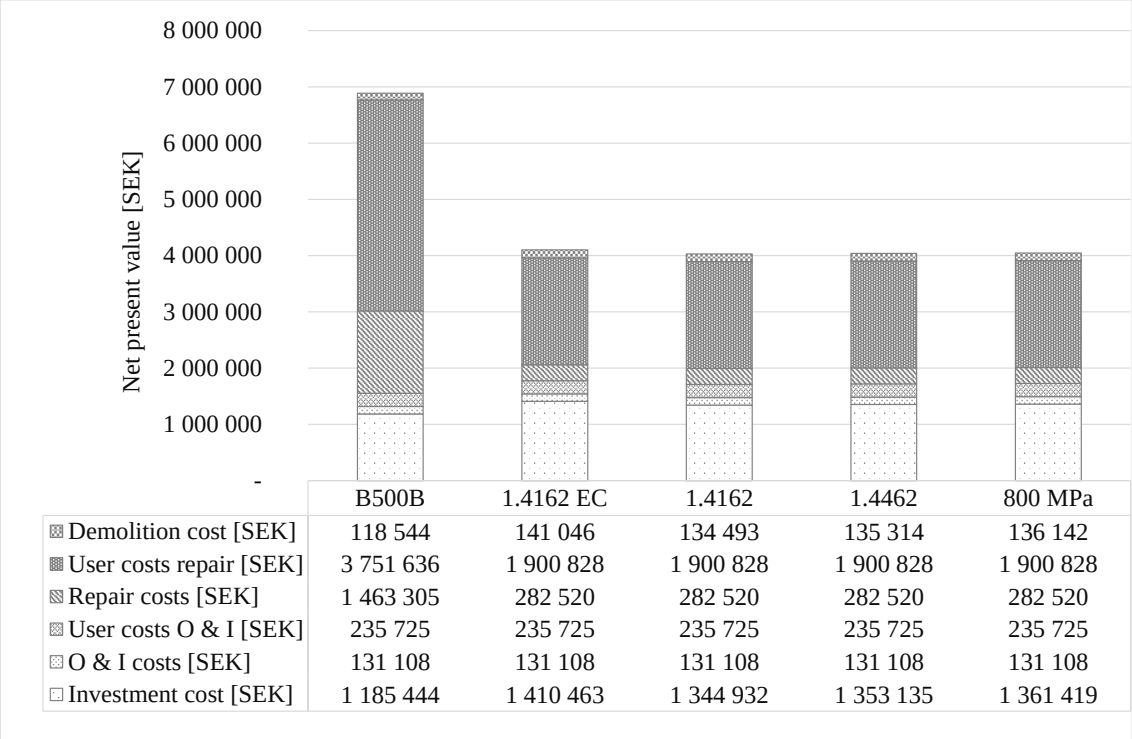

	B500B	1.4162 EC	1.4162	1.4462	800 MPa
Demolition cost [SEK]	118 544	141 046	134 493	135 314	136 142
User costs repair [SEK]	3 751 636	1 900 828	1 900 828	1 900 828	1 900 828
Repair costs [SEK]	1 463 305	282 520	282 520	282 520	282 520
User costs O & I [SEK]	235 725	235 725	235 725	235 725	235 725
O & I costs [SEK]	131 108	131 108	131 108	131 108	131 108
Investment cost [SEK]	1 185 444	1 410 463	1 344 932	1 353 135	1 361 419

Figure 7.23 The total life cycle costs for the five reinforcement layouts when assuming conditions that are most favourable to stainless steel reinforcement.

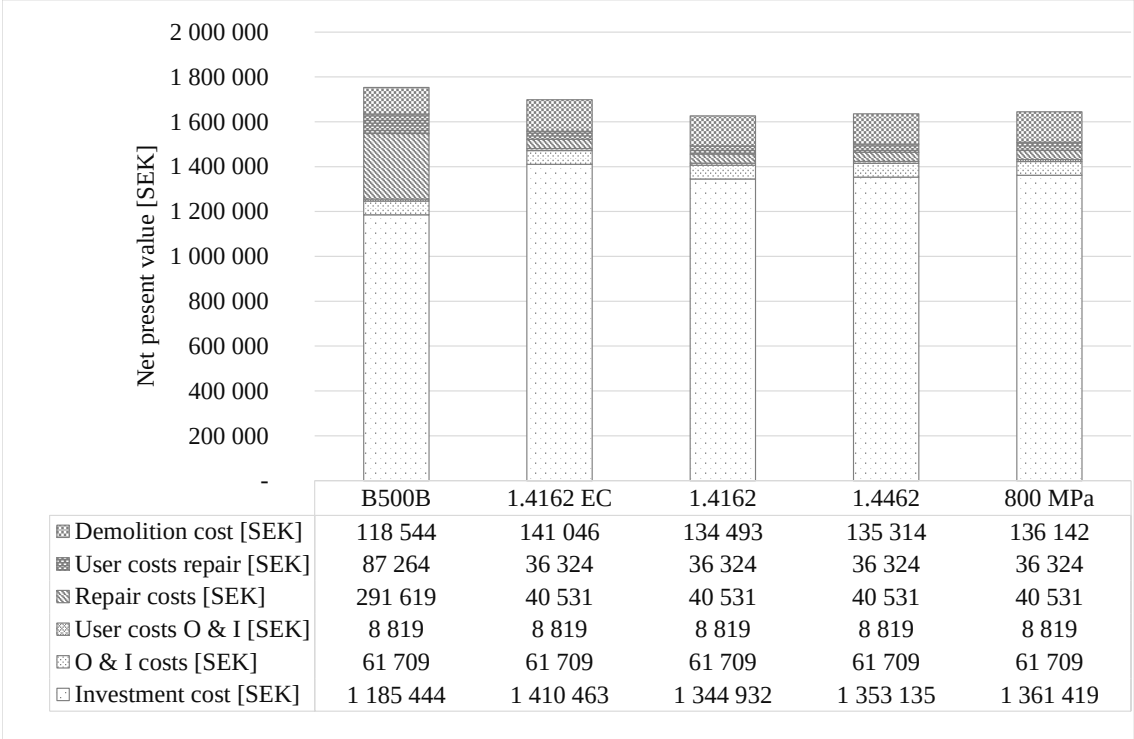

	B500B	1.4162 EC	1.4162	1.4462	800 MPa
Demolition cost [SEK]	118 544	141 046	134 493	135 314	136 142
User costs repair [SEK]	87 264	36 324	36 324	36 324	36 324
Repair costs [SEK]	291 619	40 531	40 531	40 531	40 531
User costs O & I [SEK]	8 819	8 819	8 819	8 819	8 819
O & I costs [SEK]	61 709	61 709	61 709	61 709	61 709
Investment cost [SEK]	1 185 444	1 410 463	1 344 932	1 353 135	1 361 419

Figure 7.24 The total life cycle costs for the five reinforcement layouts when assuming conditions that are least favourable to stainless steel reinforcement.

8 Discussion

In the following chapter, the results of the study are analyzed and discussed. Initially, the calculation method for the stainless steel designs are commented with potential measures for improvement, followed by a discussion of the assumptions made in the LCC, which can be a potential source of uncertainty in the study. Furthermore, the discussion mentions the areas of the study which could be improved either by a more extensive study or by more research in the specific scientific field.

8.1 Scope of the Cases Studied and Calculations

The redesign of the retaining wall was, as mentioned in Section 5.1, performed according to a calculation procedure for a retaining wall using carbon steel reinforcement and further developed to include stainless steel reinforcement. Consequently, the results are based on previous analyses, which were adapted for stainless steel. However, since the results were verified for the carbon steel design, the results were deemed viable.

Regarding the slab-frame bridge, the calculation procedure was, as mentioned in Section 5.2, partly conducted without a template for the calculation procedure and thus causing an uncertainty. These calculations were partly based on the calculations obtained from the retaining wall and partly from literature, see Section 5.2.1. The calculation procedure was verified by comparison with the original design.

Concerning the required amount of reinforcement for both cases, further optimization is possible when using stainless steel reinforcement. This is due the fact that a bi-linear relationship was assumed in ULS, which was designing for most layouts using stainless steel reinforcement. The possible increase in strength using the non-linear material model in ULS is described in Section 2.5.3. Consequently, the use of this model would lead to higher capacity and therefore to a possible reduction in reinforcement amounts, hence leading to lower investment costs.

An advantage of stainless steel reinforcement which was not exploited during this study is due to the fact that the concrete cover can be reduced leading to an increased internal lever arm. Consequently, this would result in an even lower amount of reinforcement required for the same moment capacity. However, in these cases, a reduction of concrete cover was not possible due to the fact that the maximum aggregate size was the designing factor for the concrete cover.

In Section 2.1.1, it is described how the quality of the concrete influences the durability. If the corrosion of reinforcement was not a concern, a concrete mix with a higher water to cement ratio could be used, resulting in a less expensive concrete mix. This possible reduction of concrete quality was not included

in this study, but would lead to even lower investment costs.

8.2 Limitations of the LCC Analyses

The results of the sensitivity analyses indicated that the ADT, interest rate and reduction of speed limit has a large influence on the result of LCCs. An increasing ADT results in more users and thus causing the user costs to increase. A low interest rate leads to a higher cost of future actions, consequently leading to higher repair, maintenance and user costs. In contrast, a high interest rate leads to lower future costs. Furthermore, the results of the sensitivity analyses show that it is not the reduced speed limit itself which influences the user costs, but the reduction in speed limit.

Subsequently, a higher interest rate, lower ADT and lower reduction in speed limit would result in the designs using stainless steel reinforcement becoming less favourable. This trend could be observed in the presented sensitivity analysis and what is deemed obvious is that the upper and lower bounds of the analyzed parameters is hard to estimate, resulting in the fact that the worst case scenario could become even worse in some situations.

Furthermore, there are several assumptions, such as cost of repairs, that influence the results which were not included in the sensitivity analysis and thus causes a potential source of uncertainty in the study. For the carbon steel designs, the assumption is that repair for the exposed structural members will occur one time during its service life. The cost of repair actions as well as the time intervals of the actions have a large influence on the agency costs and thus is a factor that have a large impact on the final results. In reality, the repair actions could be needed even more frequently, causing the stainless steel designs to become more beneficial.

As can be seen in Chapter 3, the cost of repair is usually higher in reality than what is assumed in the LCC analyses. However, the exact total repair cost of the existing bridges is hard to estimate. Although, it is probably safe to state that the total repair cost for the slab-frame bridge studied in Section 5.2 will be substantially higher than estimated in the LCC, consequently resulting in stainless steel becoming even more favourable. However, the interval of repair on the slab-frame bridge is set to 25 years in the LCC analysis, since the service life is only 50 years. The data presented in Section 3.7 show that the repairs usually occur more than 50 years after the inauguration of the bridge, resulting in the fact that no repairs would be required for any of the reinforcement layouts studied for the slab-frame bridge. Although, assuming a longer service life for the bridge, and that repairs take place after 50 years, the cost of repair would be reduced in the LCC as it occurs at a later time, due to a positive interest rate.

Another potential source of uncertainty for the LCC analysis is the duration and length of construction site needed for repair works. These parameters influence the user costs but are hard to estimate due to their dependency on the life cycle management plan of the structure. If all the needed repairs are conducted

at the same time, the duration of the work will be longer than if point-efforts are made to maintain the construction. To improve the accuracy of the results, a deeper investigation of the maintenance and repair of the structures would be required, but when comparing with the costs presented in Chapter 3, the cost of repairing the structures are reasonable.

8.3 Interpretation of Results

To reconnect to the purpose and problems of the study, the result shows that the reinforcement amount can be reduced when using stainless steel due to the relaxed crack width limitations, as was one of the intended investigations of the study. This result is further enhanced by the utilization of the higher strength available for stainless steel reinforcement in comparison to ordinary carbon steel reinforcement.

The results of the redesign of the retaining wall show that ULS was designing in the majority of cases. The initial idea behind this study was to implement stainless steel where SLS was designing in order to reduce the amount of reinforcement required due to crack width limitations in SLS. However, this opportunity was not exploited fully in the case studies. Thus, in structures where SLS is designing, increased profits could be expected when designing with stainless steel reinforcement.

The results of the LCC indicates in which conditions stainless steel is the most suitable. In this study, stainless steel reinforcement is the most profitable option for all cases and the profit amounts to 70 % for some specific, favourable conditions. As mentioned in the section before, only a very high interest rate in combination with a low ADT would result in stainless steel becoming more expensive over the entire service life. Consequently, the most suitable application areas for stainless steel reinforcement in bridge design would be where repair actions would cause large traffic disturbance. Although, as can be seen in the results, it can be argued that stainless steel reinforcement has a broad application area, since all the stainless steel designs are profitable also in the non-urban area.

The results of the study are in accordance with a trend worldwide, which is the use of stainless steel reinforcement as the outermost layer in exposed bridge parts, as mentioned in Chapter 4. However, the use of stainless steel reinforcement is not very common today. One possible reason behind the limited use of stainless steel could be the lack of authoritative guidelines. Another reason could be due to the fact that traditionally, only the investment cost is taken into consideration when deciding which material to use. As was seen in Section 4.2.1, stainless steel was chosen when the whole life cycle of the structure was considered.

Although this specific study investigates the profitability of stainless steel in short slab-frame bridges and retaining walls, much suggests that the use of stainless steel reinforcement could be profitably applied in other bridge types. However, the representativity of the cases in this study can be questioned since it can

be argued that small bridges are more expensive than large bridges per square meter. This is partly due to the fact that the investment cost is more affected by the higher material cost of using stainless steel reinforcement. Therefore, the results are not directly transmittable to larger bridges and more research increasing the scope of the study should be carried out.

8.4 Possible Problems when Implementing Stainless Steel Rebars

Concerning the behaviour of stainless steel reinforcement, it is somewhat unclear if it can be assumed to remain stainless under "normal" circumstances. Based on the report regarding the Progreso pier, mentioned in Section 2.5, it can be assumed that no major repairs will be needed. On the other hand, the stainless steel grade used in the Progreso pier had a very high content of Nickel, which was mentioned in Section 2.5.2 as the alloying element which contributes most to corrosion resistance. Nickel is also one of the more expensive alloys and therefore, it would be very expensive to use the same steel grade today. As was mentioned in Section 2.6.1, none of the stainless steels used in tests remained corrosion free during the extent of the tests. However, it can be argued that the environment in which the studies were carried out were not always consistent with the cold climate of Sweden and thus representative of reality. Subsequently, it is not possible to determine whether the stainless steel reinforced structures will be repair-free for at least a hundred years. The uncertainty lies in the use of lean duplex EN 1.4162, since it is a low-alloyed stainless steel and therefore more susceptible to corrosion than the duplex alternatives. On the other hand, the lean duplex steel is the most profitable according to the results of the study since it has a lower price. Although, as can be seen in the investment costs for the different cases, the design using duplex grade EN 1.4462 is only marginally more expensive, but with a considerate increase in corrosion resistance, making it a more suitable choice concerning durability aspects.

Traditionally, the risk of galvanic corrosion when combining stainless steel reinforcement with carbon steel reinforcement, as mentioned in Section 4.2, has lead to the use of polyethylene sleeves to protect the reinforcement bars. However, as is indicated in Section 2.4.4, there risk of galvanic corrosion can be eliminated when the carbon steel reinforcement is protected by the passivization of concrete. In this study, the second layer of carbon steel reinforcement is deemed to be embedded deep enough (over 100 mm) into the concrete to ensure passivization if the material during the entire service life.

9 Conclusion

The aim of this study was to build more durable concrete structures by increasing the knowledge of stainless steel reinforcement in bridge design and furthermore to evaluate the profitability along with advisable areas of application. To summarize, the following concluding remarks arose from the problem description;

1. For the studied cases and conditions, it is financially profitable to use stainless steel reinforcement in concrete bridges when considering the life-cycle of the structures.
2. The relaxation of crack width limitations, along with a higher strength leads to a reduction of the amount of reinforcement needed for the slab-frame bridge and the retaining wall.
3. When designing with stainless steel reinforcement, the literature study indicates that the crack width limitations can be relaxed while assuming fewer repairs during the service life.
4. It is possible to design a structure combining stainless steel and carbon steel reinforcement if the carbon steel is embedded in the passive state of the concrete.

An important part of the aim was to present design situations where it is advisable to use stainless steel reinforcement, these are summarized as;

- Stainless steel reinforcement is most suitable to implement as the outermost reinforcement layer in bridge members which are exposed to de-icing salts or other aggressive agents.
- The conditions where stainless steel reinforcement is considered more favorable are where there is a high volume of traffic and a high reduction of speed needed for repair or maintenance.

9.1 Suggestions for Further Study

As mentioned in Chapter 8, there are still some uncertainties regarding stainless steel reinforcement and its application in bridge design. To conclude the study, the following remarks are suggested for future research;

- Further experiments regarding the corrosion resistance of stainless steel reinforcement in cracked concrete.
- Develop a calculation procedure which utilizes the strength of stainless steel using a non-linear material model to determine the stress in ULS.
- Further develop tools to help estimate repair costs when performing a LCC analysis.

References

American Arminox (2010). *MNDOT - Hastings Bridge Project to Use 367 Tons of Arminox UNS S32304 Stainless for 3rd Bridge Project*. URL: http://americanarminox.com/html/mn%7B%5C_%7Dhastings.html (visited on 02/15/2018) (cit. on p. 41).

Bertolini, L. and M. Gastaldi (2011). "Corrosion resistance of low-nickel duplex stainless steel rebars". In: *Materials and Corrosion* 62.2, pp. 120–129. ISSN: 09475117. DOI: 10.1002/maco.201005774 (cit. on p. 27).

Bohlin, K. and R. Snibb (2016). "Carbonation of concrete Effect of mineral additions and influence on transport properties". In: (cit. on p. 12).

BSSA (2003). *the Use of Stainless Steel Reinforcement in Bridges*. Tech. rep. April, pp. 1–4 (cit. on p. 25).

Burström, P. G. (2007). *Byggnadsmaterial*. Lund: Studentlitteratur. ISBN: 978-91-44-02738-8 (cit. on pp. 6–9).

Callow, L. M. and G. Papadakis (2011). "Managing Corrosion of Stainless Steel Pipes and Heating Coils." In: URL: https://app.knovel.com/hotlink/pdf/id:kt00BDQJU3/international-conference/pitting-corrosion (cit. on pp. 14, 16).

Chong, K. P., D. Darwin, J. Balma, C. E. Locke, and P. Engineering (2001). "Accelerated Testing for Concrete Reinforcing Bar Corrosion Protection Systems". In: pp. 97–108 (cit. on pp. 12, 15).

Cochrane, D. (2003). "Success for stainless steel - Durable reinforced concrete bridges". In: *Concrete (London)* 37.3, pp. 26–28. ISSN: 00105317 (cit. on p. 14).

Cunat, P. (2004). "Alloying elements in stainless steel and other chromium-containing alloys". In: *International Chromium Development Association, ...* Pp. 1–24. URL: http://scholar.google.com/scholar?hl=en%7B%5C&%7DbtnG=Search%7B%5C&%7Dq=intitle:Alloying+Elements+in+Stainless+Steel+and+Other+Chromium-Containing+Alloys%7B%5C#%7D0 (cit. on pp. 20, 24).

Davis, J. (2001). "Stainless Steels and Heat-Resistant Alloys Stainless Steels". In: *Alloying - Understanding the Basics* (cit. on p. 19).

Dillon, C. (1982). "Forms of Corrosion Recognition and Prevention: NACE handbook 1 volume 1". In: *Corrosion: Understanding the Basics*, pp. 99–143. ISBN: 1575900262 (cit. on pp. 13–15).

Emerald Insight (2002). "Bridge using stainless steel rebar to last 120 years". In: *Anti-Corrosion Methods and Materials* 49.6. DOI: https://doi.org/10.1108/acmm.2002.12849fab.002 (cit. on pp. 42, 43).

Al-Emrani, M. (2011). *Bärande konstruktioner D.1*. Tech. rep. Department of Civil and Environmental Engineering, Chalmers University of Technology, 30, 56, 85 s. : ill. (Cit. on p. 9).

Euro Inox (2007). *Stainless Steel: Tables of Technical Properties*. Tech. rep. (cit. on p. 44).

Jing, Q. and X. Fang (2017). "Application of Stainless Steel Reinforcements in the Hong Kong-Zhuhai-Macao Bridge". In: 72, pp. 363–366 (cit. on pp. 14, 40).

Jönköpings Betong (2007). *Prislista Fabriksbetong 2007*. URL: http://www.jibabetong.com/userfiles/file/pdf/prislistor/prislista%7B%5C_%7Dfabriksbetong%7B%5C_%7D2007.pdf (visited on 04/12/2018) (cit. on p. 9).

Liljas, M. and J. O. Nilsson (1999). "Development of Commercial Nitrogen-Rich Stainless Steels". In: *Materials Science Forum* 318-320, pp. 189–200. ISSN: 1662-9752. DOI: 10.4028/www.scientific.net/MSF.318-320.189 (cit. on pp. 17, 19, 20).

Markeset, G., S. Rostam, and O. Klinghoffer (2006). *Guide for the use of stainless steel reinforcement in concrete structures*. ISBN: 8253609264. URL: http://www.sintef.no/upload/Byggforsk/Publikasjoner/Prrapp%20405.pdf (cit. on pp. 10, 16, 17, 21–24, 28, 38, 50, 57).

MEPS (2018a). *World Carbon Steel Prices*. URL: http://www.meps.co.uk/World%20Carbon%20Price.htm (visited on 02/15/2018) (cit. on p. 10).

— (2018b). *World Stainless Steel Prices*. URL: http://www.meps.co.uk/Stainless%20Prices.htm (visited on 02/15/2018) (cit. on pp. 45, 46).

Mistry, M., C. Koffler, and S. Wong (2016). "LCA and LCC of the world's longest pier: a case study on nickel-containing stainless steel rebar". In: *International Journal of Life Cycle Assessment* 21.11, pp. 1637–1644. ISSN: 16147502. DOI: 10.1007/s11367-016-1080-2. URL: http://dx.doi.org/10.1007/s11367-016-1080-2 (cit. on pp. 24, 71).

Moen, C. D. and S. R. Sharp (2016). "Bond properties between concrete and corrosion-resistant reinforcing steels". In: *ACI Structural Journal* 113.2, pp. 383–392. ISSN: 08893241. DOI: 10.14359/51688628 (cit. on p. 28).

Moore, D. (1995). *The Pantheon*. URL: http://www.romanconcrete.com/docs/chapt01/chapt01.htm (cit. on p. 6).

Nirosta, K. T. (2014). *Practical Guidelines for the Fabrication of Duplex Stainless Steels*, pp. 1–68. ISBN: 9781907470097 (cit. on p. 17).

Outokumpu (2013). “Handbook of Stainless Steel”. In: *Sandvikens Tryckeri*, pp. 1–89. ISSN: 007049147X (cit. on pp. 17, 19, 20).

Outukumpu (2017). “Sustainability for Roads”. In: (cit. on p. 39).

— (2018). *Stainless Steel Finder*. URL: http://steelfinder.outokumpu.com/properties/ (visited on 02/15/2018) (cit. on pp. 45, 56, 60).

Pajari, M. (2011). *Design with stainless steel rebars applying Eurocode 2*. Tech. rep. (cit. on pp. 21, 35, 36, 56, 59).

Safi, M. (2013). “Life-Cycle Costing”. PhD thesis. Royal Institute of Technology. ISBN: 3175723993. DOI: KTH/BKN/B--121--SE (cit. on pp. 67, 77).

SCB (2018). *Consumer Price Index (CPI)*. URL: http://www.scb.se/en/finding-statistics/statistics-by-subject-area/prices-and-consumption/consumer-price-index/consumer-price-index-cpi/ (visited on 03/23/2018) (cit. on p. 66).

Sederholm, B. and J. Almqvist (2008). *Rostfritt stål i betong - Galvaniska effekter på kolstål*. Tech. rep. (cit. on p. 14).

Sifra (n.d.). *SIFRA WP1 The use of stainless steel in steel bridges ; design , effective implementation and LCC analysis* (cit. on pp. 68, 70).

Silva, N. (2013). *Chloride Induced Corrosion of Reinforcement Steel in Concrete: Threshold Values and Ion Distributions at the Concrete-Steel Interface Department of Civil and Environmental Engineering Chloride Induced Corrosion of Reinforcement Steel in Concrete*, pp. 1–66. ISBN: 9789173858083 (cit. on p. 12).

Sundquist, H. and R. Karoumi (2008). *Life Cycle Cost Methodology and LCC Tools*. Tech. rep. URL: http://www.etsi.aalto.fi/Etsi3/PDF/TG3/LCC%20Description.pdf (cit. on p. 66).

The Highways Agency (2002). “BA84/02: Design manual for roads and bridges - Use of stainless steel reinforcement in highway structures.” In: 1.February 2002, Volume 1, Section 3, Part 15, BA84/02 (cit. on pp. 36, 37).

Trafikverket (2011). *Trafikverkets författningssamling* (cit. on p. 48).

— (2014). “Summary of the Swedish debate on the discount rate”. In: (cit. on pp. 66, 69).

— (2017). *A prislista för broåtgärder år 2017* (cit. on pp. 69, 71, 72).

Van Niejenhuis, C. B., S. Walbridge, and C. M. Hansson (2016). “The performance of austenitic and duplex stainless steels in cracked concrete exposed to concentrated chloride brine”. In: *Journal of Materials Science* 51.1, pp. 362–374. ISSN: 15734803. DOI: 10.1007/s10853-015-9387-0 (cit. on pp. 25, 26).

Ziehl, P. and M. El-Batanouny (2016). “Corrosion of Steel in Concrete Structures”. In: *Corrosion of Steel in Concrete Structures*, pp. 193–209. DOI: 10.1016/B978-1-78242-381-2.00010-9. URL: http://www.sciencedirect.com/science/article/pii/B9781782423812000109 (cit. on pp. 12, 15).

A Redesign of Reinforcement in Retaining Wall using EN 1.4162

4.2 Böjarmering

4.2.1 Armering överkant bottenplatta

Dimensionerar för det till beloppet största dimensionerande momentet:

$M_{Ed.ök.bpl.brott}$ $|M_{ök.bpl.brott}| = 191.1 \frac{kN \cdot m}{m}$

$M_{Ed.ök.bpl.bruk}$ $|M_{ök.bpl.bruk}| = 118.1 \frac{kN \cdot m}{m}$

$\phi_{s.ök.bpl}$ $12\ mm$ Armeringsdiameter överkant bottenplatta

$s_{s.ök.bpl}$ $160\ mm$ S-avstånd överkant bottenplatta

$A_{s.ök.bpl}$ $\pi \frac{\left(\frac{\phi_{s.ök.bpl}}{2}\right)^2}{s_{s.ök.bpl}} = 706.9 \frac{mm^2}{m}$ Armeringsarea

$d_{bpl.ök}$ $t_{bpl} - TB_{ök.bpl} - \frac{\phi_{s.ök.bpl}}{2} = 454\ mm$ Effektiv höjd

Minsta tillåtna armeringsarea, SS-EN 1992-1-1:2005 (9.1N) samt TRVK Bro 11 D.1.4.1.1.

$A_{s.min1}$ $4 \frac{f_{ctm}}{3\ MPa}\ b_{btg}\ cm^2 = 426.67 \frac{mm^2}{m}$

$A_{s.min2}$ $4 \frac{cm^2}{m} = 400 \frac{mm^2}{m}$

$A_{s.min3}$ $0.08\%\ t_{bpl} = 400 \frac{mm^2}{m}$

$A_{s.min4}$ $max\left(0.26 \frac{f_{ctm}}{f_{yk}}\ d_{bpl.ök}, 0.0013\ d_{bpl.ök}\right) = 629.55 \frac{mm^2}{m}$

ϕ_1 $16\ mm$

s_1 $400\ mm$

$A_{s.min5}$ $\pi \frac{\left(\frac{\phi_1}{2}\right)^2}{s_1} = 503 \frac{mm^2}{m}$

$A_{s.min.ök}$ $max\left(A_{s.min1}, A_{s.min2}, A_{s.min3}, A_{s.min4}, A_{s.min5}\right) = 629.5 \frac{mm^2}{m}$

Kontroll_min_armering_ök_bpl **if** $A_{s.ök.bpl} > A_{s.min.ök}$, "OK", "Minska s-avstånd" = "OK"

Brottgräns

Moment kring Fs:

$\alpha_{btg} \quad 0.81 \qquad \beta \quad 0.416$

$x_{ök.bpl.brott} \quad 20 \ mm$ Initiell gissning

$x_{ök.bpl.brott} \quad \textbf{root}\left(f_{cd}\ x_{ök.bpl.brott} \quad d_{bpl.ök} - \beta\ x_{ök.bpl.brott} \quad - M_{Ed.ök.bpl.brott}, x_{ök.bpl.brott}\right) = 18.35 \ mm$

$$\sigma_{sm.brott} \quad \frac{M_{Ed.ök.bpl.brott}}{d_{bpl.ök} - \frac{x_{ök.bpl.brott}}{3}\ A_{s.ök.bpl}} = 603.55 \ MPa$$

$$\varepsilon_{m.brott} \quad \frac{\sigma_{sm.brott}}{E_0} + \alpha_0 \frac{\sigma_0}{E_0} \left(\frac{\sigma_{sm.brott}}{\sigma_0}\right)^n$$

$Kontroll\_arm\_flyter\_ök\_bpl \quad \textbf{if}\left(\varepsilon_{m.brott} > \varepsilon_{s0.2}, \text{“OK”}, \text{“EJ OK”}\right) = \text{“OK”}$

Kontroll av seghet

SS-EN 1992-1-1:2005 kap. 5.6.3 (2)

$Kontroll\_arm\_seghet\_ök\_bpl \quad \textbf{if}\left(x_{ök.bpl.brott} \quad 0.45 \quad d_{bpl.ök}, \text{“OK”}, \text{“EJ OK”}\right) = \text{“OK”}$

$$A_{s.ULS.ök.bpl} \quad \frac{\alpha_{btg}\ f_{cd}\ x_{ök.bpl.brott}}{f_{yd}} = 664.6 \ \frac{mm^2}{m}$$ Erforderlig armering

$Kontroll\_ULS\_ök\_bpl \quad \textbf{if}\left(A_{s.ULS.ök.bpl} < A_{s.ök.bpl}, \text{“OK”}, \text{“INTE OK”}\right) = \text{“OK”}$

$$Nyttjandegrad\_ULS\_ök\_bpl \quad \frac{A_{s.ULS.ök.bpl}}{A_{s.ök.bpl}} = 94\%$$

Bruksgräns

$$\alpha \quad \frac{E_0}{E_{cm}} = 5$$

$x_{ök.bpl.bruk} \quad 100 \ mm$ Initiell gissning

$x_{ök.bpl.bruk} \quad \textbf{root}\left(\frac{x_{ök.bpl.bruk}^{\ 2}}{2} - \alpha\ A_{s.ök.bpl} \quad d_{bpl.ök} - x_{ök.bpl.bruk}, x_{ök.bpl.bruk}\right) = 53.2 \ mm$

Beräkning av sprickvidd i fält

$$h_{c.ef.ök} \quad min\left(2.5 \quad t_{bpl} - d_{bpl.ök}, \frac{t_{bpl} - x_{ök.bpl.bruk}}{3}, \frac{t_{bpl}}{2}\right) = 115 \ mm$$ Höjd för effektiv betongarea, SS-EN 1992-1-1:2005 kap 7.3.2 (3)

28/03/2018

$A_{ef.ök}$ $h_{c.ef.ök} = 115000 \ \frac{mm^2}{m}$ Effektiv betongarea, SS-EN 1992-1-1:2005, figur 7.1

$\rho_{p.ef.ök}$ $\frac{A_{s.ök.bpl}}{A_{ef.ök}} = 6.147 \ 10^{-3}$ Förhållande mellan dragarmerings tvärsnittsarea och effektiv betongarea, SS-EN 1992-1-1:2005 (7.10)

k_t 0.4 Faktor som beaktar lastvaraktighet, SS-EN 1992-1-1:2005 7.3.4 (2)

$\varepsilon_{cm.ök}$ $\frac{k_t \ f_{ctm}}{\rho_{p.ef.ök} \ E_0} \left(1 + \alpha \ \rho_{p.ef.ök}\right) = 1.3 \ 10^{-3}$ Betongens medeltöjning mellan sprickor, SS-EN 1992-1-1:2005 (7.9)

$\sigma_{sm.bruk}$ $\frac{M_{Ed.ök.bpl.bruk}}{d_{bpl.ök} - \frac{x_{ök.bpl.bruk}}{3}} \ A_{s.ök.bpl} = 382.82 \ MPa$ Stålets medelspänning

σ_{res} **root** $\left(\frac{M_{Ed.ök.bpl.bruk}}{d_{bpl.ök} - \frac{x_{ök.bpl.bruk}}{3}} \ A_{s.ök.bpl} - \sigma_{sm.bruk} + \alpha_0 \ \sigma_0 \left(\frac{\sigma_{sm.bruk}}{\sigma_0}\right)^n, \sigma_{sm.bruk}\right) = 380.12 \ MPa$

$\varepsilon_{s.ök}$ $\frac{\sigma_{res}}{E_0} = 2.236 \ 10^{-3}$ Stålets töjning, med icke-linjäritet

$Kontroll\_Emodul\_ök\_bpl$ **if** $\varepsilon_{s0.2} > \varepsilon_{s.ök}$, "OK", "INTE OK" = "OK"

$\varepsilon \ \sigma_{s.II}$ $\frac{\sigma_{s.II}}{E_0} + \alpha_0 \ \frac{\sigma_0}{E_0} \left(\frac{\sigma_{s.II}}{\sigma_0}\right)^n$ Samband mellan spänning och töjning enligt R-O ekv

σ_{var} $0 \ MPa \ \ 10 \ MPa \ \ 790 \ MPa$

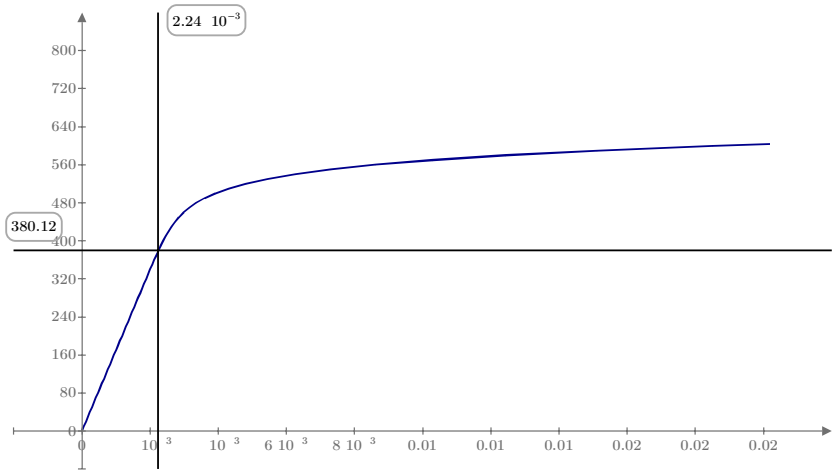

σ_{var} (MPa)

$\varepsilon \ \sigma_{var}$

$k_1 \quad 0.8 \qquad k_4 \quad 0.425 \qquad k_2 \quad 0.5$ Konstanter enligt SS-EN 1992-1-1, 7.3.4

$s_{r.max.ök} \quad 7 \ \phi_{s.ök.bpl} + k_1 \ k_2 \ k_4 \ \frac{\phi_{s.ök.bpl}}{\rho_{p.ef.ök}} = 416 \ mm$ Maximalt sprickavstånd, SS-EN 1992-1-1:2005 (7.11)

$w_{k.till.bpl.ök} \quad 0.6 \ mm$ Största tillåtna sprickbredd

$w_k \quad s_{r.max.ök} \quad max \ \varepsilon_{s.ök} - \varepsilon_{cm.ök}, \varepsilon_{s.ök} \ 0.6 \quad = 0.56 \ mm$ Karakteristisk sprickbredd, SS-EN 1992-1-1:2005 (7.8)

$Kontroll\_sprickb\_ök\_bpl \quad \textbf{if} \ w_k \quad w_{k.till.bpl.ök}, \text{“OK”}, \text{“INTE OK”} \ = \text{“OK”}$

$Nyttjandegrad\_sprickb\_ök\_bpl \quad \frac{w_k}{w_{k.till.bpl.ök}} = 93\%$

4.2.2 Armering underkant bottenplatta

Dimensionerar för det till beloppet största dimensionerande momentet:

$M_{Ed.uk.bpl.brott} \quad |M_{uk.bpl.brott}| = 0 \ \frac{kN \ m}{m}$ Moment i brottgräns

$M_{Ed.uk.bpl.bruk} \quad |M_{uk.bpl.bruk}| = 0 \ \frac{kN \ m}{m}$ Moment i brukgräns

$M_{cr} \quad \frac{f_{ctm} \ \frac{t_{bpl}^2}{6}}{\zeta_{uk.bpl}} = 133.33 \ \frac{kN \ m}{m}$ Sprickmoment

$Kontroll\_uk\_bpl \quad \textbf{if} \ M_{Ed.uk.bpl.brott} < M_{cr}, \text{“OK”}, \text{“EJ OK”} \ = \text{“OK”}$

$\phi_{s.uk.bpl} \quad 12 \ mm$ Armeringsdiameter underkant bottenplatta

$s_{s.uk.bpl} \quad 155 \ mm$ s-avstånd underkant bottenplatta

$c_{mont} \quad 16 \ mm$ Armeringsdiameter monteringsarmering

$A_{s.uk.bpl} \quad \frac{\pi \ \frac{\phi_{s.uk.bpl}^2}{2}}{s_{s.uk.bpl}} = 730 \ \frac{mm^2}{m}$ Armeringsarea

$d_{bpl.uk} \quad t_{bpl} - TB_{uk.bpl} - c_{mont} - \frac{\phi_{s.uk.bpl}}{2} = 388 \ mm$ Effektiv höjd

Minsta tillåtna armeringsarea, SS-EN 1992-1-1:2005 (9.1N) samt TRVK Bro 11 D.1.4.1.1.

$A_{s.min1} \quad 4 \quad \frac{f_{ctm}}{3 \; MPa} \; b_{btg} \; cm^2 = 426.67 \; \frac{mm^2}{m}$

$A_{s.min2} \quad 4 \quad \frac{cm^2}{m} = 400 \; \frac{mm^2}{m}$

$A_{s.min3} \quad 0.08\% \; t_{bpl} = 400 \; \frac{mm^2}{m}$

$A_{s.min4} \quad max \; 0.26 \; \frac{f_{ctm}}{f_{yk}} \; d_{bpl.uk}, 0.0013 \; d_{bpl.uk} = 538.03 \; \frac{mm^2}{m}$

$A_{s.min5} \quad \frac{\pi \; \frac{\phi_1{}^2}{4}}{s_1} = 503 \; \frac{mm^2}{m}$

$A_{s.min.uk} \quad max \; A_{s.min1}, A_{s.min2}, A_{s.min3}, A_{s.min4}, A_{s.min5} = 538 \; \frac{mm^2}{m}$

$Kontroll\_min\_armering\_uk\_bpl \quad \textbf{if} \; A_{s.uk.bpl} > A_{s.min.uk}, \text{“OK”}, \text{“Minska s-avstånd”} = \text{“OK”}$

$A_{s.uk.bpl} \quad A_{s.min.uk}$ Antar att minimiarmering är tillräckligt

Dimensionering enligt fackversanalogi

$Kontroll\_FV \quad \textbf{if} \; b_{ft} < 1.2 \; t_{bpl}, \text{“OK”}, \text{“EJ OK”} = \text{“OK”}$

Värsta fallet sker då grundtrycket är som störst.

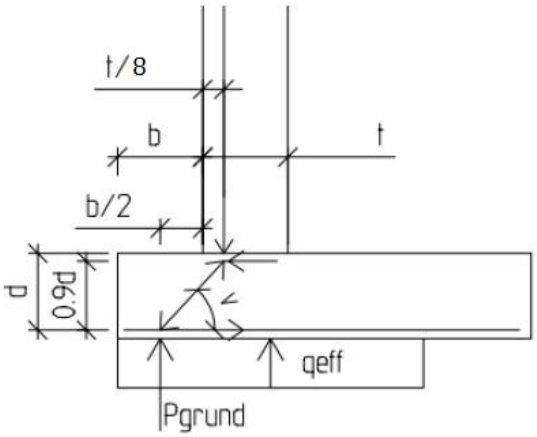

$q_{max.ft} = 156.71 \; kPa$

$P_{grund} \quad q_{max.ft} \; b_{ft} = 78.35 \; \frac{kN}{m}$

Beräkning av vinkel horisontalkraft/sned tryckstråva

$t_{mur.botten} = 400 \; mm$

$l_d \quad \frac{t_{mur.botten}}{8} + \frac{b_{ft}}{2} = 300 \; mm$

$\theta \quad atan \; \frac{0.9 \; d_{bpl.uk}}{l_d} = 49.33 \; deg$

$Kontroll\_tryckstråva \quad \textbf{if}(45 \; deg \quad \theta \quad 60 \; deg, \text{“OK”}, \text{“EJ OK”}) = \text{“OK”}$

Erforderlig armering

$F_s \quad P_{grund} \; tan(\theta) = 91.2 \; \frac{kN}{m}$ Dragkraft i armering

f_{st} $280\ MPa$ Stålspänning begränsas till 280MPa med hänsyn till sprickbredd.

A_{erf} $\frac{F_s}{f_{st}} = 325.73\ \frac{mm^2}{m}$ Erforderlig armering

Kontroll_armering **if** $A_{erf} < A_{s.uk.bpl}$, "OK", "EJ OK" = "OK"

Kontroll av tryckstråva

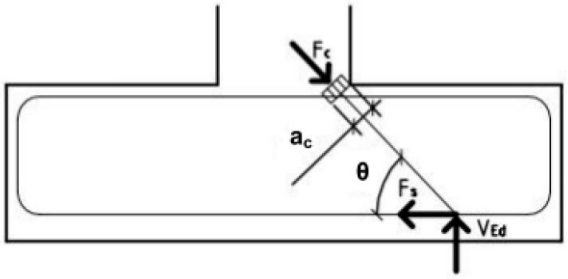

Antar a_c $100\ mm$

F_c $\frac{P_{grund}}{\sin(\theta)} = 103.3\ \frac{kN}{m}$

σ_{Ed} $\frac{F_c}{a_c} = 1.03\ MPa$

k_2 0.85 v $1 - \frac{f_{ck}}{250\ MPa} = 0.86$

$\sigma_{Rd.max}$ $k_2\ v\ f_{cd} = 17.06\ MPa$

Kontroll_tryckstråva **if** $\sigma_{Ed} < \sigma_{Rd.max}$, "OK", "EJ OK" = "OK"

4.3 Tvärkraftskapacitet

Dimensionerande tvärkraft $V_{Ed.bpl} = 127.5\ \frac{kN}{m}$

4.3.1 Livtryckbrott

$V_{Rd.bpl}$ 0.5 0.6 $1 - \frac{f_{ck}}{250\ MPa}$ f_{cd} $d_{bpl.uk} = 2335.76\ \frac{kN}{m}$ Enligt SS-EN 1992-1-1:2005 ekv. 6.5

Kontroll_livtryck_bpl **if** $V_{Ed.bpl}$ $V_{Rd.bpl}$, "OK", "INTE OK" = "OK"

Nyttjandegrad_livtryck_bpl $\frac{V_{Ed.bpl}}{V_{Rd.bpl}} = 5\%$

4.3.2 Skjuvglidbrott

Enligt SS-EN 1992-1-1:2005 kap. 6.2.2

Storleksfaktor: k_{bpl} $min\ 1 + \sqrt{\frac{200\ mm}{d_{bpl.ök}}}, 2.0$ $k_{bpl} = 1.66$

Armeringsinnehåll: $\rho_{l.bpl}$ $min\ \frac{A_{s.uk.bpl}}{d_{bpl.ök}}, 0.02$ $\rho_{l.bpl} = 0.0012$

$$V_{Rd.c.bpl} \quad \frac{0.18}{\gamma_c} \quad k_{bpl} \quad \sqrt[3]{100 \quad \rho_{l.bpl} \quad \frac{f_{ck}}{MPa}} \quad MPa \quad d_{bpl.ök} \qquad V_{Rd.c.bpl} = 145.6 \ \frac{kN}{m}$$

$$V_{Rd.c.min.bpl} \quad 0.035 \quad k_{bpl}^{\frac{3}{2}} \quad \sqrt{\frac{f_{ck}}{MPa}} \quad MPa \quad d_{bpl.ök} \qquad V_{Rd.c.min.bpl} = 201.7 \ \frac{kN}{m}$$

$$V_{Rdc.bpl} \quad max \quad V_{Rd.c.bpl}, V_{Rd.c.min.bpl} \qquad V_{Rdc.bpl} = 201.7 \ \frac{kN}{m}$$

Kontroll_tvärkraftskapacitet_bpl **if** $V_{Ed.bpl} \quad V_{Rdc.bpl}$, "OK", "INTE OK" = "OK"

Nyttkandegrad_tvärkraftkapacitet_bpl $\frac{V_{Ed.bpl}}{V_{Rdc.bpl}} = 63\%$

5 Dimensionering av frontmur

5.1 Armeringsutformning

Nr: Anges som 1, 2, 3 osv valfri text får anges. Max 20 grupper

Litt: Valfri text

Armering: Första gruppen anges på första raden och övriga grupper anges på nästkommande rader. Mellanliggande rader får inte lämnas blanka då programmet tolkar antal grupper som det antal ifyllda rader som finns ovanför den första blankraden.

x-koordinat: slut > start, x=0 ska sammanfalla med x=0 för snittangivelsen. Om stången börjar före x=0 ges minusvärde på koordinaten.

Förankringslängd: Förankringslängd anges för båda stångändarna. Start och slut.

Indatatabell för armering, OBS! Kräver minst två rader!

Littera	ϕ	s	TB	x_{start}	x_{slut}	$l_{bd.start}$	$l_{bd.slut}$
	(mm)	(mm)	(mm)	(mm)	(mm)	(mm)	(mm)
"A1"	16	220	40	−1200	7000	800	800
"A2"	16	220	40	−1200	1500	800	800

$\phi_{s.mur.jord} \quad max \quad \phi = 16\ mm$

$s_{s.mur.jord} \quad max \quad s = 220\ mm$

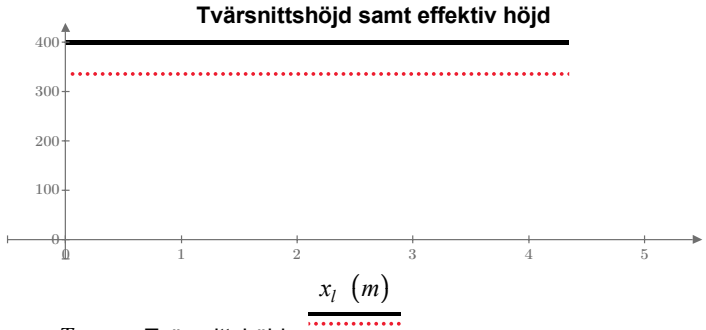

T Tvärsnittshöjd
d Effektiv höjd

$A_{s.min1} \quad 4.0 \ \frac{cm^2}{m} \quad \frac{f_{ctm}}{3\ MPa} = 427 \ \frac{mm^2}{m}$ Enligt TRVK Bro D.1.4.1.1.

$A_{s.min2} \quad 400 \ \frac{mm^2}{m}$ Enligt TRVK Bro D.1.4.1.1.

$A_{s.min3} \quad 0.08\% \ T \ x_{plot}$ Enligt TRVK Bro D.1.4.1.1.

$A_{s.min4}$ for $i \quad 0 \quad last(d)$

$A_{s.min_i} \quad max \ 0.26 \ \frac{f_{ctm}}{f_{yk}} \ d_i, 0.0013 \ d_i$

$A_{s.min}$ SS-EN 1992-1-1 avsnitt ekv 9.1N

$A_{s.min}$ for $i \in 0 \ldots last(d)$

$A_{s_i} \leftarrow max\left(A_{s.min1}, A_{s.min2}, A_{s.min3_i}, A_{s.min4_i}\right)$

A_s

Total dragarmeringsarea jämfört med minsta armeringsmängd

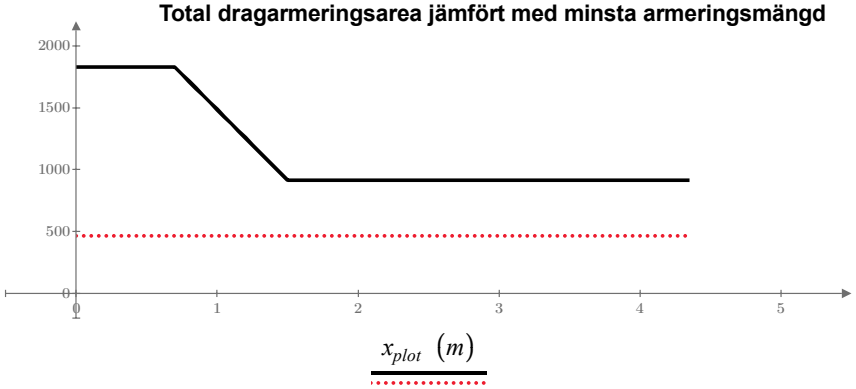

A_s Dragarmeringsarea
$A_{s.min}$ Minsta tillåtna armeringsarea

$\eta_{min.arm} \leftarrow max\left(\frac{A_{s.min}}{A_s}\right) = 51\%$ Maximal nyttjandegrad

$Kontroll\_min\_armering\_mur\_jord$ **if** $max\left(\frac{A_{s.min}}{A_s}\right) < 1$, "OK", "EJ OK" = "OK"

5.2 Snittkrafter

5.2.1 Jordlast

Funktioner för beräkning av moment och tvärkraft

$$V_{mur}(z) \leftarrow \int_0^z f_{A.j.res}(x)\,dx - \int_0^z f_{P.res}(x)\,dx$$

$$M_{mur}(z) \leftarrow \int_0^z f_{A.j.res}(x)\,x\,dx - \int_0^z f_{P.res}(x)\,x\,dx$$

5.2.2 Trafiklast

Trafiklast: $Q_{traf} \leftarrow q_{v.trafik.A} \cdot K_0 = 7.81\ kPa$

Tvärkraft: $V_{traf}(z) \leftarrow Q_{traf} \cdot z$

Moment: $M_{traf}(z) \leftarrow Q_{traf} \cdot \frac{(z)^2}{2}$

5.2.3 Dimensionerande Moment och Tvärkraft

Brottgräns

$v_{d.brott}(z) \quad V_{mur}(z) \;\; 1.1 \;\; \gamma_d + V_{traf}(z) \;\; 1.4 \;\; \gamma_d$

$m_{d.brott}(z) \quad M_{mur}(z) \;\; 1.1 \;\; \gamma_d + M_{traf}(z) \;\; 1.4 \;\; \gamma_d$

Bruksgräns

$m_{d.bruk}(z) \quad M_{mur}(z) \;\; 1.0 \;\; \begin{matrix} K_{0.bruk} \\ K_0 \end{matrix}$

5.3 Moment i brottgränstillstånd

$x_1 \quad 0.1 \;\; m$ Initiell gissning

$x_{ULS} \quad \text{for } i \;\; 0 \;\; rows(d) - 1$
$\quad s_i \;\; \textbf{root}\left(0.81 \;\; f_{cd} \;\; x_1 \;\; d_i - 0.416 \;\; x_1 \;\; - m_{d.brott} \;\; x_{1_i}, x_1\right)$
$\quad s$

Tryckzons höjd

$Ft \quad 0.81 \;\; x_{ULS} \;\; f_{cd}$

Förkjuter dragkraftskurvan med avståndet d

Förskjuten dragkraftskurva jämfört med dragkraftskapacitet

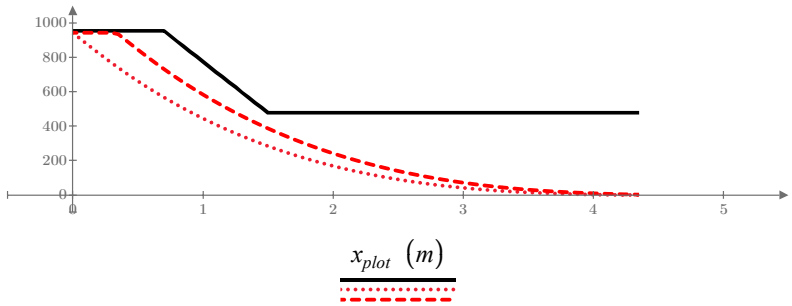

Ft	Dragkraftskurva
F_{forskj}	Förskjuten dragkraftskurva med avståndet d
F_{tot}	Dragkraftskapacitet

$Kontroll\_mur\_brott \quad \textbf{if} \;\; max\left(\frac{F_{forskj}}{F_{tot}}\right) < 1, \text{“OK”}, \text{“EJ OK”} = \text{“OK”}$

5.4 Tvärkraftskapacitet i brottgränstillstånd

$v_1 \quad 0.6 \quad 1 - \frac{f_{ck}}{250\ MPa}$ Reduktionsfaktor för betong med skjuvsprickor

$\alpha_{cw} \quad 1$ Ej förspänd struktur enl. SS-EN 1992-1-1:2005 6.2.3(3)

$\theta \quad 45\ deg$ Vinkel för betongtrycksträvan

Maximalt värde för tvärkraftskapacitet enl. SS-EN 1992-1-1:2005 6.2.3(3)

$v_{Rd.max} \quad \frac{\alpha_{cw} \ 0.9 \ d \ v_1 \ f_{cd}}{cot(\theta) + tan(\theta)}$

$C_{rd.c} \quad \frac{0.18\ MPa}{\gamma_c} = 0.12\ MPa$ Enligt SS-EN 1992-1-1:2005 6.2.2(1)

$k_1 \quad 0.15$ Enligt SS-EN 1992-1-1:2005 6.2.2(1)

$f_{ck} = 35\ MPa$ Betongens karakteristiska tryckhållfasthet

$A_c \quad T \ x_{plot}$ Betongens tvärsnittarea per meter utmed pathen.

$k \quad \text{for } i \quad 0 \quad last(d)$ Enligt SS-EN 1992-1-1:2005 6.2.2(1)

$k_i \quad min\left(1 + \left(\frac{200\ mm}{d_i}\right)^{\frac{1}{2}}, 2.0\right)$

k

$\rho_l \quad \text{for } i \quad 0 \quad last(d)$ Enligt SS-EN 1992-1-1:2005 6.2.2(1)

$\rho_{l_i} \quad min\left(\frac{A_{s_i}}{d_i}, 0.02\right)$

ρ_l

$v_{Rd.c} \quad C_{rd.c} \ k \ \left(100 \ \rho_l \ \frac{f_{ck}}{MPa}\right)^{\frac{1}{3}} \ d$ Tvärkraftskapacitet i betongen, enligt SS-EN 1992-1-1:2005 6.2.2(1)

$v_{min} \quad 0.035 \ k^{\frac{3}{2}} \ \left(\frac{f_{ck}}{MPa}\right)^{\frac{1}{2}} \ MPa \ d$ Minsta värde för tvärkraftskapacitet i betongen, enligt SS-EN 1992-1-1:2005 6.2.2(1)

$v_{Rd} \quad \text{for } i \quad 0 \quad last(d)$ Dimensionerande värde för tvärkraftskapaciteten

$v_{Rd_i} \quad max\left(v_{Rd.c_i}, v_{min_i}\right)$

v_{Rd}

utan tvärkraftsarmering

$Kontroll\_tvärkraftskapacitet\_mur \quad \textbf{if} \quad max\left(\frac{v_{d.brott} \; x_l}{v_{Rd}}\right) < 1, \text{“OK”}, \text{“EJ OK”} = \text{“OK”}$

$Nyttjandegrad\_tvärkraftskapacitet\_mur \quad max\left(\frac{v_{d.brott} \; x_l}{v_{Rd}}\right) = 59\ 1\%$

Nyttjandegraden av tvärkraft map. betongens hållfasthet.

Tvärkraftsbehov jämfört med tvärkraftskapacitet

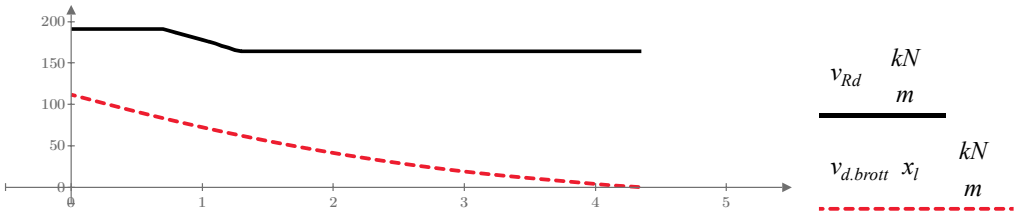

v_{Rd} Tvärkraftskapacitet

$v_{d.brott}$ Tvärkraftsbehov

5.5 Kontroll av sprickbredder i bruksgräns

$w_{k.till.fm.js} \quad w_{k.till.bpl.ök} = 0.6\ mm$ Samma tillåtna sprickbredd som ovan

$\varphi \quad 2$ Kryptal

$\alpha_e \quad \frac{E_0}{E_{cm}} \left(1+\varphi\right) = 15$ Elasticitetsmodulratio

$x_n \quad 10\ mm$ Initiell gissning

$x_{SLS} \quad \text{for } i \quad 0 \quad last\left(d\right)$

$x_i \quad \textbf{root}\left(\frac{x_n^2}{2} - \alpha_e \; A_{s_i} \; d_i - x_n, x_n\right)$

x

Beräkning av neutrala lagret

$A_{II} \quad x_{SLS} + \alpha_e \; A_s$ Area för ekvivalent tvärsnitt i Stadium II

$I_{II} \quad \frac{x_{SLS}^3}{12} + \alpha_e \; A_s \; d - x_{SLS}^2$ Tröghetsmoment för ekvivalent tvärsnitt i Stadium II

$\sigma_{s.II} \quad \frac{m_{d.bruk} \; x_I}{I_{II}} \quad d - x_{SLS} \quad \alpha_e$

Stålspänning för ekvivalent tvärsnitt i Stadium II

$\sigma_s \quad 300 \; MPa$

Initiell gissning

$\sigma_{res} \quad \text{for } i \quad 0 \quad last \; \sigma_{s.II}$

$\quad \sigma_i \quad \mathbf{root} \; \sigma_{s.II_i} - \sigma_s + \alpha_0 \; \sigma_0 \left(\frac{\sigma_s}{\sigma_0} \right)^n, \sigma_s$

$\quad \sigma$

Stålspänning med hänsyn till icke-linjärt beteende

$A_{c.eff} \quad \text{for } i \quad 0 \quad last \; x_{SLS}$

$\quad A_{1_i} \quad 2.5 \quad A_{c_i} - d_i$

$\quad A_{2_i} \quad A_{c_i} - x_{SLS_i}$

$\quad A_{3_i} \quad \frac{A_{c_i}}{3}$

$\quad A_{c.eff_i} \quad min \; A_{1_i}, A_{2_i}, A_{3_i}$

$\quad A_{c.eff}$

Effektiv betongarea, SS-EN 1992-1-1 avsn. 7.3.2(3).

$\rho_{p.eff} \quad \frac{A_s}{A_{c.eff}}$

Ratio mellan förankrad armering och effektiv betongarea.
SS-EN 1992-1-1 ekv 7.10.

$k_t \quad 0.4$

Faktor för långtidslaster

Skillnad i stålets och betongens medeltöjning, SS-EN 1992-1-1 ekv 7.9.

$\Delta\varepsilon \quad \text{for } i \quad 0 \quad last(d)$

$\quad \Delta\varepsilon_i \quad max\left(\frac{\sigma_{s.II_i} - \frac{k_t \; f_{ctm}}{\rho_{p.eff_i}} \left(1 + \alpha_e \; \rho_{p.eff_i}\right)}{E_s}, 0.6 \; \frac{\sigma_{s.II_i}}{E_s} \right)$

$\quad \Delta\varepsilon$

$k_1 \quad 0.8$

Faktor som beaktar armeringens ytegenskaper, SS-EN 1992-1-1 7.3.4 (3).

$k_2 \quad 1.0$

Faktor som beaktar inverkan av töjningsgradienten, sätts konservativt till 1, SS-EN 1992-1-1 7.3.4 (3).

$k_4 \quad 0.425$

Rekommenderat värde enl. SS-EN 1992-1-1 7.3.4(3) ANM.

$s_{r.max} \quad 7 \; \phi_{max} + k_1 \; k_2 \; k_4 \; \frac{\phi_{max}}{\rho_{p.eff}}$

Minsta sprickavstånd enl. SS-EN 1992-1-1:2005 (7.11)

$w_k \quad \Delta\varepsilon \; s_{r.max}$

Karakteristisk sprickbredd, SS-EN 1992-1-1 (7.8)

$Nyttjandegrad\_sprickb\_mur\_jord \quad max \quad \frac{w_k}{w_{k.till.fm.js}} = 85\ 1\%$ Nyttjandegrad

$Kontroll\_sprickb\_mur\_jord \quad \textbf{if} \quad max \quad \frac{w_k}{w_{k.till.fm.js}} < 1, \text{“OK”}, \text{“EJ OK”} = \text{“OK”}$

Kommentar: Eftersom stödmuren är kontrollerad för den högsta punkten samt utan tryckande normalkraft av egentyngd mur anses detta krav uppfyllt.

$\sigma_{koll} \quad max \ \sigma_{res} = 341.49\ MPa$

$\varepsilon_{s.fm} \quad \frac{\sigma_{koll}}{E_0} + \alpha_0 \left(\frac{\sigma_0}{E_0} \right) \left(\frac{\sigma_{koll}}{\sigma_0} \right)^n = 2.01 \ \ 10^{-3}$

$Kontroll\_Emodul\_fm \quad \textbf{if} \quad \varepsilon_{s0.2} > \varepsilon_{s.fm}, \text{“OK”}, \text{“INTE OK”} = \text{“OK”}$

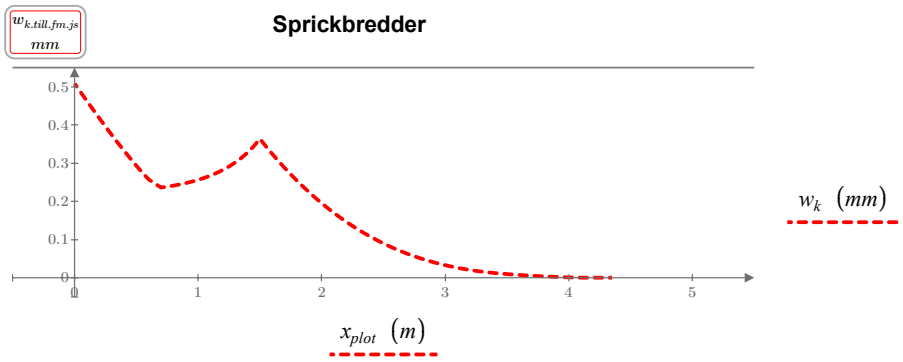

6 Kontroll av gjutfog mellan bottenplatta och frontmur

Kontrollen görs enl SS-EN 1992-1-1:2005 avsnitt 6.2.5. Fogen räknas som skrovlig rengjord yta.
Använder endast armering från baksida mur.

Armering: $A_{s.mur.jord} \quad A_{s_0} = 1827.8 \ \frac{mm^2}{m}$

Armeringsinnehåll: $b_{btg} = 1 \ m \qquad t_{mur.botten} = 0.4 \ m$

$$\rho_{gjut} \quad \frac{A_{s.mur.jord}}{t_{mur.botten}} = 4.6 \ 10^{-3}$$

Materialparametrar: $f_{yd} = 521.7 \ MPa$

$$f_{cd} = 23.3 \ MPa$$

Kraft i gjutfogen: $V_{Ed.gjutfog} \quad v_{d.brott} \ x_{l_0} = 111.7 \ \frac{kN}{m}$

$$\tau_{Ed} \quad \frac{V_{Ed.gjutfog}}{t_{mur.botten}} = 279.3 \ kPa$$

Konstanter för yta vilken klassas som skrovlig, SS-EN 1992-1-1, avsnitt 6.2.5 (2)

$c_{gjutfog} \quad 0.4 \qquad \mu_{gjutfog} \quad 0.7$

Vinkel mellan bottenplatta och mur

$\alpha \quad 90 \ deg$

SS-EN 1992-1-1 avsnitt 6.2.2 ekv 6.6N.

$$\upsilon \quad 0.6 \quad 1 - \frac{f_{ck}}{250 \ MPa} = 0.5$$

$$\tau_{Rd} \quad c_{gjutfog} \ f_{ctd} + \rho_{gjut} \ f_{yd} \quad \mu_{gjutfog} \ sin(\alpha) + cos(\alpha) = 2.3 \ MPa$$

$$\tau_{Rd.g} \quad min \ \tau_{Rd}, 0.5 \ \upsilon \ f_{cd} = 2.26 \ MPa$$

$Kapacitet\_gjutfog$ **if** $\tau_{Ed} \quad \tau_{Rd.g}$, "OK", "INTE OK" = "OK"

$$Nyttjandegrad\_gjutfog \quad \frac{\tau_{Ed}}{\tau_{Rd.g}} = 12\%$$

7 Sammanställning av kontroller

Kontroll av stjälpning, glidning och grundtryck

$Kontroll\_stjälpning = \text{“OK”}$ $Nyttjandegrad\_stjälpning = 44\%$

$Kontroll\_glidning = \text{“OK”}$ $Nyttjandegrad\_glidning = 40\%$

$Kontroll\_grundtryck\_brott = \text{“OK”}$ $Nyttjandegrad\_grundtryck\_brott = 47\%$

$Kontroll\_grundtryck\_bruk = \text{“OK”}$ $Nyttjandegrad\_grundtryck\_bruk = 57\%$

Kontroll av gjutfog

$Kapacitet\_gjutfog = \text{“OK”}$ $Nyttjandegrad\_gjutfog = 12\%$

Kontroll av bottenplattans tvärkraftskapacitet

$Kontroll\_livtryck\_bpl = \text{“OK”}$ $Nyttjandegrad\_livtryck\_bpl = 5\%$

$Kontroll\_tvärkraftskapacitet\_bpl = \text{“OK”}$ $Nyttkandegrad\_tvärkraftkapacitet\_bpl = 63\%$

Kontroll av armering bottenplatta överkant

$Kontroll\_min\_armering\_ök\_bpl = \text{“OK”}$

$Kontroll\_arm\_flyter\_ök\_bpl = \text{“OK”}$

$Kontroll\_arm\_seghet\_ök\_bpl = \text{“OK”}$

$Kontroll\_sprickb\_ök\_bpl = \text{“OK”}$

$Nyttjandegrad\_sprickb\_ök\_bpl = 93\%$

Kontroll av armering bottenplatta underkant

$Kontroll\_uk\_bpl = \text{“OK”}$

$Kontroll\_FV = \text{“OK”}$

$Kontroll\_tryckstråva = \text{“OK”}$

$Kontroll\_armering = \text{“OK”}$

$Kontroll\_tryckstråva = \text{“OK”}$

Kontroll av frontmur

$Kontroll\_mur\_brott = \text{“OK”}$

$Kontroll\_tvärkraftskapacitet\_mur = \text{“OK”}$ $Nyttjandegrad\_tvärkraftskapacitet\_mur = 59\%$

$Kontroll\_min\_armering\_mur\_jord = \text{“OK”}$

$Kontroll\_sprickb\_mur\_jord = \text{“OK”}$ $Nyttjandegrad\_sprickb\_mur\_jord = 85\%$

8 Kontroll av stöd under byggtiden

Under byggskedet kontrolleras att stödet inte välter av egenvikten. Eftersom excentriciteten för egenvikten ligger inom bottenplattans bredd finns ingen risk för att landfästet skall välta. Vidare inses att armeringen i framkant är tillräcklig för att bära egenvikten.

9 Armeringsskiss

Beroende om det skall vara kantbalk vid frontmurens topp eller inte så utformas dessa järn på olika sätt.

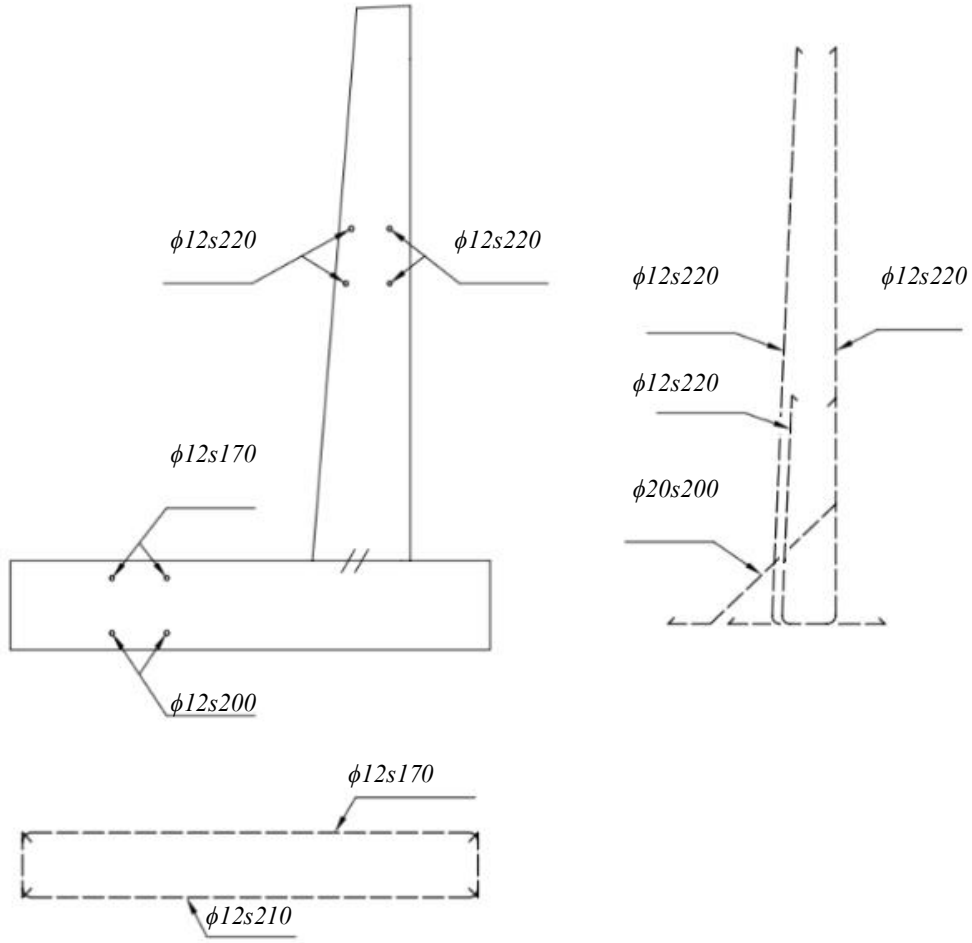

Armeringsdiameter

$\phi_{s.ök.bpl} = 12\ mm$

$\phi_{s.uk.bpl} = 12\ mm$

Centrumavstånd per för armeringsstänger

$s_{s.ök.bpl} = 160\ mm$

$s_{s.uk.bpl} = 155\ mm$

Täckande betongskikt (inkluderar ej monteringsarmering)

$TB_{ök.bpl} = 40\ mm$

$TB_{uk.bpl} = 90\ mm$

$TB_{fm.js} = 40\ mm$

$TB_{fm.ls} = 40\ mm$

Armeringsmängd

Bottenplatta

$\rho_{steel} \quad 7800 \ \frac{kg}{m^3}$

Bottenplatta, armeringsmängd dimensionerad

$V_{s.uk.bpl.} \quad A_{s.uk.bpl} \ b_{bpl} \ l_{stödmur} = 0.010653 \ m^3$

Minimiarmering i uk av bpl

$V_{s.ök.bpl.} \quad A_{s.ök.bpl} \ b_{bpl} \ l_{stödmur} = 0.013996 \ m^3$

Armeringsmängd i ök bpl dimensionerad efter momnet eller sprickbredd, alternativt minimiarmering för de höga hållfastherana

$m_{s.ök.bpl} \quad V_{s.ök.bpl.} \ \rho_{steel} = 0.1203 \ ton$

Bottenplatta, övrig armering = minimiarmering

$V_{s.bpl.} \quad A_{s.min.ök} + A_{s.min.uk} \ b_{bpl} \ l_{stödmur} = 0.0231 \ m^3$

Total minimiarmering bottenplatta

$V_{tot.min.bpl} \quad V_{s.bpl.} + V_{s.uk.bpl.} = 0.0337709 \ m^3$

$m_{tot.min.bpl} \quad V_{tot.min.bpl} \ \rho_{steel} = 0.2904 \ ton$

Frontmur

$h_{2.layer} \quad 0.7 \ m$

$A_{s.min.mur} \quad max \ A_{s.min} = 465.92 \ \frac{1}{m} \ mm^2$

Mur, minimiarmering luftsida

$A_{fm.luft.trans} \quad A_{s.min.mur} \ h_{mur} = 2269.96 \ mm^2$

$V_{fm.luft.trans} \quad A_{fm.luft.trans} \ l_{stödmur} = 0.01362 \ m^3$

$m_{fm.luft.trans} \quad V_{fm.luft.trans} \ \rho_{steel} = 106.23 \ kg$

Mur, minimiarmering längsgående

$A_{fm.long} \quad A_{s.min.mur} \ l_{stödmur} \ 2 = 5591.04 \ mm^2$

$V_{fm.long} \quad A_{fm.long} \ h_{mur} = 0.02724 \ m^3$

$m_{fm.long} \quad V_{fm.long} \ \rho_{steel} = 212.47 \ kg$

$m_{tot.min.fm} \quad m_{fm.long} + m_{fm.luft.trans} = 0.3513 \ ton$ total minimiarmering frontmur

Jordsida

$$A_{fm.jord.trans} \quad \frac{\pi \left(\frac{\phi_{s.mur.jord}}{2}\right)^2}{s_{s.mur.jord}} \ h_{mur} + \pi \left(\frac{\phi_{s.mur.jord}}{2}\right)^2 \quad h_{2.layer} = 5092.35 \ mm^2$$

$V_{fm.jord} \quad A_{fm.jord.trans} \quad l_{stödmur} = 0.03055 \ m^3$

$m_{fm.jord} \quad V_{fm.jord} \quad \rho_{steel} = 0.2627 \ ton$

B Original Drawings of Slab-Frame Bridge

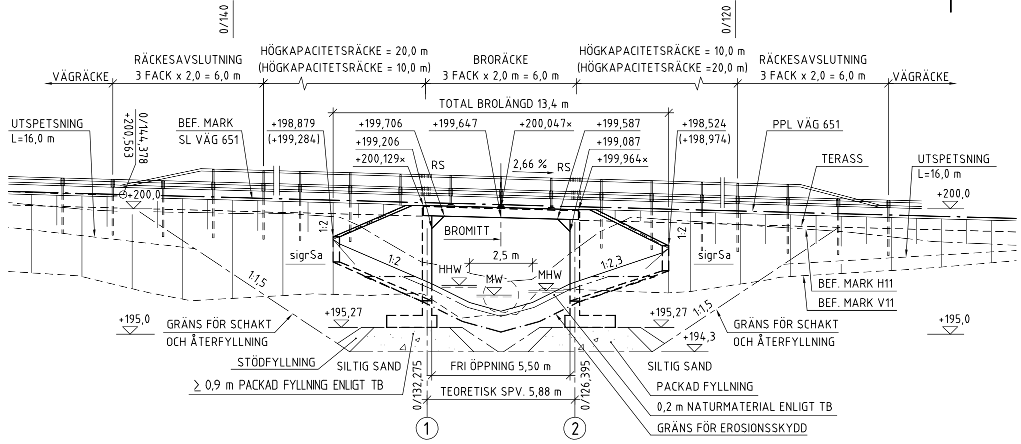
0/140
0/120
VÄGRÄCKE
RÄCKESAVSLUTNING
3 FACK x 2,0 = 6,0 m
HÖGKAPACITETSRÄCKE = 20,0 m
(HÖGKAPACITETSRÄCKE = 10,0 m)
BRORÄCKE
3 FACK x 2,0 m = 6,0 m
HÖGKAPACITETSRÄCKE = 10,0 m
(HÖGKAPACITETSRÄCKE =20,0 m)
RÄCKESAVSLUTNING
3 FACK x 2,0 = 6,0 m
VÄGRÄCKE
TOTAL BROLÄNGD 13,4 m
UTSPETSNING
L=16,0 m
+200,563
0/144,378
BEF. MARK
SL VÄG 651
+198,879
(+199,284)
+199,706
+199,206
+200,129×
+199,647
+200,047×
+199,587
+199,087
+199,964×
+198,524
(+198,974)
PPL VÄG 651
TERASS
UTSPETSNING
L=16,0 m
+200,0
RS
2,66 %
BROMITT
2,5 m
HHW
MW
MHW
1:2
1:2,3
1:5
1:1,5
sigrSa
BEF. MARK H11
BEF. MARK V11
+195,0
+195,27
+194,3
GRÄNS FÖR SCHAKT
OCH ÅTERFYLLNING
STÖDFYLLNING
SILTIG SAND
≥ 0,9 m PACKAD FYLLNING ENLIGT TB
FRI ÖPPNING 5,50 m
TEORETISK SPV. 5,88 m
0/132,275
0/126,395
PACKAD FYLLNING
0,2 m NATURMATERIAL ENLIGT TB
GRÄNS FÖR EROSIONSSKYDD
1
2

ELEVATION A-A 1:100

× AVSER HÖJD ÖK. KONSTRUKTIONSBETONG, UTSIDA KANTBALK
( ) AVSER VÄSTRA SIDAN

HÄNVISNINGAR:

FÖR ALLMÄNNA FÖRESKRIFTER SE RITNING NR. 440K2001.

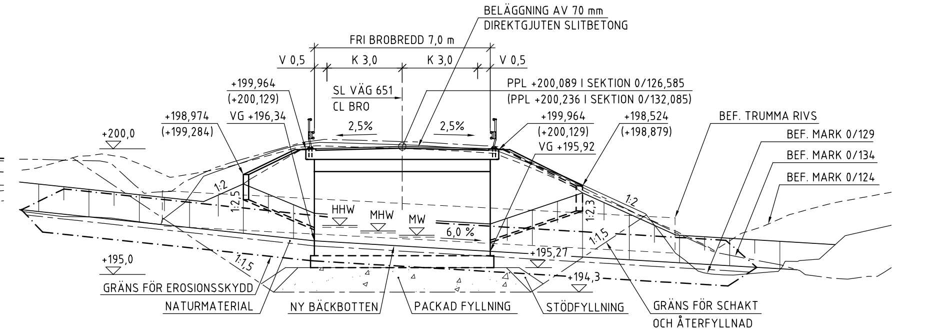
BELÄGGNING AV 70 mm
DIREKTGJUTEN SLITBETONG
FRI BROBREDD 7,0 m
V 0,5
K 3,0
K 3,0
V 0,5
+199,964
(+200,129)
VG +196,34
SL VÄG 651
CL BRO
PPL +200,089 I SEKTION 0/126,585
(PPL +200,236 I SEKTION 0/132,085)
+198,974
(+199,284)
+199,964
(+200,129)
VG +195,92
+198,524
(+198,879)
BEF. TRUMMA RIVS
BEF. MARK 0/129
BEF. MARK 0/134
BEF. MARK 0/124
+200,0
2,5%
2,5%
1:2
1:2,5
1:2,3
1:5
1:1,5
HHW
MHW
MW
6,0 %
+195,0
+195,27
+194,3
GRÄNS FÖR EROSIONSSKYDD
NATURMATERIAL
NY BÄCKBOTTEN
PACKAD FYLLNING
STÖDFYLLNING
GRÄNS FÖR SCHAKT
OCH ÅTERFYLLNAD

SEKTION B-B 1:100

STÖD 2 VISAT
(+) AVSER HÖJDER STÖD 1

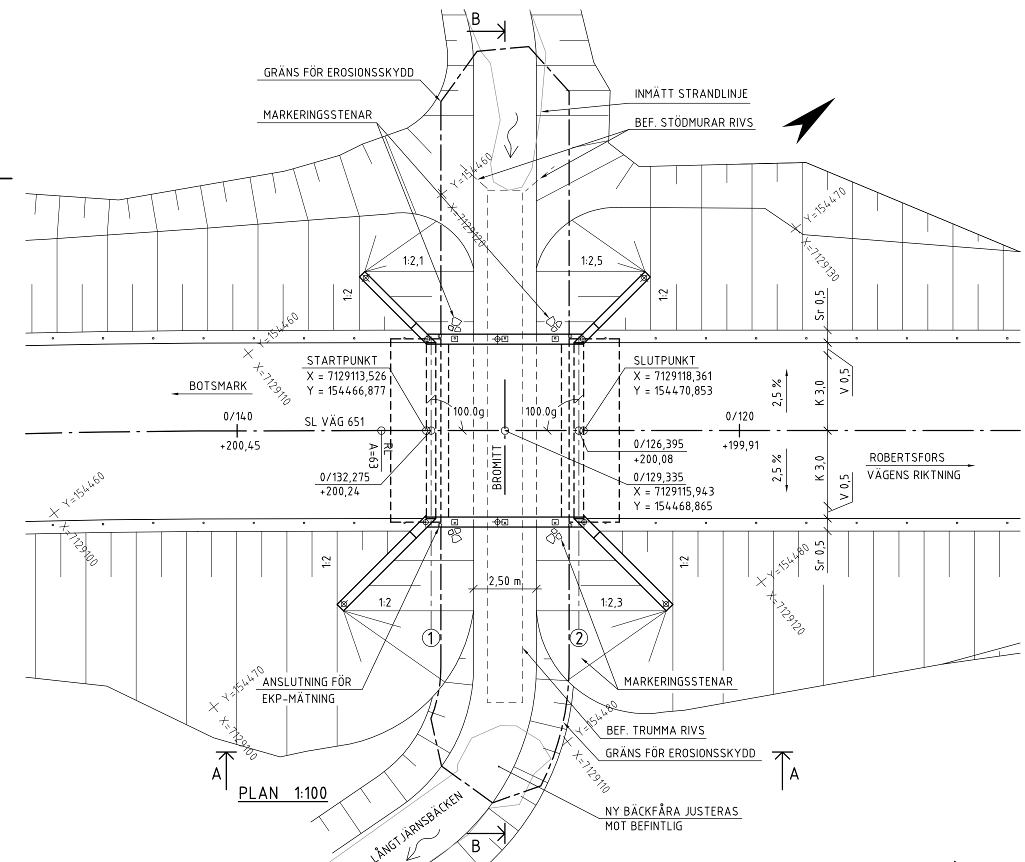
B
GRÄNS FÖR EROSIONSSKYDD
MARKERINGSSTENAR
INMÄTT STRANDLINJE
BEF. STÖDMURAR RIVS
Y=154460
X=7129120
Y=154470
X=7129130
1:2,1
1:2,5
1:2
Sr 0,5
STARTPUNKT
X = 7129113,526
Y = 154466,877
SLUTPUNKT
X = 7129118,361
Y = 154470,853
BOTSMARK
0/140
+200,45
SL VÄG 651
100,0g
100,0g
0/120
+199,91
2,5 %
K 3,0
V 0,5
0/126,395
+200,08
0/129,335
X = 7129115,943
Y = 154468,865
BROMITT
A=63
0/132,275
+200,24
ROBERTSFORS
VÄGENS RIKTNING
Y=154460
X=7129100
2,50 m
1:2
1:2,3
1
2
ANSLUTNING FÖR
EKP-MÄTNING
MARKERINGSSTENAR
BEF. TRUMMA RIVS
GRÄNS FÖR EROSIONSSKYDD
Y=154470
X=7129100
Y=154480
X=7129110
NY BÄCKFÅRA JUSTERAS
MOT BEFINTLIG
LÅNGTJÄRNSBÄCKEN
A

PLAN 1:100

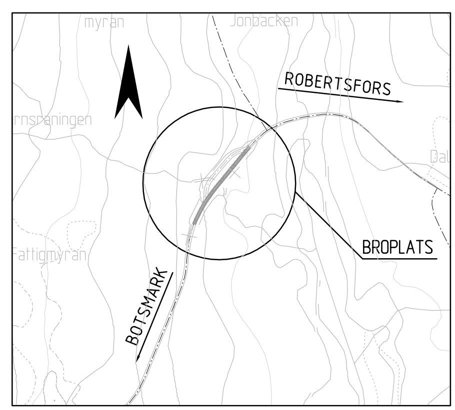

SITUATIONSPLAN 1:5000

SKALA 1:100
0 1 2 5 10
METER

100-147-1-b
Denna handling har registrerats av Trafikverket
Trafikverkets beteckning 100-147-1-b
TRVAT 2015/2155 2015-06-30

REV	ÄNT	ÄNDRINGEN AVSER	GODK	DATUM	VV DATUM	VV DIARIENUMMER

BYGGHANDLING | ARBETSHANDLING

TRAFIKVERKET

SN LIFE 10/NAT/045
REMIBAR
SÄVARÅNS AVRINNINGSOMRÅDE
BRO

ID 281
BRO ÖVER LÅNGTJÄRNSBÄCKEN
4,5 KM V ÅSJÖN PÅ VÄG 651

NCC

UPPDRAGSANSVARIG D. ANDERSSON	UPPDRAGSNUMMER 10214274	SAMMANSTÄLLNING
KONSTR C. ÅSTRÖM	GRANSK H. FRANKLIN	KONSTRUKTIONSNR 100-147-1 · FORMAT A1 · SKALA 1:100
UMEÅ H. FRANKLIN	2015-06-24	OBJEKT NR 109176 · RITNINGSNR 4 40 K 20 02 · REV

HÄNVISNINGAR:

FÖR ALLMÄNNA FÖRESKRIFTER SE RITNING NR. 440K2001.

SEKTIONER SE RITNING NR. 440K2004.

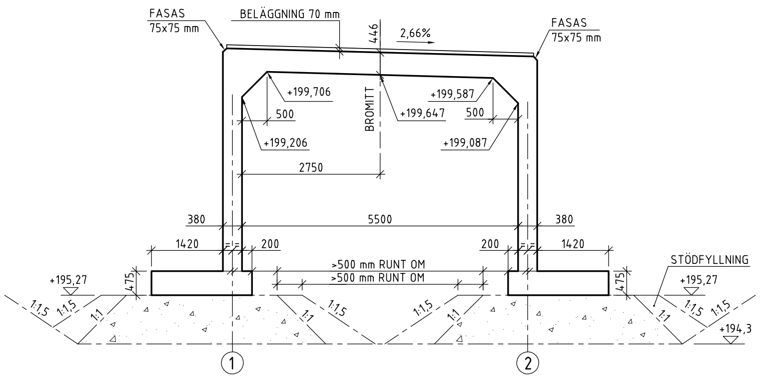

SEKTION A-A 1:50

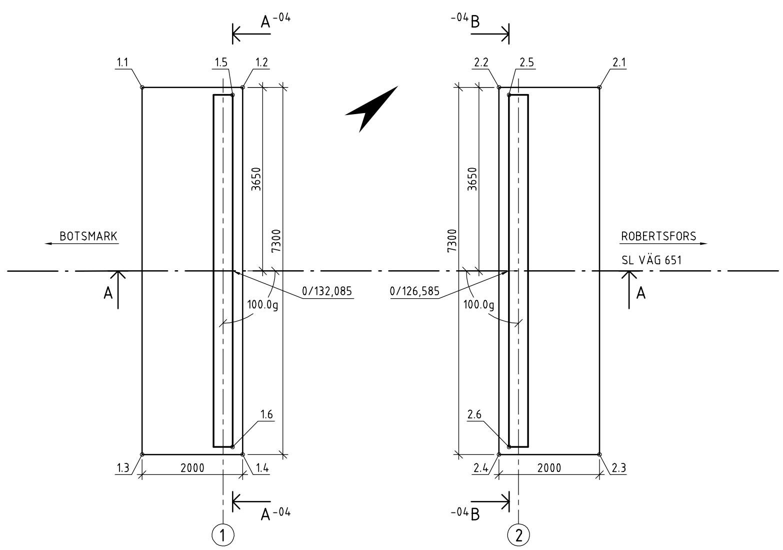

PLAN BOTTENPLATTOR 1:50

BOTTENPLATTOR		
PUNKT NR.	X	Y
1.1	7129114,748	154463,156
1.2	7129116,293	154464,426
1.3	7129110,111	154468,793
1.4	7129111,655	154470,064
1.5	7129116,043	154464,415
1.6	7129111,596	154469,821
2.1	7129121,776	154468,937
2.2	7129120,231	154467,666
2.3	7129117,138	154474,574
2.4	7129115,594	154473,304
2.5	7129120,291	154467,909
2.6	7129115,844	154473,315

KOORDINATER

SKALA 1:50
0 1 2 5
METER

100-147-1-c
Denna handling har registrerats av Trafikverket
Trafikverkets beteckning 100-147-1-c
TRVAT 2015/2155 2015-06-30

REV	ANT	ÄNDRINGEN AVSER	GODK	DATUM	VV DATUM	VV DIARIENUMMER

BYGGHANDLING — ARBETSHANDLING

TRAFIKVERKET

SN LIFE 10/NAT/045
REMIBAR
SÄVARÅNS AVRINNINGSOMRÅDE
BRO

NCC

ID 281
BRO ÖVER LÅNGTJÄRNSBÄCKEN
4,5 KM V ÅSJÖN PÅ VÄG 651

UPPDRAGSANSVARIG: D. ANDERSSON	UPPDRAGSNUMMER: 10214274	MÅTT I, PLAN, SEKTION
KONSTR: C. ÅSTRÖM	GRANSK: H. FRANKLIN	KONSTRUKTIONSNR: 100-147-1 · FORMAT: A1 · SKALA: 1:50
UMEÅ H. FRANKLIN	2015-06-24	OBJEKT NR: 109176 · RITNINGSNR: 4 40 K 20 03 · REV

HÄNVISNINGAR:

FÖR ALLMÄNNA FÖRESKRIFTER SE RITNING NR. 440K2001.

SEKTIONER TAGNA FRÅN RITNING NR. 440K2003.

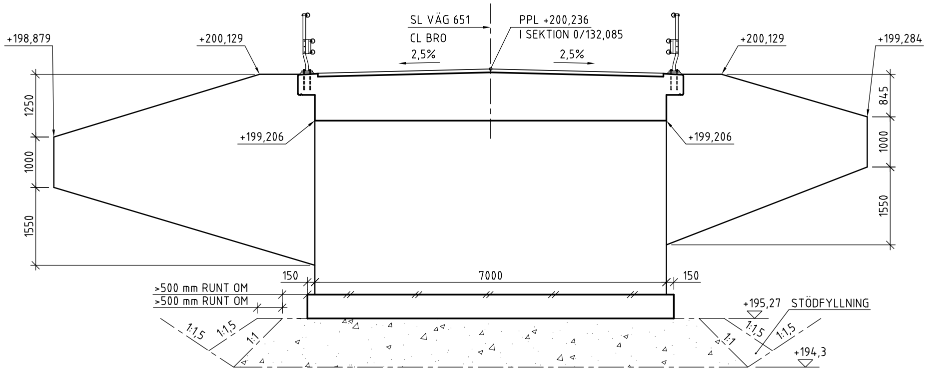

SEKTION A-A 1:50

STÖD 1

VINGARNA ÄR RITADE UTVIKTA

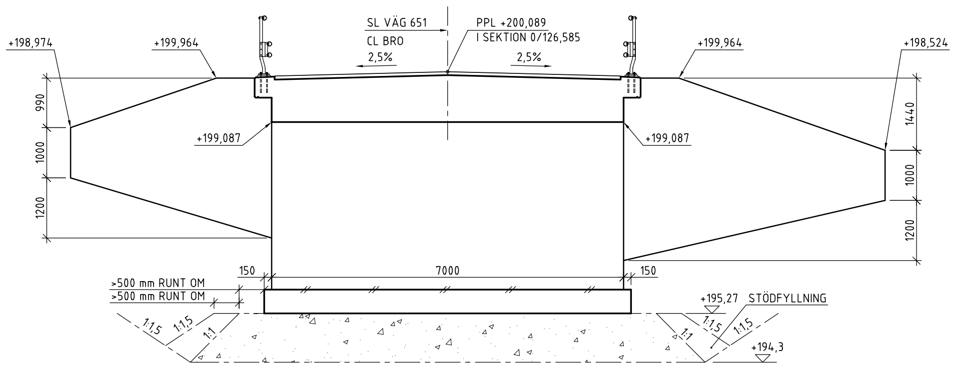

SEKTION B-B 1:50

STÖD 2

VINGARNA ÄR RITADE UTVIKTA

SKALA 1:50

0 1 2 5

METER

100-147-1-d

Denna handling har registrerats av Trafikverket

Trafikverkets beteckning 100-147-1-d

TRVAT 2015/2155 2015-06-30

REV	ANT	ÄNDRINGEN AVSER	GODK	DATUM	VV DATUM	VV DIARIENUMMER

BYGGHANDLING

ARBETSHANDLING

TRAFIKVERKET

NCC

SN LIFE 10/NAT/045
REMIBAR
SÄVARÅNS AVRINNINGSOMRÅDE
BRO

ID 281
BRO ÖVER LÅNGTJÄRNSBÄCKEN
4,5 KM V ÅSJÖN PÅ VÄG 651

UPPDRAGSANSVARIG D. ANDERSSON	UPPDRAGSNUMMER 10214274	MÅTT II, SEKTIONER		
KONSTR C. ÅSTRÖM	GRANSK H. FRANKLIN	KONSTRUKTIONSNR 100-147-1	FORMAT A1	SKALA 1:50
UMEÅ H. FRANKLIN	2015-06-24	OBJEKT NR 109176	RITNINGSNR 4 40 K 20 04	REV

Fil: \\ser01\cst\se\Common Projects\5915\10214274 - Bro över Långtjärnsbäcken\4_CAD\K\Ritdef\440K2004.dwg PLOTTAD: 2015-7-01 12:35:47 AV ANVÄNDARE: sejf11483

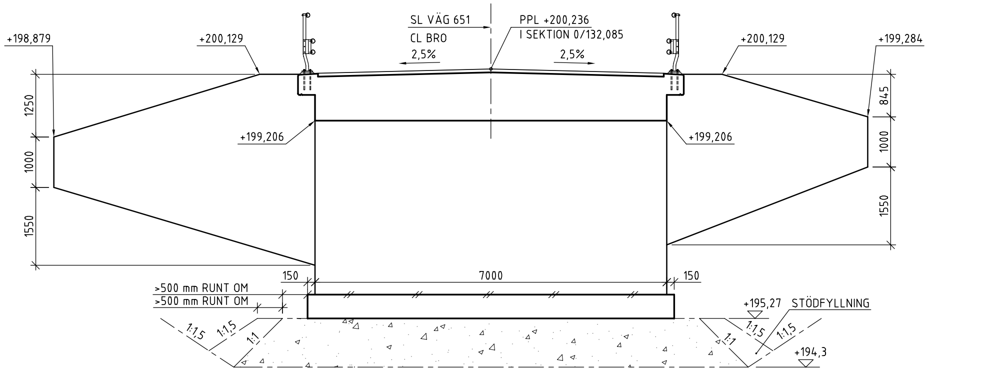

SEKTION A-A 1:50

STÖD 1

VINGARNA ÄR RITADE UTVIKTA

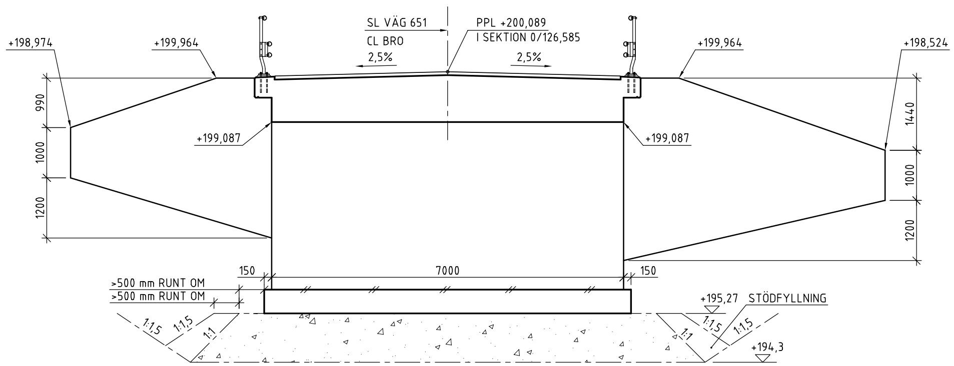

SEKTION B-B 1:50

STÖD 2

VINGARNA ÄR RITADE UTVIKTA

HÄNVISNINGAR:

FÖR ALLMÄNNA FÖRESKRIFTER SE RITNING NR. 440K2001.

SEKTIONER TAGNA FRÅN RITNING NR. 440K2003.

SKALA 1:50

0 1 2 5

METER

100-147-1-d

Denna handling har registrerats av Trafikverket
Trafikverkets beteckning 100-147-1-d
TRVAT 2015/2155 2015-06-30

REV	ÄNT	ÄNDRINGEN AVSER	GODK	DATUM	VV DATUM	VV DIARIENUMMER

BYGGHANDLING	ARBETSHANDLING
TRAFIKVERKET	SN LIFE 10/NAT/045 REMIBAR SÄVARÅNS AVRINNINGSOMRÅDE BRO
NCC	ID 281 BRO ÖVER LÅNGTJÄRNSBÄCKEN 4,5 KM V ÅSJÖN PÅ VÄG 651

UPPDRAGSANSVARIG D. ANDERSSON	UPPDRAGSNUMMER 10214274	MÅTT II, SEKTIONER		
KONSTR C. ÅSTRÖM	GRANSK H. FRANKLIN	KONSTRUKTIONSNR 100-147-1	FORMAT A1	SKALA 1:50
UMEÅ H. FRANKLIN	2015-06-24	OBJEKT NR 109176	RITNINGSNR 4 40 K 20 04	REV

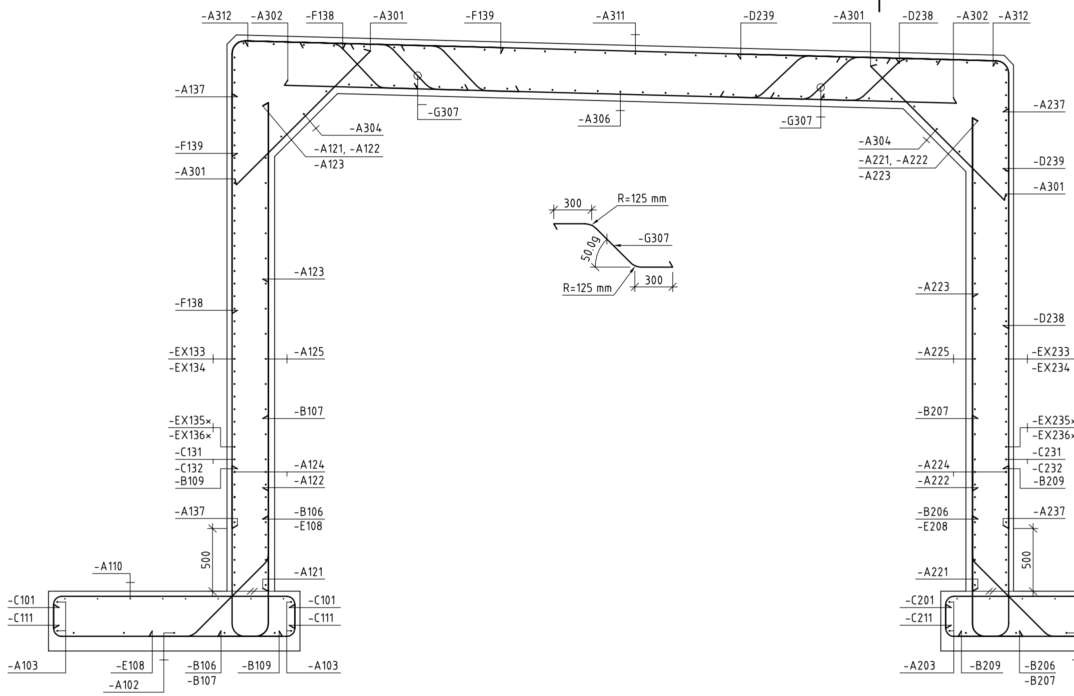
-A312
-A302
-F138
-A301
-F139
-A311
-D239
-A301
-D238
-A302
-A312
-A137
-A304
-A121, -A122
-A123
-G307
-A306
-G307
-A304
-A221, -A222
-A223
-A237
-F139
-A301
-D239
-A301
300
R=125 mm
-G307
50.0g
300
R=125 mm
-A123
-F138
-A223
-D238
-EX133
-EX134
-A125
-A225
-EX233
-EX234
-B107
-B207
-EX135×
-EX136×
-C131
-C132
-B109
-A124
-A122
-EX235×
-EX236×
-C231
-C232
-B209
-A224
-A222
-A137
-B106
-E108
-B206
-E208
-A237
500
-A110
-A121
-A221
-A210
-C101
-C111
-C201
-C211
-A103
-E108
-A102
-B106
-B107
-B109
-A203
-B209
-B206
-B207
-E208
-A202

SEKTION A-A 1:20

× LITTERA -EX135, -EX136, -EX235 ETC. REDOVISAS ENDAST FÖR ATT ILLUSTRERA ARMERINGSINLÄGGNING. FÖREKOMMER INTE I REDOVISAD SEKTION

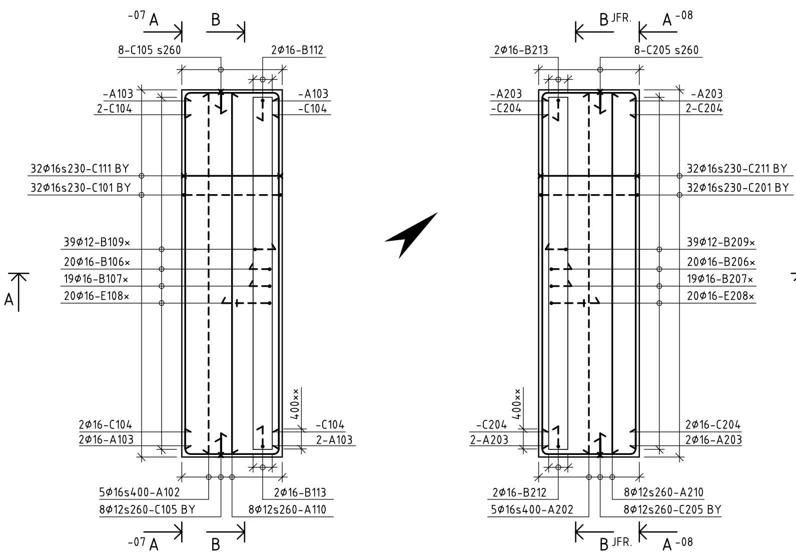
-07 A
B
8-C105 s260
2Ø16-B112
-A103
2-C104
-A103
-C104
32Ø16s230-C111 BY
32Ø16s230-C101 BY
39Ø12-B109×
20Ø16-B106×
19Ø16-B107×
20Ø16-E108×
A
2Ø16-C104
2Ø16-A103
400××
-C104
2-A103
5Ø16s400-A102
8Ø12s260-C105 BY
2Ø16-B113
8Ø12s260-A110
B JFR.
A -08
2Ø16-B213
8-C205 s260
-A203
-C204
-A203
2-C204
32Ø16s230-C211 BY
32Ø16s230-C201 BY
39Ø12-B209×
20Ø16-B206×
19Ø16-B207×
20Ø16-E208×
-C204
2-A203
2Ø16-C204
2Ø16-A203
2Ø16-B212
5Ø16s400-A202
8Ø12s260-A210
8Ø12s260-C205 BY

PLAN BOTTENPLATTOR 1:50

× INLÄGGS LIKA RAMBENSARMERING, SE ARMERINGSGRUPP TYP I, RAMBEN, RITNING NR. -07.

×× SKARVLÄNGDEN GÄLLER ÄVEN ÖVRIGA HÖRN

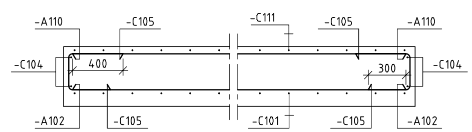

SEKTION B-B 1:20

VISAR ARMERNG FÖR STÖD 1
ARMERING STÖD 2 UTFÖRS LIKA

HÄNVISNINGAR:

FÖR ALLMÄNNA FÖRESKRIFTER SE RITNING NR. 440K2001.

VYER SE RITNING NR. 440K2007 OCH 440K2008.

ANVÄNDA ARMERINGSLITTERA:

		VAKANTA:
BOTTENPLATTA STÖD 1:	101-113	
BOTTENPLATTA STÖD 2:	201-213	

SKALA 1:50
0 1 2 5
METER

100-147-1-f
Denna handling har registrerats av Trafikverket
Trafikverkets beteckning 100-147-1-f
TRVAT 2015/2155 2015-06-30

REV	ÄNT	ÄNDRINGEN AVSER	GODK	DATUM	VV DATUM	VV DIARIENUMMER

BYGGHANDLING | ARBETSHANDLING

TRAFIKVERKET

SN LIFE 10/NAT/045
REMIBAR
SÄVARÅNS AVRINNINGSOMRÅDE
BRO

ID 281
BRO ÖVER LÅNGTJÄRNSBÄCKEN
4,5 KM V ÅSJÖN PÅ VÄG 651

NCC

ARMERING I, PLAN, SEKTIONER

UPPDRAGSANSVARIG	UPPDRAGSNUMMER	KONSTRUKTIONSNR	FORMAT	SKALA
D. ANDERSSON	10214274	100-147-1	A1	1:50, 1:20

KONSTR	GRANSK	OBJEKT NR	RITNINGSNR	REV
C. ÅSTRÖM	H. FRANKLIN	109176	4 40 K 20 06	
UMEÅ H. FRANKLIN	2015-06-24			

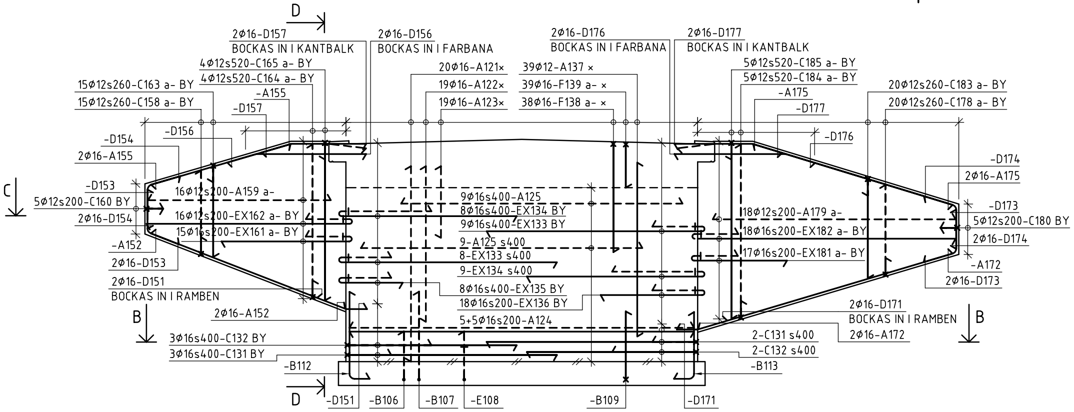
2ø16-D157
BOCKAS IN I KANTBALK
2ø16-D156
BOCKAS IN I FARBANA
2ø16-D176
BOCKAS IN I FARBANA
2ø16-D177
BOCKAS IN I KANTBALK
4ø12s520-C165 a- BY
4ø12s520-C164 a- BY
15ø12s260-C163 a- BY
15ø12s260-C158 a- BY
-A155
-D157
-D156
-D154
2ø16-A155
-D153
5ø12s200-C160 BY
2ø16-D154
-A152
2ø16-D153
2ø16-D151
BOCKAS IN I RAMBEN
2ø16-A152
3ø16s400-C132 BY
3ø16s400-C131 BY
-B112
20ø16-A121×
19ø16-A122×
19ø16-A123×
39ø12-A137 ×
39ø16-F139 a- ×
38ø16-F138 a- ×
16ø12s200-A159 a-
16ø12s200-EX162 a- BY
15ø16s200-EX161 a- BY
9ø16s400-A125
8ø16s400-EX134 BY
9ø16s400-EX133 BY
9-A125 s400
8-EX133 s400
9-EX134 s400
8ø16s400-EX135 BY
18ø16s200-EX136 BY
5+5ø16s200-A124
5ø12s520-C185 a- BY
5ø12s520-C184 a- BY
-A175
-D177
-D176
20ø12s260-C183 a- BY
20ø12s260-C178 a- BY
-D174
2ø16-A175
-D173
5ø12s200-C180 BY
2ø16-D174
-A172
2ø16-D173
18ø12s200-A179 a-
18ø16s200-EX182 a- BY
17ø16s200-EX181 a- BY
2ø16-D171
BOCKAS IN I RAMBEN
2ø16-A172
2-C131 s400
2-C132 s400
-B113
-D151
-B106
-B107
-E108
-B109
-D171
B
C
D

VY A-A 1:50

STÖD 1 VISAT (FRÅN JORDSIDAN). VINGARNA ÄR RITADE UTVIKTA

× INLÄGGS ENLIGT ARMERINGSGRUPP TYP I, RAMBEN

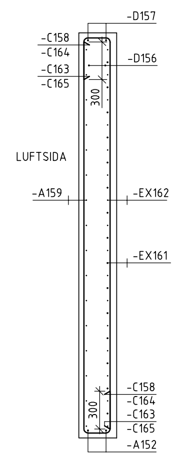

SEKTION D-D 1:20

PRINCIPEN GÄLLER ÄVEN ÖVRIGA EJ REDOVISADE VINGAR

HÄNVISNINGAR:

FÖR ALLMÄNNA FÖRESKRIFTER SE RITNING NR. 440K2001.

VY TAGEN FRÅN RITNING NR. 440K2006.

ANVÄNDA ARMERINGSLITTERA: VAKANTA:

RAMBEN STÖD 1: 121-125, 131-139

VINGAR STÖD 1: 151-165, 171-185

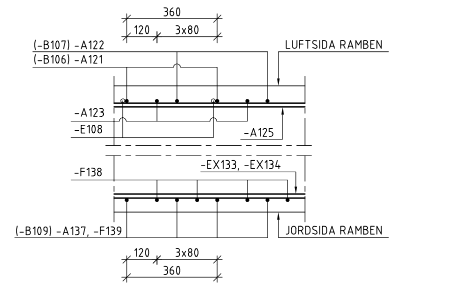

ARMERINGSGRUPP TYP I, RAMBEN 1:10

( ) SKARVAR MED DETTA JÄRN.

STÖD 2 ARMERAS PÅ LIKA SÄTT MEN MED LITTERA -B209, -D238 ETC.

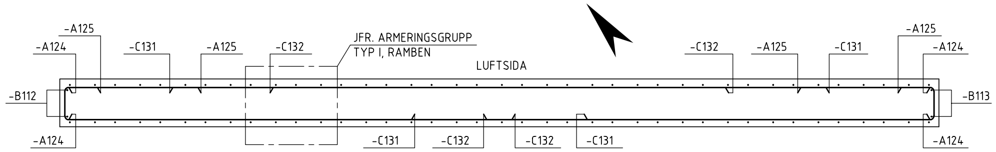

SEKTION B-B 1:20

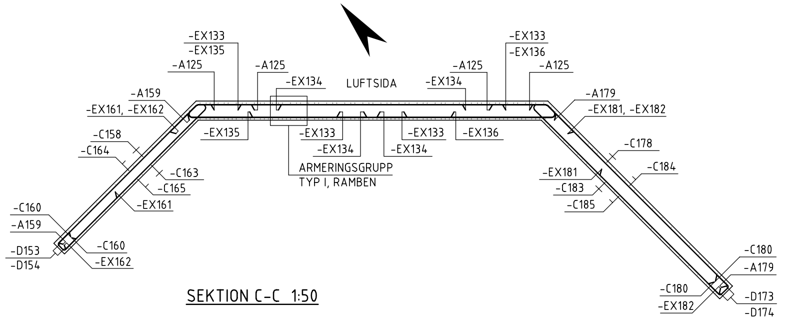
-EX133
-EX135
-A125
-A125
-EX134
LUFTSIDA
-A125
-EX134
-EX133
-EX136
-A125
-A159
-EX161, -EX162
-EX135
-EX133
-EX134
-EX134
-EX136
-A179
-EX181, -EX182
-C158
-C164
-C163
-C165
-EX161
ARMERINGSGRUPP
TYP I, RAMBEN
-C178
-C184
-EX181
-C183
-C185
-C160
-A159
-D153
-D154
-C160
-EX162
-C180
-A179
-C180
-EX182
-D173
-D174

SEKTION C-C 1:50

SKALA 1:50

0 1 2 5

METER

100-147-1-g

Denna handling har registrerats av Trafikverket

Trafikverkets beteckning 100-147-1-g

TRVAT 2015/2155 2015-06-30

REV	ÄNT	ÄNDRINGEN AVSER	GODK	DATUM	VV DATUM	VV DIARIENUMMER

BYGGHANDLING

ARBETSHANDLING

TRAFIKVERKET

NCC

SN LIFE 10/NAT/045
REMIBAR
SÄVARÅNS AVRINNINGSOMRÅDE
BRO

ID 281
BRO ÖVER LÅNGTJÄRNSBÄCKEN
4,5 KM V ÅSJÖN PÅ VÄG 651

UPPDRAGSANSVARIG D. ANDERSSON	UPPDRAGSNUMMER 10214274	ARMERING II, VY, SEKTIONER	
KONSTR C. ÅSTRÖM	GRANSK H. FRANKLIN	KONSTRUKTIONSNR 100-147-1	FORMAT A1 / SKALA 1:50, 1:20, 1:10
UMEÅ H. FRANKLIN	2015-06-24	OBJEKT NR 109176	RITNINGSNR 4 40 K 20 07 / REV

HÄNVISNINGAR:

FÖR ALLMÄNNA FÖRESKRIFTER SE RITNING NR. 440K2001.

VY TAGEN FRÅN RITNING NR. 440K2006.

ANVÄNDA ARMERINGSLITTERA:

VAKANTA:

RAMBEN STÖD 2: 221-225, 231-239

VINGAR STÖD 2: 251-265, 271-285

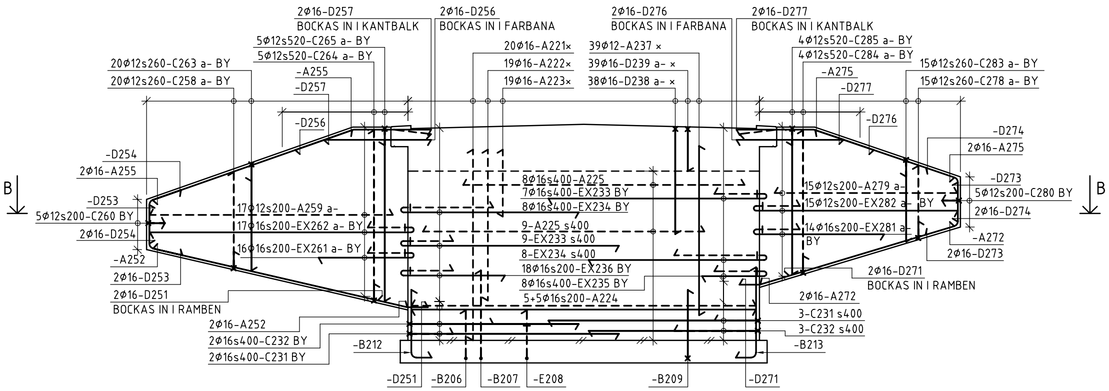

2Ø16-D257
BOCKAS IN I KANTBALK
5Ø12s520-C265 a- BY
5Ø12s520-C264 a- BY
20Ø12s260-C263 a- BY
20Ø12s260-C258 a- BY
-A255
-D257
-D256
2Ø16-D256
BOCKAS IN I FARBANA
20Ø16-A221×
19Ø16-A222×
19Ø16-A223×
2Ø16-D276
BOCKAS IN I FARBANA
39Ø12-A237 ×
39Ø16-D239 a- ×
38Ø16-D238 a- ×
2Ø16-D277
BOCKAS IN I KANTBALK
4Ø12s520-C285 a- BY
4Ø12s520-C284 a- BY
-A275
-D277
-D276
15Ø12s260-C283 a- BY
15Ø12s260-C278 a- BY
-D254
2Ø16-A255
-D253
5Ø12s200-C260 BY
2Ø16-D254
-A252
2Ø16-D253
2Ø16-D251
BOCKAS IN I RAMBEN
17Ø12s200-A259 a-
17Ø16s200-EX262 a- BY
16Ø16s200-EX261 a- BY
8Ø16s400-A225
7Ø16s400-EX233 BY
8Ø16s400-EX234 BY
9-A225 s400
9-EX233 s400
8-EX234 s400
18Ø16s200-EX236 BY
8Ø16s400-EX235 BY
5+5Ø16s200-A224
15Ø12s200-A279 a-
15Ø12s200-EX282 a- BY
14Ø16s200-EX281 a- BY
2Ø16-D271
BOCKAS IN I RAMBEN
2Ø16-A272
3-C231 s400
3-C232 s400
-B213
-D274
2Ø16-A275
-D273
5Ø12s200-C280 BY
2Ø16-D274
-A272
2Ø16-D273
2Ø16-A252
2Ø16s400-C232 BY
2Ø16s400-C231 BY
-B212
-D251
-B206
-B207
-E208
-B209
-D271
B
B

VY A-A 1:50

STÖD 2 VISAT (FRÅN JORDSIDAN). VINGARNA ÄR RITADE UTVIKTA

× JFR. ARMERINGSGRUPP TYP I, RAMBEN, SE RITNING NR. -07

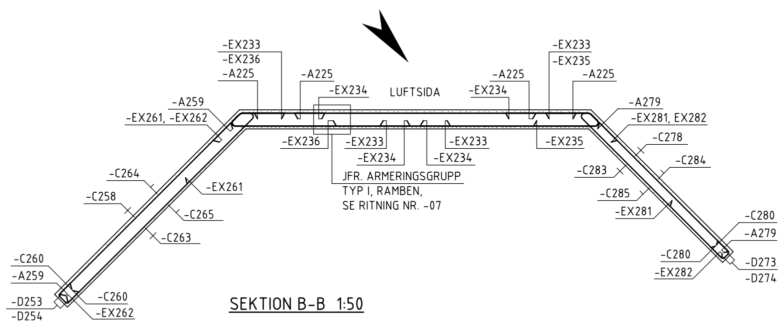

-EX233
-EX236
-A225
-A225
-EX234
LUFTSIDA
-A225
-EX234
-EX233
-EX235
-A225
-A259
-EX261, -EX262
-EX236
-EX233
-EX234
-EX233
-EX234
-EX235
-A279
-EX281, EX282
-C278
-C284
-C283
-C285
-EX281
JFR. ARMERINGSGRUPP
TYP I, RAMBEN,
SE RITNING NR. -07
-C264
-C258
-EX261
-C265
-C263
-C260
-A259
-D253
-D254
-C260
-EX262
-C280
-A279
-D273
-D274
-C280
-EX282

SEKTION B-B 1:50

SKALA 1:50

0 1 2 5

METER

100-147-1-h

Denna handling har registrerats av Trafikverket

Trafikverkets beteckning 100-147-1-h

TRVAT 2015/2155 2015-06-30

REV	ANT	ÄNDRINGEN AVSER	GODK	DATUM	VV DATUM	VV DIARIENUMMER

BYGGHANDLING | ARBETSHANDLING

TRAFIKVERKET

SN LIFE 10/NAT/045
REMIBAR
SÄVARÅNS AVRINNINGSOMRÅDE
BRO

NCC

ID 281
BRO ÖVER LÅNGTJÄRNSBÄCKEN
4,5 KM V ÅSJÖN PÅ VÄG 651

UPPDRAGSANSVARIG: D. ANDERSSON	UPPDRAGSNUMMER: 10214274	ARMERING III, VY, SEKTION
KONSTR: C. ÅSTRÖM	GRANSK: H. FRANKLIN	KONSTRUKTIONSNR: 100-147-1 · FORMAT: A1 · SKALA: 1:50
UMEÅ H. FRANKLIN	2015-06-24	OBJEKT NR: 109176 · RITNINGSNR: 4 40 K 20 08 · REV

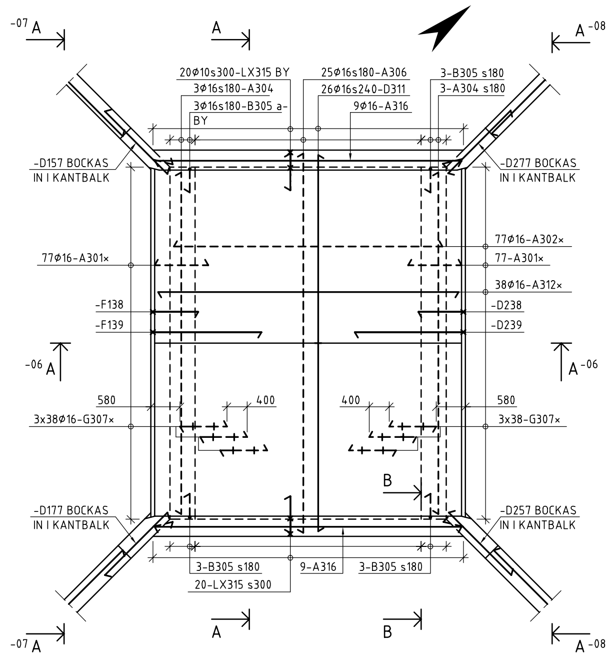
-07 A
A
A -08
20Ø10s300-LX315 BY
3Ø16s180-A304
3Ø16s180-B305 a-BY
25Ø16s180-A306
26Ø16s240-D311
9Ø16-A316
3-B305 s180
3-A304 s180
-D157 BOCKAS IN I KANTBALK
-D277 BOCKAS IN I KANTBALK
77Ø16-A301×
77Ø16-A302×
77-A301×
38Ø16-A312×
-F138
-F139
-D238
-D239
-06 A
A -06
580
400
3x38Ø16-G307×
3x38-G307×
B
-D177 BOCKAS IN I KANTBALK
-D257 BOCKAS IN I KANTBALK
3-B305 s180
20-LX315 s300
9-A316
-07 A
A
B
A -08

PLAN FARBANA 1:50

× INLÄGGS ENLIGT ARMERINGSGRUPP TYP I, FARBANA

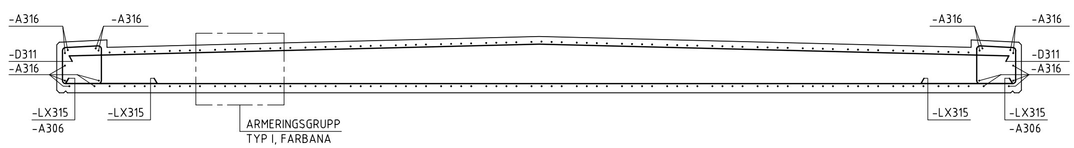

SEKTION A-A 1:20

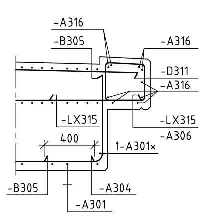

SEKTION B-B 1:20

PRINCIPEN GÄLLER ÄVEN ÖVRIGA EJ REDOVISADE HÖRN

ÖVRIG EJ REDOVISAD ARMERING SE ARMERINGSGRUPP TYP I, FARBANA

× ANTAL GÄLLER ETT HÖRN

HÄNVISNINGAR:

FÖR ALLMÄNNA FÖRESKRIFTER SE RITNING NR. 440K2001.

ANVÄNDA ARMERINGSLITTERA:
FARBANA: 301-307, 311-312, 315-316

VAKANTA:
303

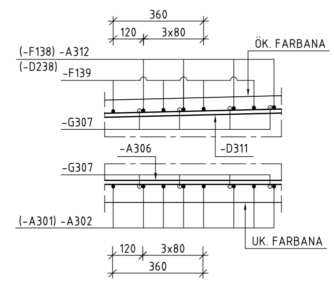

ARMERINGSGRUPP TYP I, FARBANA 1:10

( ) SKARVAR MED DETTA JÄRN.
ARMERING FRÅN RAMBEN STÖD 2 INLÄGGS PÅ LIKA SÄTT MEN MED LITTERA -D238, -D239 ETC.

SKALA 1:50
0 1 2 5
METER

100-147-1-i
Denna handling har registrerats av Trafikverket
Trafikverkets beteckning 100-147-1-i
TRVAT 2015/2155 2015-06-30

REV	ANT	ÄNDRINGEN AVSER	GODK	DATUM	VV DATUM	VV DIARIENUMMER

BYGGHANDLING	ARBETSHANDLING
TRAFIKVERKET	SN LIFE 10/NAT/045 REMIBAR SÄVARÅNS AVRINNINGSOMRÅDE BRO
NCC	ID 281 BRO ÖVER LÅNGTJÄRNSBÄCKEN 4,5 KM V ÅSJÖN PÅ VÄG 651
UPPDRAGSANSVARIG D. ANDERSSON / UPPDRAGSNUMMER 10214274	ARMERING IV, PLAN, SEKTIONER
KONSTR C. ÅSTRÖM / GRANSK H. FRANKLIN	KONSTRUKTIONSNR 100-147-1 / FORMAT A1 / SKALA 1:50, 1:20, 1:10
UMEÅ H. FRANKLIN / 2015-06-24	OBJEKT NR 109176 / RITNINGSNR 4 40 K 20 09 / REV

C Moment Distributions for the Slab-Frame Bridge

Moment distribution:
Bridge deck, longitudinal direction

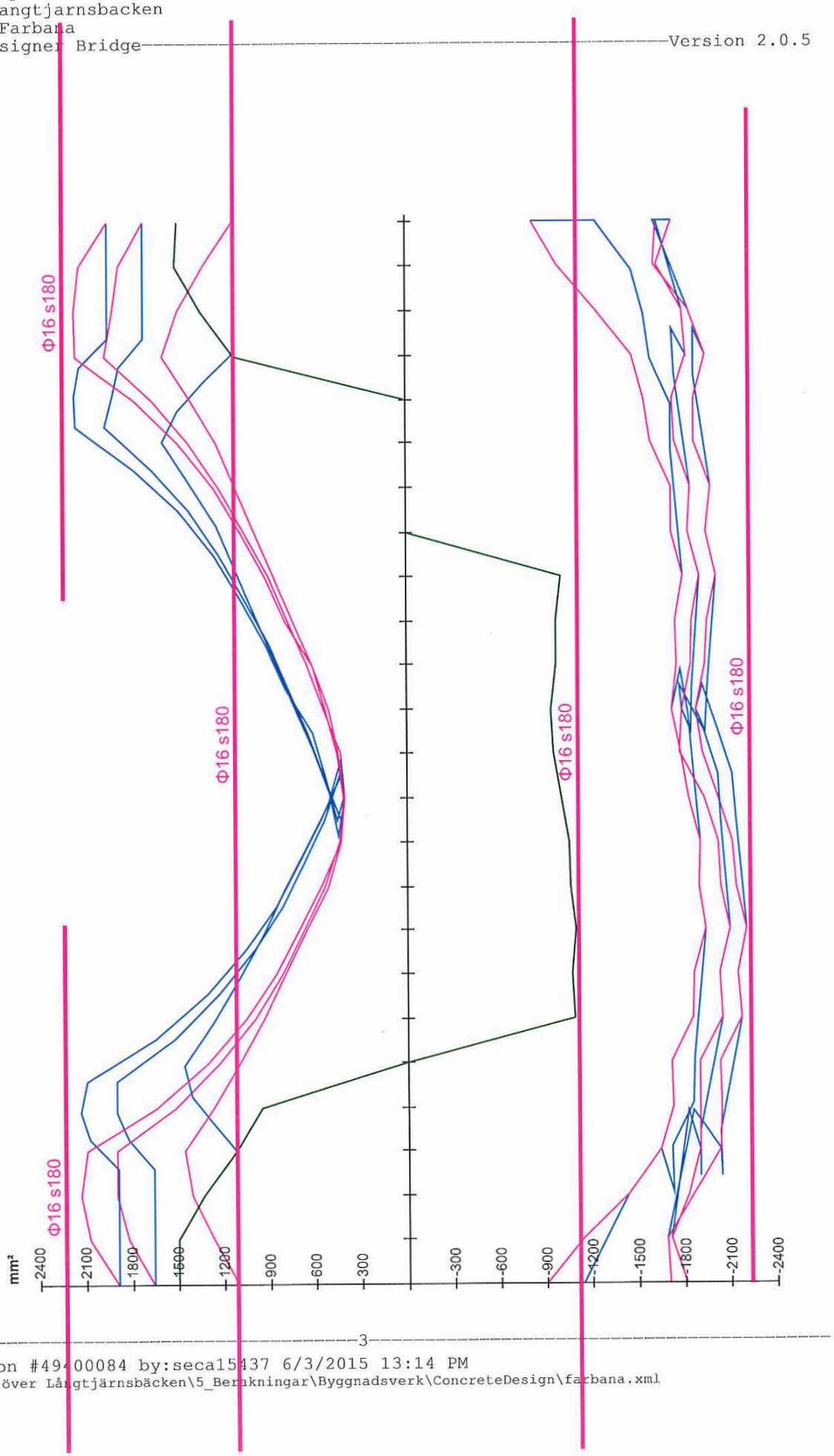

Moment distribution:
Bridge deck, transverse direction

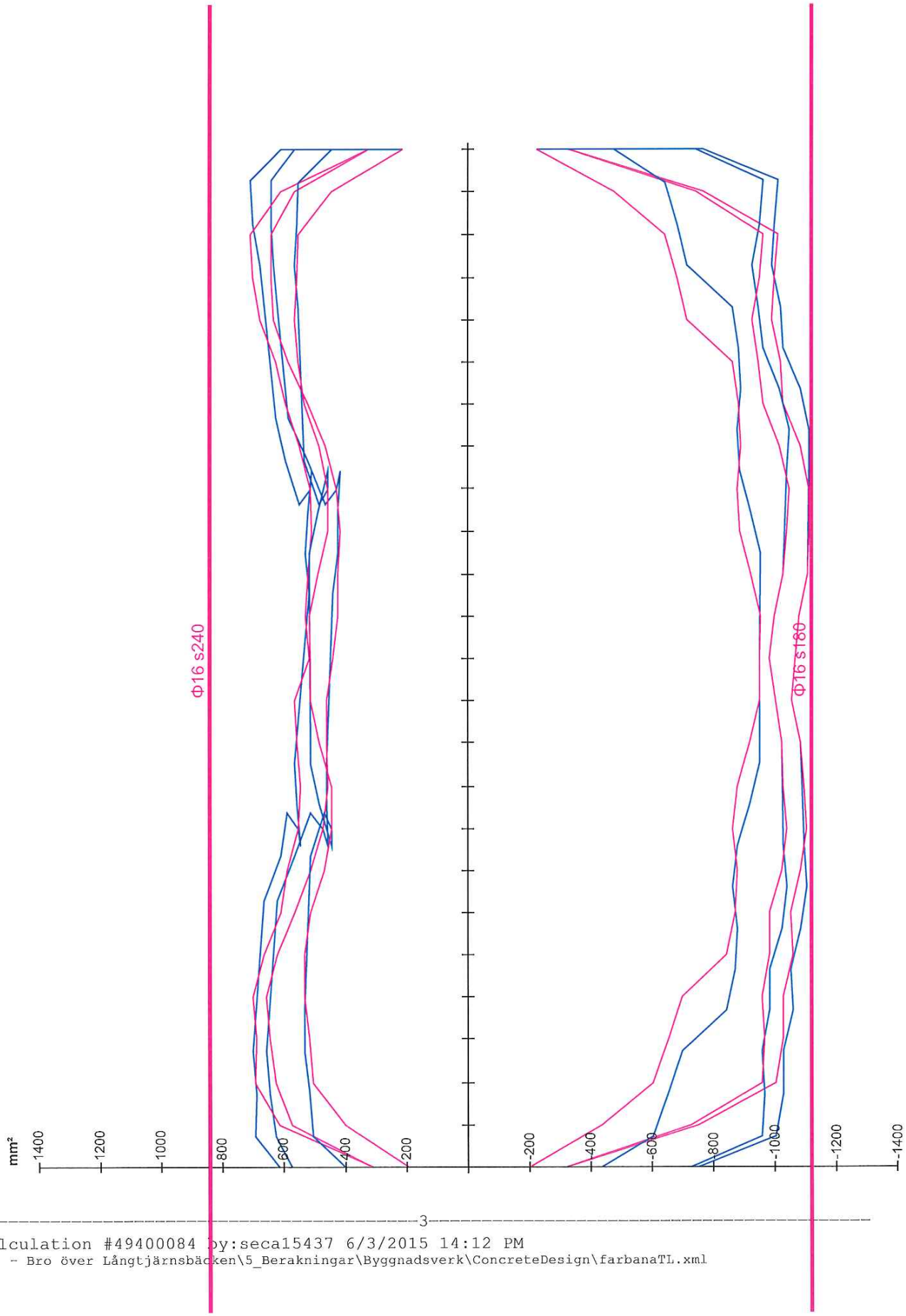

Moment distribution:
Front wall, vertical direction

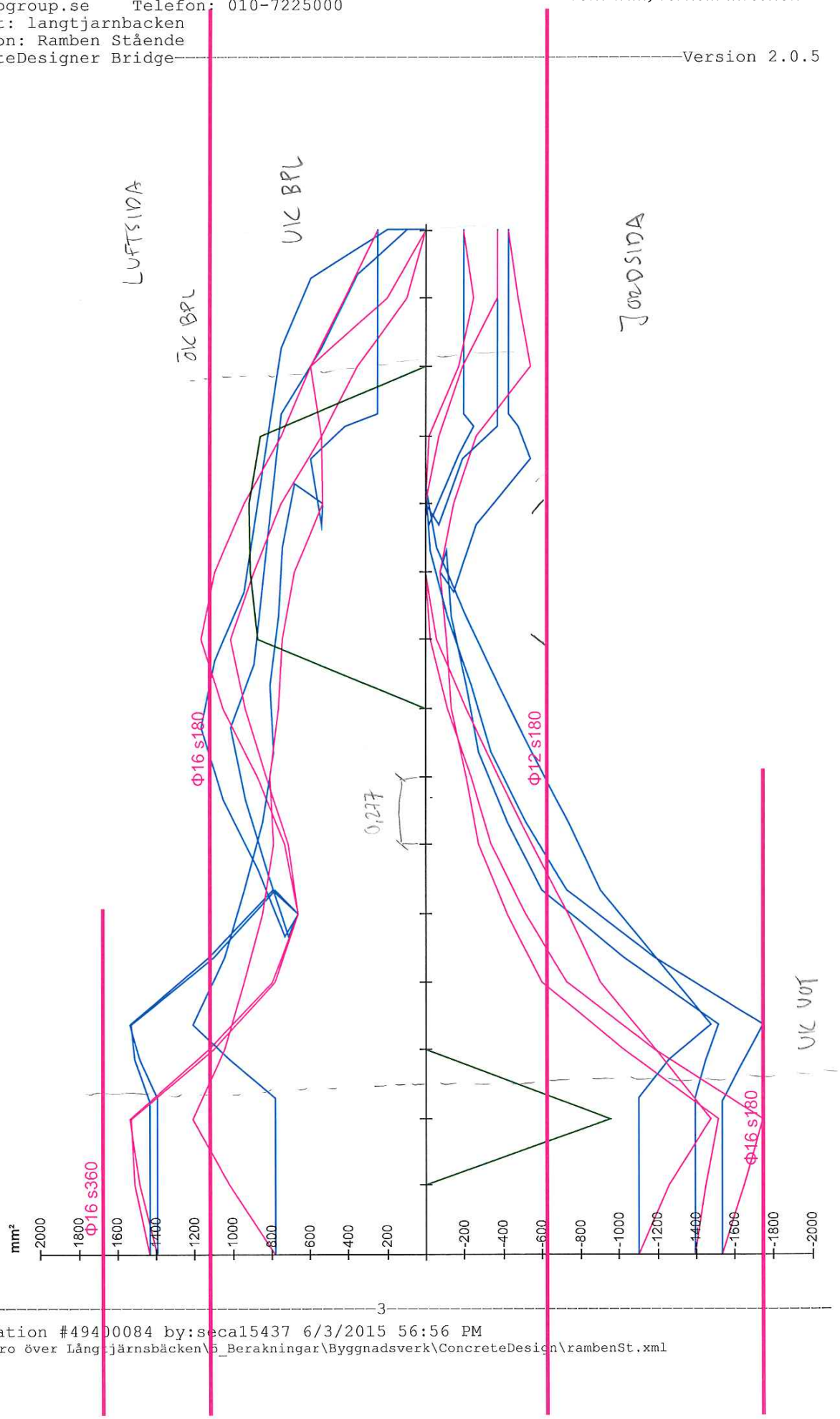

Moment distribution:
Front wall, longitudinal direction

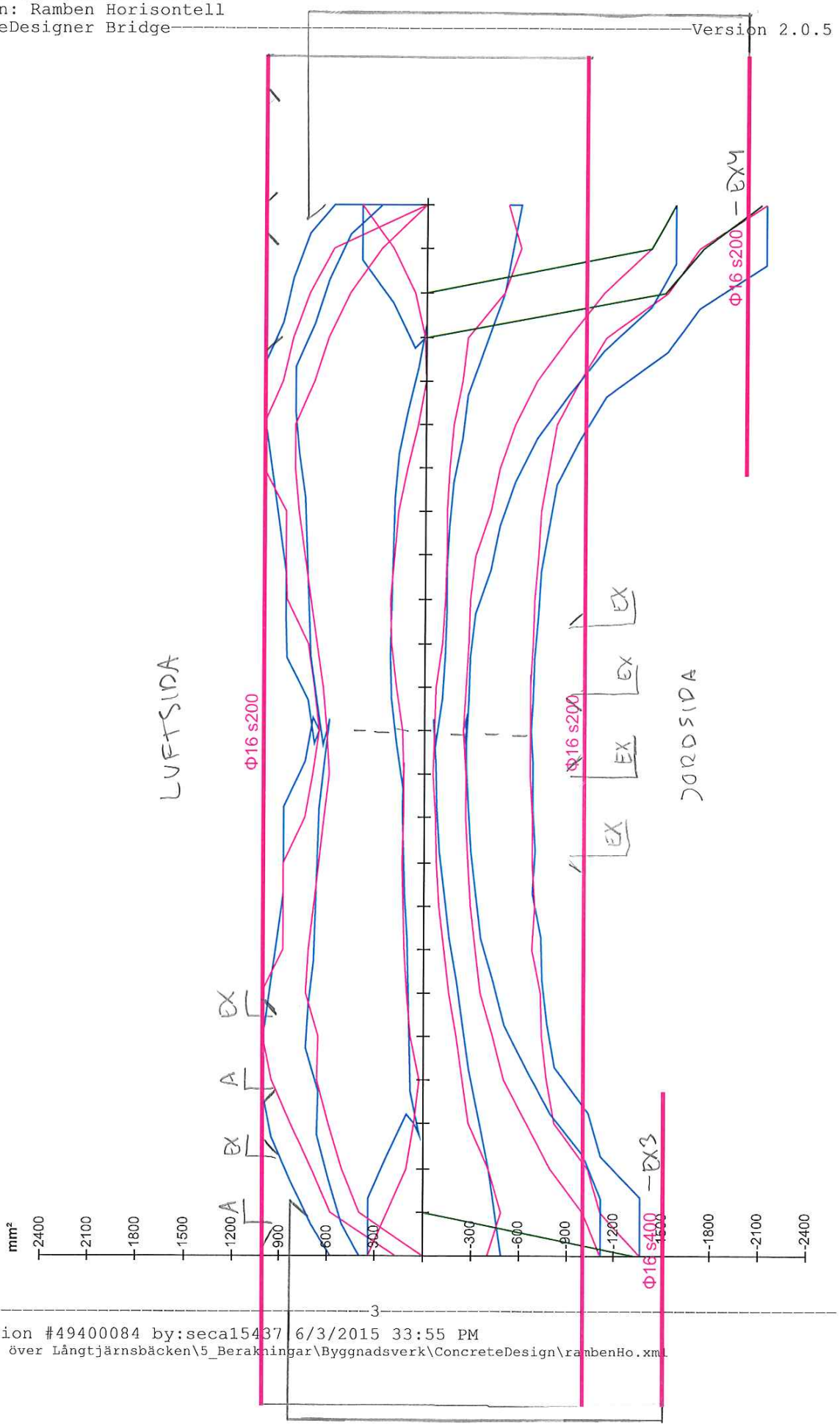

Moment distribution:
Long wing wall, horizontal direction

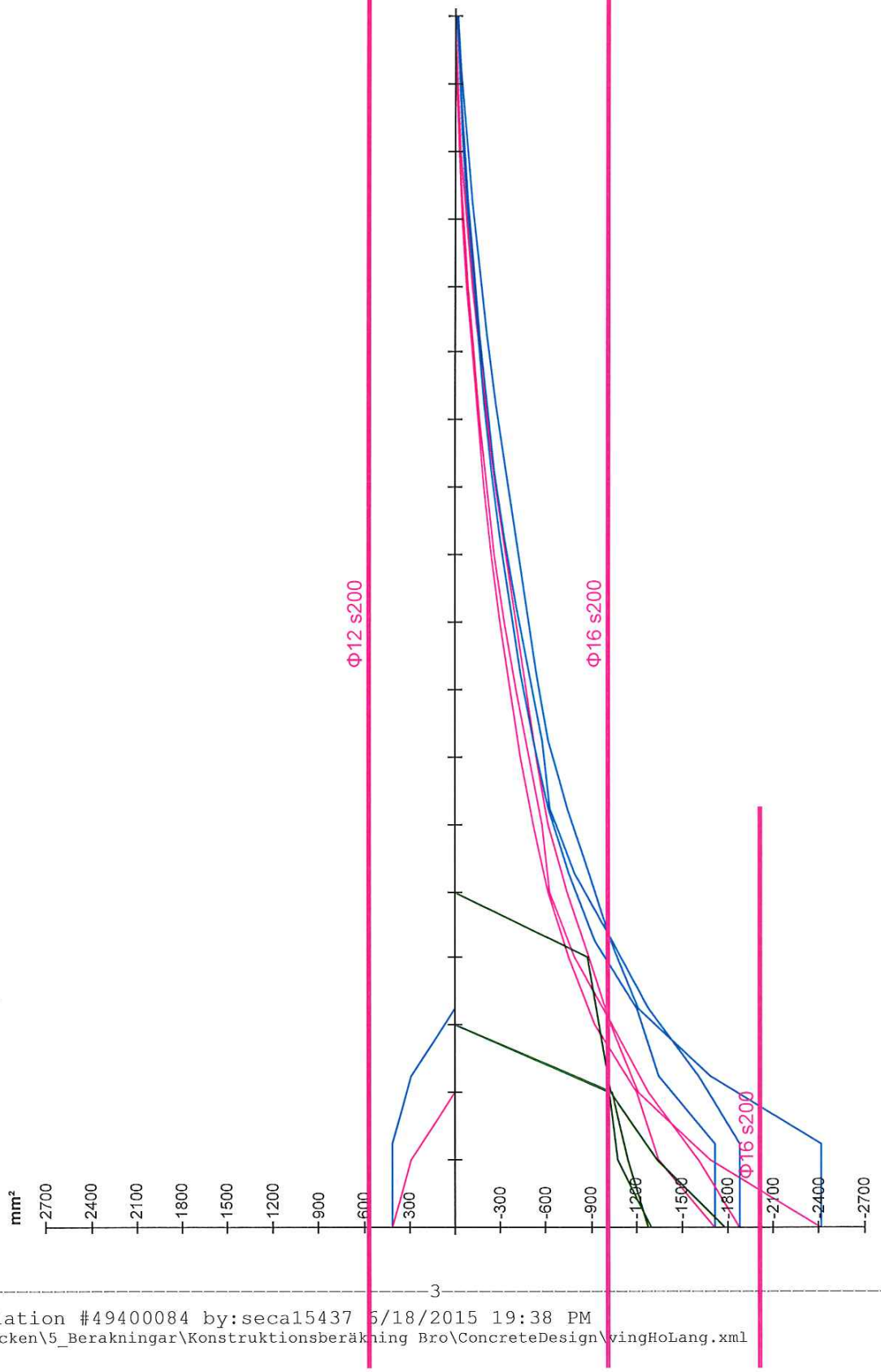

Moment distribution:
Long wing wall, vertical direction

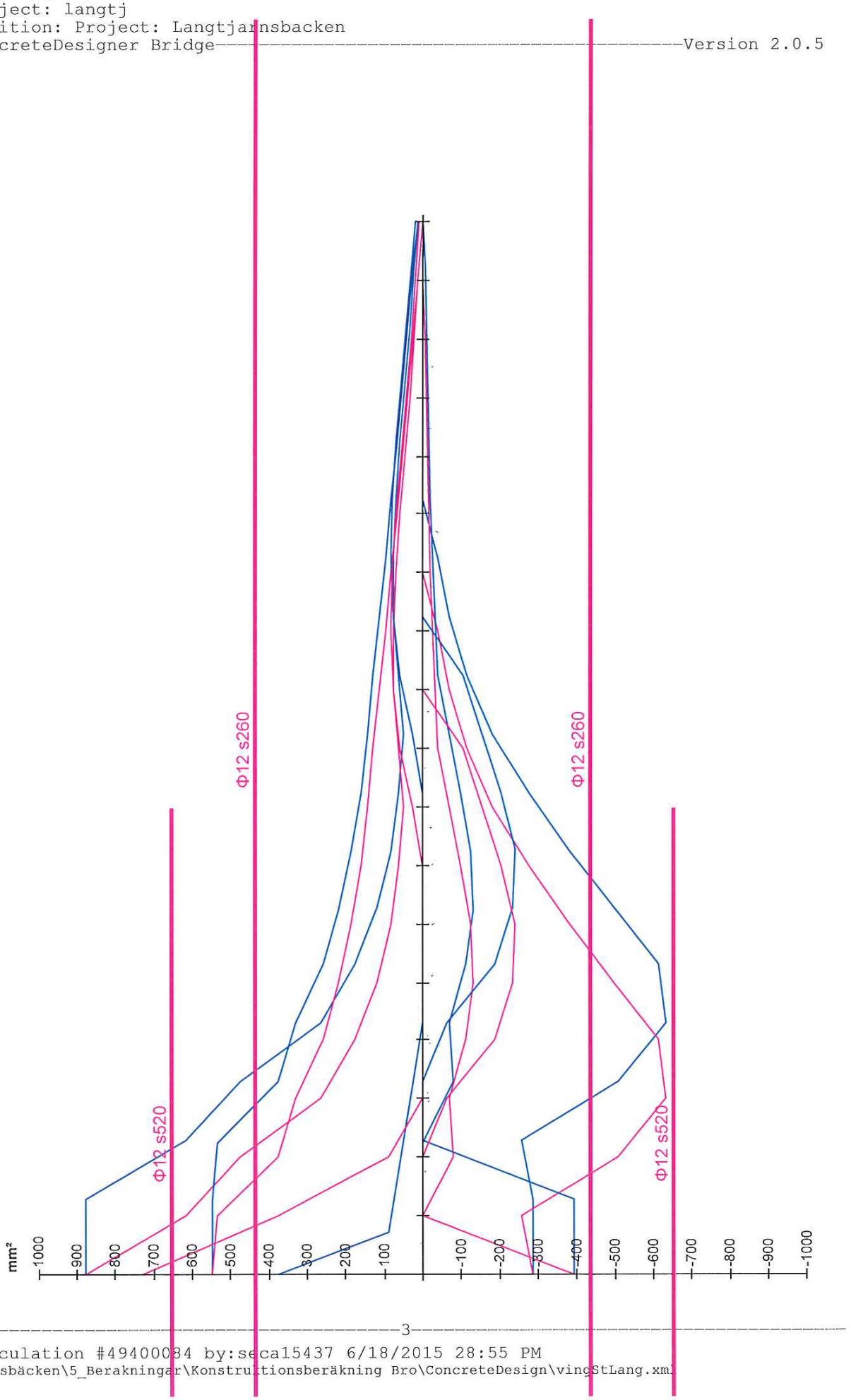

Moment distribution:
Short wing wall, horizontal direction

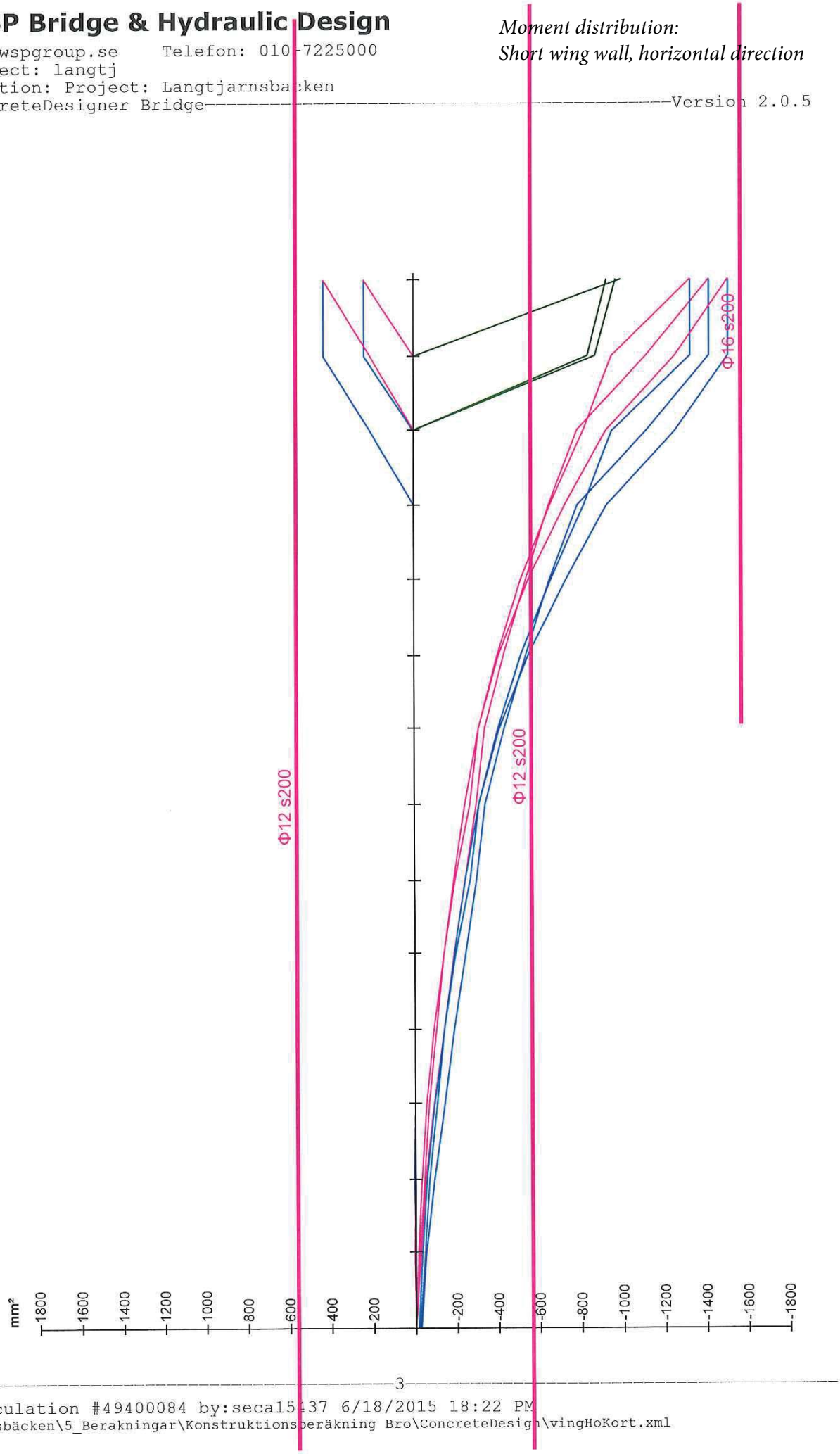

Moment distribution:
Short wing wall, vertical direction

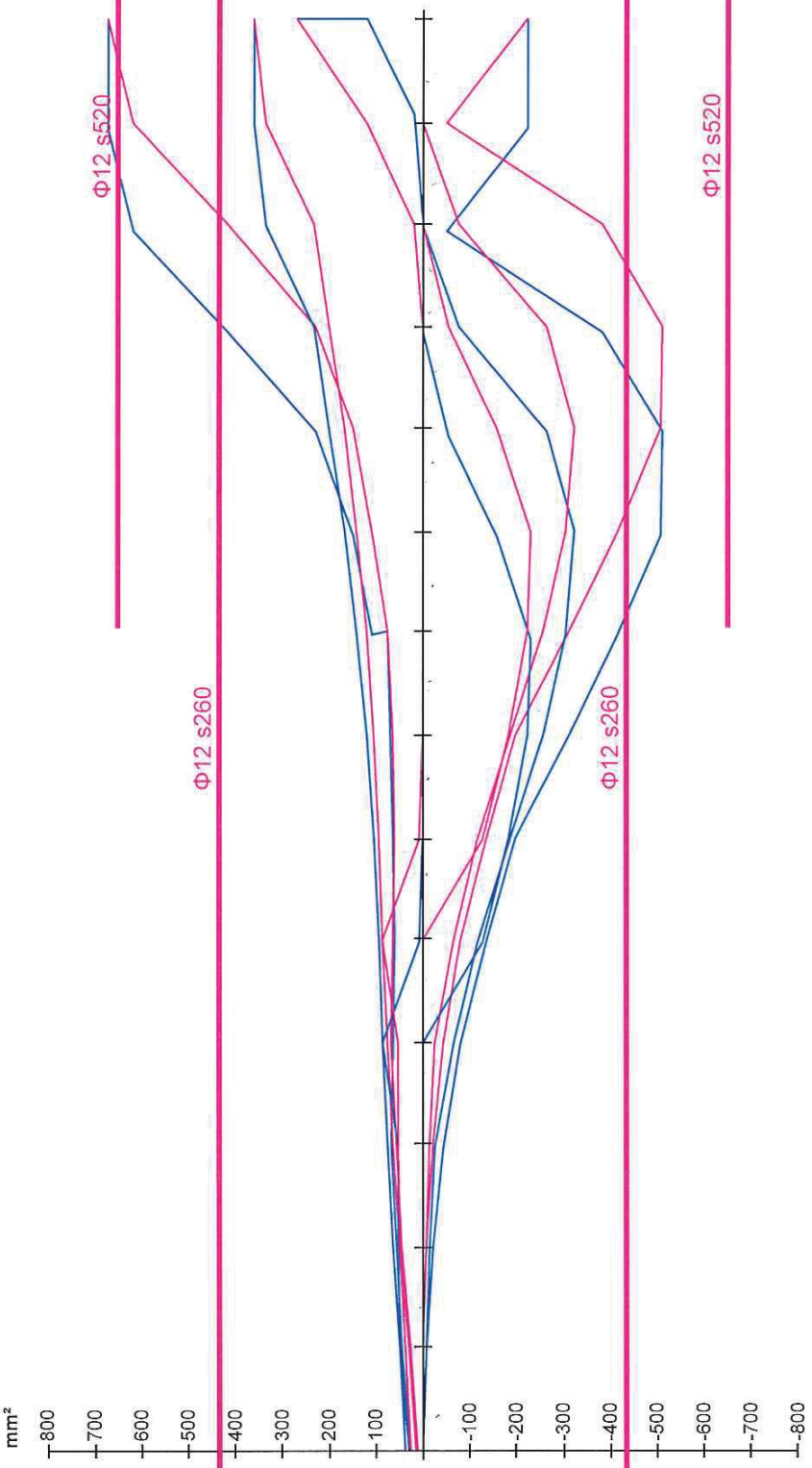

D Redesign of Reinforcement in Slab-Frame Bridge using EN 1.4162

D.1 Calculation Procudure for Bridge Deck, Longitudinal

Slab-Frame Bridge - longitudinal reinforcement in slab

Redesign using stainless steel reinforcement

Sofia Elwin Dahlström, Jonas Persson

Material Indata

Concrete C35/45 (in everything but the base plate)

$\gamma_c := 1.5$ $\alpha_{cc} := 1.0$ $\alpha_{ct} := 1.0$ Safety factors acc. to SS-EN 1992-1-1 (2.4.2.4)

$f_{ck} := 35\ MPa$ $f_{cd} := \alpha_{cc} \cdot \frac{f_{ck}}{\gamma_c} = 23.333\ MPa$ $f_{cm} := 43\ MPa$

$f_{ctk0.05} := 2.2\ MPa$ $f_{ctd} := \alpha_{cc} \cdot \frac{f_{ctk0.05}}{\gamma_c} = 1.467\ MPa$ $f_{ctm} := 3.2\ MPa$

$E_{cm} := 34\ GPa$ $\varphi := 2$ $E_{c.ef} := \frac{E_{cm}}{1+\varphi} = 11.333\ GPa$

$E_{ck} := 28.3\ GPa$

$\varepsilon_{cu} := 3.5 \cdot 10^{-3}$

Reinforcement B500B

$f_{yk} := 500\ MPa$ $\gamma_s := 1.15$

$f_{yd} := \frac{f_{yk}}{\gamma_s} = 434.783\ MPa$

$E_s := 200\ GPa$

$\varepsilon_{syd} := \frac{f_{yd}}{E_s} = 2.174 \cdot 10^{-3}$

$\alpha := \frac{E_s}{E_{cm}} = 5.882$ $\alpha_{ef} := \frac{E_s}{E_{c.ef}} = 17.647$ $\alpha_{fat} := \frac{E_s}{E_{ck}} = 7.067$

Reinforcement EN 1.4162

$f_{yk.ss} := 600\ MPa$ $f_{yd.ss} := \frac{f_{yk.ss}}{\gamma_s} = 522\ MPa$

$n := 15$ $\alpha_0 := 0.6$ Ramberg-Osgood parameters

$E_0 := 170\ GPa$

$\sigma_0 := f_{yd.ss} = 521.739\ MPa$ $\varepsilon_{s0.2} := \frac{\sigma_0}{E_0} + \alpha_0 \cdot \left(\frac{\sigma_0}{E_0}\right)^n = 3.07 \cdot 10^{-3}$

Geometry

$l := 5.88\ m$	Length of span
$b_w := 1000\ mm$	Width of section
$h_{span} := 374\ mm$	designing span moment section (ULS and SLS)
$h_{ULS.sup} := 442\ mm$	designing support moment section
$h_{SLS.sup} := 514\ mm$	designing support crack width section
$h_{fat} := 374\ mm$	designing fatigue bending section (support and span)

Prerequisites of design process

	Service life	Exposure class	Concrete cover	w.k	ξ
Slab, top	L50	XD3/XF4	45	0,20	1,5
Slab, bottom	L50	XD1/XF4	40	0,30	1,2

$w_{k.a.top} := 0.2\ mm$

$w_{k.a.bot} := 0.3\ mm$

Designing sectional forces

Span

$M_{Ed.ULS.span} := 282.3\ kN \cdot m$	$N_{Ed.ULS.span} := -35.2\ kN$	ULS, bending (line 1, section 9)
$M_{Ed.SLS.span} := 64.0\ kN \cdot m$	$N_{Ed.SLS.span} := -22.0\ kN$	SLS, crack width (line 1, section 9)
$M_{Ed.fat.span.min} := 11.1\ kN \cdot m$		Fatigue bending (line 3, section 11)
$N_{Ed.fat.span.min} := -83.8 \cdot kN$		
$M_{Ed.fat.span.max} := 54.3\ kN \cdot m$		

$N_{Ed.fat.span.max} := -84.5 \cdot kN$

Support

$M_{Ed.ULS.sup} := -365.9\ kN \cdot m$ $N_{Ed.ULS.sup} := -120.3\ kN$ ULS, bending (line 3, section 23)

$M_{Ed.SLS.sup} := -96.6\ kN \cdot m$ $N_{Ed.SLS.sup} := 110.6\ kN$ SLS, crack width (line 3, section 24)

$M_{Ed.fat.sup.min} := -66.4\ kN \cdot m$

$N_{Ed.fat.sup.min} := -49.5\ kN$ Fatigue bending (line 3, section 21)

$M_{Ed.fat.sup.max} := -22.9\ kN \cdot m$

$N_{Ed.fat.sup.max} := -51.9\ kN$

Minimum amount of reinforcement

Acc. to TDOK 2016:0204 D.1.4.1.1

$$A_{s.min.1} := \max\left(4.0\ \frac{cm^2}{m}, 4.0\ \frac{cm^2}{m} \cdot \frac{f_{ctm}}{3\ MPa}\right) = 426.667\ \frac{1}{m} \cdot mm^2$$

$$\text{if}\left(\frac{l}{h_{span}} > 5, 0.08\%, 0.05\%\right) = 0.08\%$$

$$A_{s.min.2} := \frac{0.08}{100} \cdot h_{span} = 299.2\ \frac{1}{m} \cdot mm^2$$

$$A_{s.min} := \max\left(A_{s.min.1}, A_{s.min.2}\right) \cdot b_w = 426.667\ mm^2$$

$s_{max} := 300\ mm$

Design of span section

Reinforcement

$\phi_{ss.top} := 16\ mm$ $\quad s_{ss.top} := 300\ mm$ $\quad A'_{ss} := \frac{\pi}{s_{ss.top}} \cdot \frac{\phi_{ss.top}^{2}}{4} \cdot m = 670.21\ mm^2$

$\phi_{cs.top} := 0\ mm$ $\quad s_{cs.top} := 180\ mm$ $\quad A'_{cs} := \frac{\pi}{s_{cs.top}} \cdot \frac{\phi_{cs.top}^{2}}{4} \cdot m = 0\ mm^2$

$\phi_{ss.bot} := 16\ mm$ $\quad s_{ss.bot} := 260\ mm$ $\quad A_{ss} := \frac{\pi}{s_{ss.bot}} \cdot \frac{\phi_{ss.bot}^{2}}{4} \cdot m = 773.32\ mm^2$

$\phi_{cs.bot} := 16\ mm$ $\quad s_{cs.bot} := 140\ mm$ $\quad A_{cs} := \frac{\pi}{s_{cs.bot}} \cdot \frac{\phi_{cs.bot}^{2}}{4} \cdot m = 1436.16\ mm^2$

$Check\_min\_reinf\_span := \text{if}\left(A_{ss} + A_{cs} > A_{s.min}, \text{“OK”}, \text{“NOT OK”}\right) = \text{“OK”}$

$d'_{ss} := 45\ mm + \frac{\phi_{ss.top}}{2} = 53\ mm$

$d'_{cs} := d'_{ss} + 37\ mm + \phi_{ss.top} = 106\ mm$

$d_{ss} := h_{span} - 40\ mm - \frac{\phi_{ss.bot}}{2} = 326\ mm$

$d_{cs} := d_{ss} - 37\ mm - \phi_{cs.bot} = 273\ mm$

$d_m := \frac{d_{ss} + d_{cs}}{2} = 299.5\ mm$

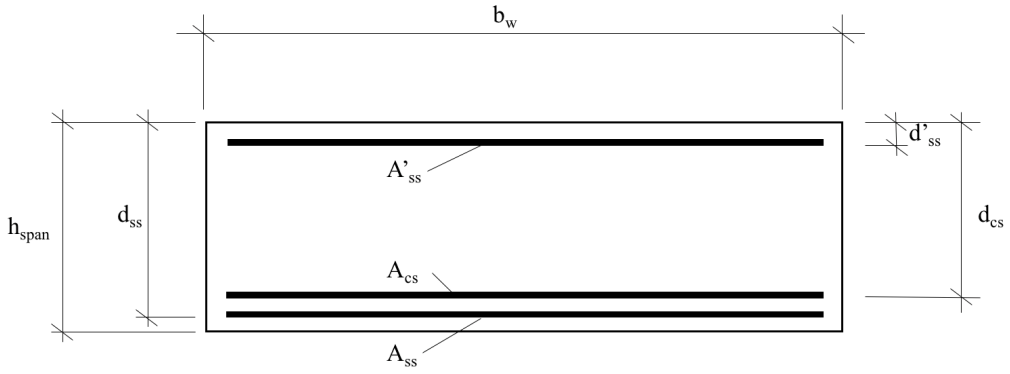

ULS, bending (section 9, line 1)

$\alpha_c := 0.81$ $\beta := 0.416$ Pressure block coefficients

$x := 40 \cdot mm$ Initial guess

$$x_{ULS} := \text{root}\left(\begin{matrix}\alpha_c \cdot f_{cd} \cdot b_w \cdot x + A'_{ss} \cdot \frac{x - d'_{ss}}{x} \cdot \varepsilon_{cu} \cdot E_0 \\ -A'_{cs} \cdot \frac{d'_{cs} - x}{x} \cdot \varepsilon_{cu} \cdot E_s - A_{cs} \cdot f_{yd} - A_{ss} \cdot \sigma_0 + N_{Ed.ULS.span}\end{matrix}, x\right) = 55.352\ mm$$

$$\varepsilon_{ss.span} := \frac{d_{ss} - x_{ULS}}{x_{ULS}} \cdot \varepsilon_{cu} = 17.114\ 10^{-3} \qquad \varepsilon'_{cs.span} := \frac{d'_{cs} - x_{ULS}}{x_{ULS}} \cdot \varepsilon_{cu} = 3.203\ 10^{-3}$$

$$\varepsilon_{cs.span} := \frac{d_{cs} - x_{ULS}}{x_{ULS}} \cdot \varepsilon_{cu} = 13.762\ 10^{-3} \qquad \varepsilon'_{ss.span} := \frac{x_{ULS} - d'_{ss}}{x_{ULS}} \cdot \varepsilon_{cu} = 0.149\ 10^{-3}$$

$Check\_yielding\_ss\_span := \text{if}\left(\varepsilon_{ss.span} > \varepsilon_{s0.2}, \text{“OK”}, \text{“NOT OK”}\right) = \text{“OK”}$

$Check\_yielding\_cs\_span := \text{if}\left(\varepsilon_{cs.span} > \varepsilon_{syd}, \text{“OK”}, \text{“NOT OK”}\right) = \text{“OK”}$

$Check\_not\_yielding\_ss'\_span := \text{if}\left(\varepsilon'_{ss.span} < \varepsilon_{s0.2}, \text{“OK”}, \text{“NOT OK”}\right) = \text{“OK”}$

$Check\_ductility\_span := \text{if}\left(x_{ULS} \le 0.45 \cdot d_{ss.span}, \text{“OK”}, \text{“NOT OK”}\right) = \text{“OK”}$

Moment capacity

$$M_{Rd.span} := \alpha_c \cdot f_{cd} \cdot b_w \cdot x_{ULS} \cdot \left(d_{ss} - \beta \cdot x_{ULS}\right) + A'_{ss} \cdot \frac{x_{ULS} - d'_{ss}}{x_{ULS}} \cdot \varepsilon_{cu} \cdot E_0 \cdot \left(d_{ss} - d'_{ss}\right) - A'_{cs} \cdot \frac{d'_{cs} - x_{ULS}}{x_{ULS}} \cdot \varepsilon_{cu} \cdot E_s \cdot \left(d_{ss} - d'_{cs}\right) - A_{cs} \cdot f_{yd} \cdot \left(d_{ss} - d_{cs}\right) + N_{Ed.ULS.span} \cdot \left(d_{ss} - \frac{h_{span}}{2}\right) = 283.592\ kN \cdot m$$

$Check\_ULS\_bending\_span := \text{if}\left(\left|M_{Ed.ULS.span}\right| \le M_{Rd.span}, \text{“OK”}, \text{“NOT OK”}\right) = \text{“OK”}$

$$Utilization\_ratio\_ULS\_bending\_span := \frac{\left|M_{Ed.ULS.span}\right|}{M_{Rd.span}} = 99.5\%$$

SLS, crack width (section 9, line 1)

Cross-section constants

$x_{SLS} := 100\ mm$ Initial guess

$x_{SLS} = 77.1844\ mm$ Value from iteration

$$A_{II} := b_w \cdot x_{SLS} + (\alpha - 1) \cdot A'_{ss} + (\alpha - 1) \cdot A'_{cs} + \alpha \cdot A_{ss} + \alpha \cdot A_{cs} = 0.093\ m^2$$

$$x_{tp} := \frac{\left(b_w \cdot \frac{x_{SLS}^2}{2} + (\alpha - 1) \cdot A'_{ss} \cdot d'_{ss} + \alpha \cdot A_{ss} \cdot d_{ss} + \alpha \cdot A_{cs} \cdot d_{cs} + (\alpha - 1) \cdot A'_{cs} \cdot d'_{cs} \right)}{A_{II}} = 0.074\ m$$

$$I_{II} := \frac{b_w \cdot x_{SLS}^3}{12} + b_w \cdot x_{SLS} \cdot \left(\frac{x_{SLS}}{2} - x_{tp} \right)^2 + (\alpha - 1) \cdot A'_{ss} \cdot \left(x_{tp} - d'_{ss} \right)^2 + \alpha \cdot A_{ss} \cdot \left(d_{ss} - x_{tp} \right)^2 + \alpha \cdot A_{cs} \cdot \left(d_{cs} - x_{tp} \right)^2 + (\alpha - 1) \cdot A'_{cs} \cdot \left(x_{tp} - d'_{cs} \right)^2 = \left(7.599 \cdot 10^{-4} \right) m^4$$

Stress in concrete and steel

x is correct when the stress is zero

$$\sigma_c := \frac{N_{Ed.SLS.span}}{A_{II}} + \left(\frac{N_{Ed.SLS.span} \cdot \left(\frac{h_{span}}{2} - x_{tp} \right) + M_{Ed.SLS.span}}{I_{II}} \right) \cdot \left(x_{SLS} - x_{tp} \right) = 0\ Pa$$

$$\sigma_{c.ss} := \frac{N_{Ed.SLS.span}}{A_{II}} + \left(\frac{N_{Ed.SLS.span} \cdot \left(\frac{h_{span}}{2} - x_{tp} \right) + M_{Ed.SLS.span}}{I_{II}} \right) \cdot \left(d_{ss} - x_{tp} \right) = 20.142\ MPa$$

$\sigma_{s.ss} := \alpha \cdot \sigma_{c.ss} = 118.485\ MPa$ Steel stress at outer layer of steel reinforcement

$$\sigma_{s.ss.nonlin} := \mathbf{root}\left(\alpha \cdot \sigma_{c.ss} - \left(\sigma_{s.ss} + \alpha_0 \cdot \sigma_0 \cdot \left(\frac{\sigma_{s.ss}}{\sigma_0} \right)^n \right), \sigma_{s.ss} \right) = 118.485\ MPa$$

Steel stress with regard to non-linearity

$$\varepsilon_{ss} := \frac{\sigma_{s.ss.nonlin}}{E_0} = 0.697\ 10^{-3}$$

Check to ensure that the assumed Youngs modulus is correct (in the linear region)

$$Check\_E\_SLS\_span := \text{if}\left(\varepsilon_{s0.2} > \varepsilon_{ss}, \text{“OK”}, \text{“INTE OK”}\right) = \text{“OK”}$$

Crack width calculation

$$h_{c.eff.bot} := min\left(2.5 \cdot \left(h_{span} - d_{ss}\right), \frac{h_{span} - x_{SLS}}{3}, \frac{h_{span}}{2}\right) = 98.939\ mm$$

Effective height concrete section, SS-EN 1992-1-1:2005 chapter 7.3.2 (3)

$$A_{c.eff} := h_{c.eff.bot} \cdot b_w = \left(9.894 \cdot 10^4\right)\ mm^2$$

Effective concrete area, SS-EN 1992-1-1:2005, figure 7.1

$$\rho_{p.eff} := \frac{A_{ss} + A_{cs}}{A_{c.eff}} = 0.022$$

Relation between area of tensile reinforcement and effective concrete area, SS-EN 1992-1-1:2005 (7.10)

$$k_t := 0.4$$

Factor that considers duration of load, SS-EN 1992-1-1:2005 7.3.4 (2)

$$\Delta\varepsilon := \frac{\sigma_{s.ss} - k_t \cdot f_{ctm} \cdot \frac{\left(1 + \alpha \cdot \rho_{p.eff}\right)}{\rho_{p.eff}}}{E_0} = 3.155 \cdot 10^{-4}$$

Difference between concrete and steel strain

$$k_1 := 0.8 \qquad k_4 := 0.425 \qquad k_2 := 0.5$$

Constants according to SS-EN 1992-1-1, 7.3.4

$$s_{r.max.bot} := 7 \cdot \phi_{ss.bot} + k_1 \cdot k_2 \cdot k_4 \cdot \frac{\phi_{ss.bot}}{\rho_{p.eff}} = 234\ mm$$

Maximum crack distance, SS-EN 1992-1-1:2005 (7.11)

$$w_{k.bot} := s_{r.max.bot} \cdot \left(\max\left(\Delta\varepsilon, 0.6 \cdot \frac{\sigma_{s.ss}}{E_0}\right)\right) = 0.10\ mm$$

Characteristic crack width SS-EN 1992-1-1:2005 (7.8)

$$Check\_crackwidth\_span := \text{if}\left(w_{k.bot} \le w_{k.a.bot}, \text{“OK”}, \text{“NOT OK”}\right) = \text{“OK”}$$

$$Utilization\_crackwidth\_span := \frac{w_{k.bot}}{w_{k.a.bot}} = 33\%$$

Fatigue, bending (section 11, line 3)

Allowable steel stress range

$N := 5 \cdot 10^5$ Number of cycles

$k_1 := 5.0$ $k_2 := 9.0$ Parameters for Wöhler-curves

$\gamma_{s.fat} := 1.15$ $\gamma_{F.fat} := 1.0$ Safety factors acc. to SS-EN 1992-1-1 (2.4.3.4) and (6.8)

$\Delta\sigma_{Rsk} := \sqrt[k_1]{162.5^5 \cdot \frac{10^6}{(N)}}\ MPa = 186.663\ MPa$ Allowable steel stress range

Maximum and minimum steel stress acc. to Betonghandboken 4.3:34

$\rho_{span} := \frac{A_{ss.span} + A_{cs.span}}{d_m} = 0.738\%$ Reinforcement content (only tensile reinforcement)

$\xi := 0.6$ Initial guess

$$\xi_{min} := \mathrm{root}\left(\begin{pmatrix} \frac{1}{2} \cdot \frac{\xi^2}{1-\xi} \\ \cdot \left(1 + \left(1 - \frac{\xi}{3}\right) \cdot \frac{N_{Ed.fat.span.min}}{M_{Ed.fat.span.min} - N_{Ed.fat.span.min} \cdot \left(d_m - \frac{h_{fat}}{2}\right)} \cdot d_m\right) \\ -\alpha_{fat} \cdot \rho_{span} \end{pmatrix}, \xi\right) = 0.702$$

$$\xi_{max} := \mathrm{root}\left(\begin{pmatrix} \frac{1}{2} \cdot \frac{\xi^2}{1-\xi} \\ \cdot \left(1 + \left(1 - \frac{\xi}{3}\right) \cdot \frac{N_{Ed.fat.span.max}}{M_{Ed.fat.span.max} - N_{Ed.fat.span.max} \cdot \left(d_m - \frac{h_{fat}}{2}\right)} \cdot d_m\right) \\ -\alpha_{fat} \cdot \rho_{span} \end{pmatrix}, \xi\right) = 0.329$$

$$\sigma_{s.min.II} := \frac{\left(M_{Ed.fat.span.min} - N_{Ed.fat.span.min} \cdot \left(d_m - \frac{h_{fat}}{2}\right)\right)}{\left(A_{ss.span} + A_{cs.span}\right) \cdot m \cdot d_m \cdot \left(1 - \frac{\xi_{min}}{3}\right)} + \frac{N_{Ed.fat.span.min}}{\left(A_{ss.span} + A_{cs.span}\right) \cdot m} = 2.561\ MPa$$

$$\sigma_{s.max.II} := \frac{\left(M_{Ed.fat.span.max} - N_{Ed.fat.span.max} \cdot \left(d_m - \frac{h_{fat}}{2}\right)\right)}{\left(A_{ss.span} + A_{cs.span}\right) \cdot m \cdot d_m \cdot \left(1 - \frac{\xi_{min}}{3}\right)} + \frac{N_{Ed.fat.span.max}}{\left(A_{ss.span} + A_{cs.span}\right) \cdot m} = 87.607\ MPa$$

$$\Delta\sigma_{s.equ.span} := \sigma_{s.max.II} - \sigma_{s.min.II} = 85.046\ MPa$$

$$\gamma_{s.fat} \cdot \Delta\sigma_{s.equ.span} = 97.803\ MPa$$

$$Check\_fatigue\_span := \text{if}\left(\gamma_{s.fat} \cdot \Delta\sigma_{s.equ.span} < \Delta\sigma_{Rsk}, \text{“OK”}, \text{“NOT OK”}\right) = \text{“OK”}$$

$$Utilization\_fatigue\_span := \frac{\Delta\sigma_{s.equ.span} \cdot \gamma_{s.fat}}{\Delta\sigma_{Rsk}} = 52.395\%$$

Fatigue, concrete compressed edge (top)

$k_1 := 0.85$ Acc. to SS-EN 1992-1-1 (6.8)

$s := 0.25$ Acc. to SS-EN 1992-1-1 (3.2)

$t := 28$

$$\beta_{cc} := \exp\left(s \cdot \left(1 - \left(\frac{28}{t}\right)^{\frac{1}{2}}\right)\right)$$

$$f_{cd.fat} := k_1 \cdot \beta_{cc} \cdot f_{cd} \cdot \left(1 - \frac{f_{ck}}{250\ MPa}\right) = 17.057\ MPa$$ Acc. to SS-EN 1992-1-1 (6.76)

Maximum and minimum concrete stress acc. to Betonghandboken 4.3:34

$$\sigma_{c.max.span} := \frac{2 \cdot \left(\left| M_{Ed.fat.span.max} \right| + N_{Ed.fat.span.max} \cdot \left(d_m - \frac{h_{fat}}{2} \right) \right)}{b_w \cdot {d_m}^2 \cdot \xi_{max} \cdot \left(1 - \frac{\xi_{max}}{3} \right)} = 3.41 \ MPa$$

$$\sigma_{c.min.span} := \frac{2 \cdot \left(\left| M_{Ed.fat.span.min} \right| + N_{Ed.fat.span.min} \cdot \left(d_m - \frac{h_{fat}}{2} \right) \right)}{b_w \cdot {d_m}^2 \cdot \xi_{min} \cdot \left(1 - \frac{\xi_{min}}{3} \right)} = 0.069 \ MPa$$

$$Check\_fat\_span := \text{if} \left(\frac{\sigma_{c.max.span}}{f_{cd.fat}} < 0.5 \ \text{↲} \quad < 0.9 \ , \text{“OK”} , \text{“NOT OK”} \right) = \text{“OK”}$$

$$+ 0.45 \cdot \frac{\sigma_{c.min.span}}{f_{cd.fat}}$$

Design of support section

Reinforcement

$\phi_{ss.top} := 16\ mm$ $\quad s_{ss.top} := 300\ mm$ $\quad A'_{ss} := \frac{\pi}{s_{ss.top}} \cdot \frac{\phi_{ss.top}^{2}}{4} \cdot m = 670.206\ mm^2$

$\phi_{cs.top} := 16\ mm$ $\quad s_{cs.top} := 135\ mm$ $\quad A'_{cs} := \frac{\pi}{s_{cs.top}} \cdot \frac{\phi_{cs.top}^{2}}{4} \cdot m = 1489.348\ mm^2$

$\phi_{ss.bot} := 16\ mm$ $\quad s_{ss.bot} := 260\ mm$ $\quad A_{ss} := \frac{\pi}{s_{ss.bot}} \cdot \frac{\phi_{ss.bot}^{2}}{4} \cdot m = 773.315\ mm^2$

$\phi_{cs.bot} := 16\ mm$ $\quad s_{cs.bot} := 140\ mm$ $\quad A_{cs} := \frac{\pi}{s_{cs.bot}} \cdot \frac{\phi_{cs.bot}^{2}}{4} \cdot m = 1436.157\ mm^2$

$Check\_min\_reinf\_support := \text{if}\left(A'_{ss} + A'_{cs} > A_{s.min}, \text{“OK”}, \text{“NOT OK”}\right) = \text{“OK”}$

$d_{ss} := 40\ mm + \frac{\phi_{ss.bot}}{2} = 48\ mm$

$d_{cs} := d_{ss} + 37\ mm + \phi_{cs.bot} = 101\ mm$

$d'_{ss} := h_{ULS.sup} - 45\ mm - \frac{\phi_{ss.top}}{2} = 389\ mm$

$d'_{cs} := d'_{ss} - 37\ mm - \phi_{cs.top} = 336\ mm$

$d'_{m} := \frac{\left(d'_{ss} + d'_{cs}\right)}{2} = 362.5\ mm$

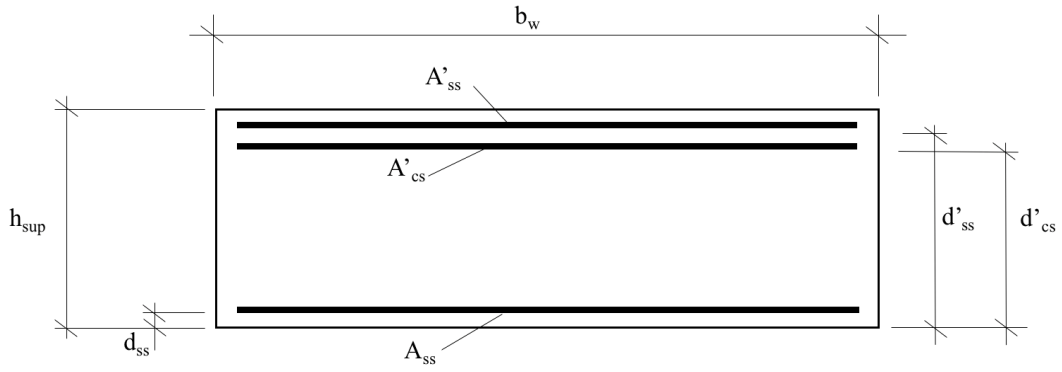

ULS, bending (line 3, section 23)

$x := 40 \cdot mm$ Initial guess

$$x_{ULS} := \text{root}\left(\begin{matrix}\alpha_c \cdot f_{cd} \cdot b_w \cdot x + A_{ss} \cdot \frac{x - d_{ss}}{x} \cdot \varepsilon_{cu} \cdot E_s - A_{cs} \cdot \frac{(d_{cs} - x)}{x} \cdot \varepsilon_{cu} \cdot E_s \\ -A'_{cs} \cdot f_{yd} - A'_{ss} \cdot \sigma_0 + N_{Ed.ULS.sup}\end{matrix}, x\right) = 71.569\ mm$$

$$\varepsilon'_{ss} := \frac{d'_{ss} - x_{ULS}}{x_{ULS}} \cdot \varepsilon_{cu} = 15.524\ 10^{-3} \qquad \varepsilon_{ss} := \frac{x_{ULS} - d_{ss}}{x_{ULS}} \cdot \varepsilon_{cu} = 0.001$$

$$\varepsilon'_{cs} := \frac{d'_{cs} - x_{ULS}}{x_{ULS}} \cdot \varepsilon_{cu} = 12.932\ 10^{-3} \qquad \varepsilon_{cs} := \frac{d_{cs} - x_{ULS}}{x_{ULS}} \cdot \varepsilon_{cu} = 0.001$$

$Check\_yielding\_ss'\_sup := \text{if}\left(\varepsilon'_{ss} > \varepsilon_{s0.2}, \text{“OK”}, \text{“NOT OK”}\right) = \text{“OK”}$

$Check\_yielding\_cs'\_sup := \text{if}\left(\varepsilon'_{cs} > \varepsilon_{syd}, \text{“OK”}, \text{“NOT OK”}\right) = \text{“OK”}$

$Check\_not\_yielding\_ss\_sup := \text{if}\left(\varepsilon_{ss} < \varepsilon_{syd}, \text{“OK”}, \text{“NOT OK”}\right) = \text{“OK”}$

$Check\_not\_yielding\_cs\_sup := \text{if}\left(\varepsilon_{cs} < \varepsilon_{syd}, \text{“OK”}, \text{“NOT OK”}\right) = \text{“OK”}$

$Check\_ductility\_sup := \text{if}\left(x_{ULS} \le 0.45 \cdot d'_m, \text{“OK”}, \text{“NOT OK”}\right) = \text{“OK”}$

$$\begin{aligned} M_{Rd.sup} := {} & \alpha_c \cdot f_{cd} \cdot b_w \cdot x_{ULS} \cdot \left(d'_{ss} - \beta \cdot x_{ULS}\right) \\ & + A_{ss} \cdot \frac{x_{ULS} - d_{ss}}{x_{ULS}} \cdot \varepsilon_{cu} \cdot E_s \cdot \left(d'_{ss} - d_{ss}\right) - A'_{cs} \cdot f_{yd} \cdot \left(d'_{ss} - d'_{cs}\right) \\ & - A_{cs} \cdot \frac{(d_{cs} - x_{ULS})}{x_{ULS}} \cdot \varepsilon_{cu} \cdot E_s \cdot \left(d'_{ss} - d_{cs}\right) \\ & - \left|N_{Ed.ULS.sup}\right| \cdot \left(d'_{ss} - \frac{h_{ULS.sup}}{2}\right) \end{aligned} = 373.108\ kN \cdot m$$

$Check\_ULS\_bending\_sup := \text{if}\left(\left|M_{Ed.ULS.sup}\right| \le M_{Rd.sup}, \text{“OK”}, \text{“NOT OK”}\right) = \text{“OK”}$

$$Utilization\_ratio\_ULS\_bending\_sup := \frac{\left|M_{Ed.ULS.sup}\right|}{M_{Rd.sup}} = 98.1\%$$

SLS, crack width (line 3, section 24)

$$d'_{ss} := h_{SLS.sup} - 45\ mm - \frac{\phi_{ss.top}}{2} = 0.461\ m$$

$x_{SLS} := 100\ mm$ Initial guess

$x_{SLS} = 73.071\ mm$

$A_{II} := b_w \cdot x_{SLS} + (\alpha - 1) \cdot A_{ss} + \alpha \cdot A'_{ss} + \alpha \cdot A'_{cs} + (\alpha - 1) \cdot A_{cs} = 0.097\ m^2$

$$x_{tp} := \frac{\left(b_w \cdot \frac{x_{SLS}^{\ 2}}{2} + (\alpha - 1) \cdot A_{ss} \cdot d_{ss} + \alpha \cdot A'_{ss} \cdot d'_{ss} + \alpha \cdot A'_{cs} \cdot d'_{cs} + (\alpha - 1) \cdot A_{cs} \cdot d_{cs} \right)}{A_{II}} = 0.086\ m$$

$$I_{II} := \frac{b_w \cdot x_{SLS}^{\ 3}}{12} + b_w \cdot x_{SLS} \cdot \left(\frac{x_{SLS}}{2} - x_{tp} \right)^2 + (\alpha - 1) \cdot A_{ss} \cdot \left(x_{tp} - d_{ss} \right)^2 = 0.001\ m^4$$
$$+ \alpha \cdot A'_{ss} \cdot \left(d'_{ss} - x_{tp} \right)^2 + \alpha \cdot A'_{cs} \cdot \left(d'_{cs} - x_{tp} \right)^2 + (\alpha - 1) \cdot A_{cs} \cdot \left(x_{tp} - d_{cs} \right)^2$$

$$\sigma_c := \frac{N_{Ed.SLS.sup}}{A_{II}} + \left(\frac{N_{Ed.SLS.sup} \cdot \left(\frac{h_{SLS.sup}}{2} - x_{tp} \right) - M_{Ed.SLS.sup}}{I_{II}} \right) \cdot \left(x_{SLS} - x_{tp} \right) = 0\ Pa$$

$$\sigma_{c.ss} := \frac{N_{Ed.SLS.sup}}{A_{II}} + \left(\frac{N_{Ed.SLS.sup} \cdot \left(\frac{h_{SLS.sup}}{2} - x_{tp} \right) - M_{Ed.SLS.sup}}{I_{II}} \right) \cdot \left(d'_{ss} - x_{tp} \right) = 33.935\ MPa$$

$\sigma_{s.ss} := \alpha \cdot \sigma_{c.ss} = 199.617\ MPa$ Steel stress at outer layer of steel reinforcement

$$\sigma_{s.ss.nonlin} := \text{root}\left(\alpha \cdot \sigma_{c.ss} - \left(\sigma_{s.ss} + \alpha_0 \cdot \sigma_0 \cdot \left(\frac{\sigma_{s.ss}}{\sigma_0} \right)^n \right), \sigma_{s.ss} \right) = 199.617\ MPa$$

Steel stress with regard to non-linearity

$\varepsilon_{ss} := \frac{\sigma_{s.ss.nonlin}}{E_0} = 1.174\ 10^{-3}$

Check to ensure that the assumed Youngs modulus is correct (in the linear region)

$Check\_E\_SLS\_span := \text{if}\left(\varepsilon_{s0.2} > \varepsilon_{ss}, \text{“OK”}, \text{“INTE OK”} \right) = \text{“OK”}$

$$h_{c.eff.top} := min\left(2.5 \cdot \left(h_{SLS.sup} - d'_{ss}\right), \frac{h_{SLS.sup} - x_{SLS}}{3}, \frac{h_{SLS.sup}}{2}\right) = 132.5\ mm$$

Effective height concrete section, SS-EN 1992-1-1:2005 7.3.2 (3)

$$A_{c.eff} := h_{c.eff.top} \cdot b_w = \left(1.325 \cdot 10^5\right)\ mm^2$$

Effective concrete area, SS-EN 1992-1-1:2005, figure 7.1

$$\rho_{p.eff} := \frac{A'_{ss} + A'_{cs}}{A_{c.eff}} = 0.016$$

Relation between area of tensile reinforcement and effective concrete area, SS-EN 1992-1-1:2005 (7.10)

$$k_t := 0.4$$

Factor that considers duration of load, SS-EN 1992-1-1:2005 7.3.4 (2)

$$\Delta\varepsilon := \frac{\sigma_{s.ss} - k_t \cdot f_{ctm} \cdot \frac{\left(1 + \alpha \cdot \rho_{p.eff}\right)}{\rho_{p.eff}}}{E_0} = 6.68 \cdot 10^{-4}$$

Difference between concrete and steel strain

$$k_1 := 0.8 \qquad k_4 := 0.425 \qquad k_2 := 0.5$$

Constants according to SS-EN 1992-1-1, 7.3.4

$$s_{r.max.top} := 7 \cdot \phi_{ss.top} + k_1 \cdot k_2 \cdot k_4 \cdot \frac{\phi_{ss.top}}{\rho_{p.eff}} = 279\ mm$$

Maximum crack distance, SS-EN 1992-1-1:2005 (7.11)

$$w_{k.top} := s_{r.max.top} \cdot \left(\max\left(\Delta\varepsilon, 0.6 \cdot \frac{\sigma_{s.ss}}{E_0}\right)\right) = 0.20\ mm$$

Characteristic crack width SS-EN 1992-1-1:2005 (7.8)

$$Check\_crackwidth\_support := \text{if}\left(w_{k.top} \le w_{k.a.top}, \text{“OK”}, \text{“NOT OK”}\right) = \text{“OK”}$$

$$Utilization\_crackwidth\_support := \frac{w_{k.top}}{w_{k.a.top}} = 98\%$$

Fatigue, bending

$\Delta\sigma_{s.equ} := 107.7\ MPa$ Value from Concrete Bridge Designer, dst 3.21

$d'_{ss} := h_{fat} - 45\ mm - \frac{\phi_{ss.top}}{2} = 0.321\ m$

$\rho_{sup} := \frac{A'_{ss.sup} + A'_{cs.sup}}{d'_m} = 0.596\%$ Reinforcement content (only tensile reinforcement)

Maximum and minimum steel stress acc. to Betonghandboken 4.3:34

$\xi := 0.6$ Initial guess

$$\xi_{min} := \text{root}\left(\begin{pmatrix} \frac{1}{2}\cdot\frac{\xi^2}{1-\xi}\cdot\left(1+\left(1-\frac{\xi}{3}\right)\cdot\frac{N_{Ed.fat.sup.min}}{\left|M_{Ed.fat.sup.min}\right| - N_{Ed.fat.sup.min}\cdot\left(d'_m - \frac{h_{fat}}{2}\right)}\cdot d'_m\right) \\ -\alpha_{fat}\cdot\rho_{sup} \end{pmatrix}, \xi\right) = 0.279$$

$$\xi_{max} := \text{root}\left(\begin{pmatrix} \frac{1}{2}\cdot\frac{\xi^2}{1-\xi}\cdot\left(1+\left(1-\frac{\xi}{3}\right)\cdot\frac{N_{Ed.fat.sup.max}}{\left|M_{Ed.fat.sup.max}\right| - N_{Ed.fat.sup.max}\cdot\left(d'_m - \frac{h_{fat}}{2}\right)}\cdot d'_m\right) \\ -\alpha_{fat}\cdot\rho_{sup} \end{pmatrix}, \xi\right) = 0.341$$

$$\sigma_{s.max.II.sup} := \frac{\left(\left|M_{Ed.fat.sup.min}\right| - N_{Ed.fat.sup.min}\cdot\left(d'_m - \frac{h_{fat}}{2}\right)\right)}{\left(A'_{ss.sup} + A'_{cs.sup}\right)\cdot m\cdot d'_m\cdot\left(1-\frac{\xi_{min}}{3}\right)} = 82.811\ MPa$$
$$+ \frac{N_{Ed.fat.sup.min}}{\left(A'_{ss.sup} + A'_{cs.sup}\right)\cdot m}$$

$$\sigma_{s.min.II.sup} := \frac{\left(\left|M_{Ed.fat.sup.max}\right| - N_{Ed.fat.sup.max} \cdot \left(d'_m - \frac{h_{fat}}{2}\right)\right)}{\left(A'_{ss.sup} + A'_{cs.sup}\right) \cdot m \cdot d'_m \cdot \left(1 - \frac{\xi_{max}}{3}\right)} = 22.09\ MPa$$
$$+ \frac{N_{Ed.fat.sup.max}}{\left(A'_{ss.sup} + A'_{cs.sup}\right) \cdot m}$$

$\Delta\sigma_{s.equ.sup} := \sigma_{s.max.II.sup} - \sigma_{s.min.II.sup} = 60.721\ MPa$ Stress range

$\gamma_{s.fat} \cdot \Delta\sigma_{s.equ.sup} = 69.829\ MPa$

$Check\_fatigue\_support\_s := \text{if}\left(\gamma_{s.fat} \cdot \Delta\sigma_{s.equ.sup} < \Delta\sigma_{Rsk}, \text{“OK”}, \text{“NOT OK”}\right) = \text{“OK”}$

$Utilization\_fatigue\_support\_s := \frac{\Delta\sigma_{s.equ.sup} \cdot \gamma_{s.fat}}{\Delta\sigma_{Rsk}} = 37.409\%$

Fatigue, concrete

Maximum and minimum concrete stress acc. to Betonghandboken 4.3:34

$$\sigma_{c.min.sup} := \frac{2 \cdot \left(\left|M_{Ed.fat.sup.max}\right| + N_{Ed.fat.sup.max} \cdot \left(d'_m - \frac{h_{fat}}{2}\right)\right)}{b_w \cdot {d'_m}^2 \cdot \xi_{max} \cdot \left(1 - \frac{\xi_{max}}{3}\right)} = 0.695\ MPa$$

$$\sigma_{c.max.sup} := \frac{2 \cdot \left(\left|M_{Ed.fat.sup.min}\right| + N_{Ed.fat.sup.min} \cdot \left(d'_m - \frac{h_{fat}}{2}\right)\right)}{b_w \cdot {d'_m}^2 \cdot \xi_{min} \cdot \left(1 - \frac{\xi_{min}}{3}\right)} = 3.477\ MPa$$

$$Check\_fatigue\_sup\_c := \text{if}\left(\frac{\sigma_{c.max.sup}}{f_{cd.fat}} < 0.5 + 0.45 \cdot \frac{\sigma_{c.min.sup}}{f_{cd.fat}} < 0.9, \text{“OK”}, \text{“NOT OK”}\right) = \text{“OK”}$$

Checks - longitudinal reinforcement

Span

$$Check\_yielding\_ss\_span := \text{if}\left(\varepsilon_{ss.span} > \varepsilon_{syd}, \text{“OK”}, \text{“NOT OK”}\right) = \text{“OK”}$$

$$Check\_yielding\_cs\_span := \text{if}\left(\varepsilon_{cs.span} > \varepsilon_{syd}, \text{“OK”}, \text{“NOT OK”}\right) = \text{“OK”}$$

$$Check\_not\_yielding\_ss'\_span := \text{if}\left(\varepsilon'_{ss.span} < \varepsilon_{syd}, \text{“OK”}, \text{“NOT OK”}\right) = \text{“OK”}$$

$$Check\_ductility\_span := \text{if}\left(x_{ULS} \le 0.45 \cdot d_{ss.span}, \text{“OK”}, \text{“NOT OK”}\right) = \text{“OK”}$$

$$Check\_ULS\_bending\_span := \text{if}\left(M_{Ed.ULS.span} \le M_{Rd.span}, \text{“OK”}, \text{“NOT OK”}\right) = \text{“OK”}$$

$$Check\_crackwidth\_span\_s := \text{if}\left(w_{k.bot} \le w_{k.a.bot}, \text{“OK”}, \text{“NOT OK”}\right) = \text{“OK”}$$

$$Check\_fatigue\_span\_s := \text{if}\left(\gamma_{s.fat} \cdot \Delta\sigma_{s.equ.span} < \Delta\sigma_{Rsk}, \text{“OK”}, \text{“NOT OK”}\right) = \text{“OK”}$$

$$Fat\_span\_c := \text{if}\left(\frac{\sigma_{c.max.span}}{f_{cd.fat}} < 0.5 + 0.45 \cdot \frac{\sigma_{c.min.span}}{f_{cd.fat}} < 0.9, \text{“OK”}, \text{“NOT OK”}\right) = \text{“OK”}$$

Support

$$Check\_min\_reinf\_support := \text{if}\left(A'_{ss} + A'_{cs} > A_{s.min}, \text{“OK”}, \text{“NOT OK”}\right) = \text{“OK”}$$

$$Check\_yielding\_ss'\_sup := \text{if}\left(\varepsilon'_{ss} > \varepsilon_{syd}, \text{“OK”}, \text{“NOT OK”}\right) = \text{“OK”}$$

$$Check\_yielding\_cs'\_sup := \text{if}\left(\varepsilon'_{cs} > \varepsilon_{syd}, \text{“OK”}, \text{“NOT OK”}\right) = \text{“OK”}$$

$$Check\_not\_yielding\_ss\_sup := \text{if}\left(\varepsilon_{ss} < \varepsilon_{syd}, \text{“OK”}, \text{“NOT OK”}\right) = \text{“OK”}$$

$$Check\_ductility\_sup := \text{if}\left(x_{ULS} \le 0.45 \cdot d'_{m}, \text{“OK”}, \text{“NOT OK”}\right) = \text{“OK”}$$

$$Check\_ULS\_bending\_sup := \text{if}\left(M_{Ed.ULS.sup} \le M_{Rd.sup}, \text{“OK”}, \text{“NOT OK”}\right) = \text{“OK”}$$

$$Check\_crackwidth\_support := \text{if}\left(w_{k.top} \le w_{k.a.top}, \text{“OK”}, \text{“NOT OK”}\right) = \text{“OK”}$$

$$Check\_fatigue\_support := \text{if}\left(\gamma_{s.fat} \cdot \Delta\sigma_{s.equ.sup} < \Delta\sigma_{Rsk}, \text{“OK”}, \text{“NOT OK”}\right) = \text{“OK”}$$

$$Fatigue\_sup\_c := \text{if}\left(\frac{\sigma_{c.max.sup}}{f_{cd.fat}} < 0.5 + 0.45 \cdot \frac{\sigma_{c.min.sup}}{f_{cd.fat}} < 0.9, \text{“OK”}, \text{“NOT OK”}\right) = \text{“OK”}$$

Utilization ratios span

$$Utilization\_ratio\_ULS\_bending\_span := \frac{M_{Ed.ULS.span}}{M_{Rd.span}} = 99.5\%$$

$$Utilization\_crackwidth\_span := \frac{w_{k.bot}}{w_{k.a.bot}} = 33\%$$

$$Utilization\_fatigue\_span := \frac{\Delta\sigma_{s.equ.span} \cdot \gamma_{s.fat}}{\Delta\sigma_{Rsk}} = 52.395\%$$

Utilization ratios support

$$Utilization\_ratio\_ULS\_bending\_support := \frac{\left|M_{Ed.ULS.sup}\right|}{M_{Rd.sup}} = 98.1\%$$

$$Utilization\_crackwidth\_support := \frac{w_{k.top}}{w_{k.a.top}} = 98\%$$

$$Utilization\_fatigue\_support := \frac{\Delta\sigma_{s.equ.sup} \cdot \gamma_{s.fat}}{\Delta\sigma_{Rsk}} = 37.409\%$$

Amount of longitudinal reinforcement

Geometry of bridge deck

$l = 5.88\ m$ — Total deck length

$b := 7\ m$ — Total deck width

$l_{span} := \frac{l}{25} \cdot 11 = 2.587\ m$ — Length of span section

$l_{sup} := l - l_{span} = 3.293\ m$ — Length of support section

Area of reinforcement

$A_{ss} := \left(A_{ss.span} + A'_{ss.span}\right) \cdot l_{span} \hookleftarrow = 8487.907\ mm^2$
$+ \left(A'_{ss.sup} + A_{ss.sup}\right) \cdot l_{sup}$ — Area of stainless steel

$A_{cs} := \left(A_{cs.span} + A'_{cs.span}\right) \cdot l_{span} \hookleftarrow = 13348.725\ mm^2$
$+ \left(A'_{cs.sup} + A_{cs.sup}\right) \cdot l_{sup}$ — Area of carbon steel

Volume of reinforcement

$V_{ss} := A_{ss} \cdot b = 0.059\ m^3$ — Volume of stainless steel

$V_{cs} := A_{cs} \cdot b = 0.093\ m^3$ — Volume of carbon steel

Mass of reinforcement

$\rho_{steel} := 7800\ \frac{kg}{m^3}$ — Density of carbon and stainless steel

$m_{ss} := V_{ss} \cdot \rho_{steel} = 463.44\ kg$ — Mass of stainless steel

$m_{cs} := V_{cs} \cdot \rho_{steel} = 728.84\ kg$ — Mass of carbon steel

D.2 Indata for Bridge Deck, Transversal

Slab-Frame Bridge - transversal reinforcement in slab

Redesign using stainless steel reinforcement

Sofia Elwin Dahlström, Jonas Persson

Material Indata

Concrete C35/45 (in everything but the base plate)

$\gamma_c = 1.5$ $\quad \alpha_{cc} = 1.0$ $\quad \alpha_{ct} = 1.0$ Safety factors acc. to SS-EN 1992-1-1 (2.4.2.4)

$f_{ck} = 35\ MPa$ $\quad f_{cd} = \alpha_{cc}\dfrac{f_{ck}}{\gamma_c} = 23.333\ MPa$ $\quad f_{cm} = 43\ MPa$

$f_{ctk0.05} = 2.2\ MPa$ $\quad f_{ctd} = \alpha_{cc}\dfrac{f_{ctk0.05}}{\gamma_c} = 1.467\ MPa$ $\quad f_{ctm} = 3.2\ MPa$

$E_{cm} = 34\ GPa$ $\quad 2$ $\quad E_{c.ef} = \dfrac{E_{cm}}{1+} = 11.333\ GPa$

$E_{ck} = 28.3\ GPa$

$\varepsilon_{cu} = 3.5\ 10^{-3}$

Reinforcement B500B

$f_{yk} = 500\ MPa$ $\quad \gamma_s = 1.15$

$f_{yd} = \dfrac{f_{yk}}{\gamma_s} = 434.783\ MPa$

$E_s = 200\ GPa$

$\varepsilon_{syd} = \dfrac{f_{yd}}{E_s} = 2.174\ 10^{-3}$

$\dfrac{E_s}{E_{cm}} = 5.882$ $\quad \alpha_{ef} = \dfrac{E_s}{E_{c.ef}} = 17.647$ $\quad \alpha_{fat} = \dfrac{E_s}{E_{ck}} = 7.067$

Reinforcement EN 1.4162

$f_{yk.ss} = 600\ MPa$

$f_{yd.ss} = \dfrac{f_{yk.ss}}{\gamma_s} = 522\ MPa$

$n \quad 15 \qquad {}_0 \quad 0.6$ Ramberg-Osgood parameters

$E_0 \quad 170 \ GPa$

${}_0 \quad f_{yd.ss} = 521.739 \ MPa$

${}_{s0.2} \quad {}^0_{E_0} + {}_0 \quad {}^0_{E_0} = 4.91 \ 10^{-3}$

Geometry

$l \quad 7 \ m$		Length of span
$b_w \quad 1000 \ mm$		Width of section
$h_{span} \quad 417 \ mm$		designing span moment section (ULS and SLS)
$h_{ULS.sup} \quad 374 \ mm$		designing support moment section
$h_{SLS.sup} \quad 374 \ mm$		designing support crack width section
$h_{fat.span} \quad 424 \ mm$		designing fatigue bending section (span)
$h_{fat.sup} \quad 374 \ mm$		designing fatigue bending section (support)

Prerequisites of design process

	Service life	Exposure class	Concrete cover	w.k	
Slab, top	L50	XD3/XF4	45	0,20	1,5
Slab, bottom	L50	XD1/XF4	40	0,30	1,2

$w_{k.a.top} \quad 0.2 \ mm$

$w_{k.a.bot} \quad 0.3 \ mm$

Designing sectional forces

Span

$M_{Ed.ULS.span}$	$149.1\ kN\ m$	$N_{Ed.ULS.span}$	$46.6\ kN$	ULS, bending (line 1, section 17)
$M_{Ed.SLS.span}$	$37.1\ kN\ m$	$N_{Ed.SLS.span}$	$24.8\ kN$	SLS, crack width (line 1, section 17)
$M_{Ed.fat.span.min}$	$-42.4\ kN\ m$			Fatigue bending (line 3, section 16)
$N_{Ed.fat.span.min}$	$-1.5\ kN$			
$M_{Ed.fat.span.max}$	$27.4\ kN\ m$			
$N_{Ed.fat.span.max}$	$-45.2\ kN$			

Support

$M_{Ed.ULS.sup}$	$-85.6\ kN\ m$	$N_{Ed.ULS.sup}$	$36.0\ kN$	ULS, bending (line 2, section 23)
$M_{Ed.SLS.sup}$	$-13.7\ kN\ m$	$N_{Ed.SLS.sup}$	$22.5\ kN$	SLS, crack width (line 2, section 23)
$M_{Ed.fat.sup.min}$	$-26.7\ kN\ m$			Fatigue bending (line 1, section 23)
$N_{Ed.fat.sup.min}$	$39.4\ kN$			
$M_{Ed.fat.sup.max}$	$7.8\ kN\ m$			
$N_{Ed.fat.sup.max}$	$37.8\ kN$			

D.3 Indata for Front Wall, Horizontal

Slab-Frame Bridge - front wall horizontal

Redesign using stainless steel reinforcement

Sofia Elwin Dahlström, Jonas Persson

Material Indata

Concrete C35/45 (in everything but the base plate)

Safety factors acc. to SS-EN 1992-1-1 (2.4.2.4)

$_c \quad 1.5$ $\qquad _{cc} \quad 1.0$ $\qquad _{ct} \quad 1.0$

$f_{ck} \quad 35\ MPa$ $\qquad f_{cd} \quad _{cc} \dfrac{f_{ck}}{_c} = 23.333\ MPa$ $\qquad f_{cm} \quad 43\ MPa$

$f_{ctk0.05} \quad 2.2\ MPa$ $\qquad f_{ctd} \quad _{cc} \dfrac{f_{ctk0.05}}{_c} = 1.467\ MPa$ $\qquad f_{ctm} \quad 3.2\ MPa$

$E_{cm} \quad 34\ GPa$ $\qquad 2$

$E_{ck} \quad 28.3\ GPa$ $\qquad E_{c.ef} \dfrac{E_{cm}}{1+} = 11.333\ GPa$ $\qquad _{cu} \quad 3.5 \quad 10^{-3}$

Reinforcement B500B

$f_{yk} \quad 500\ MPa$ $\qquad _s \quad 1.15$ $\qquad E_s \quad 200\ GPa$

$f_{yd} \quad \dfrac{f_{yk}}{_s} = 435\ MPa$ $\qquad _{syd} \quad \dfrac{f_{yd}}{E_s} = 2.174 \quad 10^{-3}$

Reinforcement EN 1.4162

$f_{yk.ss} \quad 600\ MPa$ $\qquad _s \quad 1.15$ $\qquad f_{yd.ss} \quad \dfrac{f_{yk.ss}}{_s} = 522\ MPa$

$n \quad 15$ $\qquad _0 \quad 0.6$ $\qquad$ Ramberg-Osgood parameters

$E_0 \quad 200\ GPa$

$_0 \quad f_{yd.ss} = 521.739\ MPa$ $\qquad _{s0.2} \quad \dfrac{^0}{E_0} + _0 \dfrac{^0}{E_0} = 4.17 \quad 10^{-3}$

$\dfrac{E_0}{E_{cm}} = 5.882$ $\qquad _{ef} \quad \dfrac{E_0}{E_{c.ef}} = 17.647$ $\qquad _{fat} \quad \dfrac{E_0}{E_{ck}} = 7.067$

Geometry

l	$7\ m$	Length of wall
b_w	$1000\ mm$	Width of section
h_{span}	$389\ mm$	designing span moment section (ULS and SLS)
$h_{ULS.sup}$	$389\ mm$	designing support moment section
$h_{SLS.sup}$	$389\ mm$	designing support crack width section
$h_{fat.span}$	$380\ mm$	designing fatigue bending section (span)
$h_{fat.sup}$	$389\ mm$	designing fatigue bending section (support)

Prerequisites of design process

	Service life	Exposure class	Concrete cover	w.k	
Wall	L50	XD3/XF4	40	0,30	1,2

$w_{k.a}$	$0.3\ mm$	Maximum allowed crack width

Designing sectional forces

Span

$M_{Ed.ULS.span}$	$72.7\ kN\ m$	$N_{Ed.ULS.span}$	$336.8\ kN$	ULS, bending (line 1, section 19)
$M_{Ed.SLS.span}$	$24.2\ kN\ m$	$N_{Ed.SLS.span}$	$70.2\ kN$	SLS, crack width (line 1, section 19)
$M_{Ed.fat.span.min}$	$-13.2\ kN\ m$			Fatigue bending (line 3, section 16)
$N_{Ed.fat.span.min}$	$79.8\ kN$			
$M_{Ed.fat.span.max}$	$-5.5\ kN\ m$			
$N_{Ed.fat.span.max}$	$72.1\ kN$			

Support

$M_{Ed.ULS.sup}$	$-227.8\ kN\ m$	$N_{Ed.ULS.sup}$	$364.8\ kN$	ULS, bending (line 1, section 25)
$M_{Ed.SLS.sup}$	$-115.2\ kN\ m$	$N_{Ed.SLS.sup}$	$195.0\ kN$	SLS, crack width (line 1, section 25)
$M_{Ed.fat.sup.min}$	$27.9\ kN\ m$			Fatigue bending (line 1, section 20)
$N_{Ed.fat.sup.min}$	$78.0\ kN$			
$M_{Ed.fat.sup.max}$	$44.0\ kN\ m$			
$N_{Ed.fat.sup.max}$	$81.6\ kN$			

D.4 Indata for Front Wall, Vertical

Slab-Frame Bridge - Front wall, vertical

Redesign using stainless steel reinforcement

Sofia Elwin Dahlström, Jonas Persson

Material Indata

Concrete C35/45 (in everything but the base plate)

$\gamma_c = 1.5$ $\quad \alpha_{cc} = 1.0$ $\quad \alpha_{ct} = 1.0$ Safety factors acc. to SS-EN 1992-1-1 (2.4.2.4)

$f_{ck} = 35\ MPa$ $\quad f_{cd} = \alpha_{cc}\dfrac{f_{ck}}{\gamma_c} = 23.333\ MPa$ $\quad f_{cm} = 43\ MPa$

$f_{ctk0.05} = 2.2\ MPa$ $\quad f_{ctd} = \alpha_{cc}\dfrac{f_{ctk0.05}}{\gamma_c} = 1.467\ MPa$ $\quad f_{ctm} = 3.2\ MPa$

$E_{cm} = 34\ GPa$ $\quad 2$ $\quad E_{c.ef} = \dfrac{E_{cm}}{1+} = 11.333\ GPa$

$E_{ck} = 28.3\ GPa$ $\quad \varepsilon_{cu} = 3.5\ 10^{-3}$

Reinforcement B500B

$f_{yk} = 500\ MPa$ $\quad \gamma_s = 1.15$

$f_{yd} = \dfrac{f_{yk}}{\gamma_s} = 434.783\ MPa$

$E_s = 200\ GPa$

$\varepsilon_{syd} = \dfrac{f_{yd}}{E_s} = 2.174\ 10^{-3}$

$\dfrac{E_s}{E_{cm}} = 5.882$ $\quad \eta_{ef} = \dfrac{E_s}{E_{c.ef}} = 17.647$ $\quad \eta_{fat} = \dfrac{E_s}{E_{ck}} = 7.067$

Reinforcement EN 1.4162

$f_{yk.ss} = 600\ MPa$ $\quad f_{yd.ss} = \dfrac{f_{yk.ss}}{\gamma_s} = 522\ MPa$

$n = 15$ $\quad \sigma_0 = 0.6$

$E_0 = 170\ GPa$ Ramberg-Osgood parameters

$\varepsilon_0 = f_{yd.ss} = 521.739\ MPa$ $\quad \varepsilon_{s0.2} = \dfrac{\varepsilon_0}{E_0} + \sigma_0\dfrac{\varepsilon_0}{E_0} = 4.91\ 10^{-3}$

Geometry

l	$4.44\ m$	Height of wall
b_w	$1000\ mm$	Width of section
h_{top}	$389\ mm$	designing section at top of wall (line 2 section 3)
h_{bot}	$380\ mm$	designing section at base of wall (section 10, 11, 12 & 14)
h_{fat}	$389\ mm$	designing fatigue bending section top (section 3)

Prerequisites of design process

	Service life	Exposure class	Concrete cover	w.k	
Wall	L50	XD3/XF4	40	0,30	1,2

$w_{k.a}$	$0.3\ mm$	Maximum allowed crack width

Designing sectional forces

Top outer corner

$M_{Ed.ULS.top.outer}$	$269.9\ kN\ m$	$N_{Ed.ULS.top.outer}$	$-150.3\ kN$	ULS, bending (line 2, section 3)
$M_{Ed.SLS.top.outer}$	$70.4\ kN\ m$	$N_{Ed.SLS.top.outer}$	$17.6\ kN$	SLS, crack width (line 2, section 3)
$M_{Ed.fat.top.outer.min}$	$64.2\ kN\ m$			Fatigue bending (line 2, section 3)
$N_{Ed.fat.top.outer.min}$	$-46.4\ kN$			
$M_{Ed.fat.top.outer.max}$	$102.2\ kN\ m$			
$N_{Ed.fat.top.outer.max}$	$-73.7\ kN$			

Top inner corner

$M_{Ed.ULS.top.inner}$	$-173.5\ kN\ m$	$N_{Ed.ULS.top.inner}$	$212.3\ kN$	ULS, bending (line 1, section 3)
$M_{Ed.SLS.top.inner}$	$-23.3\ kN\ m$	$N_{Ed.SLS.top.inner}$	$48.1\ kN$	SLS, crack width (line 1, section 3)
$M_{Ed.fat.top.inner.min}$	$64.2\ kN\ m$			Fatigue bending (line 2, section 3)
$N_{Ed.fat.top.inner.min}$	$-46.4\ kN$			
$M_{Ed.fat.top.inner.max}$	$102.2\ kN\ m$			
$N_{Ed.fat.top.inner.max}$	$-73.7\ kN$			

Bottom outer wall

$M_{Ed.ULS.bot.outer}$	$100.5\ kN\ m$	$N_{Ed.ULS.bot.outer}$	$-134.0\ kN$	ULS, bending (line 1, section 14)
$M_{Ed.SLS.bot.outer}$	$40.6\ kN\ m$	$N_{Ed.SLS.bot.outer}$	$-96.3\ kN$	SLS, crack width (line 1, section 14)

Bottom inner wall

$M_{Ed.ULS.bot.inner}$	$-128.6\ kN\ m$	$N_{Ed.ULS.bot.inner}$	$161.2\ kN$	ULS, bending (line 2, section 10)
$M_{Ed.SLS.bot.inner}$	$-77.7\ kN\ m$	$N_{Ed.SLS.bot.inner}$	$-68.7\ kN$	SLS, crack width (line 2, section 12)

Minimum amount of reinforcement

Acc. to TDOK 2016:0204 D.1.4.1.1

$$A_{s.min.1} \quad \max\ 4.0\ \frac{cm^2}{m}, 4.0\ \frac{cm^2}{m}\ \frac{f_{ctm}}{3\ MPa} = 426.667\ \frac{1}{m}\ mm^2$$

$$\text{if}\ \frac{l}{h_{top}} > 5, 0.08\%, 0.05\% = 0.08\%$$

$$A_{s.min.2} \quad \frac{0.08}{100}\ h_{top} = 311.2\ \frac{1}{m}\ mm^2$$

$$A_{s.min} \quad \max\ A_{s.min.1}, A_{s.min.2}\ \ b_w = 426.667\ mm^2$$

$$s_{max} \quad 300\ mm$$

D.5 Indata for Short Wing Wall, Horizontal

Slab-Frame Bridge - short wing wall horisontal

Redesign using stainless steel reinforcement

Sofia Elwin Dahlström, Jonas Persson

Material Indata

Concrete C35/45 (in everything but the base plate)

Safety factors acc. to SS-EN 1992-1-1 (2.4.2.4)

$\gamma_c = 1.5$ $\quad \alpha_{cc} = 1.0$ $\quad \alpha_{ct} = 1.0$

$f_{ck} = 35\ MPa$ $\quad f_{cd} = \alpha_{cc}\dfrac{f_{ck}}{\gamma_c} = 23.333\ MPa$ $\quad f_{cm} = 43\ MPa$

$f_{ctk0.05} = 2.2\ MPa$ $\quad f_{ctd} = \alpha_{cc}\dfrac{f_{ctk0.05}}{\gamma_c} = 1.467\ MPa$ $\quad f_{ctm} = 3.2\ MPa$

$E_{cm} = 34\ GPa$

$E_{ck} = 28.3\ GPa$ $\quad E_{c.ef} = \dfrac{E_{cm}}{1+\varphi_{ef}} = 11.333\ GPa$ $\quad \varepsilon_{cu} = 3.5\ 10^{-3}$

Reinforcement B500B

$f_{yk} = 500\ MPa$ $\quad \gamma_s = 1.15$ $\quad E_s = 200\ GPa$

$f_{yd} = \dfrac{f_{yk}}{\gamma_s} = 435\ MPa$ $\quad \varepsilon_{syd} = \dfrac{f_{yd}}{E_s} = 2.174\ 10^{-3}$

Reinforcement EN 1.4162

$f_{yk.ss} = 600\ MPa$ $\quad \gamma_s = 1.15$ $\quad f_{yd.ss} = \dfrac{f_{yk.ss}}{\gamma_s} = 522\ MPa$

$n = 15$ $\quad \sigma_0 = 0.6$ Ramberg-Osgood parameters

$E_0 = 170\ GPa$

$\sigma_0 = f_{yd.ss} = 521.739\ MPa$ $\quad \varepsilon_{s0.2} = \dfrac{\sigma_0}{E_0} + 0.002\dfrac{\sigma_0}{E_0} = 4.91\ 10^{-3}$

$\dfrac{E_0}{E_{cm}} = 5$ $\quad \eta_{ef} = \dfrac{E_0}{E_{c.ef}} = 15$ $\quad \eta_{fat} = \dfrac{E_0}{E_{ck}} = 6.007$

Geometry

l $3.19\ m$ Length of wall

b_w $1000\ mm$ Width of section

h_{span} $300\ mm$ designing moment section (ULS and SLS)

Prerequisites of design process

	Service life	Exposure class	Concrete cover	w.k	
Wall	L50	XD3/XF4	40	0,30	1,2

$w_{k.a}$ $0.3\ mm$ Maximum allowed crack width

Designing sectional forces

Section at base of wall

$M_{Ed.ULS.span}$ $98.1\ kN\ m$ $N_{Ed.ULS.span}$ $383.9\ kN$ ULS, bending (line 3, section 15)

$M_{Ed.SLS.span}$ $43.8\ kN\ m$ $N_{Ed.SLS.span}$ $141.8\ kN$ SLS, crack width (line 3, section 15)

Minimum amount of reinforcement

Acc. to TDOK 2016:0204 D.1.4.1.1

$$A_{s.min.1} \quad \max\ 4.0\ \frac{cm^2}{m}, 4.0\ \frac{cm^2}{m}\ \frac{f_{ctm}}{3\ MPa} = 426.667\ \frac{1}{m}\ mm^2$$

$$\text{if}\ \frac{l}{h_{span}} > 5, 0.08\%, 0.05\% = 0.08\%$$

$$A_{s.min.2} \quad \frac{0.08}{100}\ h_{span} = 240\ \frac{1}{m}\ mm^2$$

$$A_{s.min} \quad \max\ A_{s.min.1}, A_{s.min.2}\ \ b_w = 426.667\ mm^2$$

s_{max} $300\ mm$

D.6 Indata for Short Wing Wall, Vertical

Slab-Frame Bridge - short wing wall vertical

Redesign using stainless steel reinforcement

Sofia Elwin Dahlström, Jonas Persson

Material Indata

Concrete C35/45 (in everything but the base plate)

Safety factors acc. to SS-EN 1992-1-1 (2.4.2.4)

$_c \quad 1.5$ $\qquad _{cc} \quad 1.0$ $\qquad _{ct} \quad 1.0$

$f_{ck} \quad 35\ MPa$ $\qquad f_{cd} \quad _{cc} \dfrac{f_{ck}}{_c} = 23.333\ MPa$ $\qquad f_{cm} \quad 43\ MPa$

$f_{ctk0.05} \quad 2.2\ MPa$ $\qquad f_{ctd} \quad _{cc} \dfrac{f_{ctk0.05}}{_c} = 1.467\ MPa$ $\qquad f_{ctm} \quad 3.2\ MPa$

$E_{cm} \quad 34\ GPa$ $\qquad 2$

$E_{ck} \quad 28.3\ GPa$ $\qquad E_{c.ef} \dfrac{E_{cm}}{1+} = 11.333\ GPa$ $\qquad _{cu} \quad 3.5 \quad 10^{-3}$

Reinforcement B500B

$f_{yk} \quad 500\ MPa$ $\qquad _s \quad 1.15$ $\qquad E_s \quad 200\ GPa$

$f_{yd} \quad \dfrac{f_{yk}}{_s} = 435\ MPa$ $\qquad _{syd} \quad \dfrac{f_{yd}}{E_s} = 2.174 \quad 10^{-3}$

Reinforcement EN 1.4162

$f_{yk.ss} \quad 600\ MPa$ $\qquad _s \quad 1.15$ $\qquad f_{yd.ss} \quad \dfrac{f_{yk.ss}}{_s} = 522\ MPa$

$n \quad 15$ $\qquad _0 \quad 0.6$ $\qquad$ Ramberg-Osgood parameters

$E_0 \quad 170\ GPa$

$_0 \quad f_{yd.ss} = 521.739\ MPa$ $\qquad _{s0.2} \quad \dfrac{^0}{E_0} + _0 \dfrac{^0}{E_0} = 4.91 \quad 10^{-3}$

$\dfrac{E_0}{E_{cm}} = 5$ $\qquad _{ef} \quad \dfrac{E_0}{E_{c.ef}} = 15$ $\qquad _{fat} \quad \dfrac{E_0}{E_{ck}} = 6.007$

Geometry

l	$3.19\ m$	Length of wall
b_w	$1000\ mm$	Width of section
h_{span}	$300\ mm$	designing moment section (ULS and SLS)

Prerequisites of design process

	Service life	Exposure class	Concrete cover	w.k	
Wall	L50	XD3/XF4	40	0,30	1,2

$w_{k.a}$	$0.3\ mm$	Maximum allowed crack width

Designing sectional forces

Section at base of wall

$M_{Ed.ULS.span}$	$35\ kN\ m$	$N_{Ed.ULS.span}$	$235.1\ kN$	ULS, bending (line 1, section 15)
$M_{Ed.SLS.span}$	$21.9\ kN\ m$	$N_{Ed.SLS.span}$	$-110.4\ kN$	SLS, crack width (line 1, section 15)

Minimum amount of reinforcement

Acc. to TDOK 2016:0204 D.1.4.1.1

$$A_{s.min.1} \quad \max\ 4.0\ \frac{cm^2}{m}, 4.0\ \frac{cm^2}{m}\ \frac{f_{ctm}}{3\ MPa} = 426.667\ \frac{1}{m}\ mm^2$$

$$\text{if}\ \frac{l}{h_{span}} > 5, 0.08\%, 0.05\% = 0.08\%$$

$$A_{s.min.2} \quad \frac{0.08}{100}\ h_{span} = 240\ \frac{1}{m}\ mm^2$$

$$A_{s.min} \quad \max\ A_{s.min.1}, A_{s.min.2}\ \ b_w = 426.667\ mm^2$$

$$s_{max} \quad 300\ mm$$

D.7 Indata for Long Wing Wall, Horizontal

Slab-Frame Bridge - long wing wall horizontal

Redesign using stainless steel reinforcement

Sofia Elwin Dahlström, Jonas Persson

Material Indata

Concrete C35/45 (in everything but the base plate)

Safety factors acc. to SS-EN 1992-1-1 (2.4.2.4)

$\gamma_c = 1.5$ $\quad \alpha_{cc} = 1.0$ $\quad \alpha_{ct} = 1.0$

$f_{ck} = 35\ MPa$ $\quad f_{cd} = \alpha_{cc}\dfrac{f_{ck}}{\gamma_c} = 23.333\ MPa$ $\quad f_{cm} = 43\ MPa$

$f_{ctk0.05} = 2.2\ MPa$ $\quad f_{ctd} = \alpha_{cc}\dfrac{f_{ctk0.05}}{\gamma_c} = 1.467\ MPa$ $\quad f_{ctm} = 3.2\ MPa$

$E_{cm} = 34\ GPa$

$E_{ck} = 28.3\ GPa$ $\quad E_{c.ef} = \dfrac{E_{cm}}{1+\varphi_{ef}} = 11.333\ GPa$ $\quad \varepsilon_{cu} = 3.5\ 10^{-3}$

Reinforcement B500B

$f_{yk} = 500\ MPa$ $\quad \gamma_s = 1.15$ $\quad E_s = 200\ GPa$

$f_{yd} = \dfrac{f_{yk}}{\gamma_s} = 435\ MPa$ $\quad \varepsilon_{syd} = \dfrac{f_{yd}}{E_s} = 2.174\ 10^{-3}$

Reinforcement EN 1.4162

$f_{yk.ss} = 600\ MPa$ $\quad \gamma_s = 1.15$ $\quad f_{yd.ss} = \dfrac{f_{yk.ss}}{\gamma_s} = 522\ MPa$

$n = 15$ $\quad \sigma_0 = 0.6$ Ramberg-Osgood parameters

$E_0 = 170\ GPa$

$\sigma_0 = f_{yd.ss} = 521.739\ MPa$ $\quad \varepsilon_{s0.2} = \dfrac{\sigma_0}{E_0} + 0.002\dfrac{\sigma_0}{E_0} = 4.91\ 10^{-3}$

$\dfrac{E_0}{E_{cm}} = 5$ $\quad \varphi_{ef} = \dfrac{E_0}{E_{c.ef}} = 15$ $\quad \varphi_{fat} = \dfrac{E_0}{E_{ck}} = 6.007$

Geometry

l $3.19\ m$ Length of wall

b_w $1000\ mm$ Width of section

h_{span} $360\ mm$ designing moment section (ULS and SLS)

Prerequisites of design process

	Service life	Exposure class	Concrete cover	w.k	
Wall	L50	XD3/XF4	40	0,30	1,2

$w_{k.a}$ $0.3\ mm$ Maximum allowed crack width

Designing sectional forces

Section at base of wall

$M_{Ed.ULS.span}$ $256.8\ kN\ m$ $N_{Ed.ULS.span}$ $240.9\ kN$ ULS, bending (line 1, section 1)

$M_{Ed.SLS.span}$ $128.0\ kN\ m$ $N_{Ed.SLS.span}$ $151.9\ kN$ SLS, crack width (line 1, section 1)

Minimum amount of reinforcement

Acc. to TDOK 2016:0204 D.1.4.1.1

$$A_{s.min.1} \quad \max\ 4.0\ \frac{cm^2}{m}, 4.0\ \frac{cm^2}{m}\ \frac{f_{ctm}}{3\ MPa} = 426.667\ \frac{1}{m}\ mm^2$$

$$\text{if}\ \frac{l}{h_{span}} > 5, 0.08\%, 0.05\% = 0.08\%$$

$$A_{s.min.2} \quad \frac{0.08}{100}\ h_{span} = 288\ \frac{1}{m}\ mm^2$$

$$A_{s.min} \quad \max\ A_{s.min.1}, A_{s.min.2}\ \ b_w = 426.667\ mm^2$$

s_{max} $300\ mm$

D.8 Indta for Long Wing Wall, Vertical

Slab-Frame Bridge - long wing wall vertical

Redesign using stainless steel reinforcement

Sofia Elwin Dahlström, Jonas Persson

Material Indata

Concrete C35/45 (in everything but the base plate)

Safety factors acc. to SS-EN 1992-1-1 (2.4.2.4)

$_c \quad 1.5$ $_{cc} \quad 1.0$ $_{ct} \quad 1.0$

$f_{ck} \quad 35\ MPa$ $f_{cd} \quad _{cc} \dfrac{f_{ck}}{_c} = 23.333\ MPa$ $f_{cm} \quad 43\ MPa$

$f_{ctk0.05} \quad 2.2\ MPa$ $f_{ctd} \quad _{cc} \dfrac{f_{ctk0.05}}{_c} = 1.467\ MPa$ $f_{ctm} \quad 3.2\ MPa$

$E_{cm} \quad 34\ GPa$ 2

$E_{ck} \quad 28.3\ GPa$ $E_{c.ef} \quad \dfrac{E_{cm}}{1+} = 11.333\ GPa$ $_{cu} \quad 3.5 \quad 10^{-3}$

Reinforcement B500B

$f_{yk} \quad 500\ MPa$ $_s \quad 1.15$ $E_s \quad 200\ GPa$

$f_{yd} \quad \dfrac{f_{yk}}{_s} = 435\ MPa$ $_{syd} \quad \dfrac{f_{yd}}{E_s} = 2.174 \quad 10^{-3}$

Reinforcement EN 1.4162

$f_{yk.ss} \quad 600\ MPa$ $_s \quad 1.15$ $f_{yd.ss} \quad \dfrac{f_{yk.ss}}{_s} = 522\ MPa$

$n \quad 15$ $_0 \quad 0.6$ Ramberg-Osgood parameters

$E_0 \quad 200\ GPa$

$_0 \quad f_{yd.ss} = 521.739\ MPa$ $_{s0.2} \quad \dfrac{^0}{E_0} + {}_0 \dfrac{^0}{E_0} = 4.17 \quad 10^{-3}$

$\dfrac{E_0}{E_{cm}} = 5.882$ $_{ef} \quad \dfrac{E_0}{E_{c.ef}} = 17.647$ $_{fat} \quad \dfrac{E_0}{E_{ck}} = 7.067$

$_{s0.2} \quad _{syd}$

Geometry

l $3.64\ m$ Length of wall

b_w $1000\ mm$ Width of section

h_{span} $360\ mm$ designing moment section (ULS and SLS)

Prerequisites of design process

	Service life	Exposure class	Concrete cover	w.k	
Wall	L50	XD3/XF4	40	0,30	1,2

$w_{k.a}$ $0.3\ mm$ Maximum allowed crack width

Designing sectional forces

Section at base of wall

$M_{Ed.ULS.span}$ $40.8\ kN\ m$ $N_{Ed.ULS.span}$ $251.0\ kN$ ULS, bending (line 1, section 4)

$M_{Ed.SLS.span}$ $18.8\ kN\ m$ $N_{Ed.SLS.span}$ $-20.2\ kN$ SLS, crack width (line 1, section 4)

Minimum amount of reinforcement

Acc. to TDOK 2016:0204 D.1.4.1.1

$$A_{s.min.1} \quad \max\ 4.0\ \frac{cm^2}{m}, 4.0\ \frac{cm^2}{m}\ \frac{f_{ctm}}{3\ MPa} = 426.667\ \frac{1}{m}\ mm^2$$

$$\text{if}\ \frac{l}{h_{span}} > 5, 0.08\%, 0.05\% = 0.08\%$$

$$A_{s.min.2} \quad \frac{0.08}{100}\ h_{span} = 288\ \frac{1}{m}\ mm^2$$

$$A_{s.min} \quad \max\ A_{s.min.1}, A_{s.min.2}\ \ b_w = 426.667\ mm^2$$

s_{max} $300\ mm$